Transient and persistent aspects of human platelet activation

Transient and persistent aspects of human platelet activation

Jinmi Zou

This research in this thesis was supported by China Scholarship Council (CSC) No. 201909370052, Synapse Research Institute, and Cardiovascular Research Institute Maastricht University.

The printing of this thesis was supported by Hart Onderzoek Nederland and Synapse Research Institute.

ISBN: 978-94-6469-766-7

Date of publication: 19-03-2024

Title: Transient and persistent aspects of human platelet activation

Language: English

Manifestation / binding: Paperback / softback

Date of publication: 19-03-2024
Cover design by bing image creator

Printed by ProefschriftMaken

Transient and persistent aspects of human platelet activation

DISSERTATION

To obtain the degree of Doctor at Maastricht University on the authority of the Rector Magnificus, Prof. dr. Pamela Habibović, in accordance with the decision of Board of Deans, to be defended in public on

Tuesday, 19 March 2024 at 16:00 hours

by

Jinmi Zou

Promotors

Prof. dr. Johan W.M. Heemskerk

Prof. dr. Hugo ten Cate

Co-promotor

Dr. Frauke Swieringa, Synapse Research Institute Maastricht

Assessment Committee

Prof. dr. Rory Koenen (Chair)

Prof. dr. Chris P.M. Reutelingsperger

Prof. dr. Alastair Poole, University of Bristol

Prof. dr. David Stegner, University of Würzburg

Dr. Ingrid Dijkgraaf

Contents

Chapter 1

General introduction

Platelets are the smallest a-nucleated blood cells. They are released into the blood by matured megakaryocytes, located mainly in the bone marrow. Human platelets, once shed, remain in the circulation for 7-10 days, and act there as regulators of hemostasis, thrombosis and other processes [1]. Following vascular injury, the circulating platelets become exposed to vascular collagen fibers with von Willebrand factor (VWF) present in the subendothelial matrix. This results in platelet adhesion, activation and plug formation, such to avoid excessive blood loss [2]. The activation and aggregation processes of platelets are induced by multiple receptor agonists [3], mostly acting via phospholipase C, with as a consequence activation of the broad-spectrum serine/threonine protein kinase C (PKC) isoforms [4,5], and furthermore transient rises in cytosolic $[Ca^{2+}]_i$ [6,7]. This chapter provides a general background of central signaling pathways leading to platelet activation and aggregation, as far as relevant for this thesis.

Platelet receptors and signaling in hemostasis and thrombosis

A wide variety of receptors are expressed on the platelet surface, many of which have a role in primary hemostasis and thrombosis. The receptors are commonly divided into G-protein-coupled receptors (GPCR), immunoreceptor tyrosine-based activation motif (ITAM)-linked receptors, and adhesive receptors such as integrins.

At sites of vascular injury, VWF in the plasma deposits on collagen fibers in the extracellular matrix, which act under shear as a ligand for the glycoprotein (GP) Ib-IX-V receptor complex on platelets. Additionally, collagen serves as a receptor for the platelet integrin α2β1 and glycoprotein VI (GPVI) [8]. The subsequent activation of collagen-adhered platelets alters their shape; leads to the release of the contents of their granules; triggers the aggregation with other platelets via fibrinogen linking to integrin αIIbβ3; and provokes exposure of the anionic amino-phospholipid phosphatidylserine on their surface [9]. This translocation of phosphatidylserine from the internal to the external platelet membrane leaflets promotes a burst of thrombin generation and coagulation.

G protein-coupled receptors

GPCR are transmembrane proteins with seven transmembrane domains, which associate with heterotrimeric G proteins consisting of Gα and Gβγ subunits [10]. Binding of a soluble ligand causes a conformational change in the GPCR, which then activates the associated GTP-binding Gα protein via a GDP exchange for GTP. This event triggers its dissociation from the connected Gβγ subunit. As a result, the GTP-bound Gα subunits can interact with effector proteins, which conduct downstream responses [11]. In platelets, several GPCR contribute to activation or inhibition. The platelet-activating receptors include the protease-activated receptors (PAR) for thrombin, PAR1 and PAR4; the purinergic receptors $P2Y_1$ and $P2Y_{12}$ for adenosine 5′-disphosphate (ADP); the TPα receptor for thromboxane A_2 (TxA_2), and the $5HT_{2A}$ receptors for serotonin. Platelet-inhibiting receptors include the prostacyclin receptor IP and the prostaglandin E receptors 2 and 4 (EP_2 and EP_4). An enhancement of platelet activation is

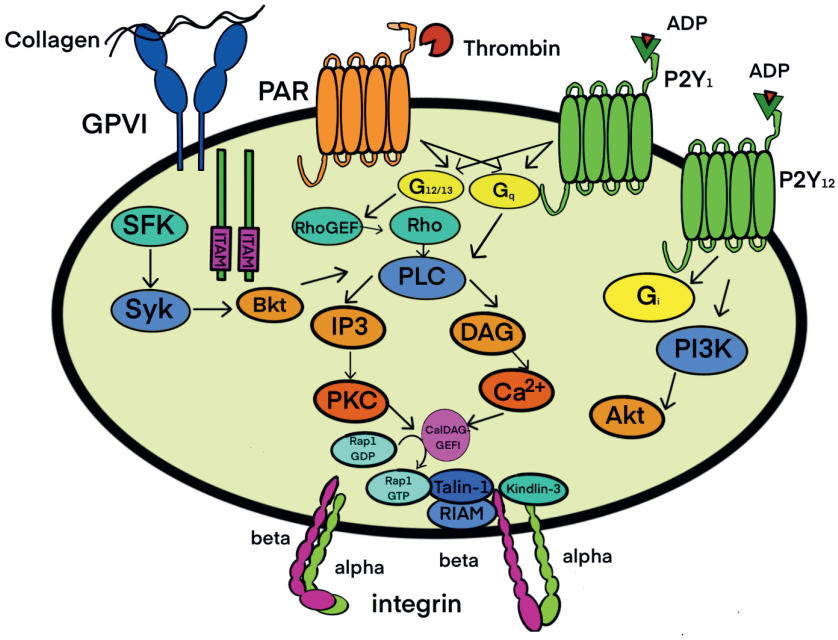

Figure 1. Key platelet receptors and signaling pathways. Thrombin cleaves PAR1/4 and ADP triggers $P2Y_1$ leading to Gq and G12/13 activation. A receptor-induced $G_{12/13}$ activation leads to shape change via Rho activation. The activation of Gq stimulates phospholipase C-β (PLCβ), which generates the secondary messengers inositol 1,4,5 trisphosphate (IP_3) and 1,2-diacylglycerol (DAG), required for Ca^{2+} mobilization and PKC activation, respectively. The components PKC and CalDAG-GEFI mediate the activation and translocation of a small GTPase Rap1 to the plasma membrane. The effector molecule RIAM interacts with Rap1-GTP and talin-1, which results in integrin αIIbβ3 conformational changes in the extracellular domains, thereby allowing ligand binding. In addition, ADP acts via the Gi-coupled $P2Y_{12}$ receptors to inhibit adenylate cyclase and activate phosphatidylinositol 3-kinase (PI3K). Collagen activates platelets via GPVI, which induces Syk docking to phosphorylated ITAM motifs. Self-activated kinase Syk propagates the signal through a tyrosine phosphorylation cascade of Bruton's tyrosine kinase (Btk), LAT and phospholipase Cγ2 (PLCγ2). Modified from Ref. 1.

achieved by stimulation of the α_{2A}-adrenergic receptor for adrenaline. Receptors and signaling paths most relevant for this thesis are summarized in **Figure 1**, and are further explained below.

Of the family of PARs, human platelets only express PAR1 and PAR4, both of which coupled to Gq and $G_{12/13}$ proteins. These receptors are key regulators of platelet function, and they become activated by the serine protease thrombin, one of the most potent platelet agonists [12]. The GTP-binding form of Gqα activates phospholipase C-β (PLCβ), then produces the secondary messengers inositol 1,4,5-trisphosphate (IP_3) and 1,2-diacylglycerol (DAG), which are essential for Ca^{2+} mobilization and protein kinase C (PKC) activation, respectively. On the other hand, $G_{12/13}$ activates Rho and Rho kinases, which confer cytoskeletal rearrangements, platelet shape changes and granule release. PAR1 becomes activated when thrombin cleaves its N-terminal outer domain at between residues Arg41 and Ser42 [13]. A special feature of the PAR1 activation mechanism is that the receptor carries its own ligand, which only becomes available after

cleavage by thrombin at this specific site. The synthetic peptide SFLLRN (TRAP6) exhibits full agonist activity to PAR1, but in contrast to thrombin does not evoke proteolysis. The receptor PAR4 becomes activated, when thrombin cleaves the amino-terminal domain between the residues Arg47 and Gly48. A potent agonist of PAR4 is the peptide AYPGKF, and this property makes it a useful tool for studying PAR4 signaling in a variety of situations [14].

The two principal ADP receptors on platelets are $P2Y_1$ and $P2Y_{12}$. The $P2Y_1$ receptors mediate platelet shape change, whereas the $P2Y_{12}$ receptors play a strong role in platelet aggregation. When ADP binds to the Gq-coupled $P2Y_1$ receptor, this activates PLCβ, and as such can initiate platelet activation [15]. When ADP binds to the Giα-coupled $P2Y_{12}$, this leads to a decrease in platelet-inhibiting cAMP production [16], and furthermore triggers the pathway of phosphatidylinositol 3-kinase (PI3K), which leads to lipid phosphorylation and thereby to activation of the protein kinase Akt, mediating platelet aggregate formation and thrombus buildup [17]. How these various signaling pathways contribute to a transient or more permanent platelet activation state is investigated in this thesis.

Glycoprotein VI as an ITAM-linked receptor

Several ligands stimulate the platelet ITAM-linked receptors, GPVI, CLEC2 (C-type lectin-like receptor 2) and FcγRIIa, all of which then signal via tyrosine protein kinases and PLC isoforms [18].

The immunoglobulin receptor GPVI on platelets is considered an antithrombotic target, given the current evidence for a major role in arterial thrombosis, and a lesser role in hemostasis [19]. Collagen-induced GPVI stimulation provides a powerful signaling trigger, involving cytosolic Ca^{2+} mobilization, activation of integrins α2β1 and αIIbβ3, release of TxA_2, secretion of storage granules, and surface exposure of phosphatidylserine [20,21]. Ligand binding to GPVI initially leads to phosphorylation of tyrosine residues in the ITAM structural domain of the co-receptor FcRγ via Src-family kinases and to the docking of the kinase Syk to this structural domain. Subsequently, Syk becomes sequentially phosphorylated at two tyrosine residues, Y323 and Y525, which then triggers a tyrosine phosphorylation cascade of several other signaling proteins, including Bruton's tyrosine kinase (Btk), adaptor protein LAT, and effector protein phospholipase Cγ2 (PLCγ2) [22,23]. Platelet activation by GPVI can be achieved with physiological collagens as well by a synthetic triple helix collagen-related peptide (CRP) containing a repetitive pattern of GPO (glycine-proline-hydroxyproline); furthermore by convulxin (Cvx), a multimeric protein from rattlesnake venom, having a high affinity for GPVI [24,25]. Monoclonal antibody binding assays have identified different sites in the functional domain of GPVI, but some of the residues share in the binding to collagen, CRP and Cvx [26].

Platelet integrins

Integrins form a family of non-covalently associated transmembrane heterodimers (α/β), which link extracellular ligands to intracellular signaling pathways.[27] Platelets express the collagen receptor integrin α2β1, the fibronectin receptor integrin α5β1 and the laminin receptor integrin

α6β1; further the fibrin(ogen) and vitronectin receptors αIIbβ3 and αvβ3, respectively, all in a low-affinity state [28]. Upon platelet activation, these integrins convert into a high-affinity state, which allows a more efficient binding of their ligands. Integrin αIIbβ3 is the most abundant receptor on platelets (80,000-120,000 copies) and, as the major fibrinogen receptor, is essential for platelet aggregation.

Integrin αIIbβ3 mediates bidirectional signaling responses. The inside-out signaling process activates the ligand-binding function, while outside-in signaling elicited by integrin-ligand binding allows contribution to activation responses. Common results of αIIbβ3 outside-in signaling are platelet spreading, contraction and migration [29].The bidirectional signaling by platelet integrin αIIbβ3 is considered to play a role in cancer progression and in inflammatory diseases [30,31]. Of note, integrin αIIbβ3 has also other endogenous ligands, such as VWF, fibronectin, thrombochondroitin and vitronectin [32].

Most platelet agonists induce activation of integrin αIIbβ3 with, as a consequence, platelet aggregate formation. Early data indicated that the Src family of kinases is involved in the protein phosphorylation events by integrin outside-in signaling [33]. This integrin-dependent activation of Src kinases also leads to activation of the tyrosine kinase Syk [34]. It is considered that the bidirectional signaling via integrin αIIbβ3 plays a role in the phenomenon of transient platelet activation, a subject that however still is underexplored. The platelet agonists and signaling pathways that can lead to a functionally reversible αIIbβ3 activation and transient aggregation are extensively discussed in the review Chapter 2. Although platelet integrin antagonists are for long used in the clinical setting, it is still debated how to finetune the treatment of thrombotic patients to prevent hemorrhage as a side effect. In the present thesis, I dived into better understanding the transiency of platelet activation.

Protein kinase C and cytosolic Ca^{2+} in the center of the platelet activation status

PKCs are a family of serine/threonine protein kinases with multiple intracellular sites. The PKC family includes 12 isoforms, which are classified into three categories based on the presence of four conserved structural domains (C1-C4) and five variable structural domains. The conventional or classical (cPKC) isoforms (α, βI/II and γ) contain a serial C1A-C1B structural domain, capable of binding DAG, and a C2 structural domain that binds Ca^{2+} [35]. The novel (nPKC) isoforms (δ, ε, η and θ) also contain the C1 domain, but lack the ability to bind Ca^{2+} due to the presence of a C2-*like* structural domain. The atypical PKC isoforms (ζ, λ) lack a C2 structural domain and moreover have an atypical C1 structural domain. Of these isoforms, human platelets mainly express cPKCα and cPKCβ, as well as nPKCδ and nPKCθ [35]. When platelets are activated, the increased cytosolic Ca^{2+} concentration $[Ca^{2+}]_i$ causes the C2 structural domain of cPKC isoforms to interact with membrane phosphatidylserine (**Figure 2**). In cPKC isoforms the C1 structural domain binds to PLC-released DAG, causing a conformational change that discharges the pseudo-substrate structural domain from the substrate binding pocket, allowing the phosphorylation of

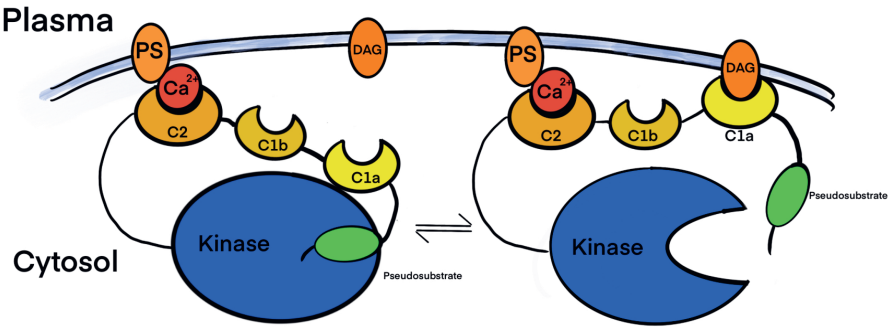

Figure 2. Activation of classical protein kinase C (cPKC) isoforms. At increased levels of cytosolic Ca^{2+}, cPKC isoforms with affinity for phosphatidylserine (PS), bind via their C2 structural domains and thereby translocate to the plasma membrane. Subsequently, the C1a structural domain binds to 1,2-diacylglycerol (DAG). Modified after Ref. 36.

adjacent substrates [36]. In contrast, nPKCs are insensitive to Ca^{2+} and become only activated by DAG. In platelets, agonist-induced increases in $[Ca^{2+}]_i$ have been reported to be enhanced by broad-spectrum PKC inhibitors [37], but the precise mechanism of this enhancement and the roles of specific isoforms are unknown.

Phorbol 12-myristate 13-acetate (PMA) is a phorbol compound extracted from the *Croton tiglium* plant of the *Euphorbiaceae* family. As a high-affinity PKC activator, PMA has been used for many years to mimic the PKC regulation mechanism in platelets [38]. In addition, several well-characterized PKC inhibitors are known, characterized by a high-affinity for the catalytic sites of PKC isoforms. Such inhibitors either prevent PKCs from binding to their substrates, reduce the PKC expression, or neutralize the effects of PKC phosphorylation events [39]. Most PKC inhibitors are ATP-competitive by binding to the catalytic C3 domain; these include the staurosporine analog Gö6976 and the bisindolylmaleimide compounds, GF109203X and RO-318425 [5,40,41]. Some of the PKC-activity inhibitors have a similar high affinity for all PKC isoforms in platelets, whereas other are more selective for specific isoforms (**Table 1**).

Inhibitors of PKC have already been used to elucidate PKC-dependent intracellular signaling pathways, as well as to study a variety of PKC-associated diseases, such as cancers, neurological disorders, cardiovascular diseases and infections [42]. However, the mechanism of action of each PKC isoform on platelets and the effect strength on platelet-related coagulation and hemorrhage are still unclear.

Rises in cytosolic free Ca^{2+} level are one of the most extensively regulated aspects of cellular activity. As a second messenger, Ca^{2+} is involved as an intracellular mediator in many cell functions, thus explaining its role in disorders, such as immunodeficiency, the York platelet syndrome, cardiovascular and metabolic pathologies, and in cancers [43]. In resting platelets, the cytosolic Ca^{2+} level is well-controlled by the Ca^{2+} pumps, sarco-endoplasmic reticulum Ca^{2+}-

Table 1. Inhibitory potential of PKC inhibitors on isolated PKC. Note that all are dissolved in DMSO and that affinities in the presence of plasma may substantially be changed. Taken from Refs. [4,35,40,41].

Name	Inhibition order
RO318425	all PKC isoforms
GF109203X	PKCε ≥ PKCα/β/γ/ε/η ≥ PKCθ
Gö6976	PKCα/β > Syk, PKD2 > PKCη > PKCε/θ
Rottlerin	PKCδ > PKCα > PKCγ > PKCβ >PKCη
PKCθ inhibitor	PKCθ > PKCδ > PKCα/β

ATPases (SERCA) and plasma membrane Ca^{2+}-ATPases (PMCA) (**Figure 3**). These Ca^{2+} pumps transfer elevated cytosolic Ca^{2+} back to the endoplasmic reticulum lumen and the extracellular medium, respectively. The extracellular Ca^{2+} entry is mediated by a number of Ca^{2+} channels, where it is recognized that store-operated Ca^{2+} entry (SOCE) is mediated by two partners: the Ca^{2+} pore-forming Orai channels (Orai1-3) and as a Ca^{2+} storage sensor, the stromal interaction molecules 1-2 (STIM1-2). It was observed that the Ca^{2+} responses to specific platelet agonists (ADP, collagen and thrombin) were significantly diminished in platelets from mice lacking functional Orai1 [44]. Other ion channels and ion exchangers may also add to Ca^{2+} entry in platelets stimulated by ITAM-linked receptors (GPVI) or GPCRs (PAR1/4); however, the roles of these have not been systematically investigated so far.

Blood coagulation and thrombin generation measurements

The hemostatic system serves to maintain continuous blood flow in intact blood vessels, and to stop blood flow upon vascular injury. Platelet aggregates form at the site of vascular injury, the so-called platelet plug, while activation of the coagulation cascade results in thrombin generation, mediating the formation of a plug-consolidating fibrin mesh [1].

During the past decades, fluorogenic thrombin generation assays have proved to be very valuable to assess the coagulation activity in plasmas from given blood samples [45,46]. Recent work has focused on creating continuous assays that can also measure thrombin generation in whole blood in order to gain a deeper understanding of the blood (patho)physiology [47,48]. An advantage of whole-blood thrombin generation tests is that these contain all blood cells, thus allowing to determine their roles in the coagulation process. Furthermore, whole-blood methods eliminate the need for centrifugation of plasma, and hence can serve for point-of-care testing. In conventional assays with platelet-rich plasma, platelets increase the initiation and velocity of thrombin generation by releasing their granule contents, by exposing phosphatidylserine, and by interacting with coagulation proteins through their surface receptors [49,50]. Hence, activated platelets can be considered as propagating factors in thrombin generation and coagulation.

Red blood cells play a variety of roles in hemostasis and thrombosis as they contribute to the viscoelasticity of the blood. There is also evidence that (activated?) red blood cells are a source

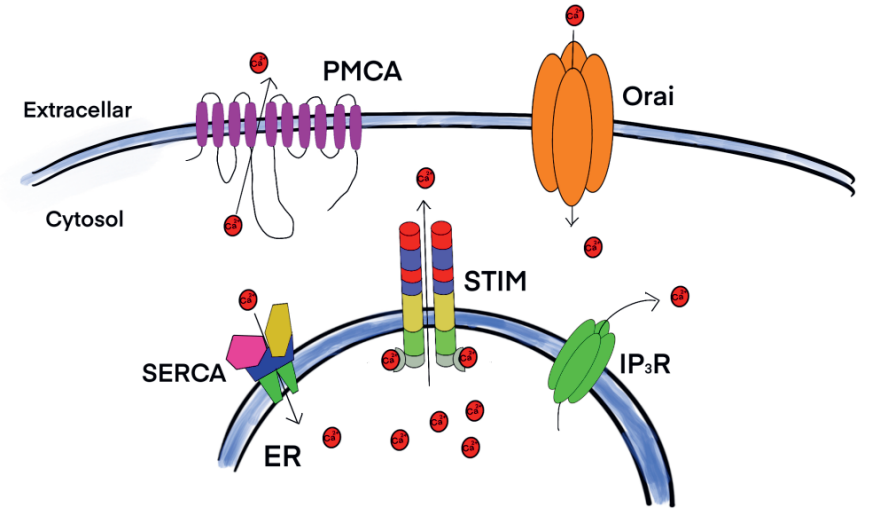

Figure 3. Mechanisms of Ca^{2+} signal generation in platelets. In resting platelets, the Ca^{2+} concentration in the cytosol is maintained at a low level by the Ca^{2+} pump action of plasma membrane Ca^{2+}-ATPases (PMCA) and sarco-endoplasmic reticulum Ca^{2+}-ATPases (SERCA). Upon platelet activation, inositol trisphosphate (IP_3) is produced, which binds to its receptor (IP_3R) in the endoplasmic reticulum (ER) membrane, then acting as a Ca^{2+} channel to release Ca^{2+} from stores in the ER. This Ca^{2+} store depletion allows STIM (stromal interaction molecule) to interact with the store-regulated Ca^{2+} entry (SOCE) Orai channels.

of surface-exposed phosphatidylserine, although the contribution to the coagulation process has not been assessed. In addition, red blood cells via their ICAM4 receptors can interact with platelet αIIbβ3, which process enhances platelet aggregation via the release of TxA_2 [51-53]. Furthermore, there is evidence that red blood cell-stimulated platelets increase in P-selectin expression and integrin αIIbβ3 activation [54]. Jointly, these pieces of evidence point to additive roles of red blood cells and platelets in blood clotting, but precisely how is unclear.

Reversible platelet aggregation

Under conditions of low-shear flow, platelet aggregation is mediated by integrin αIIbβ3-fibrinogen interactions. At wall-shear rates between 1000 and 10,000 s^{-1}, platelet adhesion initially depends on the interaction of GPIbα with immobilized VWF, after which integrin αIIbβ3 stabilizes the adhesion; unstable platelet aggregates are formed [55]. *In vivo* analyses have shown that the initial platelet aggregates are later stabilized, so that a thrombus with a dense platelet core and an outer shell with loosely connected platelets forms [56]. The core formed at the injury site is fibrin-rich and platelets are P-selectin positive. The loosely packed platelets in the shell are most sensitive to antiplatelet therapies [57,58]. One reason for this is that the autocrine mediators ADP and TxA_2 accumulate here, *i.e.,* the current antithrombotic targets [59].

Based on these *in vivo* and also on *in vitro* findings, the mechanism of platelet integrin activation is considered as an intrinsically reversible process, such as explained in Chapter 2. The vast

majority of signaling receptor agonists induce platelet aggregate formation, but interestingly, under certain conditions this aggregation can be transient. Transiency can occur in response to GPVI or GPCR stimulation, and involve the signaling pathways described, above. However, the exact conditions that lead to platelet activation reversibility, platelet detachment from a thrombus, and thrombus instability are not known.

As a weak agonist, ADP by itself induces platelet shape change and aggregation responses, without granule secretion [60,61]. ADP-stimulated platelets display a relatively small and transient Ca^{2+} signal, involving the two receptors, $P2Y_1$ and $P2Y_{12}$ [62,63]. These mild activation responses make the physiologically relevant ADP to an interesting agonist for examining the overall transiency of platelet activation processes.

Aims and outline of this thesis

This thesis aims to investigate the key signaling pathways that regulate transient platelet activation, and thereby to reveal the versatility of this process in the context of hemostasis and thrombosis. **Chapter 1** provides background knowledge on the structure and function of blood platelets, on relevant signal transduction processes, and on platelets in coagulation. As an overview of the role of platelet integrin αIIbβ3 in reversible platelet aggregation, in **Chapter 2** we review the signaling pathways involved herein, such as described in the literature. We also discuss the agonists and conditions that lead to transient ligand binding to integrin αIIbβ3. In order to determine which signaling pathways are most relevant for the opening and closure of integrin αIIbβ3, in **Chapter 3** we investigate the effects of a selected panel of signal molecule inhibitors on the time-dependent integrin activation processes induced by the collagen receptor, GPVI, and the thrombin protease-activated receptors PAR1 and PAR4. Special attention is placed on the roles of PKC isoforms. Since it is unclear how platelet agonists and the timing of their addition affect the activation process, **Chapter 4** investigates time-dependent effects on platelet aggregation and cytosolic Ca^{2+} elevation in response to the receptors GPVI and PAR1/4. To study if platelets are one-time responding cells, we also examine the responses to a sequential stimulation with agonists. **Chapter 5** describes a study that consistently compares the time-dependent roles of GPVI and PAR1/4 stimulation on extracellular Ca^{2+} entry and intracellular Ca^{2+} mobilization (from Ca^{2+} stores). The work involves parallel cytosolic Ca^{2+} measurements in the presence of either $CaCl_2$ or EGTA, using a 96-wells plate high-throughput assay. Particular attention is paid to the quantitative role of Orai1 Ca^{2+} channels in the Ca^{2+} entry induced by GPVI or PAR1/4 stimulation. In **Chapter 6** the work is continued by studying the impact of various isoforms of PKC on the regulation of Ca^{2+} entry in response to GPVI or PAR1/4 stimulation. Platelets from patients with a mutation in the Orai1 channel are the regulatory protein STIM1 are also examined. In the following **Chapter 7**, we describe a whole-blood fluorogenic assay to elucidate the non-overlapping roles of platelets and red blood cells in whole-blood thrombin generation. **Chapter 8** provides a general discussion of the most important findings of this thesis in relation to the current literature. **Chapter 9** summarizes the thesis results of the research project and lists their potential clinical importance.

References

1. Van der Meijden PE, Heemskerk JW. Platelet biology and functions: new concepts and clinical perspectives. *Nat Rev Cardiol.* **2019**, *16*, 166-179.
2. Ruggeri ZM. The role of von Willebrand factor in thrombus formation. *Thromb. Res.* **2007**, *120*, S5-S9.
3. Estevez B, Du X, New concepts and mechanisms of platelet activation signaling. *Physiology (Bethesda).* **2017**, *32,* 162-177.
4. Siess W. Molecular mechanisms of platelet activation. *Physiol. Rev.* **1989**, *69*, 158-178.
5. Gilio K, Harper MT, Cosemans JM, Konopatskaya O, Munnix IC, Prinzen L, Leitges M, Liu, Q, Molkentin JD, Heemskerk JW. Functional divergence of platelet protein kinase C (PKC) isoforms in thrombus formation on collagen. *J. Biol. Chem.* **2010**, *285*, 23410-23419.
6. Quinton TM, Kim S, Dangelmaier C, Dorsam RT, Jin J, Daniel JL, Kunapuli SP. Protein kinase C-and calcium-regulated pathways independently synergize with Gi pathways in agonist-induced fibrinogen receptor activation. *Biochem. J.* **2002**, *368*, 535-543.
7. Mattheij NJ, Gilio K, van Kruchten R, Jobe SM, Wieschhaus AJ, Chishti AH, Collins P, Heemskerk JW, Cosemans JM. Dual mechanism of integrin αIIbβ3 closure in procoagulant platelets. *J. Biol. Chem.* **2013**, *288*, 13325-13336.
8. Jennings LK. Mechanisms of platelet activation: need for new strategies to protect against platelet-mediated atherothrombosis. *Thromb. Haemost.* **2009**, *102*, 248-257.
9. Zwaal RF, Schroit AJ. Pathophysiologic implications of membrane phospho-lipid asymmetry in blood cells. *Blood.* **1997**, *89*, 1121-1132.
10. Tuteja N. Signaling through G protein coupled receptors. *Plant Sign. Behav.* **2009**, *4*, 942-947.
11. Weis WI, Kobilka BK. The molecular basis of G protein–coupled receptor activation. *Annu. Rev. Biochem.* **2018**, *87*, 897-919.
12. Chandrabalan A, Ramachandran R. Molecular mechanisms regulating proteinase-activated receptors (PARs). *FEBS J.* **2021**, *288*, 2697-2726.
13. De Candia E. Mechanisms of platelet activation by thrombin: a short history. *Thromb. Res.* **2012**, *129*, 250-256.
14. Faruqi TR, Weiss EJ, Shapiro MJ, Huang W, Coughlin SR. Structure-function analysis of protease-activated receptor 4 tethered ligand peptides: determinants of specificity and utility in assays of receptor function. *J. Biol. Chem.* **2000**, *275*, 19728-19734.
15. Gąsecka A, Rogula S, Eyileten C, Postuła M, Jaguszewski MJ, Kochman J, Mazurek T, Nieuwland R, Filipiak KJ. Role of P2Y receptors in platelet extracellular vesicle release. *Int. J. Mol. Sci.* **2020**, *21*, 6065.
16. Hechler B, Gachet C. Purinergic receptors in thrombosis and inflammation. *Arterioscler. Thromb. Vasc. Biol.* **2015,** *35*, 2307-2315.
17. Kim S, Kunapuli SP. $P2Y_{12}$ receptor in platelet activation. *Platelets.* **2011**, *22*, 54-58.
18. Fernández DI, Kuijpers MJ, Heemskerk JW. Platelet calcium signaling by G-protein coupled and ITAM-linked receptors regulating anoctamin-6 and procoagulant activity. *Platelets.* **2021**, *32*, 863-871.
19. Rayes J, Watson SP, Nieswandt B. Functional significance of the platelet immune receptors GPVI and CLEC-2. *J. Clin. Invest.* **2019**, *129*, 12-23.
20. Farndale RW. Collagen-induced platelet activation. *Blood Cells Mol. Dis.* **2006**, *36*, 162-165.

21. Heemskerk JW, Mattheij NJ, Cosemans, JM. Platelet-based coagulation: different populations, different functions. *J. Thromb. Haemost.* **2013**, *11*, 2-16.
22. Munnix IC, Strehl A, Kuijpers MJ, Auger JM, van der Meijden PE, van Zandvoort MA, oude Egbrink MG, Nieswandt B, Heemskerk JW. The glycoprotein VI-phospholipase Cγ2 signaling pathway controls thrombus formation induced by collagen and tissue factor in vitro and in vivo. *Arterioscler. Thromb. Vasc. Biol.* **2005**, *25*, 2673-2678.
23. Kusuyama J, Seong C, Makarewicz NS, Ohnishi T, Shima K, Semba I, Bandow K, Matsuguchi T. Low intensity pulsed ultrasound (LIPUS) maintains osteogenic potency by the increased expression and stability of Nanog through spleen tyrosine kinase (Syk) activation. *Cell. Sign.* **2019**, *62*, 109345.
24. Nieswandt B, Watson SP. Platelet-collagen interaction: is GPVI the central receptor? *Blood.* **2003**, *102,* 449-461.
25. Harbi MH, Smith CW, Nicolson PL, Watson SP, Thomas MR. Novel antiplatelet strategies targeting GPVI, CLEC-2 and tyrosine kinases. *Platelets.* **2021**, *32*, 29-41.
26. Niedergang F, Alcover A, Knight C, Farndale R, Barnes M, Francischetti I, Bon C, Leduc M. Convulxin binding to platelet receptor GPVI: competition with collagen related peptides. *Biochem. Biophys. Res. Commun.* **2000**, *273,* 246-250.
27. Hynes RO. Integrins: bidirectional, allosteric signaling machines. *Cell.* **2002**, *110*, 673-687.
28. Nieswandt B, Varga-Szabo D, Elvers M. Integrins in platelet activation. *J. Thromb. Haemost.* **2009**, *7*, 206-209.
29. Shen B, Delaney MK, Du X. Inside-out, outside-in, and inside-outside-in: G protein signaling in integrin-mediated cell adhesion, spreading, and retraction. *Curr. Opin. Cell Biol.* **2012**, *24*, 600-606.
30. Lavergne M, Janus-Bell E, Schaff M, Gachet C, Mangin PH. Platelet integrins in tumor metastasis: do they represent a therapeutic target? *Cancers.* **2017**, *9*, 133.
31. Kasirer-Friede A, Peuhu E, Ivaska J, Shattil SJ. Platelet SHARPIN regulates platelet adhesion and inflammatory responses through associations with αIIbβ3 and LUBAC. *Blood Adv.* **2022**, *6*, 2595-2607.
32. Bledzka K, Smyth SS, Plow EF. Integrin αIIbβ3. *Circ. Res.* **2013**, *112*, 1189-1200.
33. Durrant TN, van den Bosch MT, Hers I. Integrin αIIbβ3 outside-in signaling. *Blood.* **2017***, 130*, 1607-1619.
34. Obergfell A, Eto K, Mocsai A, Buensuceso C, Moores SL, Brugge JS, Lowell CA, Shattil SJ. Coordinate interactions of Csk, Src, and Syk kinases with αIIbβ3 initiate integrin signaling to the cytoskeleton. *J. Cell Biol.* **2002**, *157,* 265-275.
35. Harper M, Poole A. Diverse functions of protein kinase C isoforms in platelet activation and thrombus formation. *J. Thromb. Haemost.* **2010**, *8*, 454-462.
36. Steinberg SF. Structural basis of protein kinase C isoform function. *Physiol. Rev.* **2008**, *88*, 1341-1378.
37. Strehl A, Munnix IC, Kuijpers MJ, van der Meijden PE, Cosemans JM, Feijge MA, Nieswandt B, Heemskerk JW. Dual role of platelet protein kinase C in thrombus formation: stimulation of pro-aggregatory and suppression of procoagulant activity in platelets. *J. Biol. Chem.* **2007**, *282*, 7046-7055.
38. Strair RK, Schaar D, Goodell L, Aisner J, Chin KV, Eid J, Senzon R, Cui XX, Han ZT, Knox B. Administration of a phorbol ester to patients with hematological malignancies: preliminary results from a phase I clinical trial of 12-O-tetradecanoylphorbol-13-acetate. *Clin. Cancer Res.* **2002**, *8*, 2512-2518.
39. Ringvold HC, Khalil RA. Protein kinase C as regulator of vascular smooth muscle function and potential target in vascular disorders. *Adv. Pharmacol.* **2017**, *78*, 203-301.
40. Gilles P, Voets L, Van Lint J, De Borggraeve WM. Developments in the discovery and design of protein kinase D inhibitors. *Chem. Med. Chem* **2021**, *16*, 2158-2171.

41. Toullec D, Pianetti P, Coste H, Bellevergue P, Grand-Perret T, Ajakane M, Baudet V, Boissin P, Boursier E, Loriolle F. The bisindolylmaleimide GF 109203X is a potent and selective inhibitor of protein kinase C. *J. Biol. Chem.* **1991**, *266*, 15771-15781.
42. Kawano T, Inokuchi J, Eto M, Murata M, Kang JH. Activators and inhibitors of protein kinase C (PKC): their applications in clinical trials. *Pharmaceutics* **2021**, *13*, 1748.
43. Zeng B, Chen GL, Garcia-Vaz E, Bhandari S, Daskoulidou N, Berglund LM, Jiang H, Hallett T, Zhou LP, Huang L. ORAI channels are critical for receptor-mediated endocytosis of albumin. *Nat, Commun.* **2017**, *8*, 1920.
44. Van Kruchten R, Braun A, Feijge MA, Kuijpers MJ, Rivera-Galdos R, Kraft P, Stoll G, Kleinschnitz C, Bevers EM, Nieswandt B, Heemskerk JW. Antithrombotic potential of blockers of store-operated calcium channels in platelets. *Arterioscler. Thromb. Vasc. Biol.* **2012**, *32*, 1717-1723.
45. Kremers R, Peters T, Wagenvoord R, Hemker HC. The balance of pro-and anticoagulant processes underlying thrombin generation. *J. Thromb. Haemost.* **2015**, *13*, 437-447.
46. Binder NB, Depasse F, Mueller J, Wissel T, Schwers S, Germer M, Hermes B, Turecek PL. Clinical use of thrombin generation assays. *J. Thromb. Haemost.* **2021**, *19,* 2918-2929.
47. Wan J, Roberts LN, Hendrix W, Konings J, Ow TW, Rabinowich L, Barbouti O, de Laat B, Arya R, Patel VC. Whole blood thrombin generation profiles of patients with cirrhosis explored with a near patient assay. *J. Thromb. Haemost.* **2020**, *18*, 834-843.
48. Wan J, Konings J, Yan Q, Kelchtermans H, Kremers R, de Laat B, Roest M. A novel assay for studying the involvement of blood cells in whole blood thrombin generation. *J. Thromb. Haemost.* **2020**, *18*, 1291-1301.
49. Wan J, Konings J, de Laat B, Hackeng TM, Roest M. Added value of blood cells in thrombin generation testing. *Thromb. Haemost.* **2021**, *121*, 1574-1587.
50. Hoffman M, Monroe DM. A cell-based model of hemostasis. *Thromb. Haemost.* **2001**, *85*, 958-965.
51. Tombak A. Red blood cells and relation to thrombosis. *Transfusion Med. Sci. Developm.* **2017**, 43-52.
52. Du VX, Huskens D, Maas C, Al Dieri R, de Groot PG, de Laat B. New insights into the role of erythrocytes in thrombus formation. *Semin. Thromb. Hemost.* 2013; *40*, 72-80.
53. Weisel J, Litvinov R. Red blood cells: the forgotten player in hemostasis and thrombosis. *J. Thromb. Haemost.* **2019**, *17,* 271-282.
54. Byrnes JR, Wolberg AS. Red blood cells in thrombosis. *Blood.* **2017**, *130*, 1795-1799.
55. Jackson SP. The growing complexity of platelet aggregation. *Blood.* **2007**, *109*, 5087-5095.
56. Holinstat M, Normal platelet function. *Cancer Metast. Rev.* **2017**, *36*, 195-198.
57. Welsh JD, Muthard RW, Stalker TJ, Taliaferro JP, Diamond SL, Brass LF. A systems approach to hemostasis: 4. How hemostatic thrombi limit the loss of plasma-borne molecules from the microvasculature. *Blood.* **2016**, *127*, 1598-1605.
58. Welsh JD, Stalker TJ, Voronov R, Muthard R, Tomaiuolo M, Diamond SL, Brass LF. A systems approach to hemostasis: 1. The interdependence of thrombus architecture and agonist movements in the gaps between platelets. *Blood.* **2014**, *124*, 1808-1815.
59. Broos K, Feys HB, De Meyer SF, Vanhoorelbeke K, Deckmyn H. Platelets at work in primary hemostasis. *Blood Rev.* **2011**, *25*, 155-167.
60. Ohlmann P, Eckly A, Freund M, Cazenave JP, Offermanns S, Gachet C. ADP induces partial platelet aggregation without shape change and potentiates collagen-induced aggregation in the absence of Gαq. *Blood.* **2000**, *96*, 2134-2139.
61. Gachet C. ADP receptors of platelets and their inhibition. *Thromb. Haemost.* **2001**, *86*, 222-232.

62. Jones S, Evans RJ, Mahaut-Smith MP. Extracellular Ca^{2+} modulates ADP-evoked aggregation through altered agonist degradation: implications for conditions used to study P2Y receptor activation. *Br. J. Haematol.* **2011**, *153*, 83-91.
63. Hechler B, Gachet C. P_2 receptors and platelet function. *Purin. Sign.* **2011**, *7,* 293-303.

Chapter 2

Reversible platelet integrin αIIbβ3 activation and thrombus instability

Jinmi Zou,[1] Frauke Swieringa,[1] Bas de Laat,[1] Philip G. de Groot,[1] Mark Roest[1], Johan W. M. Heemskerk[1]

[1]Synapse Research Institute Maastricht, Koningin Emmaplein 7, 6217 KD Maastricht, The Netherlands

International Journal of Molecular Sciences, 2022, 23(20): 12512.

Abstract

Integrin αIIbβ3 activation is essential for platelet aggregation and, accordingly, for hemostasis and arterial thrombosis. The αIIbβ3 integrin is highly expressed on platelets and requires an activation step for binding to fibrinogen, fibrin or von Willebrand factor (VWF). A current model assumes that the process of integrin activation relies on actomyosin force-dependent molecular changes from a bent-closed and extended-closed to an extended-open conformation. In this paper we review the pathways that point to a functional reversibility of platelet αIIbβ3 activation and transient aggregation. Furthermore, we refer to mouse models indicating that genetic defects that lead to reversible platelet aggregation can also cause instable thrombus formation. We discuss the platelet agonists and signaling pathways that lead to a transient binding of ligands to integrin αIIbβ3. Our analysis points to the (autocrine) ADP $P2Y_1$ and $P2Y_{12}$ receptor signaling via phosphoinositide 3-kinases and Akt as principal pathways linked to reversible integrin activation. Downstream signaling events by protein kinase C, CalDAG-GEFI and Rap1b have not been linked to transient integrin activation. Insight into the functional reversibility of integrin activation pathways will help to better understand the effects of antiplatelet agents.

Keywords: ADP; collagen; fibrinogen; integrin; platelets; thrombin

Molecular concept of integrin activation

Integrin αIIbβ3, previously known as glycoprotein (GP)IIb/IIIa, is preferentially and highly expressed on resting platelets with 60,000–80,000 copies per cell, with additional copies from the open canicular system and granules appearing upon platelet activation [1–3]. The α and β integrin peptide chains typically consist of a large extracellular part, a transmembrane spanning region and a short intracellular tail. The αIIb extracellular part contains an N-terminal β-propeller domain, a thigh domain and two calf domains. The extracellular β3 part is composed of an A domain, a plexin/semaphorin/integrin domain, four epidermal growth factor (EGF) domains and a membrane-proximal β-tail domain. Together, the extracellular αIIb β-propeller and β3 A domains form the integrin head [2,4].

In the early 2000s, the crystal structure was resolved of αvβ3 as a typical integrin [5]. By using electron microscopy, three conformations of the extracellular domains of the structurally similar integrin αIIbβ3 were demonstrated with low, intermediate and high-affinity for its ligands [6,7]. The conformation changes appeared to be accompanied by exposure of activation epitopes, known as ligand-induced binding sites (LIBS) [4,8,9]. Structural analyses suggested that, in the resting state, the membrane-proximal regions of the cytoplasmic α and β tails along with the helixes in the transmembrane regions form a complex, which locks or clasps both integrin chains [6,7]. Agonist-induced integrin activation (described as inside-out signaling) leads to unclasping in an equilibrium-controlled process, suggesting reversibility. In-depth descriptions of these structural changes of integrins are provided elsewhere in excellent reviews [4,10].

Similarly to the integrins of other cell types, the intracellular tails of αIIbβ3 form part of an adhesion complex linked to the actin cytoskeleton, which includes isoforms of kindlin and talin, several small molecule GTP-binding (SMG) proteins and a number of protein kinases [11,12].

The integrin heterodimer with αIIb and β3 subunits resembles other integrins in that the 'unclasping' conformational change is needed for increased ligand binding affinity. It has become clear that in the bent-closed (clasped) and the extended-closed conformations, association of the transmembrane regions of αIIb and β3 hides the extracellular ligand binding site. In the extended open conformation, when the α and β chains unclasp, the ligand-binding MIDAS site (metal ion-dependent adhesion site) becomes exposed [2,3]. Thus, in its activated form αIIbβ3 serves to bind ligands as fibrinogen, fibrin and von Willebrand factor (VWF). In the cytosol, the integrin association with talin-1 and kindlin-2/3 was found to be indispensable for the activated conformational change and the ligand binding [12,13]. Other, less abundant platelet integrins such as α2β1 (collagen receptor) and α6β1 (laminin receptor) may undergo similar conformational changes as a requirement for ligand binding [14,15].

Recently, a general model of mechanical force-dependent integrin activation has been proposed, in which the actomyosin cytoskeleton mechanically pulls and transduces a force via talin-1, and possibly kindlin, to open the resting (bent) integrin conformation, which thereby allows an integrin to bind its ligands [16]. In this model, the bent-closed state is thermodynamically favored, while cytosolic integrin inactivators such as moesin, filamin A and sharpin (all highly expressed in platelets [17]) can destabilize the active integrin structure with or without

mechanical actomyosin forces [16]. A stable ligand binding to the activated integrin conformation is thought to be achieved by avidity-based clustering of multiple integrins [18].

An important implication of this model is that it considers the mechanism of integrin activation as an intrinsically reversible process. In contrast, earlier literature supposed that integrin αIIbβ3 activation in response to agonists is an irreversible event, leading to permanent platelet aggregation and adhesion. Yet, over the years, an increasing number of reports has shown reversibility of the platelet aggregation process. In the present paper, we use the terms 'reversible integrin activation' and 'integrin in-activation' from a functional perspective. Thus, integrin in-activation stands for the secondary inability of αIIbβ3 to bind fibrinogen or antibodies directed at its activated conformation, such as observed in connection to platelet disaggregation. Of note, to which extent the secondary absence of ligand binding is caused by structural reversal of the integrin chains to the bent-closed conformation is unclear.

Indirect support for reversibility of integrin activation comes from in vivo studies by the Philadelphia group, showing that in a microvascular thrombus loosely adhered platelets in the outer shell frequently detach from the thrombus core of densely packed platelets [19]. In the following sections, we discuss the agonists and signaling pathways that result in such reversibility. We explore the conditions that lead to platelet disaggregation, platelet detachment from a thrombus, and thrombus instability. In addition, we mention the relevance of this process for cardiovascular health and disease.

Reversible integrin αIIbβ3 activation and inside-out signaling

For long, integrin αIIbβ3 activation has been considered a hallmark of platelet responsiveness. The activated integrins on adjacent platelets bind with high affinity to the bivalent fibrinogen molecules, which results in the formation of platelet aggregates held together by αIIbβ3-fibrinogen bridges [2]. Under high-shear flow conditions, also the integrin-dependent interaction with VWF can contribute to the aggregate formation [20]. Low-level signaling through the GPIb-V-IX complex can support the binding of fibrinogen to αIIbβ3 and hence platelet aggregation [21].

The vast majority of signaling receptor agonists is capable to induce platelet aggregate formation [22,23]. These include agonists of G-protein coupled receptors (GPCRs), linked to the signal-transmitting Gqα and Giα proteins, and also agonists of immunoreceptor tyrosine-based activation motif (ITAM)-linked receptors (ILRs), such as the collagen receptor glycoprotein VI (GPVI). Accordingly, to mention the best-known ones, human platelet stimulation with epinephrine (via α2A receptors), ADP (via $P2Y_1$ and $P2Y_{12}$ receptors), thromboxane A_2 (TxA_2, via TP receptors), collagen (via GPVI and α2β1) and thrombin (via protease-activated receptors PAR1 and PAR4) all induce integrin αIIbβ3 activation and aggregate formation (**Figure 1**).

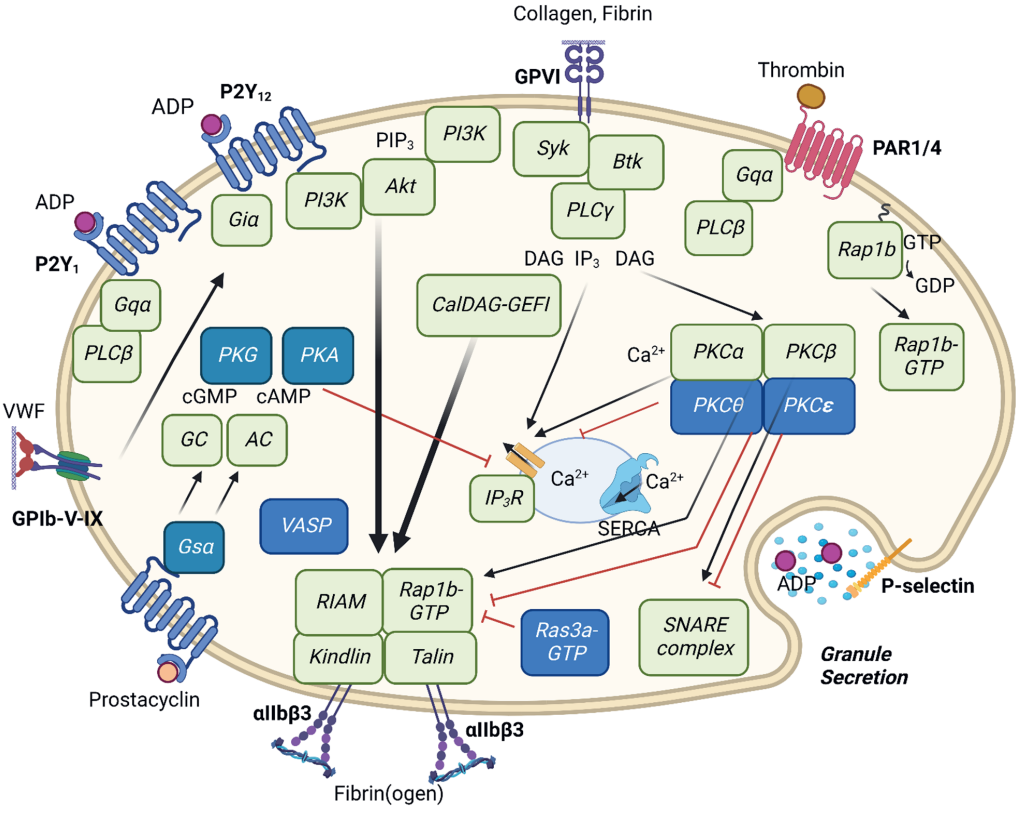

Figure 1. Key signaling pathways in platelets linked to (reversible) integrin activation αIIbβ3 and platelet aggregation. Black arrows show relative strength of activation pathway to integrin activation; red arrows represent inhibitory pathways. In short, the IP receptor for prostacyclin inhibits platelets via adenylyl cyclase (AC), while gaseous nitric oxide inhibits via guanylate cyclase (GC), which are stimuli for protein kinase A (PKA) and protein kinase G (PKG), respectively. Platelet adhesion receptors (integrins and GPIb-V-IX complex) interact with their ligands, such as fibrinogen, fibrin and VWF. The purinoceptors $P2Y_{12}$ and $P2Y_1$ operate following the autocrine release of ADP; $P2Y_{12}$ acts via the G protein Giα, inhibiting AC while stimulating phosphoinositide 3-kinase (PI3K). On the other hand, $P2Y_1$ signals via Gqα which stimulates isoforms of phospholipase C (PLC), causing Ca^{2+} release into the cytoplasm and activation of protein kinase C (PKC). As a strong platelet agonist, thrombin also activates Gqα-coupled receptors, namely PAR1 and PAR4. The collagen receptor GPVI activates a protein tyrosine kinase pathway involving Syk, leading to downstream activation of PLC and PI3K isoforms, the latter stimulating Akt protein kinases. The signaling to high-affinity conformational alterations of αIIbβ3 furthermore involves the small GTPase-regulating proteins CalDAG-GEFI (calcium and diacylglycerol regulated guanine nucleotide exchange factor I), Ras3a and Rap1b. The cytoskeleton-linked signaling is completed by kindlin and talin isoforms.

Whereas the agonist-induced signaling pathways to αIIbβ3 activation (inside-out signaling) are well understood, the subsequent events leading to (ligand-induced) integrin clustering are less clear [13]. Depending on such clustering, patches of ligand-occupied αIIbβ3 integrins can also evoke signaling responses. This is known as integrin outside-in signaling, a process that involves several protein tyrosine kinases as well as signaling adaptors and cytoskeletal components [18]. By convention, outside-in signaling is required for the spreading of platelets on a fibrinogen surface and for the contraction of a fibrin clot. It is likely, but not definitively proven, that outside-in signaling contributes to the stabilization of platelet aggregates and formed thrombi [24,25].

Below we provide a comprehensive overview on the signaling actions triggered via GPCRs or ILRs that link to reversible or transient activation of integrin αIIbβ3 and to platelet disaggregation. Herein, we focus on specific receptors, downstream signaling components, protein phosphorylations and the release of secondary mediators.

ADP receptor stimulation

The two platelet receptors for ADP, i.e., $P2Y_1$ (gene *P2RY1*) linked to Gqα, and $P2Y_{12}$ (*P2RY12*) linked to Giα [26], are both required for the full induction of platelet aggregation, such as monitored by light transmission aggregometry [27,28]. Upon ADP stimulation, P2Y1 induces a signaling route to phospholipase Cβ (PLCβ) and protein kinase C (PKC); whereas $P2Y_{12}$ causes inhibition of adenylate cyclase and activation of phosphoinositide 3-kinase (PI3K) isoforms (Figure 1) [29].

Several reports indicate that the platelet aggregation induced by ADP (as a 'weak' agonist) is particularly sensitive to disaggregation (**Table 1**). Several drugs have been described that secondarily reverse the aggregation with ADP, in particular the αIIbβ3 antagonists (abciximab, lamifiban, SR121566, tirofiban) [30,31]. These drug effects suppose that the agonist-induced binding of fibrinogen to αIIbβ3 is reversible, in a way that integrin antagonists can compete with the ligand. Under both static and flow conditions, it has indeed been shown that integrin inhibitors compete with fibrinogen and thereby reverse platelet aggregation [32,33].

Other well-studied aggregation-reversing agents are blockers of the $P2Y_1$ or $P2Y_{12}$ receptors and the enzyme apyrase, which degrades ADP. Flow cytometric evidence has shown that, following ADP-induced αIIbβ3 activation (measured as FITC-PAC1 mAb binding to platelets), the subsequent blockage of $P2Y_1$ or $P2Y_{12}$ receptors or later ADP removal resulted in a lower extent of αIIbβ3 ligand binding [31,34]. Similarly, in platelets from patients with a defect in $P2Y_{12}$ receptors, often a reversible ADP-induced aggregation is observed, even at high ADP concentrations above 10 μM [28]. The same holds for patients who are treated with $P2Y_{12}$ receptor blockers. Accordingly, platelet activation via both ADP receptors appears to be required for a persistent aggregation response, such as has been concluded earlier [35].

Another way to downregulate ADP-induced platelet responses is via ecto-nucleotidases such as CD39, which hydrolyzes ATP and ADP into AMP and adenosine [36]. In an elegant approach to make use of ecto-nucleotidases, recombinant CD39 was fused with a single chain antibody

Table 1. Drugs/interventions reported to reverse human platelet aggregation in response to given agonists.

Agonist	Reversing inhibitor	Reversing pathway	Reference
ADP	tirofiban, abciximab	αIIbβ3 antagonism	[30]
ADP	SR121566	αIIbβ3 antagonism	[115]
ADP	Gas6 depletion	TAM antagonism	[116]
ADP	citrated PRP plus $CaCl_2$	Ca^{2+}/Mg^{2+} replacement	[117]
ADP, shear	lamifiban	αIIbβ3 antagonism	[118]
ADP, collagen	ticagrelor	$P2Y_{12}$ antagonism	[31,119]
ADP, collagen	TGX-221, wortmannin	PI3K antagonism	[31]
ADP, collagen	iloprost	cAMP elevation	[31]
ADP, TRAP6	aCD62P	P-selectin blockage	[120]
TRAP6	iloprost (+ tirofiban)	cAMP elevation	[110]
PAR1p	wortmannin	PI3K antagonism	[121]
PAR4p	2-MeSADP	P2Y antagonism	[86]

Abbreviations: TAM, Tyro, Axl and Mer receptors; PAR1p, PAR1 activating peptide.

fragment recognizing the activated αIIbβ3, named Targ-CD39 [37]. This allowed the CD39 to only hydrolyze the ADP that is released from activated and aggregated platelets in a thrombus. In a mouse model of cardiac ischemia/reperfusion, the platelet-binding Targ-CD39 construct caused protection of the reperfused tissue [38].

Other drugs that secondarily reverse the ADP-induced platelet aggregation and αIIbβ3 activation appeared to be blocking agents of PI3Kβ [31], which confirms the key role of the PI3K pathway downstream of $P2Y_{12}$. Furthermore, secondary platelet inhibition with iloprost or the replacement of Mg^{2+} by Ca^{2+} (affecting the integrin MIDAS domains) were found to reverse the ADP-induced platelet aggregation (**Table 1**). The observations that $P2Y_1$ and $P2Y_{12}$ blocking as well as PI3K inhibition leads to disaggregation implies that both the Gqα and Giα signaling pathways are required for a persistent functional integrin activation and ligand binding. This might imply a transiency of the actomyosin force-dependent conformation change of integrins, although this has not yet been proven.

Collagen GPVI receptor stimulation

Platelet stimulation with collagen or collagen-related peptides induces a signaling pathway via GPVI and the ITAM-linked FcR g-chain, involving protein tyrosine kinases like Src, Syk and Btk [23,29]. As a result, PLCγ and PKC isoforms become activated as well as PI3K isoforms [39,40]. A noticeable aspect of the platelet aggregation with lower doses of collagen is that it relies on

release of the autocrine mediators, ADP and TxA_2 [22]. This can explain why the secondary inhibition of either αIIbβ3, $P2Y_{12}$ or PI3K can cause reversion of a collagen-induced platelet aggregation response (**Table 1**). In agreement with this, in microfluidics tests where whole blood is flowed over collagen, the inhibition of autocrine mediators appeared to suppress the thrombus formation and to cause disaggregation of platelets from the formed thrombi [41].

A comparison of the roles of human and mouse GPVI in platelet aggregation and thrombus stability indicated that especially the blockage of human platelet GPVI led to disaggregation [42]. In mice, most markedly a deficiency in integrin β3 led to a transient collagen-mediated platelet aggregation and an unstable thrombus formation [43].

Thrombin PAR1 and PAR4 receptor stimulation

Thrombin activates human platelets via cleavage of the GPCRs, PAR1 and PAR4, both of which receptors are coupled to Gqα and accordingly induce a common signaling route to PLCβ and PKC stimulation (**Figure 1**) [26,29]. Both receptors are cleaved at the N-terminus to uncover a so-called tethered ligand. The ligand peptide sequence of PAR1 consists of the sequence of SFLLRN, which as a hexapeptide (thrombin receptor-activating peptide: TRAP6) can also activate the receptor; for PAR4 the corresponding sequence consists of AYPGKF. Human platelet activation by TRAP6 via the PAR1 receptor results in granule release and in αIIbβ3 activation, of which the latter process has been shown to be reversible (**Table 1**). On the other hand, this reversibility has not been reported for the PAR4 peptide AYPGKF or for thrombin.

In hemostasis and thrombosis, the generation of thrombin is in part triggered by vascular-exposed tissue factor. Kinetic studies with flowed blood have shown that the role of tissue factor in platelet aggregation and thrombus formation is only short-term [44]. Interestingly, one report states that this role of tissue factor can depend on factor VII activating protein (FSAP, gene *HAPP2*). Deletion of the Happ2 gene in mouse appeared to reduce the thrombus-forming process, but did not cause thrombus instability [45]. As described below, the initial role of tissue factor in thrombin generation can be taken over by procoagulant platelets, exposing phosphatidyl-serine [22].

Integrin αIIbβ3 regulation by other extracellular proteases

A variety of proteases present in the blood plasma and in the platelet cytosol are involved in the sustained integrin αIIbβ3 activation and platelet aggregation. The majority of proteases must first be activated for instance by proteolysis, as in the case of thrombin (generated from prothrombin) and plasmin (from plasminogen) [22,46].

Regarding persistent αIIbβ3 activation, a still incompletely understood role is played by the family of zinc-dependent matrix metalloproteinases (MMP) [47]. The isoforms MMP1, 2, 9, 12, 13 and 14 are all known to modulate the platelet activation processes [46]. Both MMP1 and MMP9 enhance platelet aggregation induced by collagen under flow [48,49]. The mechanism may rely on a proteolytic cleavage of PAR1 or other receptors [46]. Additionally, the isoform

MMP2 primes for platelet activation [50], which is also the case for MMP12 [51]. The membrane-bound isoform MMP14 may induce platelet responses by a cleavage of pro-MMP2 and pro-MMP13 [52].

Integrin αIIbβ3 regulation via protease-dependent receptor cleavage

Receptor cleavage is another way to regulate integrin activation. An example is provided by the platelet-expressed proteases ADAM10 and ADAM17 (for: a disintegrin and metalloprotease), which function as sheddases for the extracellular domains of GPVI (ADAM10) and GPIbα (ADAM17) [53,54]. It has appeared that the ADAM-induced receptor cleavages are prominent in highly activated platelets, which can provide another mechanism to abrogate the aggregation response [55].

In highly activated platelets, *i.e.*, by thrombin plus collagen stimulation, prolonged and high cytosolic Ca^{2+} rises lead to opening of anoctamin-6, which is a phospholipid and ion channel, and thereby to the surface exposure of procoagulant phosphatidylserine, which promotes the assembly of coagulation factor complexes [22]. Accompanying the procoagulant response is the Ca^{2+}-dependent prolonged activation of calpains, leading to cleavage of the intracellular domain of integrin β3 [56], as well as of several proteins that are required for integrin activation (Src, filamin-A, talin-1, kindlin-3) [57]. Accordingly, in the highly activated platelets, αIIbβ3 becomes inactivated (abolishment of PAC1 mAb binding) and the aggregation response is blocked [56,58]. Uncontrolled calpain activation thus provides another pathway for functionally switching off αIIbβ3 integrins [34].

Reversible integrin activation and thrombus instability

An accepted model of murine (microvascular) thrombus formation describes the thrombus architecture as composed of an inner core with highly activated and contracted platelets, which is surrounded by a shell region with low-activation, loosely and transiently adhered platelets [59]. This heterogeneity has been explained by a different exposure of platelets to agonists like collagen, thrombin, ADP and TxA_2 together with differences in shear forces. In the core region, tissue-factor induced thrombin generation contributes to a PAR- and fibrin-dependent platelet contraction. On the other hand, the second mediators ADP and TxA_2 will act as main platelet agonists in the shell region, in which the outflow of mediators restricts the agonist concentrations [59,60].

Another form of heterogeneity has been observed in thrombi generated on collagen under flow conditions. Here, patches of aggregated platelets are formed, staining for fibrinogen, and separated from these single, balloon-shaped platelets with phosphatidylserine exposure and not binding fibrinogen [61]. It has been argued that the integrin inactivation of those platelets helps to stimulate the coagulation process [46].

Whole-blood flow chamber experiments have further shown that the platelets which disaggregate from a preformed thrombus lose their ability to bind fibrinogen and hence

inactivate their integrins [31]. In terms of thrombus formation, the reversibility of (ADP induced) platelet integrin activation likely contributes to events as thrombus instability and dissolution. However, it needs to be stated that, *in vivo*, also other processes will be involved in thrombus instability, such as local high shear forces, fibrinolysis and other proteolytic activities in an occluding artery. To which extent reversible integrin activation is important in arterial thrombosis still needs to be determined.

In mice, a deficiency of either $P2Y_1$ or $P2Y_{12}$ was found to affect arterial thrombus formation *in vivo*, and also caused instability of thrombi that still formed (**Table 2**) [62–64]. The same applied to the infusion of $P2Y_{12}$ antagonist, ticagrelor [65]. That $P2Y_{12}$ receptors have a thrombus-stabilizing role was also concluded from *in vivo* studies with *Apoe*$^{-/-}$ mice, where plaque-induced thrombus formation and stability were impaired upon receptor blockage [66]. Additionally, in mouse models, application of a reversible $P2Y_{12}$ antagonist was found to dissolve the preformed platelet thrombi [67]. Together these findings point to major roles of the two platelet ADP receptors in stable arterial thrombus formation. Although the extent of activation of αIIbβ3 cannot be followed in the *in vivo* conditions, functional reversibility of the integrin activation is a reasonable explanation of the results.

Integrin αIIbβ3 regulation by intracellular signaling molecules

Several signaling pathways are at the center of platelet integrin activation regulation, and for some of these there is evidence for reversibility.

PLC and PKC isoforms

Stimulation of GPCR-dependent (via Gqα) and ILR-dependent (via Syk) signaling routes leads to activation of isoforms of PLCβ/γ and PKC, which are essential components in platelet responses like granule secretion, integrin activation and platelet aggregation [22]. The isoforms of PKC are broad-spectrum protein kinases, of which in particular PKCα, PKCε and PKCθ have been studied in platelets [68,69]. The platelets from PKCα-deficient mice are strongly impaired in aggregation and thrombus formation [70], which leads to the conclusion that PKCα is an essential protein kinase for achieving integrin αIIbβ3 activation, such as for example induced by phorbol esters. On the other hand, in mice lacking PKCε or PKCθ, platelet aggregation and thrombus formation were increased under certain conditions (**Table 2**) [71–73].

PI3K isoforms

Enzymes of the PI3K family phosphorylate phosphoinositide lipids at the 30 position of the inositol ring, in particular to produce phosphatidylinositol 1,4,5-trisphosphate (PIP_3). Well studied in relation to platelet integrin activation are the class-I isoforms PI3K α, β and δ [74]. Upon PI3K activity, the produced PIP_3 attracts key signaling proteins with so-called pleckstrin

Table 2. Selection of genetic defects in mouse resulting altered arterial thrombus formation whether or not accompanied by platelet disaggregation or embolization *in vivo* or *in vitro*.

Gene defect	Protein defect	Thrombus formation	Disaggregation or embolization	References
Akt1	protein kinase Akt1	↓	no	[77,80,81,122]
Akt2	protein kinase Akt2	↓	**yes**	[78]
Akt3	protein kinase Akt3	↓	**yes**	[79]
Arhgef10	GEF Rho-GEF10	↓↓	**yes**	[96]
Cd18	integrin β2 (CD18)	↓	no	[123]
Gp6	GPVI receptor	↓	no (human **yes**)	[42]
Happ2	factor VII activating (FSAP)	↓	**yes**	[45]
Itga2	integrin α2	0 or ↓	no	[124-126]
Itga2b	integrin αIIb	↓↓	no	[127]
Itga6	integrin α6	↓↓	no	[128]
Itgb1	integrin β1	↓	**yes**	[129-131]
Itgb3	integrin β3	↓↓	**yes**	[43]
P2ry1	$P2Y_1$ receptor	↓↓	**yes**	[62,63]
P2ry12	$P2Y_{12}$ receptor	↓↓	**yes**	[62,64,66,67,132]
Pik3ca	PI3K alpha	↓	no	[133]
Pik3cb	PI3K beta	↓↓	**yes** (U46619)	[134]
Pik3cg	PI3K gamma	↓↓	**yes** (ADP)	[31,135]
Prkca	PKC alpha	↓↓	no	[70]
Prkcd	PKC delta	0	no	[73,136]
Prkce	PKC epsilon	↑	no	[71]
Prkcq	PKC theta	↓ or ↑	no	[72,73,137,138]
Rasa3	GAP Rasa3	↑	no	[95]
Rasgrp2	GEF CalDAG-GEFI	↓↓	no	[132,139]
Rap1b	GTPase Rap1b	↓↓	no	[90]
Rhoa	GTPase RhoA	↓↓	no	[98]
Rras2	TC21/RRas	↓	**yes**	[99]
Tln1	talin 1	↓↓	no	[11,84]
Treml1	TLT-1	↓	no	[140]
Vasp	VASP protein	0	no	[103]

Abbreviations: GAP, GTPase activating protein; GEF, GTP exchange factor; further, see text.

homology (PH) domains to the membrane. Earlier studies have indicated that the activity of PI3K isoforms is required for a perpetuated integrin activation [75,76]. Pharmacological analysis indicated non-redundant roles of PI3Kα and PI3Kβ in the GPVI-induced platelet activation and thrombus formation, in particular by contributing to Rap1b activation [40]. Furthermore, a post-treatment of collagen- or ADP-induced platelet aggregates with the PI3Kβ inhibitor TGX-221 appeared to result in immediate disaggregation and reversal of the binding of fibrinogen or PAC1 mAb to integrin αIIbβ3 (**Table 1**). Additionally, murine deficiency in either PI3Kα or PI3Kβ led to smaller sized arterial thrombi and to reversible platelet aggregation responses (**Table 2**).

Akt isoforms

Protein kinases of the Akt family (alternatively named protein kinase B) provide major PIP_3-binding proteins in the PI3K signaling cascade (**Figure 1**). From both in vivo and in vitro studies, it appeared that in mouse platelets the three isoforms Akt1, Akt2 and Akt3 contribute all to aggregate formation and thrombus stability (**Table 2**) [77–79]. In particular the deficiency of Akt1 resulted in an impaired collagen-induced platelet aggregation [77,80,81]. On the hand, murine deficiency in either Akt2 or Akt3 led to a disaggregation of platelets after stimulation with (low doses of) ADP- or thrombin-receptor agonists [78,79]. Summarizing this places the PI3K-Akt pathway as an controlling route for (persistent) platelet aggregation.

Small GTPases and integrin regulation

Platelets contain almost 500 small GTP-binding proteins and regulators [17]. These include effector GTP-binding proteins, activating guanine nucleotide exchange factors (GEF), and signal-abrogating GTPase-activating proteins (GAP). Several of these proteins are considered to be crucial for integrin αIIbβ3 activation and can be linked to functional integrin reversibility. Relevant are: *(a)* Rap1b; *(b)* its activator CalDAG-GEFI (calcium and diacylglycerol regulated guanine nucleotide exchange factor I; gene RASGRP2); *(c)* Rasa3 as a Rap1b-inactivating GAP; *(d)* the protein ARHGEF10; *(e)* the small GTPase RhoA; and *(f)* TC21/RRas (*RRAS2* gene).

Rap1b undergoes a GDP for GTP switch in response to essentially all platelet agonists, resulting in its active, GTP-bound state [82,83]. The GTP-bound Rap1b is known to support αIIbβ3 activation through RIAM (Rap1-interacting adaptor molecule), which facilitates the integrin interaction with talin and kindlin on the plasma membrane [12,84]. Depending on the type of platelet trigger, Rap1b can be activated via two signaling pathways, one via a Ca^{2+}-dependent CalDAG-GEFI activation route, and also via another slower but sustained PKC route [85–87]. The second route may require ADP co-stimulation via $P2Y_{12}$ and PI3K [88,89]. In mouse, Rap1b deficiency caused strong defects in integrin inside-out and outside-in signaling [90,91], as well as in TxA_2 release and granule secretion [91,92]. So far, there is no evidence for a particular role of Rap1b in aggregate stabilization, although its role in arterial thrombosis is clear [90].

CalDAG-GEFI, as a main Rap1b activator, becomes active via agonist-induced rises in cytosolic Ca^{2+}. The protein has a low-affinity binding site for diacylglycerol, which makes a regulation via

physiological levels of diacylglycerol unlikely [93]. CalDAG-GEFI has been identified as a rapid and reversible control switch for integrin αIIbβ3 activation. In human, a loss-of-function mutation resulted in aberrant platelet aggregation that was associated with bleeding. Supporting evidence for such a role of CalDAG-GEFI comes from *Rasgrp2* knockout mice. Platelets from these mice were severely hampered in their ability to aggregate with multiple agonists, and to contribute to arterial thrombus formation [85,94]. No thrombus instability has been reported, such in contrast to $P2Y_{12}$ inhibition (**Table 2**). An alternative, CalDAG-GEFI-independent route to integrin activation is provided by the slower diacylglycerol and PKC-dependent route [86].

Ras3a has been identified in platelets as key deactivator of Rap1b, catalyzing the hydrolysis of Rap1b-GTP to GDP [95]. Platelets from mice with a mutant Rasa3 form appeared to be hyperactive, suggesting that this protein keeps the circulating platelets in a quiescent state by restraining the CalDAG-GEFI and Rap1b signals [95]. It is suggested that $P2Y_{12}$ signaling (via PI3K) results in Rasa3 inhibition, which further enables Rap1b-dependent platelet aggregation and thrombus formation. Autocrine released ADP indeed is a potent enforcer of platelet aggregation via $P2Y_{12}$ receptors [29].

In mice lacking platelet **ARHGEF10**, platelet stimulation via ILRs or GPCRs resulted in aggregation responses which gradually declined. *In vivo* experiments pointed to an unstable arterial thrombus development and a longer tail bleeding time [96]. Mechanistically, ARHGEF10 is considered to regulate the activation of RhoA.

RhoA is known to have a role in αIIbβ3-induced outside-in signaling, and hence supports platelet spreading, cytoskeletal reorganization and clot retraction [97]. In mouse, megakaryocyte/platelet-specific RhoA deficiency thus led to impaired platelet activation responses [98].

TC21/RRas is required for full GPVI-induced platelet responses, up to now according to one paper. The reported impairments include tyrosine phosphorylation, integrin activation and secretion, as well as thrombus instability *in vivo*, as established in deficient mice [99]. Evidence is also provided that this small GTP-binding protein can control the activation of Rap 1b.

Platelet inhibition by protein kinases A and G

Two endothelial-derived mediators*, i.e.*, prostacyclin and nitric oxide, antagonize most platelet responses, including integrin αIIbβ3 activation and aggregate formation [29]. Prostacyclin acts via binding to a GPCR linked to Gsα, which stimulates adenylate cyclase to produce cAMP. This second messenger triggers the broad spectrum Ser/Thr protein kinase A (PKA) [100]. Nitric oxide diffuses across the platelet membrane, and directly stimulates guanylate cyclase to form cGMP, which activates protein kinase G (PKG) (**Figure 1**). Via stimulation of PKA and PKG a large number of proteins becomes phosphorylated, which thereby ensures a multi-targeted way of platelet inhibition, including proteins linked to integrin activation [101].

A particular phosphorylation substrate of both PKA and PKG, related to platelet inhibition, is vasodilator-stimulated phosphoprotein (VASP), which regulates the actin cytoskeletal dynamics [102]. In VASP-null platelets, it was observed that the cAMP- and cGMP-dependent inhibition of platelet aggregation was abolished, but not the secretion response [103]. In wild-type mice, VASP can form a complex that regulates Rap1b inhibition [104]. Of clinical interest, VASP phosphorylation at Ser239 is a standard method to establish PKA- and $P2Y_{12}$-dependent phosphorylation events [105]. Both prostacyclin and nitric oxide can suppress the agonist-induced activation of Rap1b [82,106].

The two platelet-inhibitory PKA and PKG pathways are halted by a negative feedback loop of cAMP and cGMP hydrolysis through cyclic nucleotide phosphodiesterases (PDE). Of these, PDE2 and PDE3 mainly lower cAMP levels, while PDE5 lowers cGMP [107]. The feedback pathway plays a role upon platelet stimulation through the Giα-coupled receptor $P2Y_{12}$, which leads to inhibition of adenylate cyclase and cAMP can no longer rise [108]. Additionally, the activity of PDE3 is increased upon thrombin stimulation [109].

The importance of PKA in suppressing platelet aggregation activation becomes clear from the fact that the secondary application of iloprost (a prostacyclin analogue) can reverse the integrin activation in response to multiple agonists (**Table 1**) [110]. In addition, gain-of-function mutations in the Gsα protein lead to elevated platelet cAMP levels, lower aggregate formation and a bleeding phenotype [111], whereas loss-of-function mutations leads to an impaired platelet inhibition with iloprost [100].

Concluding remarks and relevance

Overviewing the molecular signaling events that link to a reversible integrin αIIbβ3 activation, these are especially related to the ADP receptor pathways, including the conditions in which ADP acts as an autocrine mediator. The signaling alone via $P2Y_1$ or $P2Y_{12}$ receptors shows a certain transiency, leading to a transient way of integrin binding to its ligands. One can tentatively conclude that, to assure permanent integrin activation, the continued presence of ADP is essential acting via both P2Y receptors. Downstream of these receptors, especially the signaling via PI3K and Akt isoforms ensures irreversibility of the platelet aggregation process. In addition, the reversibility of collagen-induced (via GPVI) and TRAP6-induced (via PAR1) integrin activation can be linked to a transient PI3K activity and/or transient P2Y receptor functions. So far, there is no evidence for reversibility due to low PKC, CalDAG-GEFI or Rap1b activities, thus suggesting that the switch for a reversible offset of integrin αIIbβ3 ligand binding resides early in the signaling cascade.

From a (patho)physiological perspective, thrombus consolidation is a final stage of hemostatic plug formation. Platelet exposure to 'strong' agonists, like collagen and thrombin, appears to be required for such consolidation. The 'weaker' agonist ADP appears to extend and also restrict the initiating roles of collagen and thrombin, *e.g.*, by forming the 'loose' outer shell of an intravascular thrombus. The fact that at least part of these ADP effects – in terms of integrin activation and platelet aggregation – are reversible may explain the success of anti-$P2Y_{12}$ drugs

in thrombus suppression and possibly reversion. At the same time, realizing this, it is not a surprise that clinically used $P2Y_{12}$ antagonists have bleeding as a side effect. Improved insight into the transiency of integrin-dependent molecular pathways may thus help to better understand the (patho)physiology of hemostasis and thrombosis.

In this respect, the high αIIbβ3 expression and platelet activation recently observed in diabetic patients [112,113] may point to a shifted equilibrium in the ability to integrin ligand binding. It has been demonstrated that in diabetic platelets the force-induced integrin αIIbβ3 activation increases in a PI3K-dependent way, which resulted in an exaggerated shear-dependent platelet adhesion [114].

Author Contributions: J.Z., F.S. and J.W.M.H. conceptualized and wrote the manuscript. B.d.L., P.G.d.G. and M.R. edited the manuscript. All authors have read and agreed to the published version of the manuscript.

Funding: J.Z. is supported by the China Scholarship Council (201909370052).

Institutional Review Board Statement: This study does not contain previously unpublished data on patients, healthy subjects, or animals.

Data Availability Statement: This review does not contain novel, unpublished data.

Conflicts of Interest: J.Z., B.d.L. and M.R. are employees of Synapse Research Institute Maastricht. P.G.d.G. and J.W.M.H. are consultants at Synapse Research Institute Maastricht. The funders had no role in the design of the study; in the collection, analyses, or interpretation of data; in the writing of the manuscript, or in the decision to publish the results.

References

1. Hynes RO. Integrins: bidirectional, allosteric signaling machines. *Cell* **2002**, *110*, 673-687.
2. Plow EF, Pesho MM, Ma YQ. Integrin αIIbβ3. *In: Platelets (Michelson AD, ed.) Academic Press, Amsterdam* **2007**, 165-178.
3. Coller BS, Shattil SJ. The GPIIb/IIIa (integrin αIIbβ3) odyssey: a technology-driven saga of a receptor with twists, turns, and even a bend. *Blood. 2***008**, *112*, 3011-3025.
4. Luo BH, Carman CV, Springer TA. Structural basis of integrin regulation and signaling. *Annu. Rev Immunol.* **2007**, *25*, 619.
5. Xiong JP, Stehle T, Diefenbach B, Zhang R, Dunker R, Scott DL, Joachimiak A, Goodman SL, Arnaout MA. Crystal structure of the extracellular segment of integrin αvβ3. *Science* **2001**, *294*, 339-345.

6. Adair BD, Yeager M. Three-dimensional model of the human platelet integrin αIIbβ3 based on electron cryomicroscopy and x-ray crystallography. *Proc. Natl. Acad. Sci. USA* **2002**, *99*, 14059-14064.
7. Gottschalk KE. A coiled-coil structure of the αIIbβ3 integrin transmembrane and cytoplasmic domains in its resting state. *Structure.* **2005**, *13*, 703-712.
8. Vinogradova O, Velyvis A, Velyviene A, Hu B, Haas TA, Plow EF, Qin J. A structural mechanism of integrin αIIbβ3 inside-out activation as regulated by its cytoplasmic face. *Cell.* **2002**, *110*, 587-597.
9. Han J, Lim CJ, Watanabe N, Soriani A, Ratnikov B, Calderwood DA, Puzon-McLaughlin W, Lafuente EM, Boussiotis VA, Shattil SJ. Reconstructing and deconstructing agonist-induced activation of integrin αIIbβ3. *Curr. Biol.* **2006**, *16*, 1796-1806.
10. Arnaout MA, Goodman SL, Xiong JP. Structure and mechanics of integrin-based cell adhesion. *Curr. Opin. Cell Biol.* **2007**, *19*, 495-507.
11. Petrich BG, Marchese P, Ruggeri ZM, Spiess S, Weichert RA, Ye F, Tiedt R, Skoda RC, Monkley SJ, Critchley DR. Talin is required for integrin-mediated platelet function in hemostasis and thrombosis. *J. Exp. Med.* **2007**, *204*, 3103-3111.
12. Lagarrigue F, Kim C, Ginsberg MH. The Rap1-RIAM-talin axis of integrin activation and blood cell function. *Blood. 2***016**, *128*, 479-487.
13. Huang J, Li X, Shi X, Zhu M, Wang J, Huang S, Huang X, Wang H, Li L, Deng H, et al. Platelet integrin αIIbβ3: signal transduction, regulation, and its therapeutic targeting. *J. Hematol. Oncol.* **2019**, *12*, 26.
14. Emsley J, Knight CG, Farndale RW, Barnes MJ, Liddington RC. Structural basis of collagen recognition by integrin α2β1. *Cell.* **2000**, *101*, 47-56.
15. Nuyttens BP, Thijs T, Deckmyn H, Broos K. Platelet adhesion to collagen. *Thromb. Res.* **2011**, *127*, S26-29.
16. Sun Z, Costell M, Fassler R. Integrin activation by talin, kindlin and mechanical forces. *Nat. Cell. Biol.* **2019**, *21*, 25-31.
17. Huang J, Swieringa F, Solari FA, Provenzale I, Grassi L, De Simone I, Baaten CC, Cavill R, Sickmann A, Frontini M, et al. Assessment of a complete and classified platelet proteome from genome-wide transcripts of human platelets and megakaryocytes covering platelet functions. *Sci. Rep.* **2021**, *11*, 12358.
18. Durrant TN, van den Bosch MT, Hers I. Integrin αIIbβ3 outside-in signaling. *Blood.* **2017**, *130*, 1607-1619.
19. Welsh JD, Stalker TJ, Voronov R, Muthard RW, Tomaiuolo M, Diamond SL, Brass LF. A systems approach to hemostasis: 1. The interdependence of thrombus architecture and agonist movements in the gaps between platelets. *Blood.* **2014**, *124*, 1808-1815.
20. Hrdinova J, Fernández DI, Ercig B, Tullemans BM, Suylen DP, Agten SM, Jurk K, Hackeng TM, Vanhoorelbeke K, Voorberg J, et al. Structure-based cyclic glycoprotein Ibα-derived peptides interfering with von Willebrand factor binding affecting platelet aggregation under shear. *Int. J. Mol. Sci.* **2022**, *23*, 2046.
21. Kasirer-Friede, A, Cozzi MR, Mazzucato M, De Marco L, Ruggeri ZM, Shattil SJ. Signaling through GP Ib-IX-V activates αIIbβ3 independently of other receptors. *Blood.* **2004**, *103*, 3403-3411.
22. Versteeg HH, Heemskerk, JW, Levi M, Reitsma PS. New fundamentals in hemostasis. *Physiol. Rev.* **2013**, *93*, 327-358.
23. Fernandez DI, Kuijpers MJ, Heemskerk JW. Platelet calcium signaling by G-protein coupled and ITAM-linked receptors regulating anoctamin-6 and procoagulant activity. *Platelets.* **2021**, *32*, 863-871.
24. Van der Meijden PE, Feijge MA, Swieringa F, Gilio K, Nergiz-Unal R, Hamulyak K, Heemskerk J.W. Key role of integrin αIIbβ3 signaling to Syk kinase in tissue factor-induced thrombin generation. *Cell. Mol. Life Sci.* **2012**, *69*, 3481-3492.

25. Dai B, Wu P, Xue F, Yang R, Yu Z, Dai K, Ruan C, Liu G, Newman PJ, Gao C. Integrin-αIIbβ3-mediated outside-in signaling activates a negative feedback pathway to suppress platelet activation. *Thromb. Haemost.* **2016**, *116*, 918-930.
26. Offermanns S. Activation of platelet function through G protein-coupled receptors. *Circ. Res.* **2006**, *99*, 1293-1304.
27. Eckly A, Gendrault JL, Hechler B, Ceazenave JP, Gachet C. Differential involvement of the $P2Y_1$ and $P2Y_t$ receptors in the morphological changes of platelet aggregation. *Thromb. Haemost.* **2001**, *85*, 694-701.
28. Cattaneo M. The platelet $P2Y_{12}$ receptor for adenosine diphosphate: congenital and drug-induced defects. *Blood.* **2011**, *117*, 2102-2012.
29. Van der Meijden PE, Heemskerk JW. Platelet biology and functions: new concepts and future clinical perspectives *Nat. Rev. Cardiol.* **2019**, *16*, 166-179.
30. Moser M, Bertram U, Peter K, Bode C, Ruef J. Abciximab, eptifibatide, and tirofiban exhibit dose-dependent potencies to dissolve platelet aggregates. *J. Cardiovasc. Pharmacol.* **2003**, *41*, 586-592.
31. Cosemans JM, Munnix IC, Wetzker R, Heller R, Jackson SP, Heemskerk JW. Continuous signaling via PI3K isoforms β and γ is required for platelet ADP receptor function in dynamic thrombus stabilization. *Blood. 2***006**, *108*, 3045-3052.
32. Li YF, Spencer FA, Becker RC. Comparative efficacy of fibrinogen and platelet supplementation on the in vitro reversibility of competitive glycoprotein IIb/IIIa receptor-directed platelet inhibition. *Am. Heart J.* **2002**, *143*, 725-732.
33. Bärnthaler T, Mahla E, Toth GG, Schuligoi R, Prüller F, Buschmann E, Heinemann A. Supplemental fibrinogen restores platelet inhibitor-induced reduction in thrombus formation without altering platelet function: an in vitro study. *Thromb. Haemost.* **2020**, *120*, 1548-1556.
34. Cosemans JM, Iserbyt BF, Deckmyn H, Heemskerk JW. Multiple ways to switch platelet integrins on and off. *J. Thromb. Haemost.* **2008**, *6*, 1253-1261.
35. Hechler B, Nonne C, Roh EJ, Cattaneo, M, Cazenave JP, Lanza F, Jacobson KA, Gachet C. MRS2500 [2-iodo-N6-methyl-(N)-methanocarba-2'-deoxyadenosine-3',5'-bisphosphate], a potent, selective, and stable antagonist of the platelet $P2Y_1$ receptor with strong antithrombotic activity in mice. *J. Pharmacol. Exp. Ther.* **2006**, *316*, 556-563.
36. Atkinson B, Dwyer K, Enjyoji K, Robson SC. Ecto-nucleotidases of the CD39/NTPDase family modulate platelet activation and thrombus formation: potential as therapeutic targets. *Blood Cells Mol. Diseas.* **2006**, *36*, 217-222.
37. Hohmann JD, Wang X, Krajewski S, Selan C, Haller CA, Straub A, Chaikof EL, Nandurkar,HH, Hagemeyer CE, Peter K. Delayed targeting of CD39 to activated platelet GPIIb/IIIa via a single-chain antibody: breaking the link between antithrombotic potency and bleeding? *Blood. 2***013**, *121*, 3067-3075.
38. Ziegler M, Hohmann JD, Searle AK, Abraham MK, Nandurkar HH, Wang X, Peter K. A single-chain antibody-CD39 fusion protein targeting activated platelets protects from cardiac ischaemia/reperfusion injury. *Eur. Heart J.* **2018**, *39*, 111-116.
39. Suzuki-Inoue, K, Inoue, O, Frampton, J, Watson, S.P. Murine GPVI stimulates weak integrin activation in $PLC\gamma2^{-/-}$ platelets: involvement of PLCγ1 and PI3-kinase. *Blood. 2***003**, *102*, 1367-1373.
40. Gilio K, Munnix IC, Mangin P, Cosemans JM, Feijge MA, van der Meijden PE, Olieslagers,S, Chrzanowska-Wodnicka MB, Lillian R, Schoenwaelder S, et al. Non-redundant roles of phosphoinositide 3-kinase isoforms

α and β in glycoprotein VI-induced platelet signaling and thrombus formation. *J. Biol. Chem.* **2009**, *285*, 33750-33762.

41. Herfs L, Swieringa, F, Jooss N, Kozlowski M, Heubel-Moenen FC, van Oerle R, Machiels P, Henskens Y, Heemskerk JW. Multiparameter microfluidics assay of thrombus formation reveals increased sensitivity to contraction and antiplatelet agents at physiological temperature. *Thromb. Res.* **2021**, *203*, 46-56.
42. Janus-Bell E, Ahmed MU, Receveur N, Mouriaux C, Nieswandt B, Gardiner EE, Gachet C, Jandrot-Perrus M, Mangin PH. Differential role of glycoprotein VI in mouse and human thrombus progression and stability. *Thromb. Haemost.* **2021**, *121*, 543-546.
43. Feng W, Valiyaveettil M, Dudiki T, Mahabeleshwar GH, Andre P, Podrez EA, Byzova TV. β3 phosphorylation of platelet αIIbβ3 is crucial for stability of arterial thrombus and microparticle formation in vivo. *Thromb. J.* **2017**, *15*, 22.
44. Navarro S, Stegner D, Nieswandt B, Heemskerk JW, Kuijpers ME. Temporal roles of platelet and coagulation pathways in collagen and tissue factor induced thrombus formation. *Int. J. Mol. Sci.* **2021**, *23*, 358.
45. Subramaniam S, Thielmann I, Morowski M, Pragst I, Sandset PM, Nieswandt B, Etscheid M, Kanse SM. Defective thrombus formation in mice lacking endogenous factor VII activating protease (FSAP). *Thromb. Haemost.* **2015**, *113*, 870-880.
46. Wu J, Heemskerk JW, Baaten CC. Platelet membrane receptor proteolysis: implications for platelet function. *Front. Cardiovasc. Med.* **2021**, *7*, 608391.
47. Bäck M, Ketelhuth DF, Agewall S. Matrix metalloproteinases in atherothrombosis. *Progr. Cardiovasc. Dis.* **2010**, *52*, 410-428.
48. Fernandez-Patron C, Martinez-Cuesta MA, Salas E, Sawicki G, Wozniak M, Radomski MW, Davidge ST. Differential regulation of platelet aggregation by matrix metalloproteinases-9 and-2. *Thromb. Haemost.* **1999**, *82*, 1730-1735.
49. Mastenbroek TG, Feijge MA, Kremers RM, van den Bosch MT, Swieringa F, De Groef L, Moons L, Bennett C, Ghevaert C, Johnson JL, et al. Platelet-associated matrix metalloproteinases regulate thrombus formation and exert local collagenolytic activity. *Arterioscler. Thromb. Vasc. Biol.* **2015**, *35*, 2554-2561.
50. Falcinelli E, Guglielmini G, Torti M, Gresele P. Intraplatelet signaling mechanisms of the priming effect of matrix metalloproteinase-2 on platelet aggregation. *J. Thromb. Haemost.* **2005**, *3*, 2526-2535.
51. Wang J, Ye Y, Wei G, Hu W, Li L, Lu S, Meng Z. Matrix metalloproteinase12 facilitated platelet activation by shedding carcinoembryonic antigen related cell adhesion molecule1. *Biochem. Biophys. Res. Commun.* **2017**, *486*, 1103-1109.
52. Itoh Y. Membrane-type matrix metalloproteinases: their functions and regulations. *Matrix Biol.* **2015**, *44*, 207-223.
53. Bergmeier W, Piffath CL, Cheng G, Dole VS, Zhang Y, von Andrian UH, Wagner DD. Tumor necrosis factor-α–converting enzyme (ADAM17) mediates GPIbα shedding from platelets in vitro and in vivo. *Circ. Res.* **2004**, *95*, 677-683.
54. Montague SJ, Andrews RK, Gardiner EE. Mechanisms of receptor shedding in platelets. *Blood. 2***018**, *132*, 2535-2545.
55. Baaten CC, Swieringa F, Misztal T, Mastenbroek TG, Feijge MA, Bock PE, Donners MM, Collins PW, Li R, van der Meijden PE, et al. Platelet heterogeneity in activation-induced glycoprotein shedding: functional effects. *Blood Adv.* **2018**, *2*, 2320-2331.

56. Mattheij NJ, Gilio K, van Kruchten R, Jobe SM, Wieschhaus AJ, Chishti AH, Collins P, Heemskerk JW, Cosemans, JM. Dual mechanism of integrin αIIbβ3 closure in procoagulant platelets. *J. Biol. Chem.* **2013**, *288*, 13325-13336.
57. Solari FA, Mattheij NJ, Burkhart JM, Swieringa F, Collins PW, Cosemans JM, Sickmann A, Heemskerk JW, Zahedi RP. Combined quantification of the global proteome, phosphoproteome, and proteolytic cleavage to characterize altered platelet functions in the human Scott syndrome. *Mol. Cell. Proteomics* **2016**, *15*, 3154-3169.
58. Heemskerk JW, Mattheij NJ, Cosemans JM. Platelet-based coagulation: different populations, different functions. *J. Thromb. Haemost.* **2013**, *11*, 2-16.
59. Tomaiuolo M, Stalker TJ, Welsh JD, Diamond SL, Sinno T, Brass LF. A systems approach to hemostasis: 2. Computational analysis of molecular transport in the thrombus microenvironment. *Blood. 2***014**, *124*, 1816-1823.
60. Tomaiuolo M, Brass LF, Stalker TJ. Regulation of platelet activation and coagulation and its role in vascular injury and arterial thrombosis. *Interv. Cardiol. Clin.* **2017**, *6*, 1-12.
61. Munnix IC, Cosemans JM, Auger JM, Heemskerk JW. Platelet response heterogeneity in thrombus formation. *Thromb. Haemost.* **2009**, *102*, 1149-1156.
62. Erhardt JA, Toomey JR, Douglas SA, Johns DG. $P2X_1$ stimulation promotes thrombin receptor-mediated platelet aggregation. *J. Thromb. Haemost.* **2006**, *4*, 882-890.
63. Kahner BN, Dorsam RT, Mada SR, Kim S, Stalker TJ, Brass LF, Daniel JL, Kitamura D, Kunapuli,SP. Hematopoietic lineage cell–specific protein 1 is a functionally important signaling molecule in platelet activation. *Blood. 2***007**, *110*, 2449-2456.
64. Cornelissen I, Palmer D, David T, Wilsbacher L, Concengco C, Conley P, Pandey A, Coughlin SR. Roles and interactions among protease-activated receptors and P2ry12 in hemostasis and thrombosis. *Proc. Natl. Acad. Sci. USA* **2010**, *107*, 18605-18610.
65. Patil SB, Jackman LE, Francis SE, Judge HM, Nylander S, Storey RF. Ticagrelor effectively and reversibly blocks murine platelet $P2Y_{12}$-mediated thrombosis and demonstrates a requirement for sustained $P2Y_{12}$ inhibition to prevent subsequent neointima. *Arterioscler. Thromb. Vasc. Biol.* **2010**, *30*, 2385-2391.
66. Nergiz-Unal R, Cosemans JM, Feijge MA, van der Meijden PE, Storey, RF, van Giezen JJ, oude Egbrink MG, Heemskerk JW, Kuijpers MJ. Stabilizing role of platelet $P2Y_{12}$ receptors in shear-dependent thrombus formation on ruptured plaques. *PLoS One.* **2010**, *5*, e10130.
67. Crescence L, Kramberg M, Baumann M, Rey M, Roux S, Panicot-Dubois L, Dubois C, Riederer MA. The $P2Y_{12}$ receptor antagonist selatogrel dissolves preformed platelet thrombi in vivo. *J. Clin. Med.* **2021**, *10*, 5349.
68. Buensuceso CS, Obergfell A, Soriani A, Eto KI, Kiosses WB, Arias-Salgado,EG, Kawakami T, Shattil SJ. Regulation of outside-in signaling in platelets by integrin-associated protein kinase Cβ. *J. Biol. Chem.* **2005**, *280*, 644-653.
69. Harper MT, Poole AW. Diverse functions of protein kinase C isoforms in platelet activation and thrombus formation. *J. Thromb. Haemost.* **2010**, *8*, 454-462.
70. Konopatskaya O, Gilio K, Harper MT, Zhao Y, Cosemans JM, Karim ZA, Whiteheart SW, Molkentin JD, Verkade, P, Watson SP, et al. PKCα regulates platelet granule secretion and thrombus formation in mice. *J. Clin. Invest.* **2009**, *119*, 399-407.

71. Bynagari-Settipalli YS, Lakhani P, Jin J, Bhavaraju K, Rico MC, Kim S, Woulfe D, Kunapuli SP. Protein kinase C isoform ε negatively regulates ADP-induced calcium mobilization and thromboxane generation in platelets. *Arterioscler. Thromb. Vasc. Biol.* **2012**, *32*, 1211-1219.
72. Nagy B, Bhavaraju K, Getz T, Bynagari YS, Kim S, Kunapuli SP. Impaired activation of platelets lacking protein kinase C-θ isoform. *Blood. 2***009**, *113*, 2557-2567.
73. Gilio K, Harper MT, Cosemans JM, Konopatskaya O, Munnix IC, Prinzen L, Leitges M, Liu Q, Molkentin JD, Heemskerk JW, et al. Functional divergence of platelet protein kinase C (PKC) isoforms in thrombus formation on collagen. *J. Biol. Chem.* **2010**, *285*, 23410-23419.
74. Guidetti GF, Canobbio I, Torti M. PI3K/Akt in platelet integrin signaling and implications in thrombosis. *Adv. Biol. Regul.* **2015**, *59*, 36-52.
75. Eisenreich A, Rauch U. PI3K inhibitors in cardiovascular disease. *Cardiovasc. Therapeut.* **2011**, *29*, 29-36.
76. Yi W, Li Q, Shen J, Ren L, Liu X, Wang Q, He S, Wu Q, Hu H, Mao X. Modulation of platelet activation and thrombus formation using a pan-PI3K inhibitor S14161. *PLoS One. 2***014**, *9*, e102394.
77. Chen J, De S, Damron DS, Chen WS, Hay N, Byzova TV. Impaired platelet responses to thrombin and collagen in Akt1-deficient mice. *Blood. 2***004**, *104*, 1703-1710.
78. Woulfe DS, Jiang H, Morgans A, Monks R, Birnbaum M, Brass LF. Defects in secretion, aggregation, and thrombus formation in platelets from mice lacking Akt2. *J. Clin. Invest.* **2004**, *113*, 441-450.
79. O'Brien KA, Stojanovic-Terpo A, Hay N, Du X. An important role for Akt3 in platelet activation and thrombosis. *Blood. 2***011**, *118*, 4215-4223.
80. Kroner C, Eybrechts K, Akkerman JW. Dual regulation of platelet protein kinase B. *J. Biol. Chem.* **2000**, *275*, 27790-27798.
81. Yin H, Stojanovic A, Hay N, Du X. The role of Akt in the signaling pathway of the glycoprotein Ib-IX induced platelet activation. *Blood. 2***008**, *111*, 658-665.
82. Franke B, Akkerman JW, Bos JL. Rapid Ca^{2+}-mediated activation of Rap1 in human platelets. *EMBO J.* **1997**, *16*, 252-259.
83. Guidetti GF, Torti M. The small GTPase Rap1b: a bidirectional regulator of platelet adhesion receptors. *J. Signal Transduct.* **2012**, *2012*, 412089.
84. Stefanini L, Ye F, Snider AK, Sarabakhsh K, Piatt R, Paul DS, Bergmeier W, Petrich BG. A talin mutant that impairs talin-integrin binding in platelets decelerates αIIbβ3 activation without pathological bleeding. *Blood. 2***014**, *123*, 2722-2731.
85. Crittenden JR, Bergmeier W, Zhang Y, Piffath CL, Liang Y, Wagner DD, Housman DE, Graybiel AM. CalDAG-GEFI integrates signaling for platelet aggregation and thrombus formation. *Nat. Med.* **2004**, *10*, 982-986.
86. Cifuni SM, Wagner DD, Bergmeier W. CalDAG-GEFI and protein kinase C represent alternative pathways leading to activation of integrin αIIbβ3 in platelets. *Blood. 2***008**, *112*, 1696-1703.
87. Stefanini L, Bergmeier W. RAP1-GTPase signaling and platelet function. *J. Mol. Med.* **2016**, *94*, 13-19.
88. Lova P, Paganini S, Sinigaglia F, Balduini C, Torti M. A Gi-dependent pathway is required for activation of the small GTPase Rap1b in human platelets. *J. Biol. Chem.* **2002**, *277*, 12009-12015.
89. Woulfe DS. Akt signaling in platelets and thrombosis. *Exp.Rev. Hematol.* **2010**, *3*, 81-91.
90. Chrzanowska-Wodnicka M, Smyth SS, Schoenwaelder SM, Fischer TH, White GC. Rap1b is required for normal platelet function and hemostasis in mice. *J. Clin. Invest.* **2005**, *115*, 680-687.

91. Zhang G, Xiang B, Ye S, Chrzanowska-Wodnicka M, Morris AJ, Gartner TK, Whiteheart SW, White GC, Smyth SS, Li Z. Distinct roles for Rap1b protein in platelet secretion and integrin αIIbβ3 outside-in signaling. *J. Biol. Chem.* **2011**, *286*, 39466-39477.
92. Stefanini L, Boulaftali Y, Ouellette TD, Holinstat M, Désiré L, Leblond B, Andre P, Conley PB, Bergmeier W. Rap1-Rac1 circuits potentiate platelet activation. *Arterioscler. Thromb. Vasc. Biol.* **2012**, *32*, 434-441.
93. Czikora A, Lundberg DJ, Abramovitz A, Lewin NE, Kedei N, Peach ML, Zhou X, Merritt RC, Craft EA, Braun DC, et al. Structural basis for the failure of the C1 domain of Ras guanine nucleotide releasing protein 2 (RasGRP2) to bind phorbol ester with high affinity. *J. Biol. Chem.* **2016**, *291*, 11133-11147.
94. Stolla M, Stefanini L, Roden RC, Chavez M, Hirsch J, Greene T, Ouellette TD, Maloney SF, Diamond SL, Poncz M, et al. The kinetics of αIIbβ3 activation determines the size and stability of thrombi in mice: implications for antiplatelet therapy. *Blood. 2***011**, *117*, 1005-1013.
95. Stefanini L, Paul DS, Robledo RF, Chan ER, Getz TM, Campbell RA, Kechele DO, Casari C, Piatt R, Caron KM, et al. Rasa3 is a critical inhibitor of Rap1-dependent platelet activation. *J. Clin. Invest.* **2015**, *125*, 1419-1432.
96. Lu DH, Hsu CC, Huang SW, Tu HJ, Huang TF, Liou HC, Liao HM, Chen CH, Fu WM, Gau SS. ARHGEF 10 knockout inhibits platelet aggregation and protects mice from thrombus formation. *J. Thromb. Haemost.* **2017**, *15*, 2053-2064.
97. Shattil SJ, Kashiwagi H, Pampori N. Integrin signaling: the platelet paradigm. *Blood* **1998**, *91*, 2645-2657.
98. Pleines I, Hagedorn I, Gupta S, May F, Chakarova L, van Hengel J, Offermanns S, Krohne G, Kleinschnitz C, Brakebusch C, et al. Megakaryocyte-specific RhoA deficiency causes macrothrombocytopenia and defective platelet activation in hemostasis and thrombosis. *Blood. 2***012**, *119*, 1054-1063.
99. Janapati S, Wurtzel J, Dangelmaier C, Manne BK, Bhavanasi D, Kostyak JC, Kim S, Holinstat M, Kunapuli SP, Goldfinger LE. TC21/RRas2 regulates glycoprotein VI-FcRγ-mediated platelet activation and thrombus stability. *J. Thromb. Haemost.* **2018**, *16*, 1632-1645.
100. Swieringa F, Solari FA, Pagel O, Beck B, Faber J, Feijge MA, Jurk K, Körver-Keularts IM, Mattheij NJ, Pohlenz J, et al. Impaired iloprost-induced platelet inhibition and phosphoproteome changes in patients with confirmed pseudohypoparathyroidism type Ia, linked to genetic mutations in GNAS. *Sci. Rep.* **2020**, *10*, 11389.
101. Beck F, Geiger J, Gambaryan S, Solari FA, Dell'Aica M, Loroch S, Mattheij N, Mindukshev I, Pötz O, Jurk K, et al. Temporal quantitative phosphoproteomics of ADP stimulation reveals novel central nodes in platelet activation and inhibition. *Blood. 2***017**, *129*, e1-e12.
102. Reinhard M, Jarchau T, Walter U. Actin-based motility: stop and go with Ena/VASP proteins. *Trends Biochem. Sci.* **2001**, *26*, 243-249.
103. Aszódi A, Pfeifer A, Ahmad M, Glauner M, Zhou XH, Ny L, Andersson KE, Kehrel B, Offermanns S, Fässler R. The vasodilator-stimulated phosphoprotein (VASP) is involved in cGMP-and cAMP-mediated inhibition of agonist-induced platelet aggregation, but is dispensable for smooth muscle function. *EMBO J.* **1999**, *18*, 37-48.
104. Benz PM, Laban H, Zink J, Günther L, Walter U, Gambaryan S, Dib K. Vasodilator-stimulated phosphoprotein (VASP)-dependent and -independent pathways regulate thrombin-induced activation of Rap1b in platelets. *Cell. Commun. Signal.* **2016**, *14*, 21.
105. Schwarz UR, Geiger J, Walter U, Eigenthaler M. Flow cytometry analysis of intracellular VASP phosphorylation for the assessment of activating and inhibitory signal transduction pathways in human platelets--definition and detection of ticlopidine/clopidogrel effects. *Thromb. Haemost.* **1999**, *82*, 1145-1152.

106. Danielewski O, Schultess J, Smolenski A. The NO/cGMP pathway inhibits Rap 1 activation in human platelets via cGMP-dependent protein kinase I. *Thromb. Haemost.* **2005**, *93*, 319-325.
107. Haslam RJ, Dickinson NT, Jang EK. Cyclic nucleotides and phosphodiesterases in platelets. *Thromb. Haemost.* **1999**, *82*, 412-423.
108. Yang J, Wu J, Jiang H, Mortensen R, Austin S, Manning DR, Woulfe D, Brass LF. Signaling through Gi family members in platelets. Redundancy and specificity in the regulation of adenylyl cyclase and other effectors. *J. Biol. Chem.* **2002**, *277*, 46035-46042.
109. Zhang W, Colman RW. Thrombin regulates intracellular cyclic AMP concentration in human platelets through phosphorylation/activation of phosphodiesterase 3A. *Blood. 2***007**, *110*, 1475-1482.
110. Zou J, Wu J, Roest M, Heemskerk JW. Long-term platelet priming after glycoprotein VI stimulation in comparison to protease-activating receptor (PAR) stimulation. *PLoS One. 2***021**, *16*, e0247425.
111. Van Geet C, Izzi B, Labarque V, Freson K. Human platelet pathology related to defects in the G-protein signaling cascade. *J. Thromb. Haemost.* **2009**, *7 Suppl 1*, 282-286.
112. Pretorius L, Thomson GJ, Adams RC, Nell TA, Laubscher WA, Pretorius E. Platelet activity and hypercoagulation in type 2 diabetes. *Cardiovasc. Diabetol.* **2018**, *17*, 141.
113. Fiodorenko-Dumas Z, Dumas I, Mastej K, Jakobsche-Policht U, Bittner J, Adamiec R. Receptor GPIIb/IIIa as an indicator of risk in vascular events. *Clin. Appl. Thromb. Hemost.* **2019**, *25*, 1076029619845056.
114. Ju L, McFadyen JD, Al-Daher S, Alwis I, Chen Y, Tønnesen LL, Maiocchi S, Coulter B, Calkin AC, Felner EI. Compression force sensing regulates integrin αIIbβ3 adhesive function on diabetic platelets. *Nat. Commun.* **2018**, *9*, 1-16.
115. Savi P, Bernat A, Lalu A, Roque C, Zamboni G, Herbert JM. Effect of aspirin on platelet desaggregation induced by SR121566, a potent GPIIb/IIIa antagonist. *Platelets.* **2000**, *11*, 43-48.
116. Cosemans JM, van Kruchten R, Olieslagers S, Schurgers LJ, Verheyen FK, Munnix IC, Waltenberger J, Angelillo-Scherrer A, Hoylaerts MF, Carmeliet P, et al. Potentiating role of Gas6 and Tyro3, Axl and Mer (TAM) receptors in human and murine platelet activation and thrombus stabilization. *J. Thromb. Haemost.* **2010**, *8*, 1797-1808.
117. Filkova AA, Martyanov AA, Garzon Dasgupta AK, Panteleev MA, Sveshnikova AN. Quantitative dynamics of reversible platelet aggregation: mathematical modelling and experiments. *Sci. Rep.* **2019**, *9*, 6217.
118. Frojmovic M, Labarthe B, Legrand C. Inhibition and reversal of platelet aggregation by αIIbβ3 antagonists depends on the anticoagulant and flow conditions: differential effects of abciximab and lamifiban. *Br. J. Haematol.* **2005**, *131*, 348-355.
119. Vilahur G, Choi BG, Zafar MU, Viles-Gonzalez JF, Vorchheimer DA, Fuster V, Badimon JJ. Normalization of platelet reactivity in clopidogrel-treated subjects. *J. Thromb. Haemost.* **2007**, *5*, 82-90.
120. Merten M, Thiagarajan P. P-selectin expression on platelets determines size and stability of platelet aggregates. *Circulation* **2000**, *102*, 1931-1936.
121. Wu CC, Wu SY, Liao CY, Teng CM, Wu YC, Kuo SC. The roles and mechanisms of PAR4 and $P2Y_{12}$/phosphatidylinositol 3-kinase pathway in maintaining thrombin-induced platelet aggregation. *Br. J. Pharmacol.* **2010**, *161*, 643-658.
122. Chatterjee M, Borst O, Walker B, Fotinos A, Vogel S, Seizer P, Mack A, Alampour-Rajabi S, Rath D, Geisler T. Macrophage migration inhibitory factor limits activation-induced apoptosis of platelets via CXCR7-dependent Akt signaling. *Circ. Res.* **2014**, *115*, 939-949.

123. Rumbaut RE, Randhawa JK, Smith CW, Burns AR. Mouse cremaster venules are predisposed to light/dye-induced thrombosis independent of wall shear rate, CD18, ICAM-1, or P-selectin. *Microcirculation* **2004**, *11*, 239-247.
124. Grüner S, Prostredna,M, Schulte V, Krieg T, Eckes B, Brakebusch C, Nieswandt B. Multiple integrin-ligand interactions synergize in shear-resistant platelet adhesion at sites of arterial injury in vivo. *Blood. 2***003**, *102*, 4021-4027.
125. He L, Pappan LK, Grenache DG, Li Z, Tollefsen DM, Santoro SA, Zutter MM. The contributions of the α2β1 integrin to vascular thrombosis in vivo. *Blood. 2***003**, *102*, 3652-3657.
126. Marjoram RJ, Li Z He L, Tollefsen DM, Kunicki TJ, Dickeson SK, Santoro SA, Zutter, M.M. α2β1 integrin, GPVI receptor, and common FcRγ chain on mouse platelets mediate distinct responses to collagen in models of thrombosis. *PLoS One. 2***014**, *9*, e114035.
127. Roux D, Roullot V, Poujol C, Kortulewski T, Nurden P, Marguerie G. Thrombasthenic mice generated by replacement of the integrin αIIb gene: demonstration that transcriptional activation of this megakaryocytic locus precedes lineage commitment. *Blood. 2***000**, *96*, 1399-1408.
128. Schaff M, Tang CJ, Maurer E, Bourdon C, Receveur N, Eckly A, Hechler B, Arnold C, de Arcangelis A, Nieswandt B, et al. Integrin α6β1 is the main receptor for vascular laminins and plays a role in platelet adhesion, activation, and arterial thrombosis. *Circulation* **2013**, *128*, 541-552.
129. Kuijpers MJ, Schulte V, Bergmeier W, Lindhout T, Brakebusch C, Offermanns S, Fässler R, Heemskerk JW, Nieswandt B. Complementary roles of glycoprotein VI and α2β1 integrin in collagen-induced thrombus formation in flowing whole blood ex vivo. *FASEB J.* **2003**, *17*, 685-687.
130. Eckly A, Hechler B, Freund M, Zerr M, Cazenave JP, Lanza F, Mangin PH, Gachet C. Mechanisms underlying $FeCl_3$-induced arterial thrombosis. *J. Thromb. Haemost.* **2011**, *9*, 779-789.
131. Petzold T, Ruppert R, Pandey D, Barocke V, Meyer H, Lorenz M, Zhang L, Siess W, Massberg S, Moser M. β1 integrin-mediated signals are required for platelet granule secretion and hemostasis in mouse. *Blood. 2***013**, *122*, 2723-2731.
132. Stolla M, Stefanini L, André P, Ouellette TD, Reilly MP, McKenzie SE, Bergmeier W. CalDAG-GEFI deficiency protects mice in a novel model of Fcγ RIIA-mediated thrombosis and thrombocytopenia. *Blood.* **2011**, *118*, 1113-1120.
133. Holy EW, Jakob P, Eickner T, Camic, GG, Beer JH, Akhmedov A, Sternberg K, Schmitz KP, Lüscher TF, Tanner FC. PI3K/p110α inhibition selectively interferes with arterial thrombosis and neointima formation, but not re-endothelialization: potential implications for drug-eluting stent design. *Eur. Heart J.* **2014**, *35*, 808-820.
134. Martin V, Guillermet-Guibert J, Chicanne G, Cabou C, Jandrot-Perrus M, Plantavid M, Vanhaesebroeck B, Payrastre B, Gratacap MP. Deletion of the p110β isoform of phosphoinositide 3-kinase in platelets reveals its central role in Akt activation and thrombus formation in vitro and in vivo. *Blood. 2***010**, *115*, 2008-2013.
135. Lian L, Wang Y, Draznin J, Eslin D, Bennett JS, Poncz M, Wu D, Abrams CS. The relative role of PLCβ and PI3Kγ in platelet activation. *Blood. 2***005**, *106*, 110-117.
136. Chari R, Getz T, Nagy B, Bhavaraju K, Mao Y, Bynagari YS, Murugappan S, Nakayama K, Kunapuli SP. Protein kinase Cδ differentially regulates platelet functional responses. *Arterioscler. Thromb. Vasc. Biol.* **2009**, *29*, 699-705.
137. Unsworth AJ, Finney BA, Navarro-Nunez L, Severin S, Watson SP, Pears CJ. Protein kinase Cε and protein kinase Cθ double-deficient mice have a bleeding diathesis. *J. Thromb. Haemost.* **2012**, *10*, 1887-1894.

138. Hall KJ, Harper, MT, Gilio K, Cosemans JM, Heemskerk JW, Poole AW. Genetic analysis of the role of protein kinase Cθ in platelet function and thrombus formation. *PLoS One. 2***008**, *3*, e3277.
139. Piatt R, Paul DS, Lee RH, McKenzie SE, Parise LV, Cowley DO, Cooley BC, Bergmeier W. Mice expressing low levels of CalDAG-GEFI exhibit markedly impaired platelet activation with minor impact on hemostasis. *Arterioscler. Thromb. Vasc. Biol.* **2016**, *36*, 1838-1846.
140. Jessica MO, Fiorella R, Ocatavio S, Linnette R, Nahomy L, Kanth MB, Bismarck M, Rondina MT, Valance WA. Tlt-1 controls early thrombus formation and stability by facilitating αIIbβ3 outside-in signaling in mice. *Int. J. Adv. Res. (Indore)* **2018**, *6*, 1143-1149.

Chapter 3

Platelet activation pathways controlling reversible integrin αIIbβ3 activation

Jinmi Zou[1,2], Siyu Sun[1,2], Ilaria De Simone[1], Hugo ten Cate[2], Philip G. de Groot[1], Bas de Laat[1], Mark Roest[1], Johan W.M. Heemskerk[1], Frauke Swieringa[1]

[1]Synapse Research Institute, Maastricht, Koningin Emmaplein 7, 6217 KD Maastricht, The Netherlands; [2]Departments of Biochemistry and Internal Medicine, Maastricht University Medical Center+, Maastricht, The Netherlands.

Submitted

Chapter 4

Long-term platelet priming after glycoprotein VI stimulation in comparison to protease activating receptor stimulation

Jinmi Zou,[1] Jiayu Wu,[1] Mark Roest,[2] Johan W. M. Heemskerk[1]

[1]Department of Biochemistry, CARIM, Maastricht University, Maastricht, The Netherlands
[2]Synapse Research Institute, Maastricht, The Netherlands

PloS One, 2021, 16(3): e0247425.

Abstract

Platelets can respond to multiple antagonists and agonists, implying that their activation state is a consequence of past exposure to these substances. While platelets are often considered as one-time responsive cells, they likely can respond to sequential application of inhibitors and stimuli. We hypothesized that the ability of platelets to sequentially respond depends on the time and type of repeated agonist application. The present proof-of-concept data show that iloprost (cAMP elevation), tirofiban (integrin αIIbβ3 blocker) and Syk kinase inhibition sub-acutely modulate platelet aggregation, in other words halt this process even when applied after agonist. In comparison to thrombin-activated receptor (PAR) stimulation, glycoprotein VI (GPVI) stimulation needed to be blocked earlier for an effect on aggregation, with Syk inhibition as an exception. Furthermore, cytosolic Ca^{2+} measurements indicated that, in comparison to prior PAR stimulation, prior GPVI stimulation induced a more persistent, priming activation state that influenced the response to a next agent. Overall, these data point to an unexpected priming memory of activated platelets in sub-acutely responding to another inhibitor or stimulus, with a higher versatility and faster offset after PAR stimulation than after GPVI stimulation.

Keywords: glycoprotein VI, platelet inhibition, platelet priming, thrombin receptors

Introduction

Blood platelets are equipped with a broad range of adhesive and signaling receptors which synergize to trigger a common set of functional responses, in particular integrin activation, granular release and procoagulant activity [1,2]. Studies with genetically modified mice have established that hundreds of genes encoding for platelet receptors, signaling molecules and granule components regulate the functions of platelets in physiological hemostasis and pathological arterial thrombosis [3]. The common concept herein is that platelet activation is suppressed by vessel wall-derived inhibitors, and that this suppression is relieved in the presence of a weak or strong agonist. With exceptions [4], most of the literature implicitly considers platelets as 'single activating' cells, which idea supposes that after a first activation event the platelet response is 'over' [1]. However, the circulating platelets will be continuously exposed to (ant)agonists, suggesting that they will experience moments of inactivation and activation, the balance of which can be altered under pathophysiological conditions [5,6]. This notion implies that the inhibitory state of circulating platelets can be disturbed multiple times or, in other words, that platelets have the capacity over time to respond to series of agonists and antagonists. This has not been studied in detail before.

In the present paper, as a proof-of-concept, we tested the hypothesis that platelets can sequentially respond to more than one agonist and/or antagonist in a time-dependent manner. We therefore treated human platelets sequentially via: *(i)* the ITAM-linked collagen receptor glycoprotein VI (GPVI) using cross-linked collagen-related peptide (CRP-XL); *(ii)* the different pathway of G-protein-coupled receptors (GPCR) using the PAR1/4 agonist thrombin, the reversible PAR1 agonist TRAP6 [7], or the $P2Y_1/P2Y_{12}$ agonist Me-S-ADP; *(iii)* the platelet-inhibiting prostacyclin analogue, iloprost, elevating cAMP levels; and/or *(iv)* the integrin αIIbβ3 antagonist tirofiban, suppressing platelet-fibrinogen interactions [2]. Our first research question was in which time frame platelet aggregation induced by an agonist can be suppressed by prior or later application of inhibitor. Our second question was in which time frame a first agonist can influence the platelet responses to a second agonist.

Materials and methods

Materials

Thrombin was obtained from Enzyme Research Laboratories (South Bend IN, USA). Thrombin receptor-activating peptide 6 (SFLLRN, TRAP6) was purchased from Bachem (Bubendorf, Switzerland); cross-linked collagen-related peptide (CRP-XL) was from the University of Cambridge (Cambridge, UK); the stable ADP analog methylthio-adenosine-diphosphate (Me-S-ADP) [8] came from Santa Cruz Biotechnology (Dallas TX, USA). Fura-2 acetoxymethyl ester and human fibrinogen were obtained from Invitrogen (Carlsbad CA, USA); Pluronic F-127 from Molecular Probes (Eugene OR, USA). Integrin αIIbβ3 inhibitor tirofiban [9] and cAMP-elevating agent iloprost [2] were from Sigma-Aldrich (St. Louis MI, USA); the selective Syk kinase inhibitor

PRT-060318, 2-((1R,2S)-2-aminocyclohexylamino)-4-(m-tolylamino)pyrimidine-5-carboxamide (Syk-IN) [10] came from Bio-Connect (Huissen, The Netherlands).

Blood collection

Human blood was collected from healthy volunteers, after full informed consent according to the Declaration of Helsinki. Approval for the studies was obtained from the local Medical Ethics Committee (METC 10-30-023, Maastricht University). The subjects had not used antiplatelet medication for at least 2 weeks. Venous blood was collected from an antecubital vein into 3.2% trisodium citrate Vacuette tubes (Greiner Bio-One, Alphen a/d Rijn, The Netherlands). The first tube of blood was discarded to avoid the presence of traces of tissue factor.

Preparation of washed platelets

Platelet-rich plasma and washed platelets were prepared, basically as described before [9,11]. In brief, blood samples were centrifuged at 190 *g* for 15 min (room temperature). The yellowish upper layer of PRP was carefully collected without taking the buffy coat or the red cell bottom layer. After addition of 10 vol% ACD medium (80 mM trisodium citrate, 52 mM citric acid and 180 mM glucose), platelets in the PRP were spin down in 2 mL Eppendorf tubes at 1700 *g* for 2 min. Plasma was removed and the tubes were held upside down for 1 min to remove remaining plasma traces. The pellets then were resuspended into 1 mL of Hepes buffer pH 6.6 (136 mM NaCl, 10 mM glucose, 5 mM Hepes, 2.7 mM KCl, 2 mM $MgCl_2$, apyrase at 0.2 unit ADPase/mL, and 0.1 % (w/v) bovine serum albumin). After addition of 6.6 vol% ACD, the tubes were recentrifuged, and the washed pelleted platelets were finally resuspended into 1 mL Hepes buffer pH 7.45 (10 mM Hepes, 136 mM NaCl, 2.7 mM KCl, 2 mM $MgCl_2$, 0.1% glucose, and 0.1% bovine serum albumin). Note that apyrase during the isolation procedure retained the platelet responses to ADP and ATP [12]. Platelet count was adjusted to 250×10^9/L for aggregation and 200×10^9/L for cytosolic Ca^{2+} measurements.

Light transmission aggregometry

Aggregation responses of washed platelets were measured with a Chronology aggregometer (Havertown PA, USA) at 37 °C under stirring. The use of washed platelet suspensions in the presence of millimolar levels of extracellular Ca^{2+} and Mg^{2+} allowed direct comparison with the $[Ca^{2+}]_i$ measurements, and furthermore prevented the need for recalcification of a citrate-anticoagulated PRP. The cells were pre- or post-treated with iloprost (10 nM), tirofiban (1 µg/mL) or PRT-060318 (5 µM) as indicated. For activation, sub-maximal concentrations were used of TRAP6 (10 µM) or CRP-XL (5 µg/mL). The PAR1 agonist instead of thrombin was used to prevent fibrin formation and factor XIIIa-dependent binding of fibrin to platelets [13]. Aggregation traces of % transmission (%T) were analysed for initial slope of the curves (Δ%T/min), area under the curve (%T, 10 min after agonist addition), and maximal response [14,15].

Cytosolic Ca^{2+} measurements

Pelleted platelets in Hepes buffer pH 7.45 were incubated with Fura-2 AM (3 µM) and Pluronic (600 µg/mL) in the presence of apyrase for 40 min at 37 °C [16]. After a wash step, the Fura-2-loaded platelet were resuspended into Hepes buffer pH 7.45, and adjusted to 200 × 10^9 platelets/L. For measurements of rises in cytosolic $[Ca^{2+}]_i$, the loaded cells in 96-wells plate were pre-incubated with sub-maximal concentrations of indicated (ant)agonist (TRAP6, CRP-XL, iloprost, Me-S-ADP, thrombin or vehicle solution) for 9 min [10]. Changes in fluorescence at 340 nm and 380 nm excitation per row over time were assessed using a FlexStation 3 robotic machine at 37 °C, as described earlier [10]. After baseline fluorescence recording, $CaCl_2$ (1 mM, f.c.) was added, followed by TRAP6 (10 µM, f.c.) or CRP-XL (5 µg/mL, f.c.) as a second agonist (1 min). Automated injection speed for agonist addition was set at 8 µL/s. Note that only a single agonist at a time could be automatically injected during the ratiometric fluorescence recording. After correction for background fluorescence per excitation wavelength, ratio fluorescence values were converted into levels of nanomolar levels of $[Ca^{2+}]_i$ using minimal and maximal ratio values from calibration wells with Triton-X-100 lysed platelets [16].

Statistical analysis

Normally distributed data are presented as mean ± SEM. Excel software was used for statistical analyses. Paired values were compared by a two-sided paired Student t-test, while unpaired values were compared by a two-sided 1-way ANOVA. Values of $P < 0.05$ were considered to be statistically significant.

Results

Prolonged activation of platelets after GPVI stimulation

Platelet aggregation can be induced via the PAR1-type GPCR (for thrombin and TRAP6) or via the ITAM-linked receptor GPVI (for collagen and CRP-XL), where in either case pretreatment with the cAMP-elevating agent iloprost is known to suppress the aggregation process [1,2]. However, it has remained unclear how long such a pretreatment needs to be for affecting the platelet responses. To investigate this, we added iloprost to human platelets at various times before or after stimulation using a submaximal dose of TRAP6 or CRP-XL. Markedly, the addition of iloprost, not only before but also simultaneously with TRAP6 or CRP-XL, completely annulled the aggregation responses (**Figure 1A**, **D**). Quantification of the aggregation traces pointed to abolition of the curve slope (**Figure 1B**, **E**) and the area-under-the-aggregation-curve (**Figure 1C**, **F**). Moreover, the inhibitory effect of iloprost retained up to 0.5-2 min after TRAP6 stimulation, in that it halted or partly reversed the initial aggregation process. However, this time frame of inhibition was shorter for up to 0.5 min in case of CRP-XL stimulation. These findings pointed to a more reduced ability of GPVI-stimulated platelets in terms of post-hoc responding to cAMP elevation.

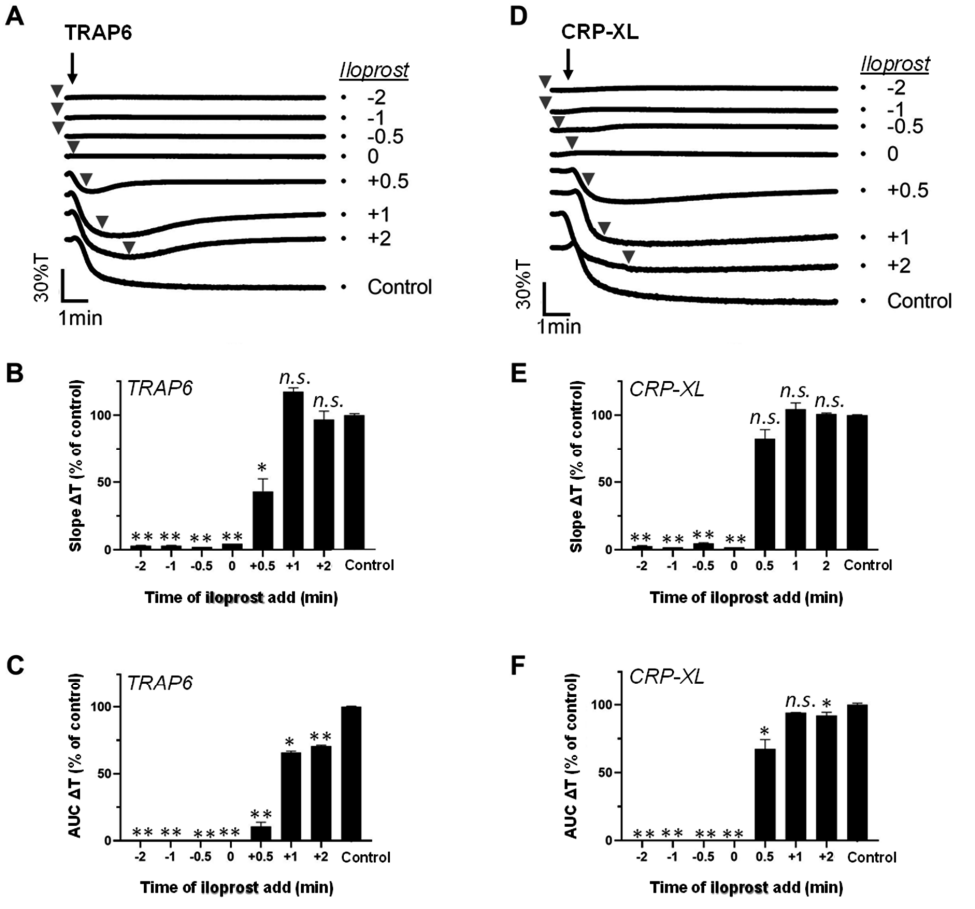

Figure 1. Post-hoc inhibitory effect of iloprost on TRAP6- and CRP-XL-induced platelet aggregation. Platelets in suspension were stimulated with 10 μM TRAP6 (**A-C**) or 5 μg/mL CRP-XL (**D-F**), and aggregation was recorded by light transmission aggregometry. Iloprost (10 nM) was added before (-2, -1 or -0.5 minutes), simultaneously with (0 minutes) or after (+0.5, +1, +2 minutes) the indicated agonist. Representative traces are shown); arrows indicate addition of agonist, arrowheads addition of iloprost (**A**, **D**). Graphs of aggregation slope as %T/minutes (**B**, **E**) and aggregation-area-under-the-curve (AUC, 10 minutes) (**C**, **F**), as fractions of control without iloprost. Mean ± SE (n = 3). **P*<0.05, ***P*<0.001 vs. control traces, paired Student t-test.

Platelet aggregation relies on integrin αIIbβ3 activation and fibrinogen-dependent platelet-platelet interactions [1]. To assess response versatility on the level of αIIbβ3 activation, we performed similar experiments, in which we applied the integrin antagonist tirofiban before or after TRAP6 or CRP-XL. The tirofiban fully suppressed the aggregation response, when added before or together with either agonist (**Figure 2A**, **D**). Quantification of the traces learned that post-addition of tirofiban for up to 2 min did not influence the initial aggregation slope (**Figure 2B**, **E**), but partly affected the aggregation integral (**Figure 2C**, **F**) with TRAP6 or CRP-XL.

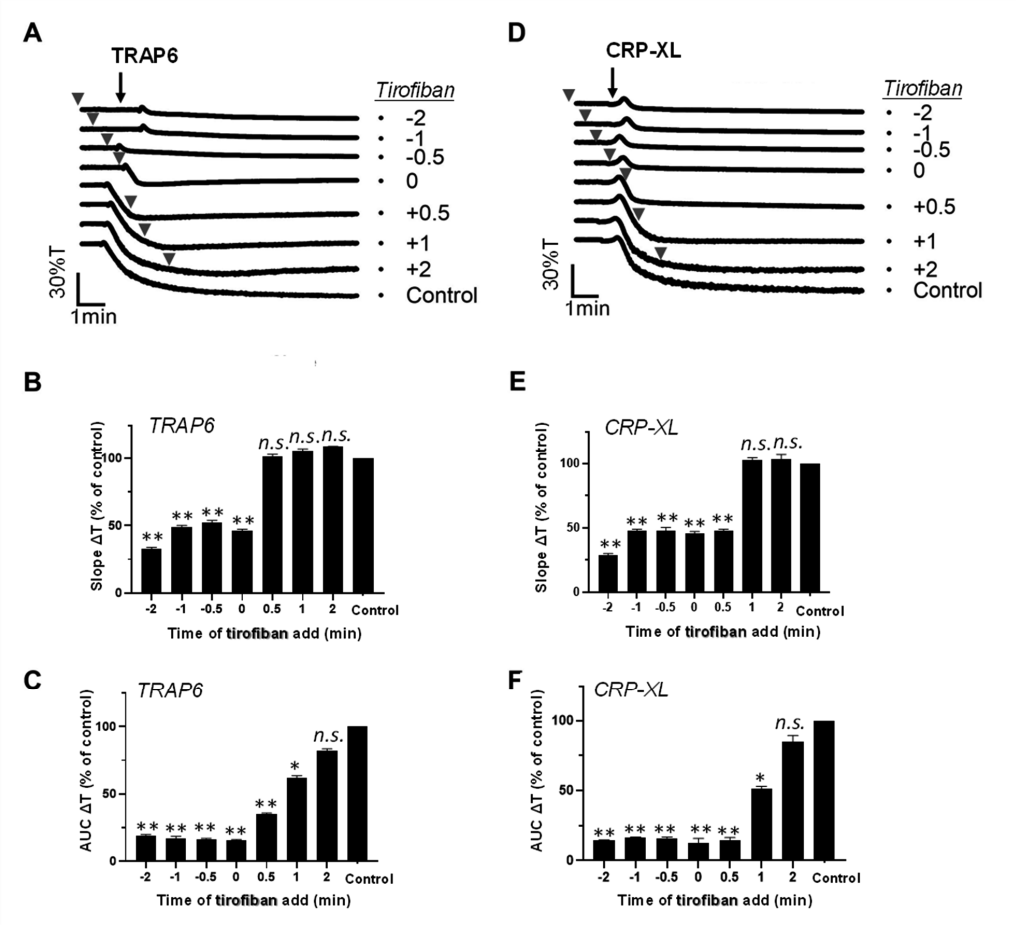

Figure 2. Post-hoc inhibitory effect of integrin antagonist on TRAP6- and CRP-XL-induced platelet aggregation. Platelets in suspension were stimulated with 10 µM TRAP6 (**A-C**) or 5 µg/mL CRP-XL (**D-F**), and aggregation was recorded by light transmission aggregometry. Tirofiban (1 µg/mL) was added before (-2, -1 or -0.5 minutes), simultaneously with (0 minutes) or after (+0.5, +1, +2 minutes) the indicated agonist. Representative traces are shown; arrows indicate addition of agonist, arrowheads addition of tirofiban (**A**, **D**). Graphs show the aggregation slope as %T/minutes (**B**, **E**) and aggregation-area-under-the-curve (AUC, 10 minutes) (**C**, **F**), as fractions of control without tirofiban. Mean ± SE (n = 3). **P*<0.05, ***P*<0.001 vs. control traces, paired Student t-test.

Platelet activation induced by GPVI is known to rely on activation of the protein tyrosine kinase Syk [10]. To reveal the requirement of Syk signaling over time, we treated platelets with the selective inhibitor PRT-060318 (Syk-IN) [10] before or after stimulation by TRAP6 or CRP-XL. As expected, Syk-IN did hardly suppress the PAR1-mediated platelet aggregation at any time point (**Figure 3A-C**). On the other hand, Syk-IN fully abrogated the GPVI-mediated aggregation, even when given after 0.5 min, *i.e.* when the aggregation normally would have started (**Figure 3D-F**). At later time points up to 2 min, Syk-IN remained partly effective in suppressing the overall aggregation process (**Figure 3F**). This suggested that a relatively prolonged GPVI signal generation via Syk is required for completion of the aggregation process.

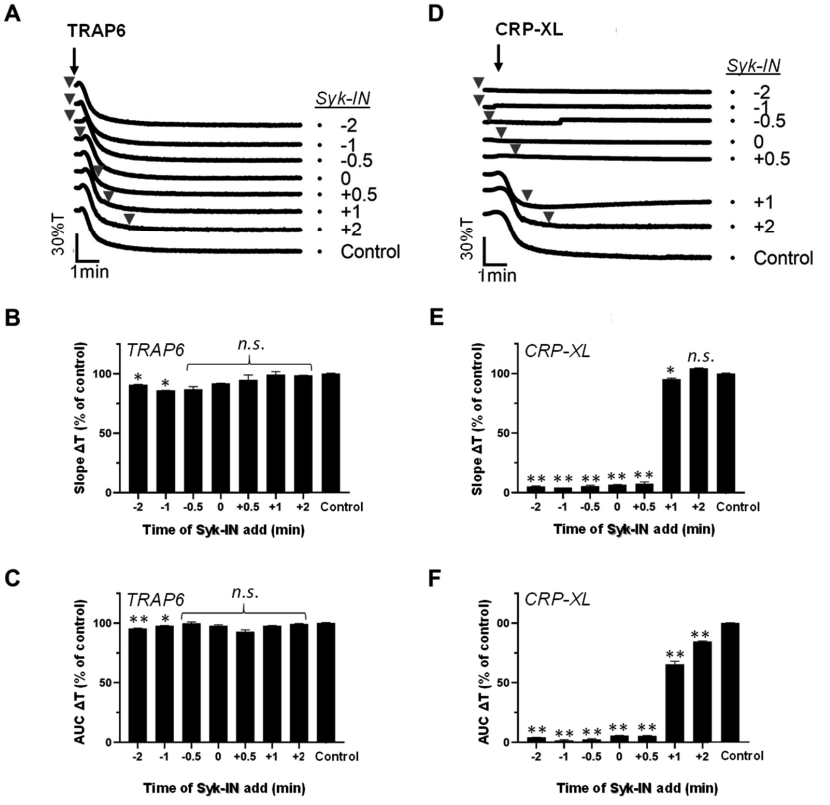

Figure 3. Post-hoc inhibitory effect of Syk blocker on CRP-XL-induced platelet aggregation. Platelets in suspension were stimulated with 10 µM TRAP6 (**A-C**) or 5 µg/mL CRP-XL (**D-F**), and aggregation was recorded by light transmission aggregometry. Syk-IN (5 µM) was added before (-2, -1 or -0.5 minutes), simultaneously with (0 minutes) or after (+0.5, +1, +2 minutes) the indicated agonist. Representative traces; arrows indicate addition of agonist, arrowheads addition of Syk-IN (**A**, **D**). Bar graphs of aggregation slope as %T/minutes (**B**, **E**) and aggregation-area-under-the-curve (AUC, 10 minutes) (**C**, **F**), expressed as fractions of control without Syk-IN. Mean ± SE (n = 3). **P*<0.05, ***P*<0.001 vs. control traces, paired Student t-test.

Given the ability of either iloprost or tirofiban to influence the aggregation after agonist addition, it was interesting to examine combined effects of the two inhibitors. When added before or up to 1 min after TRAP6 or CRP-XL stimulation, iloprost + tirofiban caused substantial suppression of the aggregation process (**Figure 4A-F**). Typically, however, examination of the aggregation traces indicated that with TRAP6 even late application of the inhibitors (6 min) caused substantial disaggregation, while this was not the case with CRP-XL (**Figure 4A-B**). This again pointed to a more continued, less reversible activation signal with CRP-XL. By comparison, it appeared that iloprost postaddition after TRAP6 to a stronger extent than tirofiban postaddition ($P<0.05$) triggered the reversal of aggregation with 15–30% transmission.

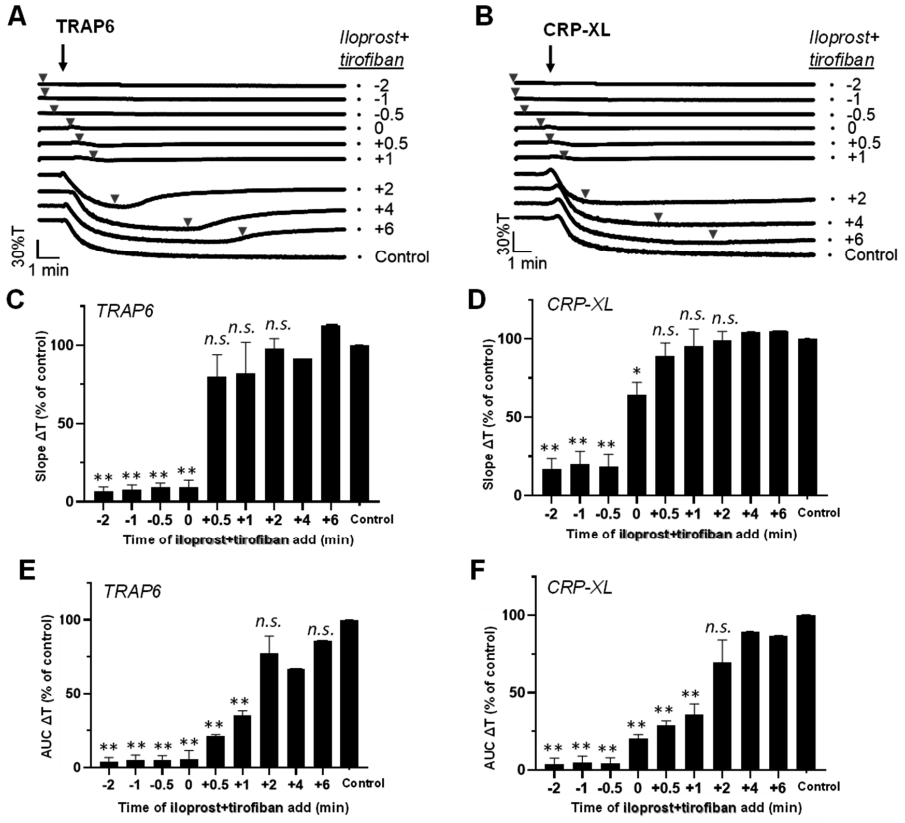

Figure 4. Post-hoc inhibitory effect of iloprost plus tirofiban on agonist-induced platelet aggregation. Platelets in suspension were stimulated with 10 µM TRAP6 (**A-C**) or 5 µg/mL CRP-XL (**D-F**), and aggregation was recorded by light transmission aggregometry. Iloprost (10 nM) in combination with tirofiban (1 µg/mL) was added before (-2, -1 or -0.5 minutes), simultaneously with (0 minutes) or after (+0.5, +1, +2, +4, +6 minutes) the indicated agonist. See Figure 1. Mean ± SE (n = 3). **P*<0.05, ***P*<0.001 vs. control traces, paired Student t-test.

In the presence of fibrinogen, iloprost on top of tirofiban also induced reversal of the aggregation response induced by Me-SADP (**Suppl. Figure 1**). Additional experiments indicated that, with supramaximal concentrations of TRAP6 (50 µM) or CRP-XL (25 µg/mL), the simultaneous

application of iloprost + tirofiban still prevented the aggregation at t = 0, but not at t = 2 min, *i.e.,* at a time point the aggregation process was completed (data not shown).

More prolonged priming of Ca^{2+} signaling after GPVI stimulation in comparison to PAR stimulation

The results so far suggested an overall higher versatility of TRAP6- than of CRP-XL-induced aggregation in terms of secondary inhibition and response reversibility. To investigate how this extended to the intracellular signaling events, we measured the cytosolic $[Ca^{2+}]_i$ rises of platelets loaded with the probe Fura-2. Measurements were performed by 340/380 nm ratio fluorometry in 96-well plates at 37 °C, in which an agonist could precisely be injected during the measurement time using a FlexStation 3 robot. This method results in diffusion-limited, but highly reproducible and calibrated $[Ca^{2+}]_i$ rises [10]. We developed an experimental setup, in which the platelets were manually treated with a first agonist or vehicle medium in wells, and then after a time window of 10 min were evaluated for changes in $[Ca^{2+}]_i$ using the FlexStation robot, which allowed to precisely record the signaling responses to the second agonist.

In agreement with earlier findings [17], initial platelet stimulation with TRAP6 alone gave a fast and transient $[Ca^{2+}]_i$ rise (**Suppl Figure 2A**). Initial stimulation with CRP-XP alone resulted in a slower and persistent $[Ca^{2+}]_i$ rise (**Suppl Figure 2B**). Markedly, after prior stimulation with CRP-XL, the subsequent application of TRAP6 again showed the transient $[Ca^{2+}]_i$ rise on top of the CRP-XL signal (**Figure 5A**). In contrast, prior stimulation with TRAP6 completely annulled the response to a second TRAP6 addition. In contrast, after initial stimulation with TRAP6 or CRP-XL, the subsequent addition of CRP-XL resulted in another prolonged Ca^{2+} signal (**Figure 5B**). This pointed to a relatively prolonged priming effect of the initial CRP-XL stimulation in comparison to initial PAR1 stimulation.

As expected, pre-incubation with iloprost (10 min) completely annulled the $[Ca^{2+}]_i$ rises evoked by TRAP6 (**Figure 5C**) or by CRP-XL (**Figure 5D**). However, after iloprost plus TRAP6, the cells responded to later CRP-XL by a greatly reduced $[Ca^{2+}]_i$ rise, pointing to a residual suppression by iloprost (**Figure 5D**). On the other hand, after iloprost plus CRP-XL, the platelets responded to later TRAP6 by a prolonged Ca^{2+} signal (**Figure 5E**), reminiscent of the normal CRP-XL response. Suppression by iloprost was also observed upon dual addition of TRAP6 (**Figure 5C**). With iloprost present, dual addition of CRP-XL resulted in a slightly increased $[Ca^{2+}]_i$ response (**Figure 5F**). Together, these data showed that, also in the presence of iloprost, initial CRP-XL stimulation enhanced the Ca^{2+} responses of later TRAP6 stimulation.

To determine if such a priming effect was confined to pre-stimulation with CRP-XL, we performed similar experiments with thrombin or ADP as a first agonist (t = -10 min). Herein, prior thrombin impaired the TRAP6-induced $[Ca^{2+}]_i$ rise (**Figure 6A**), whilst prior ADP was without effect (**Figure 6C**). On the other hand, prior thrombin (**Figure 6B**) but not ADP (**Figure**

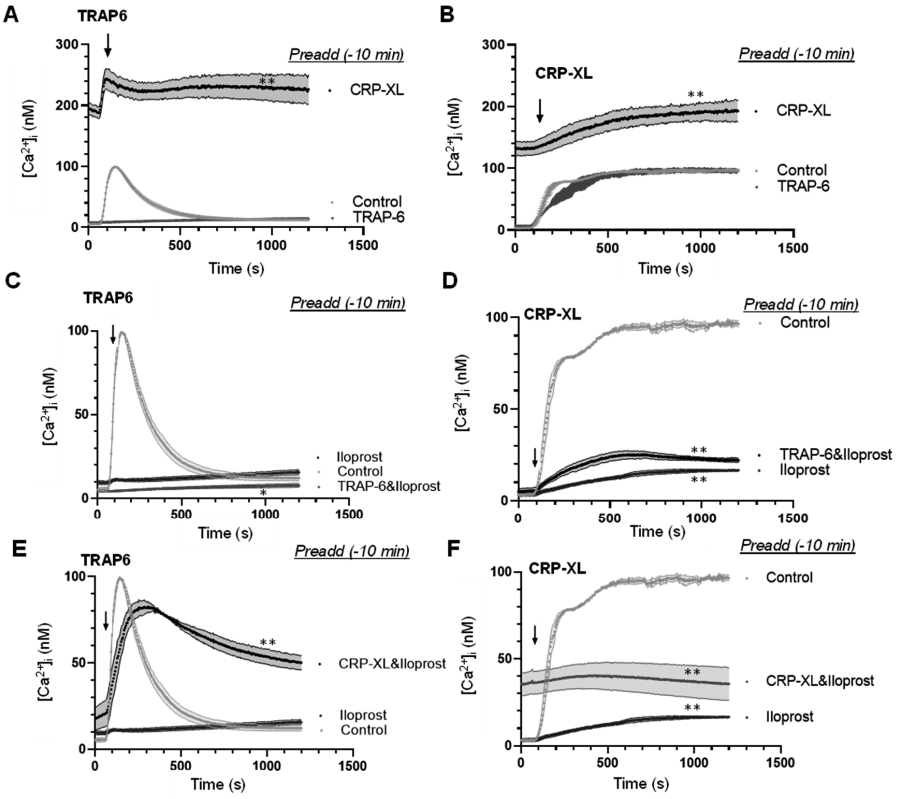

Figure 5. Recurrent Ca^{2+} signal generation induced by consecutive agonists. Calibrated $[Ca^{2+}]_i$ rises were recorded during 25 minutes of Fura-2-loaded platelets in 96-wells plates. Platelets were stimulated at indicated time point (arrow) as second agonist with 10 μM TRAP6 (**A**, **C**, **E**) or 5 μg/mL CRP-XL (**B**, **D**, **F**). (**A**, **B**) Pre-addition of vehicle (control), TRAP6 (10 μM) or CRP-XL (5 μg/mL) at 10 minutes before second agonist. (**C**, **D**) Pre-addition of vehicle control or iloprost (10 nM) with/without TRAP6 (10 μM) at 10 minutes before the second agonist. (**E**, **F**) Pre-addition of iloprost (10 nM) with/without CRP-XL (5 μg/mL) at 10 minutes before second agonist. Mean ± SE (n = 3 experiments). **P*<0.05, ***P*<0.001 vs. controls at t = 1000 seconds, paired Student t-test.

6D) enhanced the $[Ca^{2+}]_i$ rise induced by CRP-XL. Prior TRAP6 almost completely abolished the respond to secondary thrombin or ADP (**Figure 6E-F**). Markedly, however, prior CRP-XL caused a prolonged and high Ca^{2+} signal, while the platelets still responded to thrombin or ADP (**Figure 6E-F**). This indicated that PAR stimulation (with TRAP6 or thrombin) protected against secondary stimulation of these receptors. Taken together we concluded that, in terms of Ca^{2+} signaling, prior GPVI (CRP-XL) but not PAR stimulation provoked a prolonged, high activation state, which still allowed the platelets to respond to a second GPCR agonist, such as thrombin, TRAP6 or ADP.

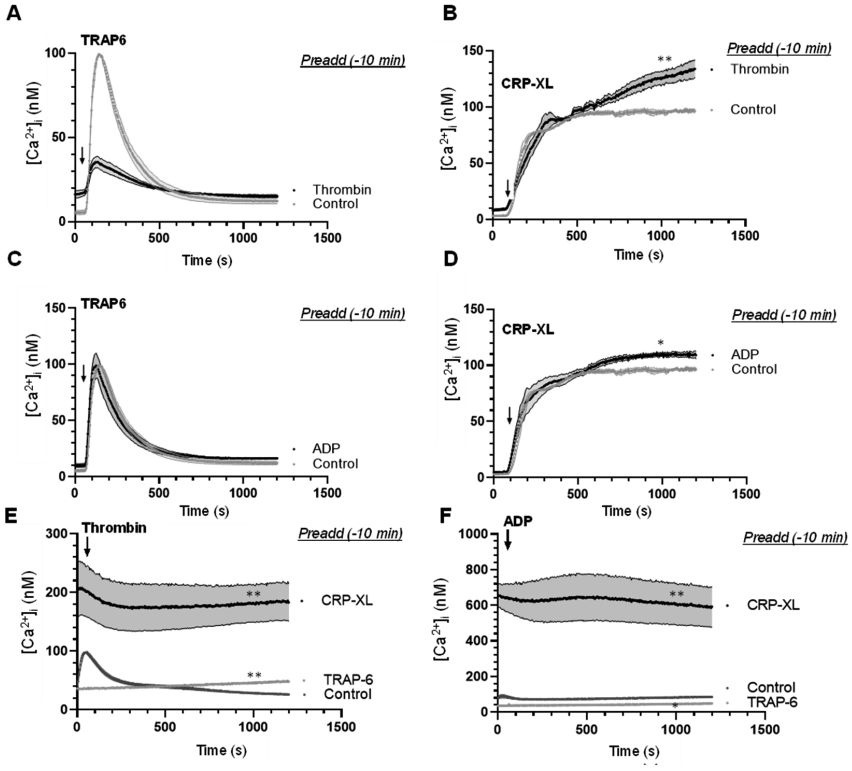

Figure 6. Effect of agonist stimulation on Ca^{2+} signaling induced by a second agonist. Calibrated $[Ca^{2+}]^i$ rises were recorded during 25 minutes of Fura-2-loaded platelets in 96-wells plates. Platelets were stimulated at indicated time point (arrow) as second agonist with 10 μM TRAP6 (**A**, **C**), 5 μg/mL CRP-XL (**B**, **D**), 1 nM thrombin (**E**) or 1 μM Me-S-ADP (**F**). (**A**, **B**) Pre-addition of vehicle (control) or thrombin (1 nM) at 10 minutes before second agonist. (**C**, **D**) Pre-addition of vehicle (control) or Me-S-ADP (1 μM) at 10 minutes before second agonist. (**E**, **F**) Pre-addition of vehicle (control), TRAP6 (10 μM) or CRP-XL (5 μg/mL) at 10 minutes before second agonist. Mean ± SE (n = 3 experiments). **P*<0.05, ***P*<0.001 vs. controls at t = 1000 sec, paired Student t-test.

Discussion

In this paper, we present new proof-of-concept data that iloprost (cAMP elevation), tirofiban (integrin αIIbβ3 blocker) and/or Syk kinase inhibition (sub)acutely affect the starting or ongoing platelet aggregation process in response to TRAP6 or CRP-XL, even when applied after these agonists. However, when compared to PAR stimulation with TRAP6, GPVI stimulation with CRP-XL provided a shorter time window for the aggregation process to stop upon secondary application of iloprost. Subacute inhibition of the tyrosine kinase Syk was only effective in case

of GPVI stimulation. This pointed to a more continued, less reversible activation signal with CRP-XL. In agreement with this, also the $[Ca^{2+}]_i$ measurements showed a more persistent activation state of the platelets after GPVI stimulation than after PAR1 stimulation, thus influencing the platelet responses to a second agonist.

Interestingly, it appeared that the platelets after initial PAR1 stimulation retained their responsiveness to GPVI stimulation, but became insensitive to a recurrent stimulation of the PAR1 receptor. Overall, tis work disclosed an unexpected high versatility of activated platelets in their ability to acutely respond to a subsequent receptor agonist, with a more prolonged signal memory effect after GPVI than after PAR stimulation.

Iloprost as a prostacyclin mimetic has been used in the clinic for platelet inhibition and vasodilatation in pulmonary hypertension treatment [18]. Our aggregation experiments indicate that late application of this inhibitor can reverse the platelet activation process even after initial receptor stimulation, yet in a way depending on the agonist and receptor type. Typically, the post-hoc inhibitory effect of iloprost decreased in the order of TRAP6 > CRP-XL. In combination with integrin αIIbβ3 antagonist tirofiban, iloprost acted even stronger, by causing substantial disaggregation after TRAP6, but not CRP-XL stimulation.

In agreement with our findings, it is known that iloprost pretreatment strongly affects TRAP6-induced platelet responses [19]. Iloprost, acting on the level of G-proteins (Gs) via adenylyl cyclase, directly competes with soluble GPCR agonists (thrombin, ADP, TxA_2) also acting on adenylyl cyclase via Gi [20-22]. Hence, the joint regulation of adenylyl cyclase activity can result in a versatile modulation of cAMP levels and PKA activity. Earlier, we have established that iloprost and ADP in terms of PKA-dependent phosphorylation act partly in an antagonistic way [23]. Several of the PKA-regulated phosphorylation sites are cytoskeletal proteins, which agrees with the notion that platelet disaggregation is accompanied by a reversal of cytoskeletal changes [24].

Mechanistically, both the prior and subacute effects of iloprost will be due to an immediate elevation in cAMP and protein kinase A (PKA), which then suppresses phospholipase C activity and ensuing $[Ca^{2+}]_i$ rises [25-27]. The more limited ability of iloprost to revert the CRP-XL induced aggregation (in comparison to TRAP6) can be explained by the longer Ca^{2+} signal with this GPVI agonist, implying a lower ability of PKA to overrule this signal. On the other hand, our laboratories have described that iloprost and other cAMP-elevating agents, as a pretreatment, are able to affect the collagen-induced platelet adhesion under stasis and flow conditions [28, 29].

Tirofiban as an integrin antagonist is in use for the prevention of thrombus formation in ischemic stroke [30]. The observed reversal of TRAP6-induced aggregation by tirofiban/iloprost is compatible with evidence from preclinical studies that integrin activation per se is a reversible process [1,31]. The acute halting of the CRP-XL-induced aggregation with inhibitor Syk-IN (with antithrombotic potential in mouse) is explained by the evidence that it is an upstream blocker of GPVI- and CLEC2-induced signaling pathways [10,32]. Markedly, the blockage of Syk activation (Syk-IN) or of integrin αIIbβ activation (tirofiban) primarily stopped the ongoing aggregation process without reversal. It thus appears that interference at different levels of the

signaling scheme (early Syk activation, or late integrin activation) can halt the further assembly of platelet aggregates, but cannot disassemble the aggregates, such as is the case with the PKA-activating compound iloprost.

The $[Ca^{2+}]_i$ measurements provided proof-of-principle evidence that platelets have the ability to respond consecutively to PAR1, P2Y and GPVI stimulation, even when these receptors are triggered 10 min apart. Interestingly, such sequential responses were not seen for dual exposure to PAR1 agonist (TRAP6, thrombin), in that a first stimulation inactivated the Ca^{2+} signal of a second stimulation. This points to a mechanism of thrombin receptor desensitization after platelet exposure to PAR agonists [33,34]. It also underlines the idea that platelet exposure to a gradient of GPCR agonists causes response diminishment [35].

Whilst it is known that continued receptor occupancy is needed for the completion of thrombin-induced $[Ca^{2+}]_i$ rises [17,36], we now find that – on the longer term (10-30 min) –, PAR1-stimulated platelets in some way become reset by a desensitization mechanism. Interestingly, such a desensitization process does not occur following GPVI stimulation, hence excluding a role of cleavage of the GPVI receptors [37]. Rather, the maintained Ca^{2+} signal with CRP-XL points to a longer-term high activation state (priming) of the platelets, which can be linked to the prolonged ability of store-regulated Ca^{2+} entry with GPVI ligands [38].

Regarding the translation relevance of our findings, at the one hand, we show that platelets have the ability to respond to multiple agonists, for instance when (in the circulation) exposed to soluble agonists or when adhered to subendothelial vascular agonists like collagen. At the other hand, our data provide more insight into the mechanism of positive and (secondarily) negative platelet priming by dual exposure to agonists and/or antagonists. More precisely, our findings suggest that the acute exposure of circulating platelets to locally generated thrombin (before it is inactivated by antithrombin) results in an only shortly increased activation state, which is antagonized by the simultaneous exposure to prostacyclin. On the other hand, it appears that platelet adhesion to vascular collagen resulting in a GPVI-mediated aggregation leads to a more persistent activation state, which influences the ensuing responses to a next agent.

Summarizing, we provide novel data that GPVI stimulation causes a more prolonged and robust priming and memory activating effect on platelets, when compared to PAR or P2Y stimulation. This work thereby revealed unexpected differences between a high versatility of platelets in sequentially responding to specific agonists and antagonists.

Declaration of interest

The authors declare that no relevant conflicts of interest exist.

Acknowledgements

J.Z. and J.W. acknowledge a bursary support from the China Scholarship Council (CSC).

Author Contributions

Conceptualization: J.W.M.H. Data curation: J.Z., J.W. Formal analysis: J. Z., J. W. Funding acquisition: J.Z., M.R., J.W.M.H. Investigation: J.Z., J.W., M.R., J.W.M.H. Methodology: J.Z., J.W. Project administration: J.W.M.H. Resources and supervision: M.R., J.W.M.H. Validation: M.R. Writing – original draft & editing: J.Z., J.W., J.W.M.H.

References

1. Versteeg HH, Heemskerk JW, Levi M, Reitsma PS. New fundamentals in hemostasis. *Physiol. Rev.* **2013**, *93*, 327-358.
2. Swieringa F, Kuijpers MJ, Heemskerk JW, van der Meijden PE. Targeting platelet receptor function in thrombus formation, the risk of bleeding. *Blood Rev*. **2014**, 2*8*, 9-21.
3. Baaten CC, Meacham S, de Witt SM, Feijge MA, Adams DJ, Akkerman JW, Cosemans JM, Grassi L, Jupe S, Kostadima M, et al. A synthesis approach of mouse studies to identify genes and proteins in arterial thrombosis and bleeding. *Blood.* **2018**, *132,* e35-e46.
4. Heemskerk JW, Vis P, Feijge MA, Hoyland J, Mason WT, Sage SO. Roles of phospholipase C and Ca^{2+}-ATPase in calcium responses of single, fibrinogen-bound platelets. *J. Biol. Chem.* **1993**, *268*, 356-363.
5. Baaten CC, ten Cate H, van der Meijden PE, Heemskerk JW. Platelet populations and priming in hematological diseases. *Blood Rev.* **2017**, *31*,389-399.
6. Van der Meijden PE, Heemskerk JW. Platelet biology and functions, new concepts and future clinical perspectives. *Nat. Rev. Cardiol*. **2019**, *16*, 166-179.
7. Heuberger DM, Schuepbach RA. Protease-activated receptors (PARs), mechanisms of action and potential therapeutic modulators in PAR-driven inflammatory diseases. *Thromb. J*. **2019**, *17*, 4.
8. Bourdon DM, Mahanty SK, Jacobson KA, Boyer JL, Harden TK. N-Methanocarba-2MeSADP (MRS2365) is a subtype-specific agonist that induces rapid desensitization of the $P2Y_1$ receptor of human platelets. *J. Thromb. Haemost.* **2006**, *4*, 861-868.
9. Gilio K, Harper MT, Cosemans JM, Konopatskaya O, Munnix IC, Prinzen L, Leitges M, Liu Q, Molkentin JD, Heemskerk JW, et al. Functional divergence of platelet protein kinase C (PKC) isoforms in thrombus formation on collagen. *J. Biol. Chem*. **2010**, *285*, 23410-23419.
10. Jooss NJ, De Simone I, Provenzale I, Fernandez DI, Brouns SL, Farndale RW, Henskens YM, Kuijpers MJ, ten Cate H, van der Meijden PE, et al. Role of platelet glycoprotein VI and tyrosine kinase Syk in thrombus formation on collagen-like surfaces. *Int. J. Mol. Sci.* **2019**, *20*, e2788.
11. Heemskerk JWM, Willems GM, Rook MB, Sage SO. Ragged spiking in free calcium in ADP-stimulated platelets, regulation of puff-like calcium signal in vitro and ex vivo. *J. Physiol*. **2001**, *535*, 625-635.
12. Hechler B, Dupuis A, Mangin PH, Gachet C. Platelet preparation for function testing in the laboratory and clinic, historical and practical aspects. *Res. Pract. Thromb. Haemost*. **2019**, *3*, 615-625.
13. Mattheij NJ, Swieringa F, Mastenbroek TG, Berny-Lang MA, May F, Baaten CC, van der Meijden PE, Henskens YM, Beckers EA, Suylen DP, et al. Coated platelets function in platelet-dependent fibrin formation via integrin αIIbβ3 and transglutaminase factor XIII. *Haematologica.* **2016**, *101*, 427-436.

14. Strehl A, Munnix IC, Kuijpers MJ, van der Meijden PE, Cosemans JM, Feijge MA, Nieswandt B, Heemskerk JW. Dual role of platelet protein kinase C in thrombus formation, stimulation of pro-aggregatory and suppression of procoagulant activity in platelets. *J. Biol. Chem.* **2007**, *282*, 7046-7055.
15. Alessi MC, Sié P, Payrastre B. Strengths and weaknesses of light transmission aggregometry in diagnosing hereditary platelet function disorders. *J. Clin. Med.* **2020**, *12*, 763.
16. Feijge MA, van Pampus EC, Lacabaratz-Porret C, Hamulyak K, Lévy-Toledano S, Enouf J, Heemskerk JW. Inter-individual varability in Ca^{2+} signaling in platelets from healthy volunteers, relation with expression of endomembrane Ca^{2+}-ATPases. *Br. J. Haematol.* **1998**, *102*, 850-859.
17. Heemskerk JW, Feijge MA, Henneman L, Rosing J, Hemker HC. The Ca^{2+}-mobilizing potency of a-thrombin and thrombin-receptor-activating peptide on human platelets. Concentration and time effects of thrombin-induced Ca^{2+} signaling. *Eur. J. Biochem*. **1997**, *249*, 547-555.
18. Higenbottam T, Butt AY, McMahon A, Westerbeck R, Sharples L. Long-term intravenous prostaglandin (epoprostenol or iloprost) for treatment of severe pulmonary hypertension. *Heart.* **1998**, *80*, 151-155.
19. McCoy KL, Traynelis SF, Hepler JR. PAR1 and PAR2 couple to overlapping and distinct sets of G proteins and linked signaling pathways to differentially regulate cell physiology. *Mol. Pharmacol*. **2010**, *77*, 1005-1015.
20. Feinstein MB, Egan JJ, Opas EE. Reversal of thrombin-induced myosin phosphorylation and the assembly of cytoskeletal structures in platelets by the adenylate cyclase stimulants prostaglandin D2 and forskolin. *J. Biol. Chem.* **1983**, *258*, 1260-1267.
21. Nagy Z, Smolenski A. Cyclic nucleotide-dependent inhibitory signaling interweaves with activating pathways to determine platelet responses. *Res. Pract. Thromb. Haemost.* **2018**, *2*, 558-571.
22. Fernandez DI, Kuijpers MJ, Heemskerk JW. Platelet calcium signaling by G-protein coupled and ITAM-linked receptors regulating anoctamin-6 and procoagulant activity. *Platelets*. **2021**, *32*, 863-871.
23. Beck F, Geiger J, Gambaryan S, Solari FA, Dell'Aica M, Loroch S, Mattheij N, Mindukshev I, Pötz O, Jurk K, et al. Temporal quantitative phosphoproteomics of ADP stimulation reveals novel central nodes in platelet activation and inhibition. *Blood*. **2017**, *129*, e 1-e12.
24. May JA, Glenn JR, Spangenberg P, Heptinstall S. The composition of the platelet cytoskeleton following activation by ADP, effects of various agents that modulate platelet function. *Platelets*. **1996**, *7*, 159-168.
25. Grant SM, Goa KL. Iloprost, a review of its pharmacodynamic and pharmacokinetic properties, and therapeutic potential in peripheral vascular disease, myocardial ischaemia and extracorporeal circulation procedures. *Drugs*. **1992**, *43*, 889-924.
26. Cavallini L, Coassin M, Borean A, Alexandre A. Prostacyclin and sodium nitroprusside inhibit the activity of the platelet inositol 1,4,5-trisphosphate receptor and promote its phosphorylation. *J. Biol. Chem*. **1996**, *271*, 5545-5551.
27. Van Gorp RM, Feijge MA, Vuist WM, Rook MB, Heemskerk JW. Irregular spiking in free calcium concentration in human platelets. Regulation by modulation of the inositol trisphosphate receptors. *Eur. J. Biochem*. **2002**, *269*, 1543-1552.
28. Margarucci L, Roest M, Preisinger C, Bleijerveld OB, van Holten TC, Heck AJ, Scholten A. Collagen stimulation of platelets induces a rapid spatial response of cAMP and cGMP signaling scaffolds. *Mol. Biosyst.* **2011**, *7*, 2311-2319.
29. Swieringa F, Solari FA, Pagel O, Beck B, Faber J, Feijge MA, Jurk K, Körver-Keularts IML, Mattheij NJ, Pohlenz J, et al. Diagnostic potential of phosphoproteome of prostaglandin-treated platelets from patients with

confirmed or suspected pseudohypoparathyroidism type 1a linked to platelet functions. *Sci. Rep.* **2020**, *10*, 11389.

30. Yang M, Huo X, Miao Z, Wang Y. Platelet glycoprotein IIb/IIIa receptor inhibitor tirofiban in acute ischemic stroke. *Drugs.* **2019**, *79*, 515-529.
31. Cosemans JM, Iserbyt BF, Deckmyn H, Heemskerk JW. Multiple pathways to switch platelet integrins on and off. *J. Thromb. Haemost.* **2008**, *6*, 1253-1261.
32. Reilly MP, Sinha U, André P, Taylor SM, Pak Y, Deguzman FR, Nanda N, Pandey A, Stolla M, Bergmeier W, et al. PRT-060318, a novel Syk inhibitor, prevents heparin-induced thrombocytopenia and thrombosis in a transgenic mouse model. *Blood*. **2011**, *117*, 2241-2246.
33. Ghilotti M, Lova P, Balduini CL, Torti M. Epinephrine induces intracellular Ca^{2+} mobilization in thrombin-desensitized platelets, a role for GPIb/IX/V. *Platelets*. **2007**, *18*, 135-142.
34. Shapiro MJ, Weiss EJ, Faruqi TR, Coughlin SR. Protease-activated receptors 1 and 4 are shut off with distinct kinetics after activation by thrombin. *J. Biol. Chem*. **2000**, *275*, 25216-25221.
35. Macwan AS, Boknäs N, Ntzouni MP, Ramström S, Gibbins JM, Faxälv L, Lindahl TL. Gradient-dependent inhibition of stimulatory signaling from platelet G protein-coupled receptors. *Haematologica*. **2019**, *104*, 1482-1492.
36. Brüne B, von Appen F, Ullrich V. Receptor occupancy regulates Ca^{2+} entry and intracellular Ca^{2+} redistribution in activated human platelets. *Biochem. J.* **1994**, *304*, 993-999.
37. Baaten CC, Swieringa F, Misztal T, Mastenbroek TG, Feijge MA, Bock PE, Donners MM, Collins PW, Li R, van der Meijden PE, et al. Platelet heterogeneity in activation-induced glycoprotein shedding, functional effects. *Blood Adv.* **2018**, *2*, 2320-2331.
38. Mammadova-Bach E, Nagy M, Heemskerk JW, Nieswandt N, Braun A. Store-operated calcium entry in blood cells in thrombo-inflammation. *Cell Calcium*. **2019**, *77,* 39-48.
39. Heemskerk JW, Calcium and platelets. In, The Molecular Basis of Calcium Action in Biology and Medicine (Pochet R, Donato R, Haiech J, Heinzmann C, Gerke V, eds.), Kluwer Acad. Publ., The Hague (the Netherlands). **2000** p. 45-71.

Supplementary Materials to Chapter 4

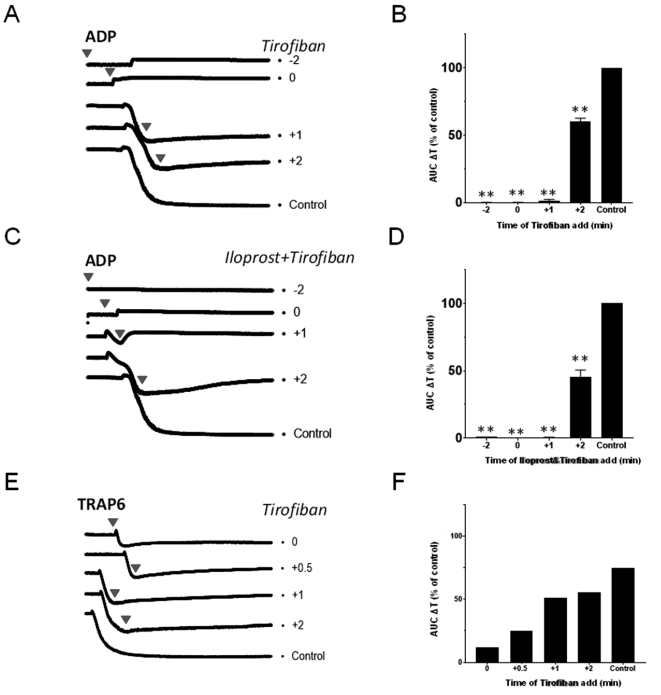

Suppl. Figure 1. Post-hoc inhibitory effect of iloprost and/or tirofiban on agonist-induced platelet aggregation in the presence of fibrinogen. Platelets in suspension containing 50 µg/mL fibrinogen were stimulated with 1 µM Me-S-ADP (**A-D**) or 10 µM TRAP6 (**E**, **F**), and aggregation was recorded by light transmission aggregometry. Iloprost (10 nM) and/or tirofiban (1 µg/mL) was added before (-2 minutes), simultaneously with (0 minutes) or after (+0.5, +1, +2 minutes) the indicated agonist. Shown are representative aggregation traces (**A**, **C**, **E**). Arrowheads indicate addition of iloprost and/or tirofiban. Bar graphs indicate the aggregation-area-under-the-curve (AUC, 10 minutes), as fractions of control (**B**, **D**, **F**). See further Figure 1. Mean ± SE (n = 3). $^{**}P<0.001$ *vs.* control traces, paired Student t-test.

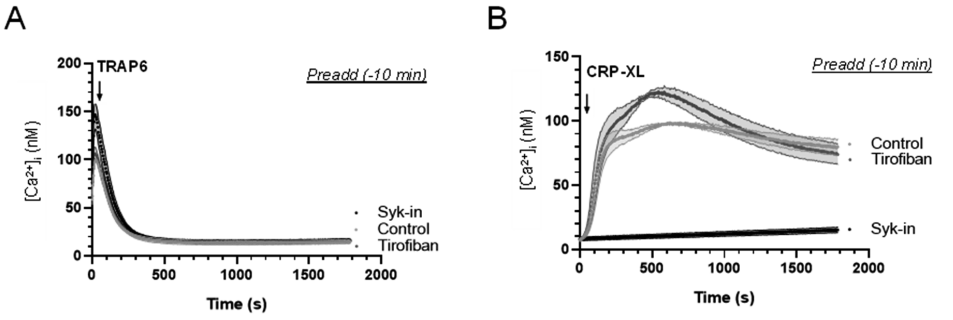

Suppl. Figure 2. Calcium responses by one agonist. Cytosolic Ca^{2+} rises were recorded of Fura-2-loaded platelets in 96-wells plates during 33 minutes. (A) Cells were preincubated with vehicle (control), tirofiban (1 µg/mL) or Syk-IN (5 µM). The platelets were stimulated with 10 µM TRAP6 (**A**) or 5 µg/mL CRP-XL (**B**) during fluorescence recording. Mean ± SE (n = 3 experiments).

Supplemental 3: Datafile containing raw data of all figures.

Chapter 5

High-throughput assessment identifying major platelet Ca^{2+} entry pathway via tyrosine kinase-linked and G protein-coupled receptors

Hilaire Yam Fung Cheung[1,2,3*], Jinmi Zou[1,4*], Chukiat Tantiwong[1,5], Delia I. Fernandez,[1,6] Jingnan Huang,[1,2,6] Robert Ahrends[2,7], Mark Roest[4], Rachel Cavill[9], Jon Gibbins[5], Steve P. Watson[3], Johan W. M. Heemskerk[1,4]

*These authors equally contributed for this work.

[1]Department of Biochemistry, Cardiovascular Research Institute Maastricht (CARIM), Maastricht University, Maastricht, The Netherlands; [2]Leibniz-Institut für Analytische Wissenschaften-ISAS-e.V, Dortmund, Germany; [3]Institute of Cardiovascular Sciences, College of Medical and Dental Sciences, University of Birmingham, Birmingham, United Kingdom; [4]Synapse Research Institute Maastricht, 6217 KD Maastricht, The Netherlands; [5]Institute for Cardiovascular and Metabolic Research (ICMR), School of Biological Sciences, University of Reading, Reading, United Kingdom; [6]Center for Research in Molecular Medicine and Chronic Diseases (CIMUS), Universidade de Santiago de Compostela, 15706 Santiago de Compostela, Spain; [7]Dept. of Analytical Chemistry, University of Vienna, Vienna, Austria; [8]Department of Advanced Computing Sciences, Maastricht University, 6229 ER Maastricht, The Netherlands; [9]Department of Pediatrics and Adolescent Medicine, Division of Pediatric Hematology and Oncology, Medical Center, University of Freiburg, Freiburg, Germany.

Cell Calcium, 2023, 112: 102738.

Abstract

In platelets, increased cytosolic Ca^{2+} is a crucial second messenger, directly or indirectly involved in all functional responses. As in other non-excitable cells, the platelet Ca^{2+} response consists of Ca^{2+} mobilization from the endoplasmic reticulum stores, complemented with store-operated and receptor-operated Ca^{2+} entry pathways. Whereas several channel types have proposed to contribute to the Ca^{2+} entry process, their relative strength and contribution are unknown in response to agonists of ITAM-linked receptors such as glycoprotein VI (GPVI) and G-protein coupled receptors such as the protease-activated receptors (PAR) for thrombin. Here, we used a 96-well plate-based high throughput assay to perform parallel $[Ca^{2+}]_i$ measurements with Fura-2-loaded human platelets in the presence of external EGTA or $CaCl_2$. Analysis resulted in sets of $CaCl_2$, EGTA and Ca^{2+} entry ratio curves, all defined by six curve parameters, reflecting the relevant Ca^{2+} ion fluxes. We report that threshold levels GPVI or PAR, with a variable contribution of secondary mediators released by platelets, induced a maximal Ca^{2+} entry ratio of 3-7. Strikingly, under conditions of Ca^{2+}-ATPase inhibition with thapsigargin, the maximal Ca^{2+} entry ratio increased to 400 (GPVI) and 40 (PAR), pointing to a receptor-dependent enhancement of store-operated Ca^{2+} entry. Upon pharmacological blockage of relevant Ca^{2+} channels in platelets, we found that, for both GPVI and PAR stimulation, the Ca^{2+} entry ratio was strongest affected by inhibition of Orai1 (2-APB, Synta66) > Na^+/Ca^{2+} exchangers (NCE), $P2X_1$ (only initial curve value); while the inhibition of TRPC6, Piezo-2 or STIM1 was of no effect. Together, these data reveal Orai1 and NCE as a dominating Ca^{2+} carriers regulating GPVI- and PAR-induced Ca^{2+} entry in human platelets.

Keywords: Orai1, platelets, sodium-calcium exchange, STIM1, store-regulated calcium entry

Introduction

Increased cytosolic Ca^{2+} is a crucial second messenger, involved in essentially all functional platelet responses, ranging from shape change, spreading, adhesion by integrin activation, dense and alpha-granule secretion, platelet aggregation and thrombus assembly up to the processes of clot retraction and development of platelet procoagulant activity [1–4]. Most platelet agonists induce a rise in cytosolic $[Ca^{2+}]_i$ to steer a variety of signaling pathways, in order to regulate actin and tubulin cytoskeleton reorganization, small molecular weight GTPase activation, networks of protein kinases and phosphatases, calpain protease activation, secretome organization, thromboxane release, and phosphoinositide and other phospholipid alterations [5–8].

In situations of hemostasis and thrombosis, platelet Ca^{2+} signaling can be evoked by ITAM-linked receptors (ILR) acting through protein tyrosine kinases, as well as by G-protein coupled receptors (GPCR) working the Gqα and Giα proteins [9]. Regarding ILR, the collagen receptor glycoprotein VI (GPVI) has been extensively studied in the context of thrombosis and hemostasis, with several anti-GPVI drugs being evaluated in clinical trials [10]. Vascular collagens and the soluble mimetic collagen-related peptide (CRP), as established GPVI agonists, operate via tyrosine phosphorylation and activation of phospholipase Cγ2 (PLCγ2) [11]. On the other hand, activation of platelet GPCR in particular occurs by soluble agonists, like thrombin (acting via PAR1 and PAR4), ADP (acting via $P2Y_1$ and $P2Y_{12}$) and thromboxane A_2 (acting via TP receptors). The common activation mechanism is Gqα-mediated activation of PLCβ isoforms with an additional Giα-mediated activation phosphoinositide 3-kinases [2,4,12]. Drugs interfering with these GPCR pathways are regularly prescribed to patients with prior cardiovascular disease. The success of the so-called secondary mediator inhibitors (SMI) – *i.e.*, aspirin to block thromboxane synthesis and ADP-receptor antagonists – relies on the fact that they suppress amplification mechanisms, rather than primary processes of platelet activation [10,13].

In human and mouse platelets, classical Ca^{2+}-signaling mechanisms operate, *i.e.*, primary internal Ca^{2+} mobilization and secondary store operated Ca^{2+} entry (SOCE) or receptor-operated Ca^{2+} entry (ROCE), such as reviewed recently [4]. These pathways are crucially involved in platelet-dependent immune responses, intravascular thrombosis formation and thrombo-inflammation in mouse, and by extension also in man [4,14,15]. In brief, PLCβ/γ activity results in the formation of inositol 1,4,5 trisphosphate ($InsP_3$), which by way of a Ca^{2+}-induced Ca^{2+} release stimulates the $InsP_3$-operated Ca^{2+} channels in the endoplasmic reticulum. Pumping back of the released Ca^{2+} from the cytosol into Ca^{2+} stores occurs by sarco- and endoplasmic reticulum Ca^{2+}-ATPases (SERCAs), which are selectively inhibited by thapsigargin, a compound that prolongs the $[Ca^{2+}]_i$ signal [9,16].

Regarding SOCE, an important role in platelets has been confirmed for the Ca^{2+} channel Orai1 [17], which via the BIN2 protein couples to the Ca^{2+} store sensor STIM1 [18]. This mechanism contributes to both the ILR- and GPCR-induced Ca^{2+} entry [4,19,20]. It has been shown that platelets from mice with a defect in STIM1, BIN2 or Orai1 display impaired Ca^{2+} responses with common agonists [20–23]. The low platelet Ca^{2+} responses were accompanied by a protection against arterial thrombus formation *in vivo* and a lowered collagen-dependent thrombus formation in vitro [4]. Similarly, in blood from immunodeficient patients with a loss-of-function

mutation in Orai1 or STIM1, in vitro thrombus formation on collagen was found to be impaired [24]. Yet, other studies suggest the operation of additional ROCE pathways in platelets as well [23,25].

Established for platelet activation is also the $P2X_1$ cation channel, as a fast way to increase $[Ca^{2+}]_i$, in response to the secondary mediator ATP [26,27]. Other papers indicate that a significant proportion of the diacylglycerol-induced ROCE in platelets is carried by transient receptor potential C (TRPC) type of cation channels, TRPC3 and TRPC6, so far with an unclear contribution to hemostasis and thrombosis [28,29]. The murine TRPC6 protein appeared to support the Orai1-dependent SOCE mechanism [30]. Additional proteins with a possible contribution to Ca^{2+} entry in platelets are the mechanosensitive Piezo1/2 ion channels [31], and Na^+/Ca^{2+} exchangers (NCE) operating in reverse mode [32].

While several channel types are considered to contribute to SOCE and ROCE in human platelets, their relative strength and contribution to the agonist-induced Ca^{2+} entry process are unknown. In the present paper, we investigated this in Fura-2-loaded platelets by parallel measurements of $[Ca^{2+}]_i$ in the presence of external EGTA or $CaCl_2$, thus blocking or allowing Ca^{2+} entry, respectively, using a previously established 96-well plate-based high throughput assay [33]. For the studies we used two GPVI (ILR) agonists, *i.e.,* CRP and collagen, and two PAR (GPCR) agonists, thrombin and TRAP, as well as the SERCA inhibitor thapsigargin. By systematic comparison of the Ca^{2+} entry traces we were able to directly compare the effects of pharmacological blockage of Orai1, STIM1, TRPC6, P2X1, Piezo1/2 or NCE.

Materials and methods

Materials

Thrombin was obtained from Enzyme Research Laboratories (South Bend IN, USA). Thrombin receptor-activating peptide SFLLRN (TRAP) was purchased from Bachem (Bubendorf, Switzerland); cross-linked collagen-related peptide (CRP) came from the University of Cambridge (Cambridge, United Kingdom); Fura-2 acetoxymethyl ester and human fibrinogen were obtained from Invitrogen (Carlsbad, CA, USA); Pluronic F-127 from Molecular Probes (Eugene OR, USA). 2-aminoethyl diphenylborinate (2-APB) and ORM-10,103, 2-[(3,4-dihydro-2-phenyl-2H-1-benzopyran-6-yl)oxy]- 5-nitro-pyridine were from Sigma-Aldrich (St. Louis, MO, USA), GsMTx4 was from Tocris Bioscience (Bristol, United Kingdom), MRS-2159 from Santa-Cruz (Santa-Cruz, CA, USA), ML-9 and BI-749327 were from MedChem Express (Monmouth Junction, NJ, USA). Human α-thrombin came from Kordia (Leiden, The Netherlands). Standard Horm-type collagen (dissolved in 0.1 M acetic acid) was obtained from Nycomed (Hoofddorp, The Netherlands). Synta-66, 3-fluoropyridine-4-carboxylic acid (2′,5′-dimethoxybiphenyl-4-yl) amide, came from GlaxoSmithKline (London, UK). The PAR4-activating peptide AYPGKF-NH_2 was a kind gift of Synpeptide Ltd. (Pudong, Shanghai, China). Other materials were from sources, described before [34].

Subjects and blood collection

Blood was taken by venipuncture from healthy male and female volunteers who had not taken anti-platelets in the previous ten days, after full informed consent according to the Helsinki declaration. The study was approved by the Medical Ethics Committee of Maastricht University. According to the approval, blood donor age and sex were not recorded. Blood was collected into 3.2% sodium citrate (Vacuette tubes, Greiner Bio-One, Alphen a/d Rijn, the Netherlands). Blood donors had platelet counts within the reference range, as measured with a Sysmex XN-9000 analyzer (Sysmex, Kobe, Japan).

Platelet isolation and loading with Fura-2

Platelet-rich plasma (PRP) and washed platelets were obtained from citrated blood, as described earlier [23,35]. PRP was obtained through centrifugation of blood samples at 260 *g* for 10 minutes, after supplementation of 1:10 vol/vol acid citrate dextrose (ACD; 80 mM trisodium citrate, 183 mM glucose, 52 mM citric acid). The collected PRP was then centrifuged in Eppendorf tubes at 2360 g for 2 minutes. The pelleted platelets were resuspended into Hepes buffer pH 6.6 (10 mM Hepes, 136 mM NaCl, 2.7 mM KCl, 2 mM $MgCl_2$, 5.5 mM glucose, and 0.1% bovine serum albumin). After addition of apyrase (1 unit/mL) and 1:15 vol/vol ACD to the platelet suspension, another centrifugation step was performed to obtain washed platelets. Based on an earlier protocol [36], the washed platelets resuspended into Hepes buffer pH 7.45 at a count of 2×10^8/mL were loaded with Fura-2 acetoxymethyl ester (3 μM) and Pluronic F-127 (0.4 μg/mL) for 40 minutes at room temperature. In comparison to a previous protocol, the loading at room temperature and the pre-mixing of probe with Pluronic F-127 prevented accumulation of de-esterified dye in the intracellular organelles [37]. Once loaded with Fura-2, the cells were centrifuged in the presence of apyrase (1 unit/mL) and 1:15 vol/vol ACD. The final platelet count after resuspension into Hepes buffer pH 7.45 was 2×10^8/mL. Adequacy of Fura-2 loading in the cytoplasm was confirmed by a >90% quenching of the isosbestic Fura-2 signal (360 nm excitation) with $MnCl_2$ [16]. In addition, microscopic examination of spread platelets did not show compartmentalization of the Fura-2 fluorescence.

The commonly used procedure of ACD and apyrase silencing of platelets prevented autocrine activation, while maintaining resting cyclic-AMP levels [38]. Platelet activation markers (P-selectin and PAC1 antigen) were <2% using the platelet isolation procedure [39].

Calibrated high-throughput platelet $[Ca^{2+}]_i$ measurements

Changes in $[Ca^{2+}]_i$ of Fura-2-loaded platelets were measured in 96-well plates using a FlexStation 3 robot (Molecular Devices, San Jose, CA, USA), basically as described [33,40]. The Xenon flash light-based measurements of fluorescence, in combination with the excellent optics of the FlexStation3 reader chip allowed to measure with limited fluorescence bleaching.

In brief, 200 μL samples of platelets (2×10^8/mL) per well were left untreated or were pretreated with apyrase (0.1 U/mL) and indomethacin (20 μM) for 10 minutes at room

Table 1. Platelet agonists, receptors and channels reported to modulate Ca^{2+} responses. For full inhibitor names, see methods section. Protein copy numbers per platelet were taken from Ref. [57].

Compound	1st target	Copies	2nd targets	Ref. conc.	Ref.
Agonists					
CRP	GPVI	9577	n.a.	0.1-30 µg/mL	[33]
Collagen	GPVI	9577	α2β1	1-10 µg/mL	[35]
Thrombin	PAR1/4	n.a./ 1095	GPIbα	0.3-30 nM	[33]
TRAP	PAR1	n.a.	n.a.	0.5-15 µM	[33]
Modulators					
SMI*	$P2Y_1$, COX1	~1000	$P2Y_{12}$	0.1 U/mL, 20 µM	[33]
Thapsigargin	SERCA2b	25,272	SERCA3	1 µM	[24]
Channel inhibitors					
2-APB	Orai1	1,658	$InsP_3$ R**	10 µM	[45]
BI-749327	TRPC6	1,101	n.a.	0.1 µM	[47]
GsMTx4	Piezo1/2	2***	n.a.	3 µM	[31]
ML-9	STIM1	7,423	MLCK, Akt	30 µM	[46]
MRS-2159	$P2X_1$	1,441	$P2Y_1$	1 µM	[27]
ORM-10103	NCX3	578	NCX1	10 µM	[32]
Synta66	Orai1	1,658	n.a.	10 µM	[45]

*Secondary mediator inhibitors (SMI) = apyrase + indomethacin; **$InsP_3$ receptors type 1-3 (4,873 copies); ***for mouse platelets [58].

temperature. Where indicated, pharmacological inhibitors to block Ca^{2+} entry were added (at room temperature) (see **Table 1**). After the addition of either 0.1 mM EGTA or 2 mM $CaCl_2$, the platelets in wells were temperature adjusted (37 °C), and fluorescence was recorded at two excitation wavelengths for 10 minutes. During the measurements, 20 µL of agonist solution was added by automated pipetting. Note that the mixing of agonist with Fura-2-loaded platelets was diffusion-limited, and occurred by high-speed injection of 10% volume of the agonist solution. Prior to default use, injection volume and speed (125 µL/sec) were optimized as to obtain maximal platelet responses [33].

Changes in Fura-2 fluorescence (37 °C) were measured per row by ratiometric fluorometry, using excitation wavelengths of 340 and 380 nm and a single emission wavelength of 510 nm [33]. Fura-2 fluorescence ratio values per well were obtained every 4 seconds. Separate calibration wells contained Fura-2-loaded platelets that were lysed with 0.1% Triton-X-100 in the presence of either 1 mM $CaCl_2$ or 1 mM EGTA/Tris for determining R_{max} and R_{min} values [35]. After the correction for 340 and 380 nm background fluorescence levels, nanomolar changes in $[Ca^{2+}]_i$ were calculated according to the Grynkiewicz equation with a K_d of 224 nM [41]. All measurements were completed within 2–3 hours of isolation of cells.

For the present measurements, the loading concentration with Fura- 2 AM was optimized, giving a stable calibrated Ca^{2+} responses at 1.5 to 3 µM, and highest 340 nm fluorescent agonist signals (+22%, n = 3) and lowest a noise at 3 µM. Dye leakage from the platelets appeared to be negligible; this was observed by a minimal, <5 nM apparent $[Ca^{2+}]_i$ rise upon addition of 1 mM $CaCl_2$ to unstimulated cells.

For the relative assessment of Ca^{2+} entry, activation experiments were routinely performed in parallel (duplicate) wells, containing either 0.1 mM EGTA or 2 mM $CaCl_2$. Accordingly, after calibration, sets of nM $[Ca^{2+}]_i$ traces were obtained without (EGTA) or with ($CaCl_2$) Ca^{2+} entry.

Data analysis and molecular calculations

The nanomolar $[Ca^{2+}]_i$ traces (4–6 second intervals during 600 seconds) were floating-point averaged before further processing. Per agonist and inhibitor condition, then ratioed Ca^{2+} entry traces were calculated. These were obtained by dividing the nanomolar traces in the presence of $CaCl_2$ by the corresponding traces in the presence of EGTA. Taking into account the assumptions mentioned below, the ratioed $[Ca^{2+}]_i$ traces represent the relative amount of Ca^{2+} entry per unit of intracellular Ca^{2+} release (Eq. 1):

$$\frac{[\text{Ca}]\text{i in CaCl2}}{[\text{Ca}]\text{i in EGTA}} = \frac{\text{ER release} + \text{Entry}}{\text{ER release}} = 1 + \frac{\text{Entry}}{\text{ER release}}$$

Using a script in Excel, the $[Ca^{2+}]_i$ traces with $CaCl_2$ or EGTA were analyzed on six curve parameters: the nM levels at start (P1), at first peak (P4) and final (P6); the initial slope after agonist addition as nM/s (P2) and the change of slope (P3); furthermore, the agonist-induced increase in area-under-curve over 600 seconds (P5). For the Ca^{2+} entry ratio curves, these curve parameters were calculated as well. The following assumptions were used for the molecular calculation of Ca^{2+} fluxes in a representative platelet (of average size). Mean platelet volume (average from 96 volunteers) was set at 10.24 fL [42]. Based on electron microscopic images [43], the volume contribution of intracellular organelles and open canicular system was set at 20%, which resulted in a mean cytosolic volume of 8.92 fL. For 0.4×10^8 platelets per well, this gave a total cytosolic volume of 3.57×10^{-7} L. Considering the single-platelet cytosolic volume of 8.92 fL, then a $[Ca^{2+}]_i$ increase of 1 nM represents 8.92×10^{-24} mol, *i.e.* 5.37 mobilized Ca^{2+} ions per single platelet. Considerations for interpretation of the $[Ca^{2+}]_i$ traces were as follows. *(i)* In Fura-2-loaded platelets, the low resting $[Ca^{2+}]_i$ was set at ~20 nM. *(ii)* Rises in $[Ca^{2+}]_i$ in response to agonists were considered to be the mathematical summation of $InsP_3$-induced Ca^{2+} release from the endoplasmic reticulum (ER, taken as one undivided compartment) and from extracellular Ca^{2+} entry via ion channels and exchangers. This implies that any enforcement of $InsP_3$ channel activity by extracellular $CaCl_2$ via Ca^{2+}-induced Ca^{2+} release [1] is attributed to the entry part. Concerning the mitochondrial and lysosomal Ca^{2+} compartments, of which the sizes and regulation are poorly established [4], these are considered as a providing a fixed fractional contribution to the total Ca^{2+} stores, not contributing to $InsP_3$-induced Ca^{2+} release. *(iii)* It is thus assumed that measurements in the presence of 0.1 mM EGTA reflect only intracellular Ca^{2+} release, while measurements in the presence of 2 mM $CaCl_2$ reflect the summed contribution of intracellular Ca^{2+} release and extracellular Ca^{2+} entry. *(iv)* By using suspensions of 0.4×10^8 platelets, intercellular heterogeneity due to single-cell oscillations will be averaged out [44]. *(v)* Transient decreases in $[Ca^{2+}]_i$ are considered to result from the combined Ca^{2+}-ATPase activities of SERCA and PMCA (plasma membrane Ca^{2+}-ATPases) isoforms, unless indicated otherwise. *(vi)*

In calculations, the cytosolic Ca^{2+}-buffering capacity of Fura-2 and the likely fractional uptake into mitochondria were discarded. *(vii)* Finally, the maximal $[Ca^{2+}]_i$ level to be achieved was set at 200 × K_d (44.8 μM).

Pharmacologic inhibition of Ca^{2+} responses

An overview of relevant platelet receptors and channels with protein copy numbers is provided in **Table 1**. The table also contains the compounds reported to block Ca^{2+} channels or exchangers with reasonable selectivity at indicated concentration. In experiments with Fura-2- loaded platelets in the presence of EGTA or $CaCl_2$, the indicated compounds were always tested versus relevant vehicle solution (final DMSO concentration <0.5%).

Heatmaps and statistics

Data are expressed as means ± SD. The program GraphPad Prism 8 (San Diego, CA, USA) was used for statistical analyses. Regression analysis was performed with the program R, which was also used for heatmap generation. For heatmap representation, values per curve parameter sets (P1+4+6, P2+3, or P5) were univariate-scaled at 0–100% per indicated set of conditions, as indicated in the figure legends. Statistical significance, calculated by a two-tailed *t*-test, was defined as $P<0.05$.

Results

High Ca^{2+} entry ratio in GPVI-stimulated platelets

To quantify how GPVI-induced extracellular Ca^{2+} entry (via ILR) relied on intracellular Ca^{2+} mobilization in platelets, we performed dose-response experiments, using the strong agonist CRP and the weaker agonist collagen type-I for this receptor [9]. Employing the 96-well plate method with automated agonist injection [33,40], each agonist was added to Fura-2-loaded platelets in the presence of external $CaCl_2$ or EGTA. After calibration we obtained parallel curves of nanomolar rises in $[Ca^{2+}]_i$ for 600 seconds, either with or without Ca^{2+} entry, which were analyzed for 6 curve parameters (P1, basal nM level; P2, slope to initial peak; P3, change of slope; P4, first nM peak level; P5, area-under-the-activation curve; and P6, final nM level). By ratioing the two parallel curves, we obtained corresponding Ca^{2+} entry ratio curves, which were analyzed for the same parameters.

Platelet stimulation with CRP (1–30 μg/mL) resulted in a dose dependent increased $[Ca^{2+}]_i$ peak level, followed by a sustained phase in the presence of either $CaCl_2$ or EGTA (**Figure 1A i-ii**). Quantification versus the reference condition of $CaCl_2$/CRP 10 μg/mL indicated that the first peak level (P4) at all agonist doses was 3–5 fold higher with CaCl2 than with EGTA presence (**Table 2**). Further comparison of the curves indicated a longer time-to-peak, when the Ca^{2+}

entry was eliminated (**Figure 1A i-ii**). The Ca^{2+} entry ratio curves showed a dose-dependent enhancement of slope, reaching a maximal level of 4–7 (**Figure 1A iii**).

To examine the contribution of autocrine platelet agonists (i.e. released thromboxane A_2 and ADP) to the CRP-induced Ca^{2+} responses, the Fura-2-loaded platelets in wells were pre-incubated with secondary mediator inhibitors (SMI) apyrase (0.1 units/mL) and indomethacin (20 μM), *i.e.* a treatment sufficient to block the autocrine Ca^{2+} release events [45]. At all CRP concentrations, we observed a lowering and delay of the $[Ca^{2+}]_i$ traces, although the SMI effects were relatively larger in the presence of $CaCl_2$ than with EGTA (**Figure 1A iv-v**). Quantitation of the first peak indicated a 20–55% reduction with SMI, which percentage increased with the CRP dose in the presence of $CaCl_2$. In contrast, there was a consistent ~25% reduction by SMI in the presence of EGTA (**Table 1**). Concerning in the Ca^{2+} entry ratio traces, the presence of SMI reduced the curve maximum from 7 to 3 in cases of ≥10 μg/mL CRP, while no agonist signal was observed at the lower doses (**Figure 1A vi**). Platelet stimulation with collagen (1–30 μg/mL) in the presence of $CaCl_2$ led to relatively low $[Ca^{2+}]_i$ peak levels (**Suppl. Figure 1A i**), not exceeding 9 ± 1% to 19 ± 1% of the peak levels obtained at 10 μg/mL CRP (**Table 2**). This is in agreement with earlier findings that collagen in platelet suspensions acts as a weak GPVI agonist [40]. The observed flat $[Ca^{2+}]_i$ traces with EGTA indicated that the collagen-induced Ca^{2+} signal relied on Ca^{2+} entry, but with Ca^{2+} ratio curves not exceeding a peak value of 2 (**Suppl. Figure 1A ii-iii**). The presence of SMI annulled the collagen-induced $[Ca^{2+}]_i$ traces, indicating a necessarily enforcement by autocrine agonists (**Supp. Figure 1A iv-vi**). Jointly, these findings indicated that a certain activation level of GPVI, supported by secondary mediators, needs to be reached to induce a Ca^{2+} entry ratio peak value of 3–7.

Table 2. Relative agonist-induced first-peak rises of $[Ca^{2+}]_i$ of platelets under conditions of Ca^{2+} entry (+$CaCl_2$) or only intracellular Ca^{2+} mobilization (+EGTA). Experiments performed as in Figures 1-2; peak levels were reached at 75-150 seconds. Agonist doses 1-4 were ordered from low to high, as indicated. Secondary mediator inhibitors (SMI) were used, where indicated. Peak values in nM per donor were normalized for conditions of CRP 10 + $CaCl_2$ or thrombin (10 nM) + $CaCl_2$. Data are mean ± SD (n = 3-7). All $P<0.05$ versus 100% (t test). Full data are presented in Suppl. Datafile 1.

Condition	Basal	Dose 1	Dose 2	Dose3	Dose 4
CRP *(0, 1, 3, 10, 30 μg/mL)*					
$CaCl_2$	10 ± 4%	36 ± 4%	64 ± 5%	**100%**	142 ± 8%
$CaCl_2$ + SMI	8 ± 4%	29 ± 7%	46 ± 1%	59 ± 1%	64 ± 2%
EGTA	8 ± 4%	11 ± 2%	18 ± 2%	22 ± 3%	28 ± 3%
EGTA + SMI	6 ± 2%	9 ± 1%	14 ± 1%	17 ± 1%	21 ± 3%
Thrombin *(0, 0.3, 1, 3, 10 nM)*					
$CaCl_2$	10 ± 4%	20 ± 3%	35 ± 8%	57 ± 6%	**100%**
$CaCl_2$ + SMI	8 ± 4%	14 ± 1%	29 ± 1%	46 ± 10%	88 ± 3%
EGTA	8 ± 4%	13 ± 3%	19 ± 3%	26 ± 4%	39 ± 7%
EGTA + SMI	6 ± 2%	10 ± 1%	14 ± 2%	20 ± 2%	26 ± 4%

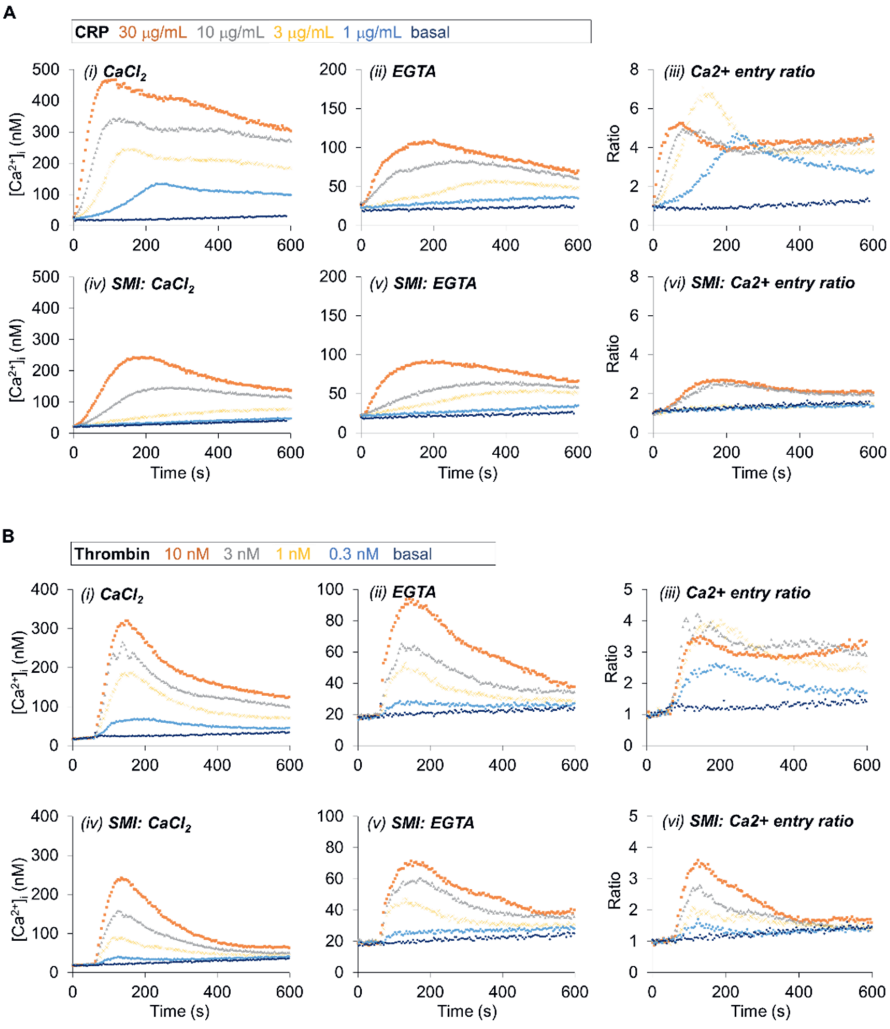

Figure 1. Dose-dependency of Ca^{2+} entry by strong collagen and thrombin receptor agonists. Fura-2-loaded platelets in 96-well plates were left untreated or were pre-incubated with SMI (0.1 U/mL apyrase and 20 µM indomethacin). Roboted stimulation in the presence of 2 mM $CaCl_2$ or 0.1 mM EGTA was with CRP (1-30 µg/mL) or thrombin (0.3-10 nM). Measurements by ratio fluorometry were performed for 600 seconds using a FlexStation 3, and values were converted into calibrated nM levels of $[Ca^{2+}]_i$. Agonists were injected into wells at 60 seconds (t = 0) and reached platelets in a diffusion-limited way. (**A-B**) Calibrated $[Ca^{2+}]_i$ traces (non-smoothed) upon stimulation with CRP (**A**) or thrombin (**B**), obtained in the absence (**i-iii**) or presence (**iv-vi**) of SMI (non-smoothed). Parallel traces were measured in the presence of $CaCl_2$ (left panels) or EGTA (middle panels). Curves of Ca^{2+} entry ratio (right panels) were obtained by dividing the corresponding $CaCl_2$/EGTA curves, indicating the relative Ca^{2+} entry over time. Data are representative of at least three experiments (n = 3-5 donors). For curve parameters, see Suppl. Datafile 1.

Moderate Ca^{2+} entry ratio in PAR-stimulated platelets

For comparison to the GPVI-induced $[Ca^{2+}]_i$ traces in platelets, we performed similar experiments employing the PAR agonists thrombin (activates PAR1 and PAR4) and TRAP (activates only PAR1). With $CaCl_2$ present, thrombin (0.3–10 nM) induced transient increases in $[Ca^{2+}]_i$, which were dose-dependent in size (**Figure 1B i**). In the presence of EGTA, thrombin gave 30–50% lower peak values (**Table 2**), which resulted in Ca^{2+} entry ratio curves that reached a maximum of 3–4 (**Figure 1B ii-iii**). Upon incubation with SMI, thrombin provoked similar $[Ca^{2+}]_i$ traces, which were only 20% lower regardless of the presence of $CaCl_2$ or EGTA (**Figure 1B iv-v**). With SMI present, the overall peak values were reduced to the same extent (**Table 2**), while the Ca^{2+} entry ratio curves had a more transient shape (**Figure 1B vi**). Accordingly, both the individual Ca^{2+} peak values (**Table 2**) and the Ca^{2+} entry ratio curves pointed to a higher threshold of the thrombin dose for Ca^{2+} entry in the presence than in the absence of SMI (3 nM versus 0.3 nM). The PAR1 agonist TRAP (0.5–15 μM) with $CaCl_2$ present evoked similar dose-dependent $[Ca^{2+}]_i$ traces as seen with thrombin, although at 25% lower peak values and an early decrease to basal level within 7 minutes (**Suppl. Figure 1B i**). The derived Ca^{2+} entry ratio curves showed peak values of 3–4 (**Suppl. Figure 1B ii-iii**). When the platelets were treated with SMI and stimulated by TRAP, the (Ca^{2+} entry ratio) curves were more transient (**Suppl. Figure 1B iv-vi**). These data collectively pointed to a moderate Ca^{2+} entry ratio upon threshold levels of PAR activation, with a relatively limited contribution of secondary mediators.

Comparing of GPVI and PAR agonist effects on Ca^{2+} entry

To provide an overall comparison of the various conditions of GPVI stimulation, we compared the obtained curve parameters between experiments, and averaged these per condition (for raw data, see **Datafile 1**). The six curve parameters P1–6 were considered to reflect the net amounts and rates of Ca^{2+} mobilization and entry into the cytosol, under conditions of back-pumping by Ca^{2+}-ATPases in the endoplasmic reticulum and plasma membrane. Heatmapping after univariate scaling of relevant parameter sets was then performed to make a direct comparison of the Ca^{2+} responses between agonists and doses. For CRP, the obtained heatmap indicated a stronger dose-dependent increase of all scaled parameters (except for P1) in the presence of $CaCl_2$, when compared to the EGTA condition (**Figure 2A**). The $CaCl_2$-dependent effect was also apparent from the heatmapped Ca^{2+} entry ratio parameters. In the presence of SMI, parameter values of the $CaCl_2$ and Ca^{2+} entry ratio curves were reduced to half. For the weaker GPVI agonist collagen, this scaling underlined the low, both $CaCl_2$- and SMI-dependent responses (**Figure 2B**).

A separate heatmap of scaled parameters for thrombin (**Figure 2C**) and TRAP (**Figure 2D**) demonstrated also dose-dependency, but with smaller differences between $CaCl_2$ and EGTA curves than for the GPVI agonists. A reducing effect by SMI was seen that is limited at all doses. When compared to thrombin, PAR1 stimulation with TRAP gave a similar heatmap profile, but with overall lower parameter values. Taken together, these results point to a higher reliance on Ca^{2+} entry and secondary mediators for the prolonged $[Ca^{2+}]_i$ traces induced by the GPVI agonists than for traces of the PAR agonists.

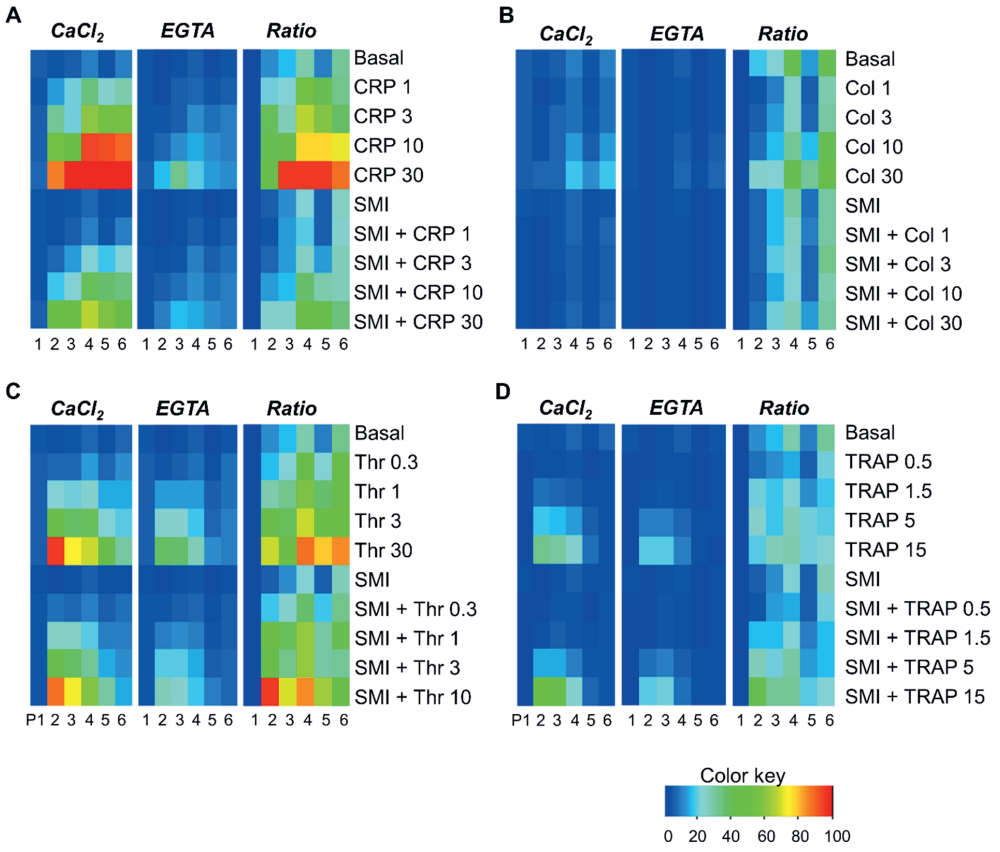

Figure 2. Comparative dose-dependent effects on Ca^{2+} entry by collagen and thrombin receptor agonists. Fura-2-loaded platelets were stimulated with 1-30 µg/mL CRP (**A**), 1-30 µg/mL collagen (**B**), 0.3-10 nM thrombin (**C**) or 0.5-15 µM TRAP (**D**), as in (Suppl.) Figure 1. The cells were pre-incubated with secondary mediator inhibitors (SMI), as indicated. In parallel smoothed $[Ca^{2+}]_i$ curves were generated with $CaCl_2$ or EGTA present, as well as Ca^{2+} entry ratio curves. Data are mean values from at least three experiments (n = 3-5 donors), scaled at 0-140% across $CaCl_2$ and EGTA conditions. Scaling was separate for Ca^{2+} entry ratio curves. Heatmaps are shown of scaled curve parameters per agonist. Color key shows scale %. Consecutive columns indicate: level at start (P1), slope to first peak (P2), maximal change of slope (P3), maximal peak level (P4), area under the response curve over 600 s (P5), and end level after 600 seconds (P6). Note that scaling was combined for parameters of (**i**) all $[Ca^{2+}]_i$ values (P1,3,6), (**ii**) all $[Ca^{2+}]_i$ slopes (P2,3), and (**iii**) $[Ca^{2+}]_i$ integrals (P5). For values, see Suppl. Datafile 1.

Potent enforcement of GPVI-induced Ca^{2+} entry ratio by SERCA inhibition

Considering that the SERCA inhibitor thapsigargin (**Table 1**) stimulates Ca^{2+} entry by a continued Ca^{2+} store depletion [4], we performed a similar series of experiments by combining the GPVI or PAR agonists with an optimal dose of 1 µM thapsigargin. When combined with thapsigargin, CRP dose-dependently induced a higher increase in $[Ca^{2+}]_i$ in the presence of $CaCl_2$ and EGTA (**Figure 3A i-ii**). Quantification of the $[Ca^{2+}]_i$ levels at peak time indicated a 30–150

higher increase in the presence of $CaCl_2$ (**Table 2**). Similarly, the Ca^{2+} entry ratio curves showed a progressive increase, reaching ratio levels as high of 300–400, hence pointing to a massively enhanced entry of Ca^{2+} (**Figure 3A iii**). Of note, at very high $[Ca^{2+}]_i$ of >10 μM far above the K_d of Fura-2 of 224 nM, the traces showed fluctuations caused by even minimal changes in fluorescence ratio.

When the platelets were treated with SMI, the traces with CRP + thapsigargin traces reduced 3–4 fold with $CaCl_2$, while those with EGTA lowered by 25% (**Figure 3A iv-v**). The changes are also apparent from the quantified peak values (**Table 3**). With SMI, the Ca^{2+} entry ratio curves reached a lower maximum, but still reaching a value to 150 at the highest CRP dose (**Figure 3A vi**).

Platelet stimulation with collagen (1–10 μg/mL) + thapsigargin (1 μM) led to higher $[Ca^{2+}]_i$ traces in the presence of $CaCl_2$, but not of EGTA (**Suppl. Figure 2A i-ii**). Of note, the highest collagen dose of 30 μg/mL gave a lower Ca^{2+} response, due to the presence of acetic acid and the pH sensitivity of the Ca^{2+} entry process [46,47]. At 10 μg/mL collagen + thapsigargin, the Ca^{2+} entry ratio curves still reached levels of 30–40 (**Suppl. Figure 2A iii**). Again, the traces flattened in the presence of SMI (**Suppl. Figure 2A iv-vi**). Together, these data indicate a potent enforcement of extracellular Ca^{2+} entry in GPVI-activated platelets under conditions of SERCA inhibition with thapsigargin.

Moderate enforcement of PAR-induced Ca^{2+} entry ratio by SERCA inhibition

Similar experiments were performed by activating the platelets with thapsigargin (1 μM) plus thrombin (0.3–30 nM). With $CaCl_2$ present this led to a dose-dependent ~2 μM peak increase in $[Ca^{2+}]_i$, which was followed by a sustained $[Ca^{2+}]_i$ elevation (**Figure 3B i**). With EGTA present, the $[Ca^{2+}]_i$ peak maximally reached 150 nM (**Figure 3B ii**). The combination of thapsigargin and thrombin raised the maximal and final levels of Ca^{2+} entry ratio curves to 15 and 40, respectively (**Figure 3B iii**). This pointed to a lower Ca^{2+} entry than that seen with CRP. In the presence of SMI, thrombin + thapsigargin showed similarly shaped $[Ca^{2+}]_i$ traces, although amplitudes of the $CaCl_2$ and Ca^{2+} entry curves were lower (**Figure 3B iv-vi**). This reduction, especially at lower thrombin concentrations, also appeared from the quantified peak levels (**Table 3**).

For platelet stimulation of TRAP plus thapsigargin, a peak increase to 2–5 μM was observed in the presence of $CaCl_2$, which was similar to that of thrombin (**Suppl. Figure 2B i**). For traces in the presence of EGTA, amplitudes reached 90 nM, *i.e.,* lower than with thrombin (**Suppl. Figure 2B ii**). The Ca^{2+} entry ratio curves were reminiscent to those of (lower doses of) thrombin (**Suppl. Figure 2B iii**). With SMI and $CaCl_2$ present, the $[Ca^{2+}]_i$ traces of TRAP + thapsigargin though were markedly reduced, with Ca^{2+} entry ratio curves not exceeding 20 (**Suppl. Figure 2B iv-vi**). Accordingly, the enforcement of thapsigargin-induced Ca^{2+} entry was lower with PAR agonists than with the strong GPVI agonist CRP.

Table 3. Relative agonist-induced peak rises of $[Ca^{2+}]_i$ in the presence of thapsigargin under conditions of Ca^{2+} entry (+$CaCl_2$) or only intracellular Ca^{2+} mobilization (+EGTA). Experiments performed as in Figure 1-2; peak levels of traces with EGTA were at 75-150 seconds, and with $CaCl_2$ at 450-500 s (CRP) or 250-300 seconds (thrombin). Agonist doses 1-4 were ordered from low to high, as indicated. Final thapsigargin concentration was 1 μM. Secondary mediator inhibitors (SMI) were present, where indicated. Peak values in nM per donor were normalized for conditions of CRP (10 μg/mL) + $CaCl_2$ or for thrombin (10 nM) + $CaCl_2$. Data are mean ± SD (n = 3-6). All $P<0.05$ versus 100%, except for *not significant (t test). Full data are presented in Suppl. Datafile 1.

Condition	Basal	Dose 1	Dose 2	Dose 3	Dose 4
Thapsigargin + CRP *(0, 1, 3, 10, 30 μg/mL)*					
$CaCl_2$	3 ± 2%	23 ± 14%	56 ± 45%	**100%**	140 ± 98%*
$CaCl_2$ + SMI	1.0 ± 0.1%	5 ± 4%	10 ± 8%	22 ± 19%	42 ± 46%
EGTA	0.3 ± 0.1%	0.8 ± 0.3%	0.8 ± 0.3%	0.9 ± 0.3%	0.9 ± 0.3%
EGTA + SMI	0.3 ± 0.1%	0.5 ± 0.1%	0.5 ± 0.1%	0.6 ± 0.1%	0.7 ± 0.2%
Thapsigargin + thrombin *(0, 0.3, 1, 3, 10 nM)*					
$CaCl_2$	19 ± 8%	46 ± 24%	66 ± 35%	63 ± 29%	**100%**
$CaCl_2$ + SMI	6 ± 3%	22 ± 10%	34 ± 13%	71 ± 39%*	92 ± 51%*
EGTA	1.7 ± 0.8%	4.1 ± 0.3%	4.6 ± 0.4%	5.2 ± 0.5%	7.7 ± 1.3%
EGTA + SMI	1.5 ± 0.4%	3.1 ± 0.8%	3.7 ± 0.3%	4.5 ± 0.8%	5.6 ± 0.5%

Comparing of GPVI- and PAR-induced Ca^{2+} entry with SERCA inhibition

We also constructed heatmaps of scaled curve parameters for the four agonists (CRP, collagen, thrombin, TRAP) combined with thapsigargin in the presence of $CaCl_2$ or EGTA. The heatmaps illustrated the very potent stimulation of CRP + thapsigargin on the $CaCl_2$ curves and the Ca^{2+} entry ratio curves, when compared to the other agonists (**Figure 4**). Nevertheless, the scaled parameters of Ca^{2+} entry ratio curves for all combinations with thapsigargin showed a consistent, dose-dependent enhancement of the entry of Ca^{2+}, as well as a consistent dependency on secondary mediators. To sum up, these results point to a potent enforcement of receptor agonist-induced Ca^{2+} entry upon SERCA inhibition, which is partly dependent on secondary mediators.

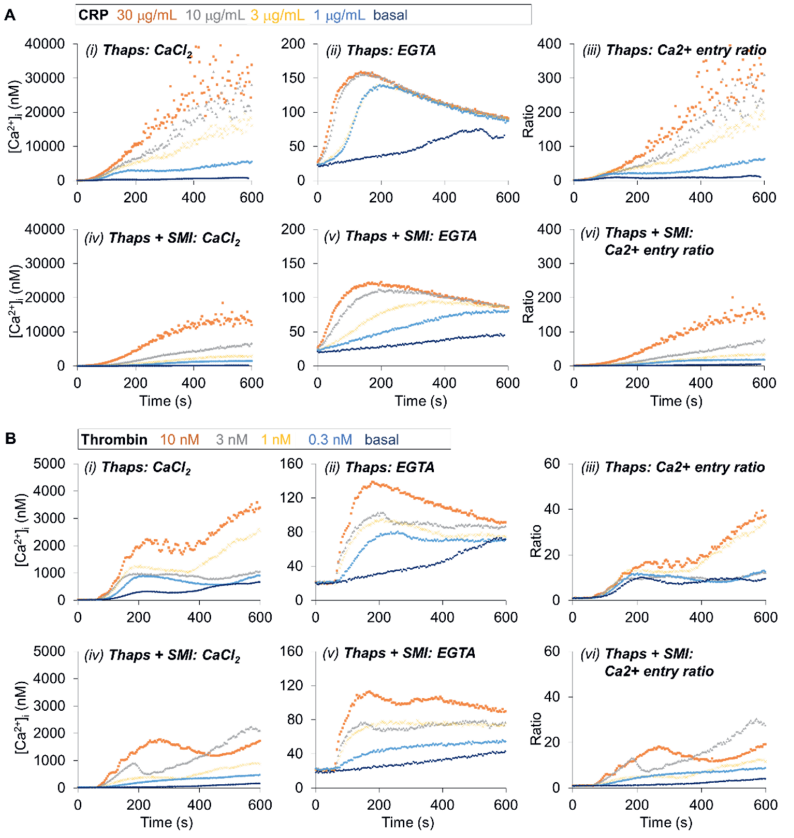

Figure 3. Dose-dependency of Ca^{2+} entry by strong collagen and thrombin receptor agonists upon SERCA inhibition. Fura-2-loaded platelets in 96-well plates were left untreated or pre-incubated with SMI (0.1 U/mL apyrase and 20 µM indomethacin). Roboted stimulation in the presence of 2 mM $CaCl_2$ or 0.1 mM EGTA was with thapsigargin (1 µM) plus CRP (1-30 µg/mL) or thrombin (0.3-10 nM). Measurements of $[Ca^{2+}]_i$ were performed, as for Figure 1. (**A-B**) Calibrated $[Ca^{2+}]_i$ traces (non-smoothed) with thapsigargin plus CRP (**A**), or thapsigargin plus thrombin (**B**), in the absence (**i-iii**) or presence (**iv-vi**) of SMI. Parallel traces were observed in the presence of $CaCl_2$ (left panels) or EGTA (middle panels). The Ca^{2+} entry ratio curves (right panels) were obtained by dividing corresponding $CaCl_2$/EGTA curves, thus representing the fractional Ca^{2+} entry over time. Data are representative of at least 3 experiments (n = 3-6 donors). For curve parameters, see Suppl. Datafile 1.

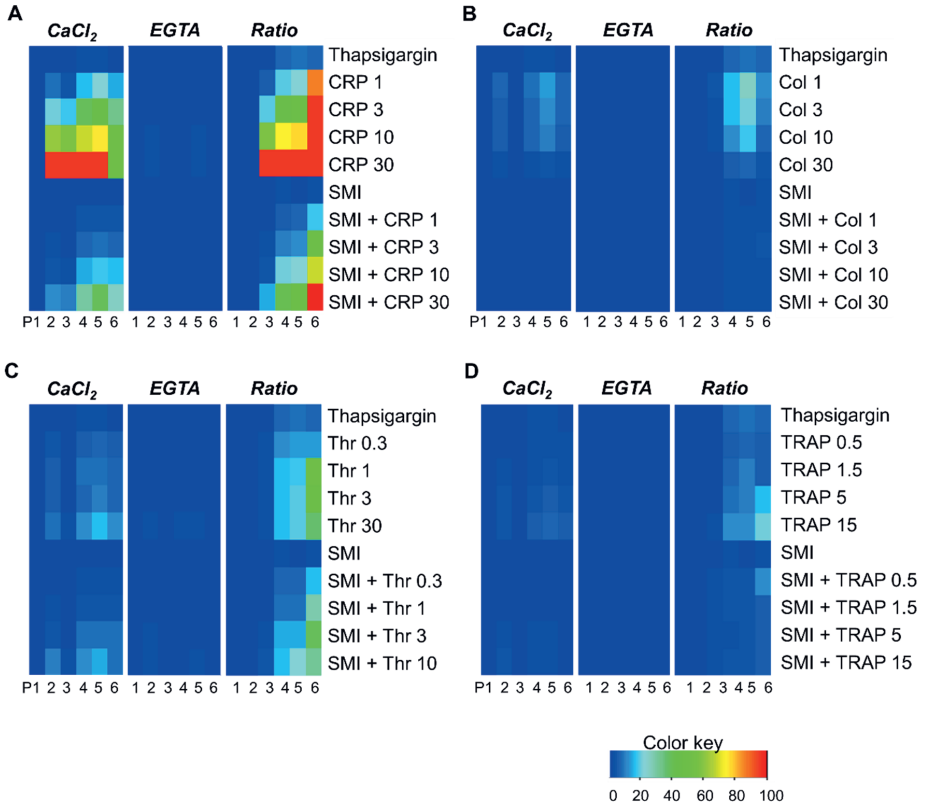

Figure 4. Comparative dose-dependent effects on Ca^{2+} entry by collagen and thrombin receptor agonists upon SERCA inhibition. Fura-2-loaded platelets in the presence of 2 mM $CaCl_2$ or 0.1 mM EGTA were stimulated with 1-30 µg/mL CRP (**A**), 1-30 µg/mL collagen (**B**), 0.3-10 nM thrombin (**C**) or 0.5-15 µM TRAP (**D**), as in (Suppl.) Figure 3. In all conditions, thapsigargin (1 µM) was added to the agonist mixture. The cells were pre-incubated with secondary mediator inhibitors (SMI), as indicated. In parallel smoothed $[Ca^{2+}]_i$ curves were generated with $CaCl_2$ or EGTA present, as well as Ca^{2+} entry ratio curves. Data are mean values from at least three experiments (n = 3-6 donors), scaled at 0-140% across all conditions, but separately for $CaCl_2$/EGTA curves and for Ca^{2+} entry ratio curves. Heatmaps are shown of the scaled curve parameters per agonist. Color key shows scale %. Consecutive columns indicate: level at start (P1), slope to first peak (P2) maximal change of slope (P3), maximal peak level (P4), area under the response curve over 600 seconds (P5) and level at end (P6). Note combined scaling of parameters of (**i**) all $[Ca^{2+}]_i$ values (P1,3,6), (**ii**) the $[Ca^{2+}]_i$ slopes (P2,3), and (**iii**) $[Ca^{2+}]_i$ integrals (P5). For values, see Suppl. Datafile 1.

Relative contribution of Ca^{2+} entry channels to GPVI- and PAR-induced Ca^{2+} entry

For investigating the comparative roles of known or presumed Ca^{2+}-permeable cation channels or transporters in the Ca^{2+} entry process, we used a panel of pharmacological inhibitors. **Table 1** gives the targets and commonly used concentrations of the used inhibitors in platelet research. The compound 2-ABP was used a blocker of the STIM1-coupled Orai1 channel, although it also affects the $InsP_3$-induced Ca^{2+} mobilization [48,49]. For comparison, we used the Orai channel

blocker Synta66 [49], and also the STIM1 inhibitor ML-9 (also blocking MLCK and Akt isoforms) [50]. Earlier dose-response curves with human platelets showed a more selective inhibitory effect of Synta66 than 2-APB on SOCE in comparison to intracellular Ca^{2+} mobilization [49]. Other non-specific effects are not commonly described [51].

To block the most abundantly expressed TRPC isoform, TRPC6, we used the compound BI-749327 [52], which has recently been used as a specific TRPC6 inhibitor to improve platelet preservation upon storage [53]. Furthermore, the mechanosensitive Piezo1/2 ion channels were blocked with the compound GsMTx4 [31]. In human platelets, GsMTx4 (micromolar range) was shown not to affect Ca^{2+} influx via Orai1 or TRPC6 channels [54].

As a most specific antagonist of ATP-induced Ca^{2+} entry via $P2X_1$ channels, we tested MRS-2159 [55,56]. Furthermore, for blockage of the NCX3 Na^+/Ca^{2+} exchanger, we used the compound ORM-10103. In other cells types this has been described as a specific inhibitor of NCX and L-type Ca^{2+} currents in the 3–10 μM dose range [57]. For human platelets, dosing of ORM-10103 indicated a IC_{50} of ~10 μM on the Ca^{2+}-dependent procoagulant activity induced by GPVI and PAR stimulation [32].

Although almost all of these compounds have been used in the 1–10 μM range, we first performed a 1–30 μM dose-response experiment using the standard agonist concentrations of CRP (10 μg/mL) or thrombin (10 nM). By comparing the CaCl2 and EGTA curves, the largest $[Ca^{2+}]_i$ altering effects (if any) of 2-APB, BI-749327, ORM-10103 and Synta66 were obtained at 30 μM, while of ML-9 and MRS-21593 these were reached at 10 μM (not shown). Since for GsMTx4 no clear effects were observed, this compound was discarded. Accordingly, these concentrations were chosen for further experiments.

In a large set of experiments, the six compounds were systematically tested for effects on CRP- or thrombin-induced $[Ca^{2+}]_i$ traces in $CaCl_2$ or EGTA medium, also using the modifying conditions with SMI and/or thapsigargin present. The resulting, representative Ca^{2+} entry ratio traces showed for 2-ABP a potent suppression with either agonist (**Figure 5A**); for BI-749327 no more than small effects (**Figure 5B**); for MRS-2159 small reductions in the first part of the curves (**Figure 5C**); for ORM-10103 longer-term reductions (**Figure 5D**); and for Synta66 a continued inhibition (**Figure 5E**).

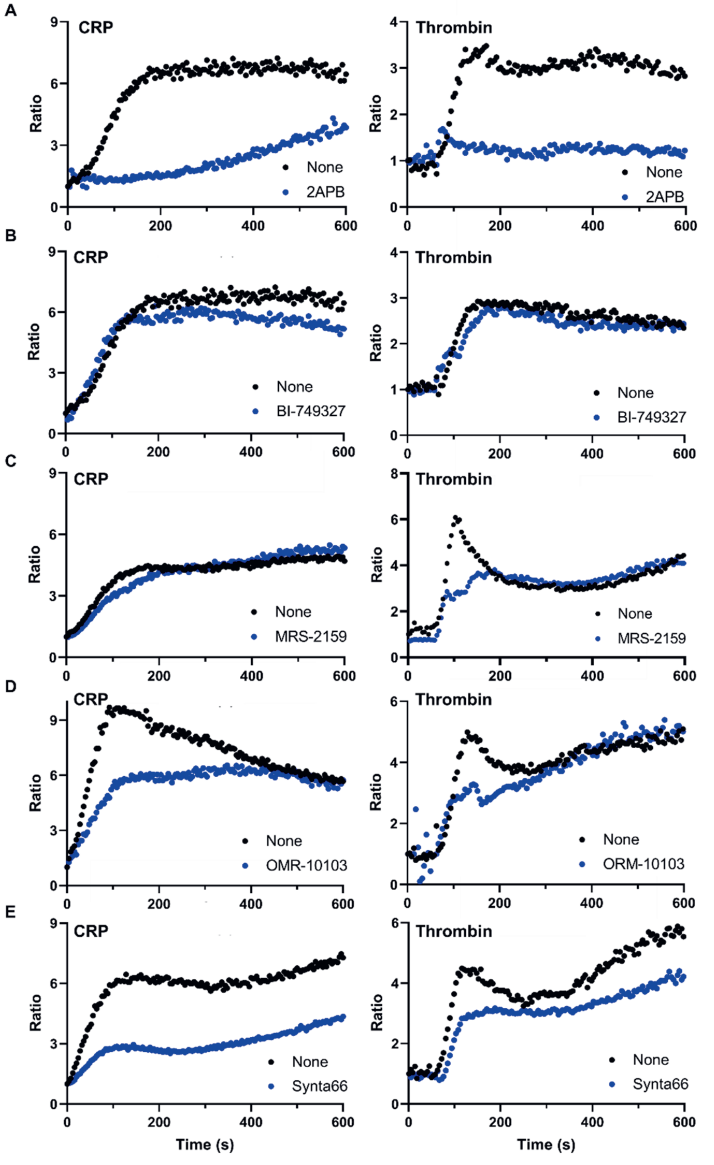

Figure 5. Effect of pharmacological inhibitors on Ca^{2+} entry by collagen and thrombin receptor agonists. Fura-2-loaded platelets in the presence of 2 mM $CaCl_2$ or 0.1 mM EGTA were stimulated with 10 µg/mL CRP (left panels) or 10 nM thrombin (right panels) after pre-incubation with vehicle solution (none) or indicated inhibitor. Final concentrations were as follows: 2-APB (30 µM), BI-749327 (30 µM), ML-9 (not shown, 10 µM), MRS-2159 (10 µM), ORM-10103 (30 µM) and Synta66 (30 µM). Parallel $[Ca^{2+}]_i$ curves generated with $CaCl_2$ or EGTA during 600 s were converted into Ca^{2+} entry ratio curves. Shown are representative Ca^{2+} entry ratio curves for n = 3-5 independent experiments. For values, see Suppl. Datafile 2.

For all inhibitor experiments, we determined the curve parameters (P1–6) in the presence of $CaCl_2$ or EGTA, as well as from the calculated Ca^{2+} entry ratio traces. To assess the inhibitor effects on the Ca^{2+} entry process, we used two approaches: a calculation of effects per parameter and curve type, and a calculation of relative effects per parameter on $CaCl_2$ curves ratioed to EGTA curves. Upon CRP stimulation, heatmapping of the effects on Ca^{2+} entry ratio curves and on relative effect parameters indicated a strong, significant inhibition for all Ca^{2+} entry parameters (2 × 5) with 2-APB, which remained in the presence of SMI (**Figure 6A**). For Synta66 and ORM-10,103, most of the Ca^{2+} entry parameters showed a less strong, but still significant inhibition. With MRS- 2159, only the initial parameter P2 (slope to first peak) was lowered. With BI-749317 or ML-9 the Ca^{2+} entry parameters did not decrease or rather increased.

In comparison, upon thrombin stimulation without or with SMI (**Figure 6B**), heatmapping showed with 2-APB again a strong and significant reduction in all Ca^{2+} entry parameters. The effects of Synta66 and ORM-10103, while mostly significant, were smaller in size. MRS-2159 again affected only parameter P2. While BI-749317 was without effect, ML-9 increased some parameter values although of no significance.

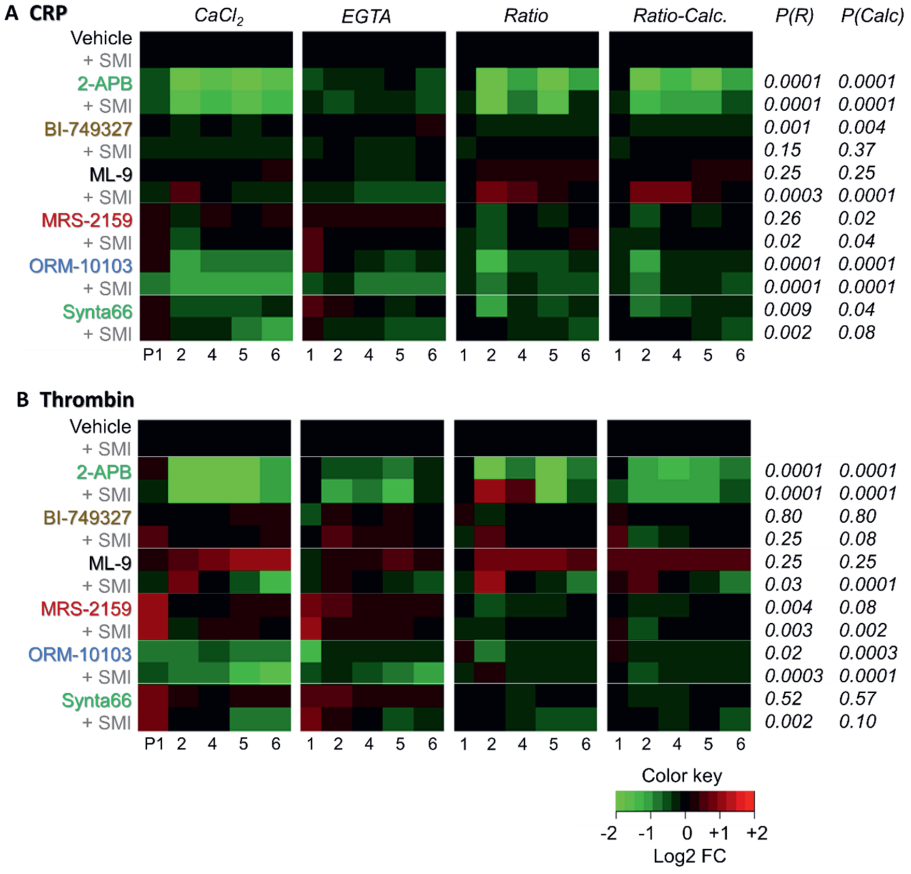

Figure 6. Integrative effects of pharmacological inhibitors on Ca^{2+} entry by collagen and thrombin receptor agonists. Fura-2-loaded platelets in the presence of 2 mM $CaCl_2$ or 0.1 mM EGTA were stimulated with CRP (**A**) or thrombin (**B**) after pre-incubation with vehicle solution or indicated channel inhibitor. Secondary mediator inhibitors (SMI, indomethacin and apyrase) were added, where indicated. Final concentrations were as in Fig 5: 2-APB (30 µM), BI-749327 (30 µM), ML-9 (10 µM), MRS-2159 (10 µM), ORM-10103 (30 µM) or Synta66 (30 µM). Parallel $[Ca^{2+}]_i$ curves generated with $CaCl_2$ or EGTA were smoothed and converted into Ca^{2+} entry ratio curves. Curve parameters analyzed were: level at start (*P1),* slope to first peak (P2), maximal peak level (P4), area under the response curve (P5), and level at end (P6). Inhibitor effects compared to vehicle were calculated per experiment, curve type and parameter. In addition, the ratios of inhibitor effects for $CaCl_2$ vs. EGTA curves were also calculated (Ratio-Calc.). Heatmaps show mean log2 fold changes (FC) of inhibitor effects per curve and parameter vs. the vehicle-control condition. Green = decrease, red = increase. Data are for n = 3-5 donors. *P* values of combined parameters *vs.* control condition are indicated for Ca^{2+} entry ratio curves = *P(R)* and for Ratio-Calc. curves = *P(Calc)* (repetitive t-test). For values, see Suppl. Datafile 2

For the inhibitors with largest effect sizes upon thrombin stimulation (PAR1+4), we also compared the effects on Ca^{2+} entry curve parameters in response to peptide stimulation of PAR1 (TRAP), PAR4 (AYPGKF) or the combination of PAR1+4 (TRAP + AYPGKF). As shown in **Suppl. Figure 3**, we found similar size effects on the Ca^{2+} entry parameters upon PAR1 and/or PAR4 stimulation, Heatmap presentation indicated that, regardless of the agonist used (thrombin TRAP, AYPGKF, TRAP+AYPGKF), suppressive effects of 2-ABP were larger than those of ORM-10103.

Similar heatmaps were generated for the assessment of inhibitor effects in platelets stimulated with CRP or thrombin in the presence of thapsigargin. Representative Ca^{2+} entry ratio curves indicate a potent, almost abolishing effect of 2-APB on the entry process with either agonist combination (**Figure 7A-B**). This reduction was also apparent from generated heatmaps, which for CRP + thapsigargin showed strong and significant reducing effects of 2-APB and Synta66 on all Ca^{2+} entry parameters (**Figure 7C**). This reduction remained in the presence of SMI. For thrombin + thapsigargin, again strongly reducing effects of 2-APB and Synta66 were obtained (**Figure 7D**). Furthermore, for either agonist combination, also ORM-10103 showed a significant inhibitory profile on most Ca^{2+} entry parameters, although of a greater effect size with thrombin than with CRP (**Figure 7C-D**). Regarding the other inhibitors, BI-749427 and ML-9 tended to increase rather than decrease a subset of parameters, whereas MRS-2159 was essentially without effect. Altogether, these data point, for the collagen and thrombin receptor agonists, to an inhibitory effect on Ca^{2+} entry in the order of 2-APB > Synta66 (strongest with thapsigargin) > ORM-10103 > MRS-2159 (initial parameter) >BI-749327, ML-9.

Figure 7

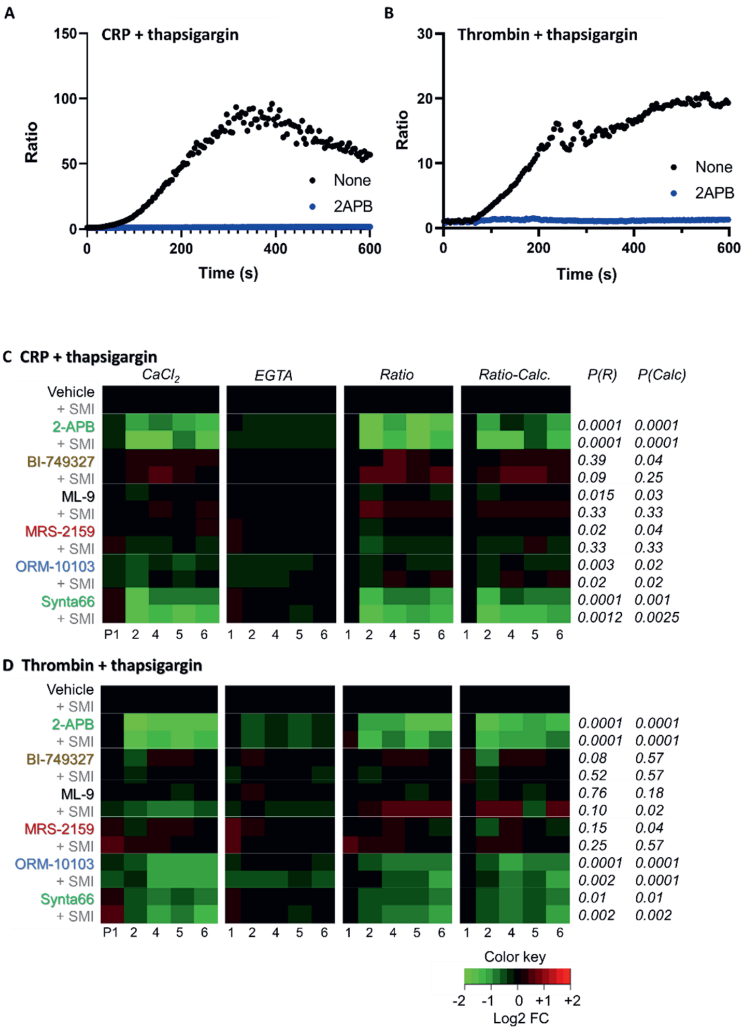

Figure 7. Integrative effects of pharmacological inhibitors on Ca^{2+} entry by collagen and thrombin receptor agonists upon SERCA inhibition. Inhibitor experiments with Fura-2-loaded platelets were performed as for Figure 6, but additionally thapsigargin (1 µM) was added as agonist together with CRP (**A**, **C**) or thrombin (**B**, **D**). Effects on parameters of $CaCl_2$, EGTA, Ca^{2+} entry ratio and calculated ratios (Ratio-Calc.) were also obtained as for Figure 6. Shown are representative Ca^{2+} entry ratio curves for 2-ABP (**A**, **B**). Furthermore, heatmaps of mean log2 fold changes (FC) of inhibitor effects per curve and parameter *vs*. the vehicle-control condition (**C**, **D**). Green = decrease, red = increase. Data are for n = 3-5 donors. *P* values of combined parameters vs. control condition are indicated for Ca^{2+} entry ratio curves = *P(R)* and for Ratio-Calc. curves = *P(Calc)* (repetitive t-test). For values, see Suppl. Datafile 2.

Discussion

In this paper, we employed a high-throughput assay with Fura-2- loaded platelets, for obtaining sets of calibrated agonist-induced $[Ca^{2+}]_i$ traces in the presence of either extracellular $CaCl_2$ or EGTA. As reviewed earlier [1,4], these traces were assumed to reflect the summation of Ca^{2+} fluxes by $InsP_3$-induced Ca^{2+} mobilization from stores and Ca^{2+} entry mechanisms, restrained by a back pumping of mobilized Ca^{2+} by SERCA and PMCA isoforms. Of note, when observed per individual platelet, the Ca^{2+} fluxes are higher than currently measured, as the steeply spiking Ca^{2+} transients in platelet suspensions are averaged out [16]. By considering that the traces with $CaCl_2$ result from the addition of Ca^{2+} entry to the traces with EGTA, we constructed sets of Ca^{2+} entry ratio curves, which provide a quantitative indication of the size over time of the Ca^{2+} entry process.

In our calculations of Ca^{2+} fluxes, due to lack of quantitative affinity and expression data, we did not separate out Ca^{2+} uptake by the mitochondrial calcium uniporter [58] or by Ca^{2+}-induced Ca^{2+} release via the mitochondrial permeability transition pore [9,15]. However, for mouse platelets it was established that mitochondrial uniporters do take up Ca^{2+} ions in activated platelets [58], whereas the mitochondrial permeability transition pore mostly in highly activated, procoagulant platelets contributes to persistently high, entry-dependent $[Ca^{2+}]_i$ levels [9,15].

The constructed Ca^{2+} entry ratio curves indicated for strong platelet agonists, i.e. CRP (GPVI ligand) and thrombin (PAR1/4 ligand), a 3–7 fold enhanced Ca^{2+} entry, when added above threshold doses, while these levels were lower upon inhibition of the secondary mediators ADP and thromboxane A_2. On the other hand, the weaker agonists collagen (for GPVI) and TRAP (for PAR1) triggered a moderately enhanced Ca^{2+} entry, which again depended on secondary mediator release. Strikingly, by combining the agonists with the SERCA inhibitor thapsigargin, we observed a dramatically increased Ca^{2+} entry, with ratio levels reaching 400 (with CRP) or 40 (with thrombin). These values suggest a better degree of coupling of SOCE to Ca^{2+} store depletion in response to GPVI than to PAR stimulation. A high level of SOCE in human or mouse platelets was also previously seen with the GPVI agonist convulxin [19,49]. A novel finding is that also in the presence of thapsigargin the high Ca^{2+} entry greatly relied on platelet co-activation by secondary mediators. Together, these data indicate that the approach of calculating Ca^{2+} entry ratios can provide novel and relevant information on the agonist-induced Ca^{2+} entry, and by extension to the platelet activation process.

Regarding the net Ca^{2+} fluxes in platelets, we obtained a maximal Ca^{2+} mobilization with CRP and thapsigargin in the presence of EGTA of 150 nM $[Ca^{2+}]_i$. Based on a mean cytosolic volume of platelet of 8.92 fL (see methods), this points to a net estimate of $5.37 \times 150 = 80^5$ mobilizable Ca^{2+} ions from stores per single platelet. With $CaCl_2$ present, this net Ca^{2+} entry can raise up to 400-fold higher. For these calculations it should be noted that these do not take into account interindividual variation in platelet Ca^{2+} signaling [35,59,60], nor intra-individual differences between platelet populations [39,61], and neither effects of combinations of agonists [62,63].

Table 4 summarizes the overall effects of the various pharmacological inhibitors on extracellular Ca^{2+} entry and intracellular Ca^{2+} mobilization. The consistent inhibition of Ca^{2+}

entry with 2-APB (50–80%) and Synta66 (15–80%) point to Orai1 as a main Ca^{2+} channel regulating GPVI- and PAR-induced Ca^{2+} entry in the presence of thapsigargin. The difference between 2-APB and Synta66 can be explained by an additional, known inhibitory effect of 2-APB, but not Synta66, on Ca^{2+} store depletion [48,64]. This also suggests a certain degree of synergy between both processes, *e.g.* via the mechanism of Ca^{2+}-induced Ca^{2+} release. Confirming evidence for a major role of the Orai1-STIM1 pathway indeed comes from patients with a homozygous R91W mutation in Orai1 or an R429C mutation in STIM1, where in platelets the thapsigargin-mediated Ca^{2+} entry was fully annulled [24]. Interestingly, the Ca^{2+} entry after convulxin stimulation was stronger impaired with the Orai1 mutation than with the STIM1 mutation [24], pointing to a more crucial role of the Orai1 channel activity. This may also be concluded from the absence of inhibitory effects (rather a tendency to stimulation) of the STIM1 inhibitor ML-9, with the note that it also targets MLCK and Akt isoforms (**Table 1**). In human platelets, the isoforms Orai2/Orai3 and STIM2 are expressed at no more than low levels [65].

Table 4 furthermore summarizes that the TRPC6 inhibitor BI-749327 [52] at the dose applied failed to suppress Ca^{2+} entry. In line with this finding, for mouse platelets, the role of TRPC6 was found to rely on Orai1 activity [30]. We note here that we did not study the oleoyl-acetyl glycerol-induced Ca^{2+} entry, which pathway requires TRPC6 activity [28,29].

In platelets, the ATP-induced P2X1 Ca^{2+} channel is an early onset which is rapidly desensitized by its ligand [26,27]. Using the inhibitor MRS-2159, our data also point to an only early contribution of $P2X_1$ in the Ca^{2+} entry process (*i.e.,* parameter P2). However, in our experiments with washed platelets, we may not have fully prevented desensitization of the channel. On the other hand, due to autocrine ATP release, $P2X_1$ desensitization will already occur in the beginning of the 10-minute Ca^{2+} responses.

Platelet Na^+/Ca^{2+} exchangers (NCEs), operating in reverse mode have been shown to contribute to the prolongedly high $[Ca^{2+}]_i$ required for the formation of procoagulant platelets, such as measured with the probe annexin A5 [32]. Our experiments with ORM-10103 point to a partial inhibition (20–60%) of Ca^{2+} entry, along with a smaller effect on Ca^{2+} mobilization (**Table 4**). Human platelets express five Na^+/Ca^{2+} exchangers (genes *SLC8A1,3* and *SLC24A1,3,4*) [65]. The compound ORM-10103 is primarily directed to NCX3 (*SLC8A3*). To which extent the other isoforms contribute to the regulation of Ca^{2+} fluxes is still unclear. Collectively, our data thus reveal Orai1 and NCE as the dominating Ca^{2+} transporters regulating the long-term GPVI- and PAR-induced Ca^{2+} entry in human platelets.

For essentially all agonists and combinations, we found reducing effects on the various (ratioed) $[Ca^{2+}]_i$ traces in the presence of SMI, blocking the autocrine effects of released ADP and thromboxane A_2 (**Figures 2**, **4**). This agrees with a reference paper reporting on the major contributions of these feedback mediators to platelet aggregation and secretion in response to GPVI or PAR agonists, sch as measured by light transmission aggregometry [66].

This study provides novel information on platelet Ca^{2+} signaling, but also has some limitations. First, our data provide new quantitative insight into the key importance of the Orai1-STIM1 Ca^{2+} entry pathway for platelet activation, such in agreement with the impaired thrombus formation reported mice or patients with a genetic Orai1 or STIM1 dysfunction [19,22,24].

Table 4. Relative effects of inhibitors on CRP- or thrombin-induced Ca^{2+} entry and Ca^{2+} mobilization. Note presence of SMI and/or thapsigargin (thaps.). Shown are mean (SD) effects of inhibitors on parameters (P2,4,5,6) of Ca^{2+} ratio and EGTA curves. NEEDS BETTER OUTLINE

Condition	**Ca^{2+} entry**				**Ca^{2+} mobilization**			
	- SMI	+ SMI	- SMI + thaps.	+ SMI + thaps.	- SMI	+ SMI	- SMI + thaps.	+ SMI + thaps.
CRP								
2-APB (Orai1, IP3R)	0.36 (0.13)	0.49 (0.19)	0.28 (0.26)	0.18 (0.16)	0.83 (0.10)	0.76 (0.07)	0.70 (0.05)	0.76 (0.04)
Synta66 (Orai1)	0.70 (0.11)	0.85 (0.10)	0.29 (0.10)	0.16 (0.04)	1.01 (0.09)	0.76 (0.08)	0.95 (0.04)	0.89 (0.06)
BI-749327 (TRPC6)	0.85 (0.05)	1.02 (0.04)	1.41 (0.29)	1.98 (0.54)	1.05 (0.06)	0.91 (0.02)	1.00 (0.06)	0.94 (0.02)
ML-9 (STIM1, Akt)	1.11 (0.04)	1.43 (0.33)	0.87 (0.12)	1.52 (0.15)	0.90 (0.09)	0.73 (0.05)	1.00 (0.02)	0.89 (0.00)
MRS-2159 (P2X1)	0.87 (0.12)	0.94 (0.12)	0.96 (0.15)	0.75 (0.25)	1.21 (0.03)	0.97 (0.06)	1.03 (0.04)	0.97 (0.03)
ORM-10103 (NCE)	0.68 (0.17)	0.72 (0.08)	0.75 (0.12)	1.08 (0.34)	0.82 (0.11)	0.66 (0.11)	0.82 (0.04)	0.83 (0.01)
Thrombin								
2-APB (Orai1, IP3R)	0.46 (0.15)	0.64 (0.39)	0.16 (0.05)	0.23 (0.07)	0.66 (0.13)	0.60 (0.18)	0.59 (0.11)	0.59 (0.09)
Synta66 (Orai1)	0.92 (0.07)	0.86 (0.15)	0.45 (0.07)	0.35 (0.13)	1.30 (0.14)	0.90 (0.22)	0.98 (0.08)	0.91 (0.10)
BI-749327 (TRPC6)	0.97 (0.08)	1.00 (0.17)	1.20 (0.46)	1.01 (0.20)	1.12 (0.04)	1.15 (0.14)	1.07 (0.12)	0.94 (0.16)
ML-9 (STIM1, Akt)	1.57 (0.16)	0.91 (0.26)	0.88 (0.12)	1.95 (0.86)	1.24 (0.07)	0.92 (0.22)	1.12 (0.12)	0.73 (0.11)
MRS-2159 (P2X1)	0.87 (0.11)	0.91 (0.12)	0.96 (0.28)	1.23 (0.19)	1.26 (0.06)	1.16 (0.12)	1.19 (0.18)	1.02 (0.10)
ORM-10103 (NCE)	0.78 (0.09)	0.83 (0.12)	0.35 (0.10)	0.48 (0.23)	0.78 (0.01)	0.64 (0.18)	0.89 (0.11)	0.52 (0.06)

Hence, pharmacological targeting of the Orai1 channel may be an interesting approach to treat arterial thrombosis, although it should be remarked that complete abrogation of the channel activity associates with immune deficiency [4,14]. Also new is our evidence for a general role of NCE isoforms in Ca^{2+} signaling, thus taking further the recognition that these ion transporters are involved in the Ca^{2+} elevation preceding procoagulant platelet formation [32]. The OMIM database of human genetics only reports on night blindness in carriers of an SLC24A1 mutation and on pigmentation abnormalities linked to *SLC24A4* mutations [67]. The NCE channel types may thus be interesting and novel drug targets. Third, the observed effects of Orai1 or NCE inhibition in the presence of SMI (inhibiting cyclooxygenase and ADP receptors) suggests that those drugs affecting Orai1 or NCEs will be effective on top of the current antiplatelet agents, aspirin and $P2Y_{12}$ inhibitors. A limitation of our approach – high throughput screening setup to define and quantify Ca^{2+} entry mechanisms – is that the multitude of assay variables did not allow simultaneous measurements of other functional responses of platelets. For the functional relevance of the Ca^{2+} entry process we like to refer to papers using flow cytometric or microfluidic approaches. For instance, the blockage Orai1 in human platelets with 2-APB or Synta66 has been shown to suppress collagen-induced thrombus formation and annexin A5 binding (phosphatidylserine expression) [49]. A second limitation is that we considered the intracellular Ca^{2+} stores of platelets as one compartment, not taking into account separate Ca^{2+} uptake or release from mitochondria or lysosomes. Reason for this is that the Ca^{2+} fluxes in these organelles were not easy to assess. Third, the followed pharmacological approach to quantify Ca^{2+} entry fluxes in platelets implies a certain degree of dose-dependent non-specificity of the inhibitors used. Additional preclinical studies will be needed to show the suitability of the compounds and their targets in the field of thrombosis and hemostasis.

Authorship contribution statement

H.Y.F.C. conceptualization, data curation, formal analysis, writing – original draft, writing – review & editing. J.Z. conceptualization, data curation, formal analysis, writing – original draft, writing – review & editing. C.T. investigation, methodology, validation, writing – review & editing. D.I.F. investigation, methodology, validation, writing – review & editing. J.H. investigation, methodology, validation, writing – review & editing. R.A. funding acquisition, supervision, writing – review & editing. M.R. funding acquisition, supervision, writing – review & editing. R.C. investigation, methodology, validation, writing – review & editing. J.G. funding acquisition, supervision, writing – review & editing. J.W.M.H. funding acquisition, supervision, writing – original draft, writing – review & editing.

Declaration of competing interest

M.R. is an employee of Synapse Research Institute. J.W.M.H. is a scientific advisor of Synapse Research Institute. The other authors report no relevant conflicts of interest.

Data availability

Data will be made available on request.

Acknowledgements

We thank Dr. S. P. Watson (University of Birmingham) for helpful advice throughout the studies. We acknowledge Dr. D. Tian (Synpeptide, Shanghai) for the kind gift of AYPGKF. Authors H.Y.F.C., C.T., J.H. and D.I.F. are supported by the European Union's Horizon 2020 research and innovation program under the Marie Sklodowska-Curie grant agreement TAPAS No. 766118, H.Y.F.C. is enrolled in a joint PhD program with the Universities of Maastricht (The Netherlands) and Birmingham (United Kingdom). C.T. is enrolled in a joint PhD program with the Universities of Reading (United Kingdom) and Maastricht. J.Z. acknowledges bursary support from the China Scholarship Council (CSC) 201909370052.

References

1. Heemskerk JW. Calcium and platelets. In: The Molecular Basis of Calcium Action in Biology and Medicine (Pochet R, Donato R, Haiech J, Heinzmann C, Gerke V, eds.), Kluwer Acad. Publ., The Hague (the Netherlands). **2000**, p. 45-71.
2. Varga-Szabo D, Braun A, Nieswandt B. Calcium signaling in platelets. *J. Thromb. Haemost.* **2009**, *7*, 1057-1066.
3. Versteeg HH, Heemskerk JW, Levi M, Reitsma PH. New fundamentals in hemostasis. *Physiol. Rev*. **2013**, *93*, 327-358.
4. Mammadova-Bach E, Nagy M, Heemskerk JW, Nieswandt B, Braun A. Store-operated calcium entry in thrombosis and thrombo-inflammation. *Cell Calcium.* **2019**, *77,* 39-48.
5. Solari FA, Mattheij NJ, Burkhart JM, Swieringa F, Collins PW, Cosemans JM, Sickmann A, Heemskerk JW, Zahedi RP. Combined quantification of the global proteome, phosphoproteome, and proteolytic cleavage to characterize altered platelet functions in the human Scott syndrome. *Mol. Cell. Proteomics.* **2016**, *15,* 3154-3169.
6. Beck F, Geiger J, Gambaryan S, Solari FA, Dell'Aica M, Loroch S, Mattheij NJ, Mindukshev I, Pötz O, Jurk K, Burkhart JM, Fufezan C, Heemskerk JW, Walter U, Zahedi RP, Sickmann A. Temporal quantitative phosphoproteomics of ADP stimulation reveals novel central nodes in platelet activation and inhibition. *Blood.* 2017*, 129*, e1-e12.
7. Cheung HY, Coman C, Westhoff P, Manke M, Sickmann A, Borst O, Gawaz M, Watson SP, Heemskerk JW, Ahrends R. Targeted phosphoinositides analysis using high-performance ion chromatography-coupled selected reaction monitoring mass spectrometry. *J. Proteome Res.* **2021**, *20,* 3114-3123.
8. Wu J, Heemskerk JW, Baaten CC. Platelet membrane receptor proteolysis: implications for platelet function, *Front. Cardiovasc. Med.* **2021**, *7,* 608391.
9. Fernandez DI, Kuijpers MJ, Heemskerk JW. Platelet calcium signaling by G-protein coupled and ITAM-linked receptors regulating anoctamin-6 and procoagulant activity. *Platelets.* **2021**, *32*, 863-871.
10. Van der Meijden PE, Heemskerk JW. Platelet biology and functions: new concepts and clinical perspectives, *Nat. Rev. Cardiol.* **2019**, *16,* 166-179.
11. Watson SP, Auger JM, McCarty OJ, Pearce AC. GPVI and integrin αIIbβ3 signaling in platelets. *J. Thromb. Haemost.* **2005**, *3,* 1752-1762.
12. Offermanns S. Activation of platelet function through G protein-coupled receptors. *Circ. Res.* **2006**, *99,* 1293-1304.
13. De Gaetano G, Cerletti C, Dejana E, R. Latini R. Pharmacology of platelet inhibition in humans: implications of the salicylate-aspirin interaction. *Circulation.* **1985**, *72,* 1185-1193.
14. Feske S, Gwack Y, Prakriya M, Srikanth S, Puppel SH, Tanasa B, Hogan PG, Lewis RS, Daly M, Rao AK. A mutation in Orai1 causes immune deficiency by abrogating CRAC channel function. *Nature,* **2006,** *441,* 179-185.
15. Lang F, Münzer P, Gawaz M, Borst O. Regulation of STIM1/Orai1-dependent Ca^{2+} signaling in platelets. *Thromb. Haemost.* **2013**, *110,* 925-930.
16. Heemskerk JW, Vis P, Feijge MA, Hoyland J, Mason WT, Sage, SO. Roles of phospholipase C and Ca^{2+}-ATPase in calcium responses of single, fibrinogen-bound platelets. *J. Biol. Chem.* **1993**, *268,* 356-363.
17. Prakriya M, Feske S, Gwack Y, Srikanth S, Rao A, Hogan PG. Orai1 is an essential pore subunit of the CRAC channel. *Nature.* **2006**, *443,* 230-233.

18. Luik RM, Wang B, Prakriya M, Wu M, Lewis RS. Oligomerization of STIM1 couples ER calcium depletion to CRAC channel activation. *Nature.* **2008***, 454,* 538-542.
19. Varga-Szabo D, Braun A, Nieswandt B. STIM1 and Orai1 in platelet function. *Cell Calcium.* **2011***, 50,* 70-278.
20. Volz J, Kusch C, Beck S, Popp M, Vögtle T, Meub M, Scheller I, Heil HS, et al. BIN2 orchestrates platelet calcium signaling in thrombosis and thrombo-inflammation, *J. Clin. Invest.* **2020**, *130*, 6064-6079.
21. Bergmeier W, Oh-Hora M, McCarl CA, Roden RC, Bray PF, Feske S. R93W mutation in Orai1 causes impaired calcium calcium influx in platelets. *Blood.* **2009**, *109*, 6875-6878.
22. Braun A, Varga-Szabo D, Kleinschnitz C, Pleines I, Bender M, Austinat M, Bösi M, Stoll G, Nieswandt B. Orai1 (CRACM1) is the platelet SOC channel and essential for pathological thrombus formation. *Blood.* **2009***, 113,* 2056-2063.
23. Gilio K, van Kruchten R, Braun A, Berna-Erro A, Feijge MA, Stegner D, van der Meijden PE, Kuijpers MJ, Varga-Szabo D, Heemskerk JW, Nieswandt B. Roles of platelet STIM1 and Orai1 in glycoprotein VI- and thrombin-dependent procoagulant activity and thrombus formation. *J. Biol. Chem.* **2010**, *285,* 23629-29638.
24. Nagy M, Mastenbroek TG, Mattheij NJ, de Witt S, Clemetson KJ, Kirschner J, Schulz JA, Braun A, Cosemans JM, Zieger B, Heemskerk JW. Variable impairment of platelet functions in patients with severe, genetically linked immune deficiencies. *Haematologica.* **2018***, 103,* 540-549.
25. Harper MT, Poole AW. Store-operated calcium entry and non-capacitative calcium entry have distinct roles in thrombin-induced calcium signaling in human platelets. *Cell Calcium.* **2011**, *50,* 351-358.
26. Mahaut-Smith MP, Ennion SJ, Rolf MG, Evans RJ. ADP is not an agonist at $P2X_1$ receptors: evidence for separate receptors stimulated by ATP and ADP on human platelets. *Br. J. Pharmacol.* ***2000****, 131,* 108-114.
27. Mahaut-Smith MP, Taylor KA, Evans RJ. Calcium signaling through ligand-gated ion channels such as $P2X_1$ receptors in the platelet and other non-excitable cells. *Adv. Exp. Med. Biol.* **2016**, *898,* 305-329.
28. Harper MT, Camacho-Londono JE, Quick K, Camacho-Londono J, Flockerzi V, Phillipp SE, Birnbaumer L, Freichei M, Poole AW. Transient receptor potential channels function as a coincidence signal mediating phosphatidylserine exposure. *Sci. Signal.* **2013***, 6,* ra50.
29. Ramanathan G, Gupta S, Thielmann, Pleines I, Varga-Szabo D, May F, Mannhalter C, Dietrich A, Nieswandt B, Braun A. Defective diacylglycerol-induced Ca^{2+} entry but normal agonist-induced activation responses in TRPC6-deficient mouse platelets. *J. Thromb. Haemost.* **2012**, *10,* 419-429.
30. Chen W, Thielmann I, Gupta S, Subramanian H, Stegner D, van Kruchten R, Dietrich A, Gambaryan S, Heemskerk JW, Hermanns HM, Nieswandt B, Braun A. Orai1-induced store-operated Ca^{2+} entry enhances phospholipase activity and modulates canonical transient receptor potential channel 6 function in murine platelets. *J. Thromb. Haemost.* **2014**, *12*, 528-539.
31. Bae C, Sachs F, Gottlieb PA. The mechanosensitive ion channel Piezo1 is inhibited by the peptide GsMTx4. *Biochemistry.* **2011**, *50*, 6295-6300.
32. Aliotta A, Bertaggia Calderara D, Zermatten MG, Alberio L. Sodium-calcium exchanger reverse mode sustains dichotomous ion fluxes required for procoagulant COAT platelet formation. *Thromb. Haemost.* **2020***, 121,* 309-321.
33. Fernandez DI, Provenzale I, van Groningen J, Tullemans BM, Veninga A, Dunster JL, Honarnejad S, van den Hurk H, Kuijpers MJ, Heemskerk JW. Ultra-high throughput Ca^{2+} response patterns in platelets to distinguish between ITAM-linked and G- protein coupled receptor activation, *iScience*. **2022**, *25,* 103718.
34. Gilio K, Munnix IC, Mangin P, Cosemans JM, Feijge MA, van der Meijden PE, Olieslagers S, Chrzanowska-Wodnicka MB, Lillian R, Schoenwaelder S, Koyasu S, Sage SO, Jackson SP, Heemskerk JW. Non-redundant roles

of phosphoinositide 3-kinase isoforms alpha and beta in glycoprotein VI-induced platelet signaling and thrombus formation, *J. Biol. Chem.* **2009**, *284*, 33750-33762.

35. Jooss NJ, De Simone I, Provenzale I, Fernandez DI, Brouns SL, Farndale RW, Henskens YM, Kuijpers ME, ten Cate H, van der Meijden PE, Cavill R, Heemskerk JW. Role of platelet glycoprotein VI and tyrosine kinase Syk in thrombus formation on collagen-like surfaces. *Int. J. Mol. Sci.* **2019***, 20,* e2788.
36. Feijge MA, van Pampus EC, Lacabaratz-Porret C, Hamulyak K, Lévy-Toledano S, Enouf J, Heemskerk JW. Inter-individual varability in Ca^{2+} signaling in platelets from healthy volunteers, relation with expression of endomembrane Ca^{2+}-ATPases, *Br. J. Haematol.* **1998**, *102,* 850-859.
37. Grynkiewicz G, Poenie M, Tsien RY. A new generation of Ca^{2+} indicators with greatly improved fluorescence properties. *J. Biol. Chem.* **1985***, 260,* 3440-3450.
38. Van Geffen JP, Brouns SL, Batista J, McKinney H, Kempster C, Nagy M, Sivapalaratnam S, Baaten CC, Bourry N, Frontini M, Jurk K, Krause M, Pillitteri D, Swieringa F, Verdoold R, Cavill R, Kuijpers MJ, Ouwehand WH, Downes K, Heemskerk JW. High-throughput elucidation of thrombus formation reveals sources of platelet function variability. *Haematologica.* **2019***, 104,* 1256-1267.
39. White JG. Platelet structure. In: Platelets, 2nd edition (Michelson A, ed.) Academic Press, Amsterdam. **2007**, p. 45-73.
40. Heemskerk JW, Willems GM, Rook MB, Sage SO. Ragged spiking of free calcium in ADP-stimulated human platelets: regulation of puff-like calcium signals in vitro and ex vivo. *J. Physiol.* **2001***, 535,* 625-635.
41. Sargeant P, Sage SO. Calcium signaling in platelets and other nonexcitable cells. *Pharmacol. Ther.* **1994***, 64,* 395-443.
42. Malayev A, Nelson DJ. Extracellular pH modulates the Ca^{2+} current activated by depletion of intracellular Ca^{2+} stores in human macrophages. *J. Membr. Biol.* **1995***, 146,* 101-111.
43. Beck A, Fleig A, Penner R, Peinelt C. Regulation of endogenous and heterologous Ca^{2+} release-activated Ca^{2+} currents by pH. *Cell Calcium.* **2014***, 56,* 235-243.
44. Bootman MD, Collins TJ, Mackenzie L, Roderick HL, Berridge MJ, Peppiatt CM. 2-aminoethoxydiphenyl borate (2-APB) is a reliable blocker of store-operated Ca^{2+} entry but an inconsistent inhibitor of $InsP_3$-induced Ca^{2+} release. *FASEB J.* **2002**, *16*, 1145-1150.
45. Van Kruchten R, Braun A, Feijge MA, Kuijpers MJ, Rivera-Galdos R, Kraft P, Stoll G, Kleinschnitz G, Bevers EM, Nieswandt B, Heemskerk JW. Antithrombotic potential of blockers of store-operated calcium channels in platelets. *Arterioscler. Thromb. Vasc. Biol.* **2012**, *32*, 1717-1723.
46. Kondratskyi A, Yassine M, Slomianny C, Kondratska K, Gordienko D, Dewailly E, Lehen'kyi V, Skryma R, Prevarskaya N. Identification of ML-9 as a lysosomotropic agent targeting autophagy and cell death. *Cell Death Dis.* **2014***, 5,* e1193.
47. Lin BL, Matera D, Doerner JF, Zheng N, Del Camino D, Mishra S, Bian H, Zeveleva S, Zhen X, et al. In vivo selective inhibition of TRPC6 by antagonist BI 749327 ameliorates fibrosis and dysfunction in cardiac and renal disease, *Proc. Natl. Acad. Sci. USA.* **2019**, *116,* 10156-10161.
48. Harper MT, Mason MJ, Sage SO, Harper AG. Phorbol ester-evoked Ca^{2+} signaling in human platelets is via autocrine activation of $P2X_1$ receptors, not a novel non-capacitative Ca^{2+} entry. *J. Thromb. Haemost.* **2010**, *8*, 1604-1613.
49. Flamm MH, Colace TV, Chatterjee MS, Jing H, Zhou S, Jaeger D, Brass LF, Sinno T, Diamond SL. Multiscale prediction of patient-specific platelet function under flow. *Blood.* **2012**, *120*, 190-198.

50. Joutsi-Korhonen L, Smethurst PA, Rankin A, Gray E, IJsseldijk M, Onley CM, Watkins NA, Williamson LM, Goodall AH, de Groot PG, Farndale RW, Ouwehand WH. The low-frequency allele of the platelet collagen signaling receptor glycoprotein VI is associated with reduced functional responses and expression. *Blood.* **2003**, *101*, 4372-4379.
51. Baaten CC, ten Cate H, van der Meijden PE, Heemskerk JW. Platelet populations and priming in hematological diseases. *Blood Rev.* **2017**, *31*, 389-399.
52. Veninga A, Baaten CC, Tullemans BM, De Simone I, Kuijpers MJ, Heemskerk JW, van der Meijden PW. Effects of platelet agonists and priming on the formation of platelet populations. *Thromb. Haemost*. **2022**, *122*, 726-738.
53. Chatterjee MS, Purvis JE, Brass LF, Diamond SL. Pairwise agonist scanning predicts cellular signaling responses to combinatorial stimuli. *Nat. Biotechnol.* **2010**, *28*, 727-732.
54. Dolan AT, Diamond SL. Systems modeling of Ca^{2+} homeostasis and mobilization in platelets mediated by IP_3 and store-operated Ca^{2+} entry. *Biophys. J.* **2014**, *106*, 2049-2060.
55. Goto JI, Suzuki AZ, Ozaki S, Matsumoto N, Nakamura T, Ebisui E, Fleig A, Penner R, Mikoshiba K. Two novel 2-aminoethyl diphenylborinate (2-APB) analogues differentially activate and inhibit store-operated Ca^{2+} entry via STIM proteins. *Cell Calcium.* **2010**, *47*, 1-10.
56. Huang J, Swieringa F, Solari FA, Provenzale I, Grassi L, De Simone I, Baaten CC, Cavill R, Sickmann A, Frontini M, Heemskerk JW. Assessment of a complete and classified platelet proteome from genome-wide transcripts of human platelets and megakaryocytes covering platelet functions. *Sci. Rep.* **2021***, 11,* 12358.
57. Burkhart JM, Vaudel M, Gambaryan S, Radau S, Walter U, Martens L, Sickmann A, Zahedi RP. The first comprehensive and quantitative analysis of human platelet protein composition allows the comparative analysis of structural and functional pathways. *Blood*. **2012**, *120,* e73-e82.
58. Zeiler M, Moser M, Mann M. Copy number analysis of the murine platelet proteome spanning the complete abundance range. *Mol. Cell. Proteomics*. **2014**, *13*, 3435-3445.

Supplementary Materials to Chapter 5

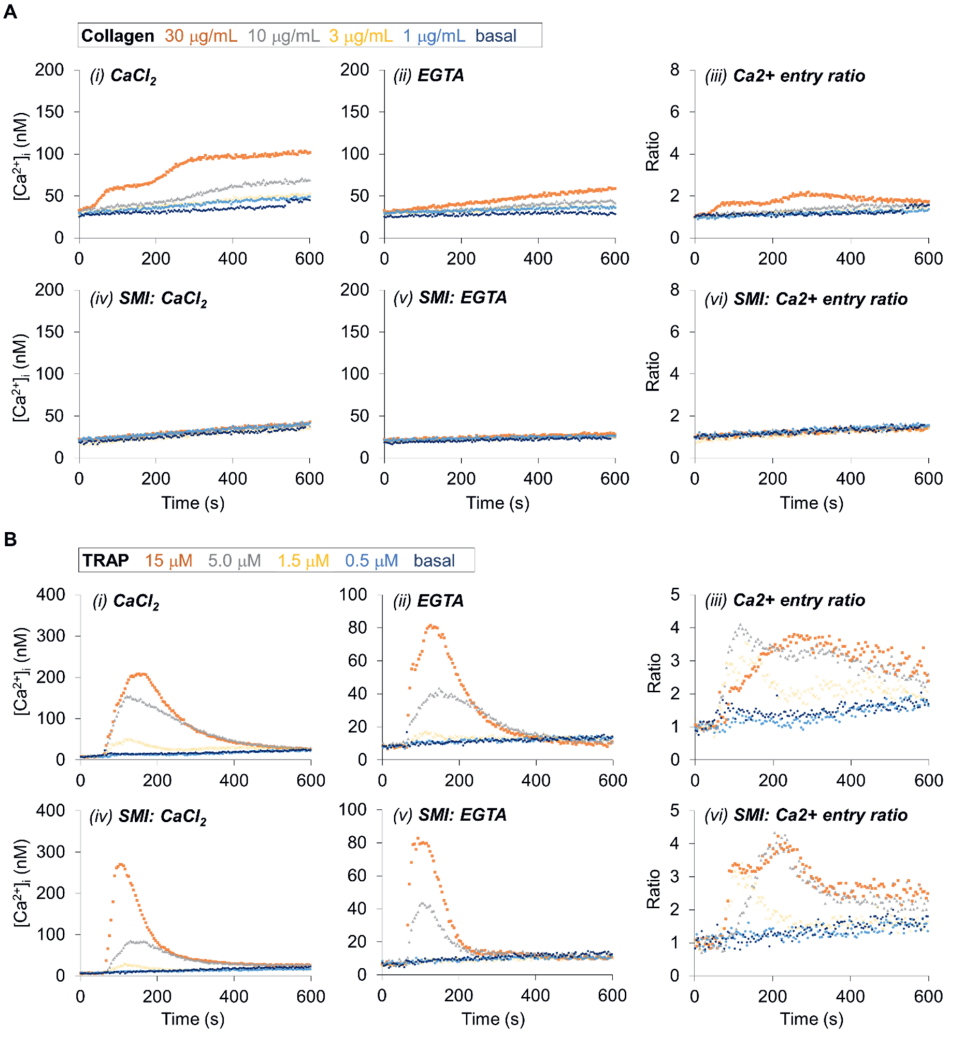

Suppl. Figure 1. Dose-dependency of Ca^{2+} entry ratio by collagen and TRAP. Fura-2-loaded platelets in 96-well plates were left untreated or were pre-incubated with SMI (0.1 unit/mL apyrase and 20 µM indomethacin). Fura-2-loaded platelets in 96-well plates were pre-incubated with SMI (0.1 unit/mL apyrase and 20 µM indomethacin), or left untreated. Stimulation in the presence of 2 mM $CaCl_2$ or 0.1 mM EGTA was with collagen (1-30 µg/mL) or TRAP (0.5-15 µM). Changes in $[Ca^{2+}]_i$ were monitored over 600 seconds, as for Figure 1. (**A-B**) Calibrated $[Ca^{2+}]_i$ traces after stimulation with collagen (**A**) or TRAP (**B**), in the absence (**i-iii**) or presence (**iv-vi**) of SMI. Parallel traces were observed in the presence of $CaCl_2$ (left panels) or EGTA (middle panels). The Ca^{2+} entry ratio curves (right panels) were obtained by dividing the $CaCl_2$/EGTA curves, representing the relative Ca^{2+} entry over time. Data are representative of at least three experiments (n = 3-5 donors). For parameters, see Suppl. Datafile 1.

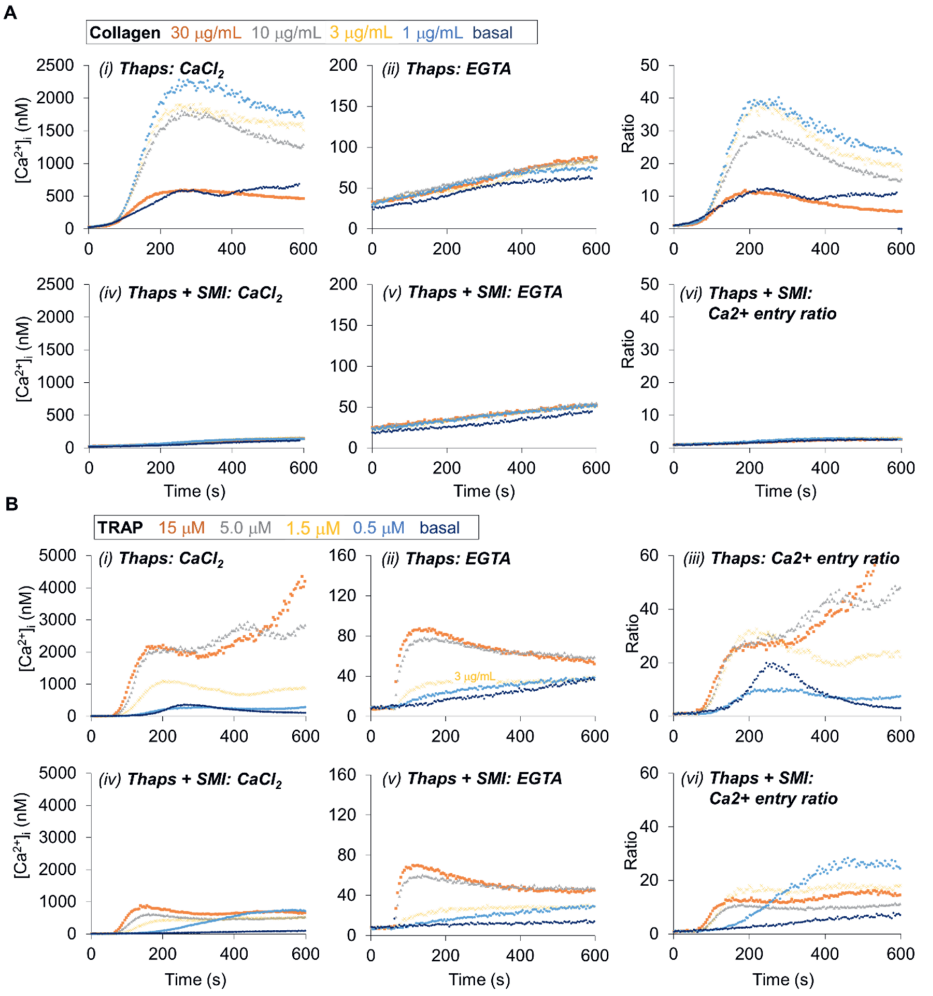

Suppl. Figure 2. Dose-dependency of Ca^{2+} entry by collagen and TRAP in the presence of SERCA inhibition. Fura-2-loaded platelets in 96-well plates were left untreated or pre-incubated with SMI (0.1 unit/mL apyrase and 20 µM indomethacin). Stimulation in the presence of 2 mM $CaCl_2$ or 0.1 mM EGTA was with thapsigargin (1 µM) plus collagen (0.3-30 nM) or thapsigargin plus TRAP (0.5-15 µM). Changes in $[Ca^{2+}]_i$ were obtained over 600 seconds, as indicated for Figure 1. (**A-B**) Calibrated $[Ca^{2+}]_i$ traces after stimulation with thapsigargin plus collagen (**A**) or thapsigargin plus TRAP (**B**), in the absence (**i-iii**) or presence (**iv-vi**) of SMI. Traces obtained with $CaCl_2$ (left panels), EGTA (middle panels) or $CaCl_2$/EGTA ratio curves representing Ca^{2+} entry ratios (right panels). Data are representative of at least three experiments (n= 3-6 donors). For parameter values, see Suppl. Datafile 1.

Chapter 6

Negative regulation of store-operated Ca^{2+} entry in platelets by protein kinase C isoforms

Jinmi Zou,[1,2*] Pengyu Zhang,[2,3,4*] Fiorella A. Solari,[1] Nadine J. A. Mattheij,[5] Claudia Schönichen,[2,3] Marijke J. E. Kuijpers,[2] Frauke Swieringa,[1] Albert Sickmann,[5] Barbara Zieger,[6] Kerstin Jurk,[3] Johan W. M. Heemskerk[1]

*Equal contribution

[1]Synapse Research Institute Maastricht, Koningin Emmaplein 6217 KD Maastricht, he Netherlands; [2]Department of Biochemistry, CARIM, 6200 MD Maastricht University, Maastricht, The Netherlands; [3]Center for Thrombosis and Hemostasis CTH, University Medical Center of the Johannes Gutenberg University Mainz, 55131 Mainz, Germany; [4]Leibniz-Institut für Analytische Wissenschaften-ISAS-e.V, Dortmund, Germany; [5]Department of Clinical Chemistry and Hematology, Maxima Medical Center Veldhoven, 5500 MB Veldhoven, The Netherlands; [6]Department of Pediatrics and Adolescent Medicine, Division of Pediatric Hematology and Oncology, Medical Center, University of Freiburg, Freiburg, Germany

Submitted

Chapter 7

Crucial roles of red blood cells and platelets in whole blood thrombin generation

Siyu Sun[1,2], Elena Campello [3]*, Jinmi Zou[1,2]*, Joke Konings[1], Dana Huskens[1], Jun Wan[1], Delia I. Fernandez[2], Chris P. M. Reutelingsperger[2], Hugo ten Cate[2,4], Serena Toffanin[3], Cristiana Bulato[3], Philip G. de Groot[1], Bas de Laat[1], Paolo Simioni[3]*, Johan W. M. Heemskerk[1,2]*, Mark Roest[1]

*Equal contribution

[1]Synapse Research Institute, Maastricht, The Netherlands; [2]Department of Biochemistry, Cardiovascular Research Institute Maastricht (CARIM), Maastricht University, The Netherlands; [3]Department of Medicine, University of Padua, Padova, Italy; [4]Department of Internal Medicine, Maastricht University Medical Center+, Maastricht, The Netherlands

Blood Adv. 2023;bloodadvances.2023010027

Abstract

Red blood cells (RBC) and platelets contribute to the coagulation capacity in bleeding and thrombotic disorders. The thrombin generation (TG) process is considered to reflect the interactions between plasma coagulation and the various blood cells. Using a new high-throughput method capturing the complete TG curve, we were able to compare TG in whole blood and in autologous platelet-rich and platelet-poor plasma to redefine the blood cell contributions to the clotting process. We report a faster and initially higher generation of thrombin and a shorter coagulation time in whole blood than in PRP upon low concentrations of coagulant triggers, including tissue factor, Russell's viper venom factor X factor Xa, factor XIa and thrombin. The TG accelerated with increased hematocrit, and delayed after prior treatment of RBC with phosphatidylserine-blocking annexin A5. RBC treatment with ionomycin increased phosphatidylserine exposure, confirmed by flow cytometry, and increased the TG process. In reconstituted blood samples, the prior selective blockage of phosphatidylserine on RBC with annexin A5 enhanced glycoprotein VI-induced platelet procoagulant activity. In patients with anemia or erythrocytosis, cluster analysis revealed high or low whole blood TG profiles in specific cases of anemia. The TG profiles lowered upon annexin A5 addition in the presence of RBC, and thus were determined by the extent of phosphatidylserine exposure of blood cells. Profiles for patients with polycythemia vera undergoing treatment were similar to control subjects. We concluded that RBC and platelets, in a phosphatidylserine-dependent way, contribute to the TG process. Determination of the whole blood hypo-or hyper-coagulant activity may help to characterize a bleeding or thrombosis risk.

Keywords: anemia; coagulation; erythrocytosis; phosphatidylserine; polycythemia vera

Introduction

Enhanced blood clotting is a primary cause of venous thromboembolism [1]. To understand the pathophysiology this process, the contribution of all blood components should be considered. In addition to plasma (anti)coagulation proteins and platelets, there is evidence that also abnormalities in red blood cells (RBC) can be risk factors for thrombosis [2]. Experimental studies have indicated that RBC contribute to thrombus and clot formation, for instance by enhancing thrombus stability [3-5]. Furthermore, in patients with hemolytic anemia, sickle cell disease or polycythemia [6-8], qualitative or quantitative alterations in RBC might be linked to thromboembolic events [9,10]. It is known that (ageing) RBC express procoagulant phosphatidylserine in a manner that is increased in sickle cell anemia [11-13]. Therefore, it is important to assess whether and how RBC can contribute in the coagulation process to achieve a thrombotic phenotype.

In the past decade, fluorogenic thrombin generation (TG) assays have frequently been used to evaluate coagulation in blood plasma to link to thrombosis or bleeding risks [14,15]. However, in such plasma-based tests the contribution of blood cells is not taken into account. Initially, whole blood TG – with all blood cells present – was challenging due to repeated sampling and low throughput [16]. Later higher throughput methods for blood TG were hampered by RBC fluorescence quenching [17,18], which allowed to capture only the initial phase of TG [19].

For the present study, we solved earlier issues with a 96 well-plate based method using non-diluted blood samples, providing completed, calibrated kinetics of TG, and allowing direct comparison by TG of blood and plasma samples. This allowed us to test the effects of various coagulation triggers as well as the role of exposed phosphatidylserine on RBC and platelets, as potent procoagulant membrane surfaces [20]. As a proof-of-concept, we also analyzed blood samples from patients with RBC complications and an assumed pro-thrombotic phenotype. Collectively, our data point to additive roles of RBC and platelets in this coagulant process.

Materials and methods

An extended version of the materials and methods is available in the supplement below.

Study subjects

Human blood was collected from healthy volunteers, who had not taken medication for >2 weeks. Studies were conducted as guided by the Declaration of Helsinki and approved by the Medical Ethics Committee of Maastricht University Medical Center. The patient study was approved by the Research and Ethics Committee of Padua University Hospital. Patients with potential RBC abnormalities and day controls were included in September 2022.

Blood sample preparation

Blood samples were collected into 3.2 % trisodium citrate Vacuette tubes (Greiner Bio-One, Alphen a/d Rijn, The Netherlands). Platelet-rich plasma (PRP) and platelet-poor plasma (PPP) [17,21] were prepared as detailed in the supplement. Double washed RBC in Hepes buffer pH 7.35 (136 mM NaCl, 2.7 mM KCl, 10 mM Hepes, 2 mM $MgCl_2$, 0.1% w/v BSA and 0.1% w/v glucose) reconstituted with autologous PRP or PPP, where indicated.

Measurement of thrombin generation in whole blood and platelet-rich plasma

Calibrated measurements of TG were performed in 96-well plates at 37 °C with major modifications from previous TG measurements in whole blood [19]. Samples of citrated whole blood (WB), PRP or PPP (3 volumes) were mixed with 2 volumes Z-Gly-Gly-Arg-AMC substrate solution (ZGGR-AMC in BSA-60 buffer) and 1 volume trigger solution in BSA5 buffer. Optimized final concentrations (f.c.) of cations in blood (PRR, PPP) were 6 (11) mM $CaCl_2$ and 3 (5.5) mM $MgCl_2$. For mixing procedure, see supplement. The use of ZGGR-AMC as the thrombin substrate (417 µM, f.c.) together with adapted fluorescence optics allowed first measurement of complete TG curves in whole-blood. Fluorescence signals were recorded with a Fluoroskan Ascent microplate fluorometer (Thermolabsystems, Helsinki, Finland) at fluorescence wavelengths of λ_{ex} 355 nm and λ_{em} 460 nm. Fluorescence was collected in parallel from sample and corresponding calibrator wells using Fluoroskan Ascent Software (version 2.6). An Excel-based calculation template was used to automatically generate first derivative TG curves from raw fluorescence data. And then five TG parameters were calculated from those first derivative TG curves corresponding blood and plasma samples: lagtime in minutes (P1), time-to-peak in minutes (TTP; P2), velocity index in nM/minutes (VI; P3), thrombin peak in nM (P4), and endogenous thrombin potential in nM × minutes (ETP; P5). Absence of hemolysis was routinely checked at the end of measurements.

Triggering of blood and plasma samples

In blood or PRP, TG was triggered as appropriate with tissue factor (0.1-1.0 pM), Rvv-X activator (dilution $1e^{-3}$ to $1e^{-7}$), factor Xa (0.1-10 nM), factor XIa (0.3-3 pM), or thrombin (0.1-10 nM). Platelet activation was induced (10 minutes) with the glycoprotein VI (GPVI) agonist cross-linked collagen-related peptide (CRP-XL, 25 µg/mL), which enhances procoagulant activity. For specific experiments, wells containing blood or PRP were preincubated with selected inhibitors of platelet activation or thrombin exosite 1/2.

Red blood cell treatment and reconstitution

Washed annexin A5-treated RBC were reconstituted with autologous PRP or PPP for TG experiments, as described in the supplemental methods. Note that the RBC treatment and washing step were performed in a way to retain annexin A5 binding to the phosphatidylserine-exposing RBC by a continued presence of millimolar $CaCl_2$.

Statistical analysis and data clustering

Statistical analyses were performed with GraphPad Prism 8 (San Diego, USA) and R package version 4.2.1 (www.r-project.org). Data are presented as mean ± SD. Significance was determined using a one-way or two-way ANOVA, as required ($P<0.05$ as statistically significant). Clustered (subtraction) heatmaps of univariate scaled parameters were constructed, as before [22]. For correlation matrices, normality was assessed with a Shapiro-Wilk's test. When parameters were non-normally distributed, this was followed by Spearman correlation analysis. Principal component analysis and k-means clustering analysis used the scaling function in R.

Agreement to share publication-related data

The macro to calculate WB-TG parameters is freely available, and is shared by the corresponding author on reasonable request.

Results

Simultaneous assessment of a completed thrombin generation in whole blood and plasma

Earlier attempts to measure thrombin generation in whole blood samples using 96-well plates only captured the first, rising part of TG [19,23]. We now improved the method using the thrombin substrate ZGGR-AMC in combination with altered fluorescence optics. Other changes were a consistent handling of the viscous blood samples in 96-well plates, adapted calibrator wells, and new data processing scripts. Application with blood from healthy subjects resulted in complete, calibrated TG curves at high throughput. Triplicate measurements with 0.1 pM tissue factor triggering gave an acceptable 5-10% intra-assay variation of curve parameters, *i.e.* lagtime (P1), time-to-peak (P2), velocity index (maximal initial slope, P3), thrombin peak level (P4), and endogenous thrombin potential (ETP, area-under-the-curve, P5).

Since extracellular Ca^{2+} and Mg^{2+} both affect platelet and coagulant activities [24,25], we optimized the two cations concentrations by adding different combinations of these to citrated blood (0-10 mM) or PRP (0-15 mM), and triggering the TG process with 1 pM tissue factor. Heatmapping of the curve variables indicated relatively broad millimolar ranges for maximal TG curves in blood and PRP (**Suppl. Figure 1A-B**). Within the optimum, we choose for using 6 mM $CaCl_2$ and 3 mM $MgCl_2$ in citrated blood, and 11 mM $CaCl_2$ and 5.5 mM $MgCl_2$ in citrated PRP.

In parallel blood and PRP samples, we compared the kinetics of TG induced by $CaCl_2$/$MgCl_2$ and distinct coagulant triggers, *i.e.,* with vehicle, tissue factor (activating the extrinsic factor VII pathway), snake venom Rvv-X (activating factor X), factor Xa, or thrombin. With vehicle solution or low coagulant triggers, the majority of TG curves showed a faster onset and stronger response in whole blood than in PRP (**Figure 1A-D** panels **i-ii**). At higher coagulant triggers, the differences decreased, although factor Xa and thrombin remained more active in blood (**Figure 1A-D iii**). Curve quantification indicated that at low Rvv-X (dilution $1e^{-7}$), factor Xa (≤0.3 nM) or

thrombin (≤0.3 nM) lag times were significantly shorter in blood than in PRP (**Figure 1E**). Furthermore, over a wider concentration range for all triggers, TG peak levels were higher in blood than in PRP (**Figure 1F**). In addition, triggering with factor XIa (0.3-3.0 pM) caused a more enhanced TG response in blood than in PRP (**Suppl. Figure 2A**). Together, this suggested that blood components other than platelets and plasma contribute to the initial phase of TG. This idea was confirmed by measuring clotting times in corresponding blood and PRP samples, indicating a significant shortening in case of blood (**Suppl. Figure 2B**).

Considering a possible role of blood-borne tissue factor in blood samples [20], we compared the TG in blood and PRP samples preincubated with factor VIIa inhibitor (1 μg/mL) [26]. Coagulation triggering with vehicle solution or low Rvv-X (dilution $1e^{-6}$) gave similar profiles with factor VIIai present, for both blood (**Figure 2A-B**) and PRP (**Figure 2C-D**). Statistical analysis confirmed an unchanged lagtime and peak thrombin level (**Figure 2E-F**). On the other hand, blood pretreatment with corn trypsin inhibitor (suppressing the contact activation pathway) resulted in a marked delay in TG even at low 0.1 pM tissue factor concentration (**Suppl. Figure 2C i**).

We also examined the effect of GPVI agonist CRP-XL, which enhances the procoagulant activity of platelets.[26,27] Using weak triggers (vehicle or Rvv-X $1e^{-6}$), CRP-XL accelerated and enhanced the TG in both whole blood and PRP, in which case the extra addition of factor VIIai was again without effect (**Figure 2A-D**). Jointly, these data indicated that, at low dose of coagulant triggers, the generation of thrombin is enhanced and increased in whole blood versus PRP by mechanisms involving other blood cells than platelets, by contact activation, and by GPVI-induced platelet activation.

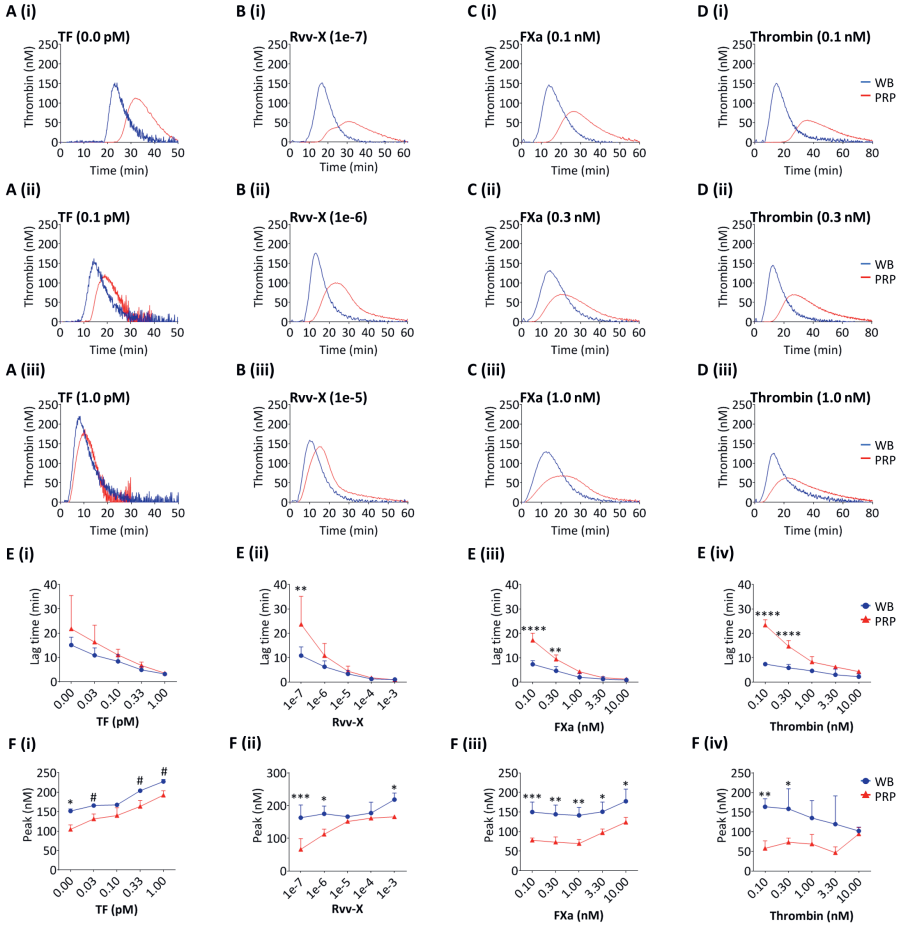

Figure 1. Enhanced thrombin generation in blood compared to PRP for all coagulant triggers. Thrombin generation in whole blood or PRP was triggered in the presence of $CaCl_2$/$MgCl_2$ with vehicle medium or tissue factor (TF, 0.1-1.0 pM) (**A i-iii**), Rvv-X activator (dilutions $1e^{-3}$ to $1e^{-7}$) (**B i-iii**), factor Xa (FXa, 0.1-10 nM) (**C i-iii**), or 0.1-10 nM thrombin (**D i-iii**). Shown are representative curves of nanomolar calibrated TG for each trigger. Calibrated curves of TG were quantitatively assessed for lagtime (**E**) and thrombin peak level (**F**) per trigger and dose. Each condition was performed in parallel with whole blood and corresponding PRP from three donors (n = 3) two-way ANOVA, #*P*<0.10, **P*<0.05, ***P*<0.01, ****P*<0.001. Full data are provided in Datafile 1.

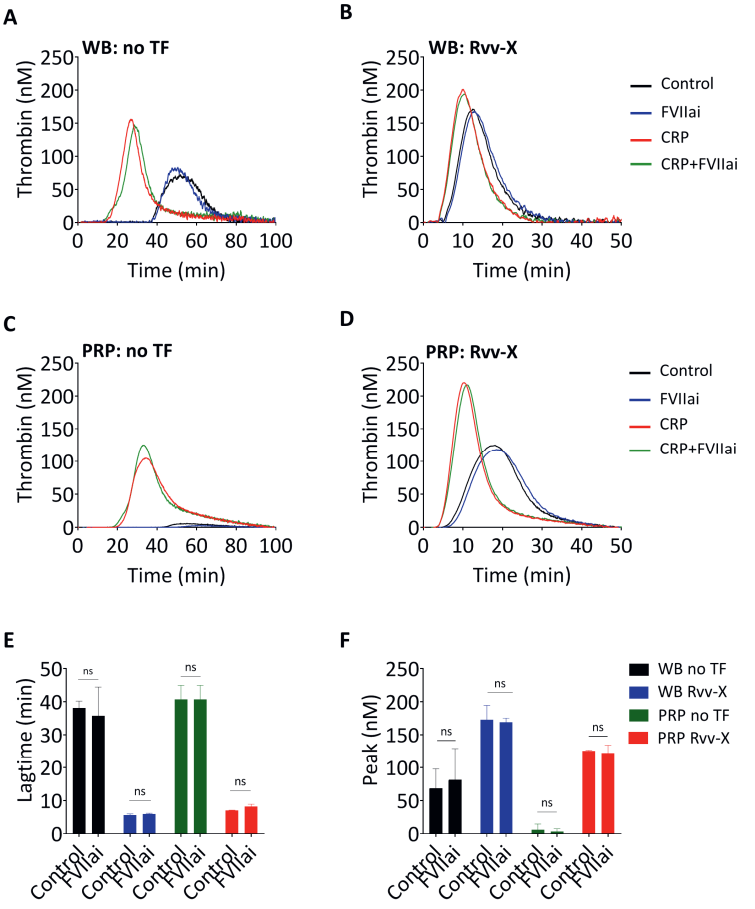

Figure 2. No detectable role of blood-borne tissue factor in whole blood thrombin generation. (**A-D**) Thrombin generation in whole blood (WB) or PRP was triggered with vehicle medium (**A**, **C**) or Rvv-X activator (dilution $1e^{-6}$) (**B**, **D**). Where indicated, samples were pretreated with CRP-XL (25 µg/mL) and/or factor VIIai (FVIIai, 1 µg/mL). Given are representative TG curves (n = 3), as well as the curve parameters lagtime (**E**) and thrombin peak level (**F**). Mean ± SD (n = 3), two-way ANOVA.

Role of phosphatidylserine exposed on red blood cells

A proportion of circulating RBC is known to have surface-exposed phosphatidylserine due to age-dependent eryptosis [28] and by other triggers [29-31]. We investigated RBC phosphatidylserine exposure as an explanation for the enhanced TG in blood samples. For this purposed we used the high-affinity blocking agent annexin A5, which provides 2-dimensional shields on phosphatidylserine of cells and vesicles; a mutant annexin analog lacking the four Ca^{2+}-binding sites (M1-4 annexin A5) acted as control [21,32].

In blood triggered with 0.1 pM tissue factor, we observed a dose-dependent TG inhibition by the wildtype but not the mutant annexin A5 (**Figure 3A**). To check for binding to RBC, we designed

whole blood reconstitution experiments. We first treated isolated RBC with increasing concentrations of annexin A5 (0, 18.75, 37.5, 75 µg/mL) in the presence of $CaCl_2$. After another triple wash in the continuous presence of $CaCl_2$, we reconstituted the annexin A5-blocked RBC (35% hematocrit) with autologous PRP (**Figure 3B**). According to this procedure, the annexin A5 was retained on phosphatidylserine-exposing RBC, while the residual unbound annexin A5 was washed away. In these reconstituted samples, the RBC pretreated with the lowest dose of annexin A5 delayed showed a lowered TG, while higher treatment doses did not have a significant additional effect (**Figure 3C** and **F**). When changing in reconstituted samples the hematocrit from 20 to 40%, the TG lagtime shortened and the peak level increased (**Figure 3D**). However, the annexin-treated RBC invariably reduced the TG curve to the level as seen in PRP, *i.e.* absence of RBC (**Figure 3D** and **G**). Together, this pointed to a hematocrit-dependent enhancing effect on TG that was annulled by pretreatment of the RBC with annexin A5. To further confirm a role of phosphatidylserine-exposing RBC in the enhancement of whole blood TG, we also reconstituted (annexin A5-treated) RBC with PPP. In this case, we noticed an annexin-treatment dose-dependent lowering of TG (**Figure 3E** and **H**), likely due to the fact that phosphatidylserine-exposing platelets could not take over the TG process.

To check for a role of the contact activation pathway, we treated part of the blood samples with corn trypsin inhibitor (CTI). When the isolated plasma samples were reconstituted with RBC, the prior CTI treatment caused a delay and suppression of TG curves (with or without platelets), similarly as in whole blood samples (**Suppl. Figure 2C ii-iii**). On the other hand, extra addition of WBC-enriched buffy coat to the blood did not alter the TG curves (**Suppl. Figure 3**). Together, this pointed to phosphatidylserine exposure on RBC and the contact activation system as major factors in the initial enhancement of TG in blood.

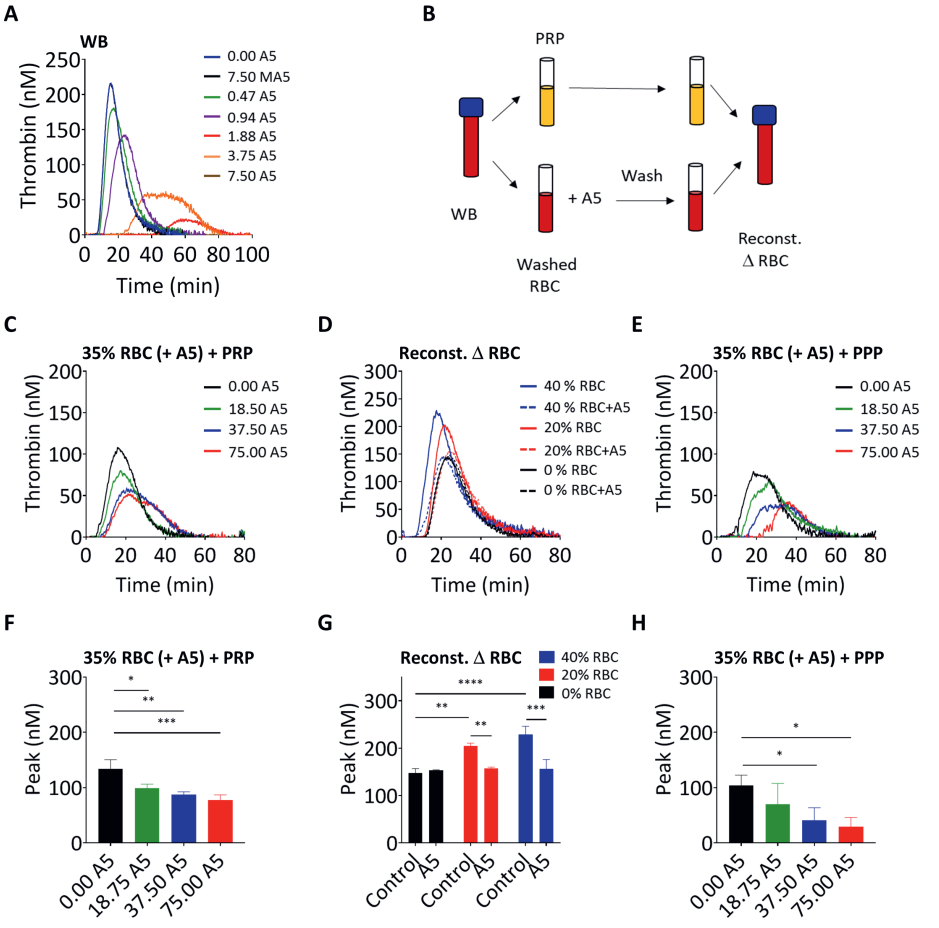

Figure 3. Contribution of red blood cell exposed phosphatidylserine to thrombin generation. (**A**) Thrombin generation was triggered by 0.1 pM tissue factor in whole blood (WB) in the presence of annexin A5 (A5, 0.47-7.50 µg/mL) or mutant annexin A5 (MA5, 7.50 µg/mL), which lacks Ca^{2+}- and phosphatidylserine-binding sites. Shown are representative calibrated curves of 3 independent experiments. (**B**) Schematic procedure of using isolated RBC, treatment with annexin A5, triple wash in the presence of 2 mM $CaCl_2$, and reconstitution with autologous PRP. (**C** and **F**) Thrombin generation effect of RBC treatment with different annexin A5 concentrations (A5, 18.5-75.0 µg/mL) reconstituted at 35% hematocrit in the presence of platelets. Indicated are representative TG curves (**C**) and thrombin peak levels (**F**). Means ± SD (n = 3), one-way ANOVA, **P*<0.05, ***P*<0.01, ****P*<0.001. (**D** and **G**) Thrombin generation effect of RBC treatment with vehicle or (37.5 µg/mL annexin A5, reconstituted at 20% or 40% hematocrit. Note: 0% RBC plus annexin A5 refers to a triple washing with Hepes buffer. Representative TG curves (**D**) and quantified thrombin peak levels (**G**). Means ± SD (n = 3), two-way ANOVA, *P<0.05, **P<0.01. E and H, Thrombin generation effect of RBC treatment with different annexin A5 concentrations (A5, 18.5-75.0 µg/mL) reconstituted at 35% hematocrit in the absence of platelets. Representative TG curves (**E**) and quantified thrombin peak levels (**H**). Mean ± SD (n = 3), one-way ANOVA, **P*<0.05. Full data in Datafile 1.

Role of platelet activation in blood and platelet-rich plasma

To better examine the impact of GPVI-induced platelet activation, we compared how this agonist changed the TG at different concentrations of tissue factor. When tested in blood, CRP-XL appeared to accelerate in the absence or presence of low 0.1 pM tissue factor. On the other hand, in PRP the enhancing effect of CRP-XL continued at higher tissue factor doses (**Figure 4A-B i-iv**). These changes were confirmed by statistical analysis of the TG lag times and peak values (**Figure 4C-F**).

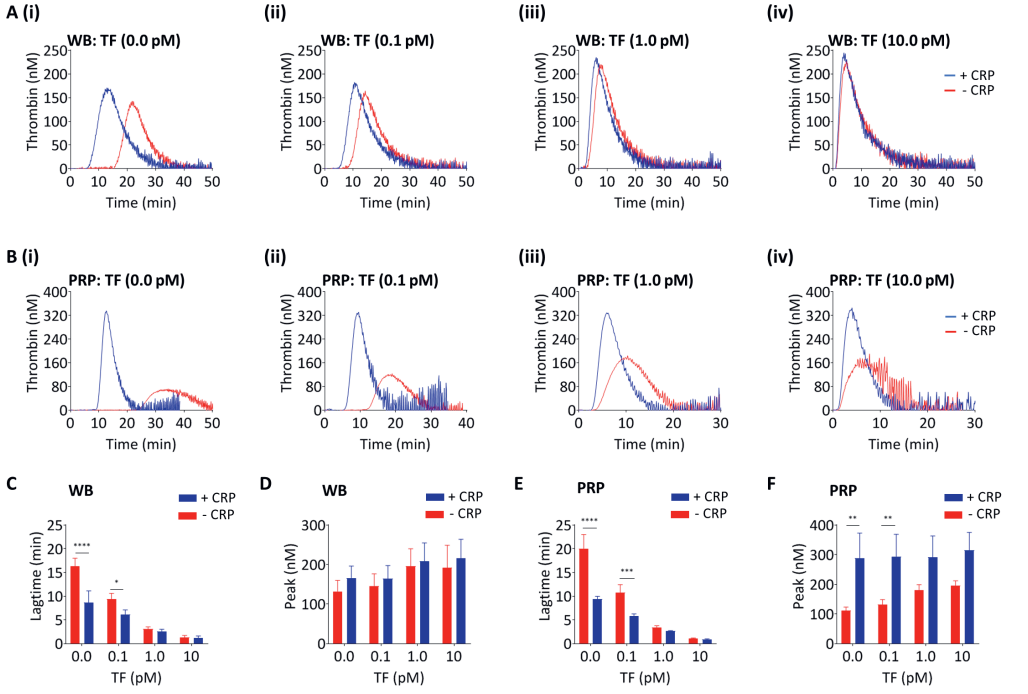

Figure 4. Tissue factor concentration dependent effect of glycoprotein VI-induced platelet activation in thrombin generation. Parallel samples of whole blood (**A**) and PRP (**B**) were triggered in the absence of tissue factor (TF, panels **i**), or with 0.1 pM TF (**ii**), 1 pM TF (**iii**) or 10 pM TF (**iv**). Pre-incubation was with 25 µg/mL CRP-XL, where indicated (+CRP). Traces are representative of three independent experiments. Plots of TG lagtime and thrombin peak levels in whole blood(**C**, **D**) or PRP (**E**, **F**). Data are Mean ± SD (n = 3), two-way ANOVA, **P*<0.05, ***P*<0.01, ****P*<0.001, *****P*<0. 0001. For details, see Datafile 1.

Markedly, in whole blood with added annexin A5 – most strongly at 1.88 and 3.75 µg/mL – platelet pre-activation with CRP-XL caused a shortening and increase in TG (**Suppl. Figure 4A**). In contrast, in reconstituted RBC plus plasma (without platelets), CRP-XL was without effects, and TG was already fully blocked at 1.88 µg/mL annexin A5 (**Suppl. Figure 4B**). Together, these results support a procoagulant role of phosphatidylserine-positive RBC at low trigger dose, which is supplemented with CRP-XL-induced platelet procoagulant activity.

To further assess the roles of platelets in the whole blood system, we checked in a dose-dependent way a number of established inhibitors: the PAR1 antagonists vorapaxar and atopaxar [33], the PAR4 antagonist BMS-986120, aptamers against thrombin exosite 1 and/or 2 [34,35], integrin αIIbβ3 antagonist tirofiban and Syk kinase inhibitor PRT-060318. Heatmapping of the effects on TG parameters lagtime (P1), peak level (P4) and ETP (P5) in blood samples (**Figure 5A**) and in parallel PRP samples (**Figure 5B**) indicated no major effects of the three thrombin receptor antagonists, even not in combination. An integrin-like receptor for fibrinogen on RBC has been reported [36]. Additionally, in mice a role of fibrin(ogen) in RBC capturing has been observed [3]. This raises the option that tirofiban can also interfere in the contact of RBC with platelets and certain coagulation factors.

On the other hand, inhibition of thrombin exosite 1 or exosite 1+2 prolonged and reduced the TG in blood and PRP (**Figure 5A-B**). Platelet integrin or Syk inhibition stronger influenced the coagulation in PRP than in whole blood, in agreement with earlier PRP data [25]. These results overall indicated a more pronounced effect of known platelet inhibitors in the PRP setting.

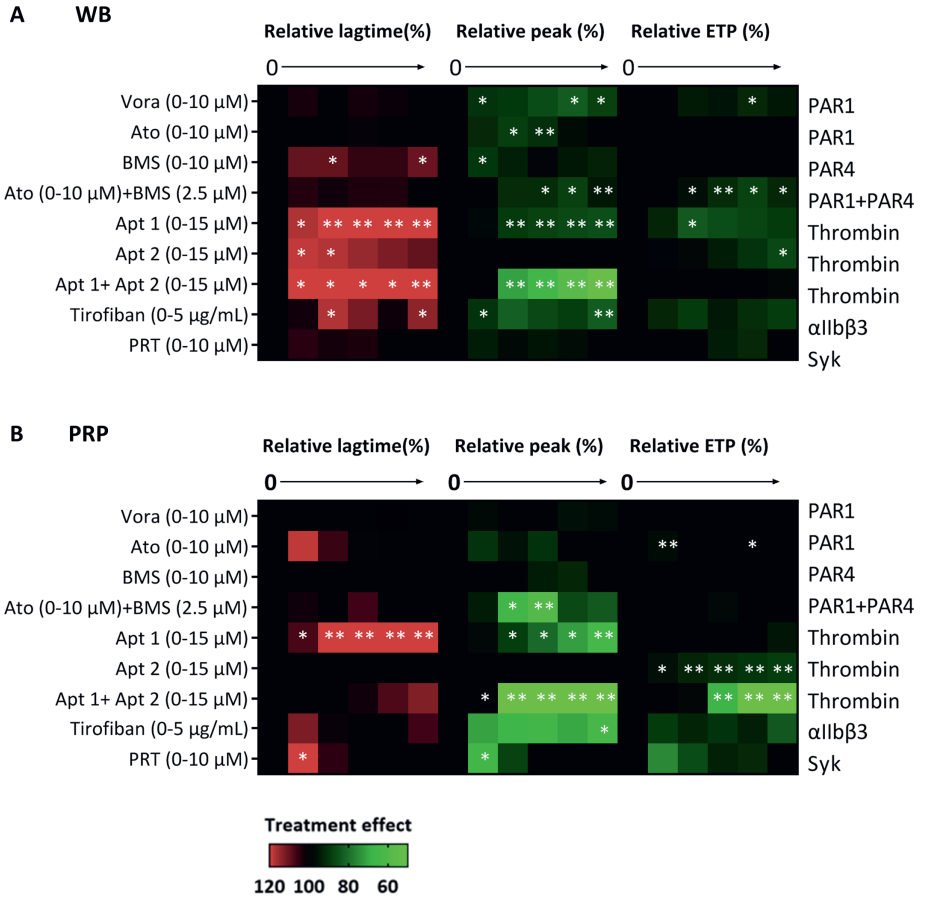

Figure 5. Effects of receptor-directed platelet inhibitors on thrombin generation. Thrombin generation was measured in parallel in whole blood (**A**) and autologous PRP (**B**). Samples were pre-incubated with vehicle medium or inhibitor at 5 increasing concentrations: vorapaxar (Vora, 0.04, 0.16, 0.63, 2.5 or 10 µM; PAR1 antagonist), atopaxar (Ato, idem), BMS-986120 (BM, idem; PAR4 antagonist), aptamer 1 (Apt1, 0.50, 1.75, 3, 9 or 15 µM; thrombin exosite-1 antagonist), aptamer 2 (Apt2, idem exosite-2), aptamer 1+2 (Apt1+2, idem exosite- 1+2), tirofiban (0.31, 0.63, 1.25, 2.5 or 5 µg/mL; integrin αIIbβ3 antagonist) or PRT-060318 (PRT, 0.02, 0.08, 0.4, 2 or 10 µM; Syk antagonist), for 10 minutes at 37 °C. Thrombin generation parameters were compared relative to the vehicle condition (set at 100%). Heatmap presentation of % treatment effect at increasing dose on lagtime (left 6 rows), thrombin peak levels (middle 6 rows), and ETP (area under the curve; right 6 rows). Color code showing increase (red) or decrease (green) in comparison to the vehicle control condition (black, 100%). Each condition was measured three times. Significance from vehicle controls, **P*<0.05, ***P*<0.01, ****P*<0.001, *****P*<0. 0001 (paired t-test).

Modulation of red blood cell phosphatidylserine exposure

Previous flow cytometric studies indicated that a small fraction of isolated human RBC expresses phosphatidylserine[37,38]. This was confirmed by flow cytometry with FITC-annexin A5, showing 0.57 ± 0.33% (mean ± SD, n = 3) in freshly washed RBC (**Suppl. Figure 5A**). To study the suspected procoagulant effect of phosphatidylserine-exposing RBC, we treated the washed RBC with ionomycin or unlabeled annexin A5. This resulted in increased (12%) and decreased (0.2%) percentages of positive RBC, respectively (**Figure 6A-B**). Microscopic examination indicated a small, spherical shape of part of the ionomycin-treated RBC (**Figure 6C**). Markedly, reconstitution of the ionomycin-treated RBC with PRP resulted in an over two-fold increase in the rising phase of TG, when compared to untreated RBC (**Figure 6D**). In agreement with a procoagulant role of the phosphatidylserine exposure, ionomycin-treated RBC strongly increased the factor Xa activity in a purified system (**Figure 6E**). In control experiments, we also checked for the presence of phosphatidylserine-exposing vesicles. In platelet-free plasma obtained from freshly isolated blood samples, however, TG remained very low in response to Rvv-X, but not when triggered with tissue factor plus phospholipids (**Suppl. Figure 5B**).

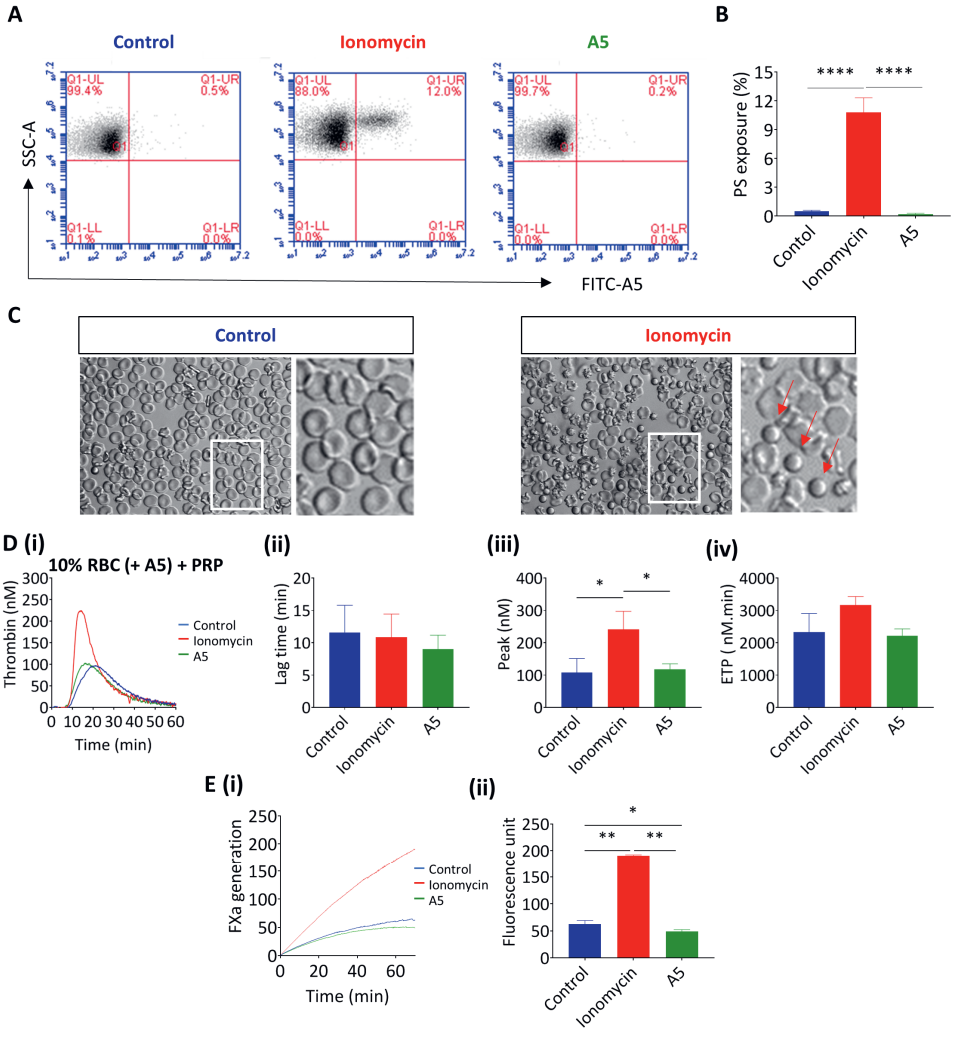

Figure 6. Altered thrombin generation by increasing or blocking phosphatidylserine exposure on RBC. (**A-B**) Flow cytometry of phosphatidylserine exposure of washed RBC after 30 minutes treatment with 10 µM ionomycin/$CaCl_2$ or with 7.5 µg/mL annexin A5/$CaCl_2$ (A5), analyzed after labeling with FITC-annexin A5. Shown are representative fluorescence-scatter profiles (F1 *vs.* SSC) (**A**) and fractions of phosphatidylserine-exposing RBC (**B**). Visualization of RBC without or with ionomycin/$CaCl_2$ treatment (**C**). Arrows indicate activated, rounded RBC. (**D**) Effect of RBC treatment with ionomycin/$CaCl_2$ or annexin A5/$CaCl_2$ and wash, in comparison to no treatment (control) on TG in PRP samples reconstituted at 10% hematocrit at 0.1 pM tissue factor. Panels give representative curves (**i**); quantified lag times (**ii**), thrombin peak levels (**iii**) and ETP values (**iv**). (**E**) Effect of RBC treatment with ionomycin/$CaCl_2$ or annexin A5/$CaCl_2$ on factor Xa generation in a purified system. Indicated are representative factor Xa generation curves (**i**), and increased fluorescence units over 40 minutes (**ii**). Mean ± SD (n = 3), one-way ANOVA, **P*<0.05, ***P*<0.01, ****P*<0.001.

Proof-of-principle patient study

Considering the contribution of RBC to whole blood TG, we also tested this in patients with typical RBC abnormalities. The subjects, investigated during a limited period, included healthy day-controls, five patients with mostly familial polycythemia vera (treated by phlebotomy), two patients with erythrocytosis (treated by phlebotomy), and eight untreated patients with distinct forms of anemia, two of whom had hemolytic anemia or sickle cell disease (**Table 1**). The treated polycythemia vera patients had mostly normal hematological parameters, the erythrocytosis patients characteristically showed high hemoglobin levels, and the anemia patients all had low RBC counts, in part of the cases together with sub-normal platelet counts (**Table 1**).

Using the collected blood samples, we obtained triplicate TG curves triggered by vehicle, 0.1 or 1.0 pM TF, Rvv-X ($1e^{-5}$, $1e^{-6}$, $1e^{-7}$) or CRP-XL. Representative curves per patient are given in Suppl. Figure 6. A subtraction heatmap of the five TG parameters per trigger (scaled 0-10) versus the means of controls indicated an overall high consistency in the alterations per patient (**Figure 7A**). In particular, low values were obtained for one patient with polycythemia vera (Pcv4) and two patients with anemia (Ane1, Ane2, both had also low platelet counts). In contrast, high values were seen for other anemia patients (Ane6, Ane7, Ane8). Levels of ETP only were high for the patient with sickle cell disease (Ane7). A two-factor plot of RBC versus peak level indicated close grouping of the healthy controls and polycythemia patients, but a separation of 6 anemia patients with a relatively high TG and 2 with low TG, based on the RBC count (**Figure 7B**).

As an unbiased approach comparing the hematological (10) and TG curve (5x6) parameters, we performed a Spearman correlation analysis, which showed high consistency within the RBC and TG parameters, but not between the parameter sets (**Suppl. Figure 7**). A principal component analysis (PCA) on the same dataset identified four clusters in two dimensions, explaining 80.6% of the variance (**Figure 7C**). The matrix for all dimensions showed a high contribution of most TG parameters to dimension 1, and stronger contribution of the RBC parameters to dimension 2 (**Suppl. Figure 8**). Interestingly, cluster 1 was formed by the anemia patients with relatively high TG (Ane6-8). Cluster 2 by most control subjects together with the polycythemia vera patients. Cluster 3 consisted of a mixed set of individuals, while cluster 4 included only the anemia patients with low TG and low platelet counts (Ane1, Ane2).

With the various blood samples, we also studied the effect of two doses of annexin A5 on TG triggered by low tissue factor (0.1 pM). Analysis indicated overall dose-dependent annexin A5 effects by prolonging the lagtime P1 (**Figure 7D**) and lowering the peak level P4 (**Figure 7E**). Per cluster of subjects, annexin A5 addition led to similar absolute, but not relative decreases in peak level. These results hence pointed to different levels of RBC phosphatidylserine exposure in a cluster-dependent way, with in particular cluster 1 patients (sickle cell and hemolytic anemia) requiring high concentrations of annexin A5 to completely block the TG process.

Table 1. Baseline characteristics and hematologic variables of patient study.

Subject code	Sex	Age	Subject class	Diagnosis and genetics	Prior treatment	WBC	RBC	HBG	HCT	MCV	PLT	MPV
						10^3/mL	10^6/mL	g/dL	%	fL	10^3/mL	fL
Con1	F	53	healthy control	none	none	5.4	4.1	13.9	37.4	90.1	191	8.6
Con2	M	31	healthy control	none	none	9.2	4.7	15.7	43.2	91.2	333	8.7
Con3	F	38	healthy control	none	none	5.1	4.1	13.8	39.1	93.6	287	6.9
Con4	M	27	healthy control	none	none	5.8	5.6	17.5	47.5	85.9	150	8.5
Con5	F	28	healthy control	none	none	5.2	**3.9***	12.6	36.2	93.3	**132***	9.0
Con6	M	32	healthy control	none	none	9.8	4.8	15.1	41.9	88.1	256	8.6
Pcv1	F	57	primary polycythemia	*JAK2* mutation V617F	periodic phlebotomy	6.7	5.2	15.1	42.5	81.4	**48***	8.4
Pcv2	M	70	primary polycythemia	myeloproliferative syndrome, JAK2 negative	periodic phlebotomy	6.1	5.1	16.5	46.0	89.9	**141***	8.3
Pcv3	M	61	primary polycythemia	*JAK2* mutation V617F	periodic phlebotomy + cytoreductive therapy	8.4	4.1	16.5	44.6	**109.1†**	332	7.9
Pcv4	F	74	familial erythrocytosis	*EGLN1* mutation (ECYT3)	warfarin	6.6	5.5	16.3	46.5	84.3	206	**9.1†**
Pcv5	M	65	primary polycythemia	*JAK2* mutation V617F	periodic phlebotomy + cytoreductive therapy	8.4	4.1	15.6	43.5	**104.8†**	281	7.9
Ery1	M	68	primary erythrocytosis	*PHD2* C127S, not pathogenetic. Ongoing genotyping	phlebotomy	7.4	5.3	**18.4†**	51.3	**97.4†**	176	**9.1†**
Ery2	M	21	familial erythrocytosis	*EPAS1* mutation (ECYT4)	periodic phlebotomy	6.3	5.6	**18.2†**	48.8	86.5	164	7.9
Ane1	M	55	anemia	GI bleeding in alcoholic liver failure	none	4.8	**1.9***	**6.9***	**18.5***	**97.7†**	**81***	8.5
Ane2	F	57	anemia	myeloid leukemia after chemotherapy	none	**0.2***	**1.8***	**6.2***	**16.2***	90.4	**15***	7.5
Ane3	M	67	anemia	sepsis in acute cholecystitis	none	5.0	**2.6***	**6.3***	**18.0***	**70.2***	256	8.0
Ane4	M	79	anemia	refractory anemia	none	4.7	**2.1***	**7.2***	**19.9***	92.9	223	**10.1†**
Ane5	F	95	anemia	Gl bleeding and malnutrition	none	6.3	**1.3***	**4.5***	**12.0***	95.8	**149***	8.0
Ane6	M	91	chronic anemia	chronic GI bleeding	none	5.3	**2.4***	**6.8***	**18.8***	79.6	223	7.6
Ane7	M	46	sickle cell anemia	homozygous sickle cell disease	none	**13.2†**	**2.4***	**9.1***	**24.6***	**103.8†**	282	7.2
Ane8	M	84	hemolytic anemia	immune hemolytic anemia	none	7.4	**2.1***	**6.4***	**18.2***	87.7	**67***	n.d.
Normal range						4-10	4.0-5.8	12.0-18.0	35.0-52.0	79.0-96.0	150-400	5.0-9.0

GI, gastrointestinal; HBG, hemoglobin; HCT, hematopoietic cell transplant; MCV, mean corpuscular volume; MPV, mean platelet volume; nd, not defined; PLT, platelet; WBC, white blood cell.

The bold values indicate values below or above the normal range. Values below normal ranges are marked with *, and those above normal ranges are marked with †.

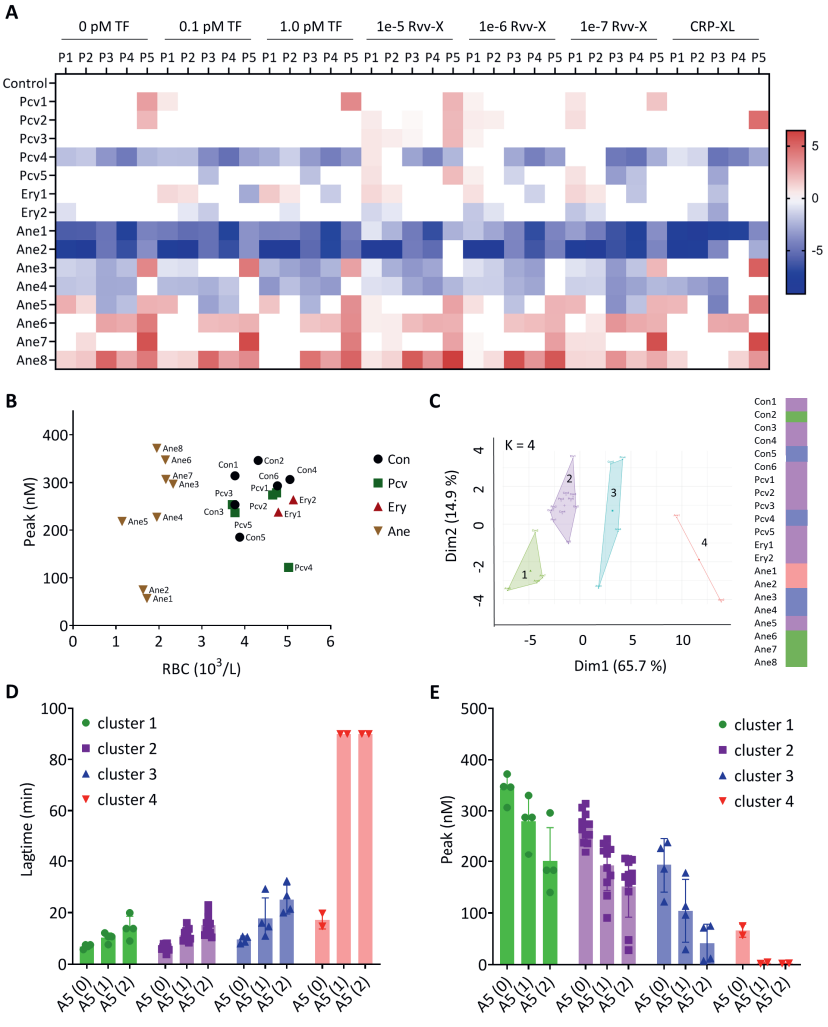

Figure 7. Changes in thrombin generation in blood from patients with altered red blood cell traits. Blood was investigated from day-control subjects (Con), or from patients with polycythemia vera (Pcv), erythrocytosis (Ery) or anemia (Ane) of various causes (Table 1). Whole blood TG was measured in response to vehicle, tissue factor (TF, 0.1, 1.0 pM) or Rvv-X (dilutions $1e^{-5}$, $1e^{-6}$, $1e^{-7}$). Where indicated, platelets in blood were stimulated with CRP-XL (25 µg/mL, 0.1 pM TF). Parameters of TG curves were univariate scaled 0-10 across all conditions, and differences per patient *vs.* means of control subjects were obtained. (**A**) Subtraction heatmap of TG parameters (scaled 0-10) from 15 patient samples per indicated trigger. Note reversed scaling for lagtime and TTP. Differences were filtered for changes outside of mean ± SD. Color code: blue = decrease, red = increase. (**B**) Plot of RBC count and thrombin peak level (0.1 pM TF) per subject. (**C**) Results of principal component analysis of combined TG and hematological parameters (Suppl. Figures 7-8). Colors indicate 4 clusters, with each dot representing one subject. (**D-E**) Effect annexin A5 addition (vehicle, 1 or 2 µg/mL) on lagtime (**D**) and peak level (**E**) at 0.1 pM TF per cluster of subjects (clustered according to panel **C**). For full data, see Datafile 1.

Discussion

In this paper, we describe a manner of obtaining first derivative, calibrated thrombin generation curves in 96-well plates, which for the first time allows to make a complete quantitative comparison of this coagulation process in whole blood and (platelet-rich) plasma from the same subjects. Our results revealed an initial role of RBC, a minor contribution of WBC and a secondary contribution of activated platelets in the TG process. The annexin A5 inhibition and reconstitution studies indicated a priming role of RBC surface-expressed phosphatidylserine, with an additional contribution of the contact activation system. The observation of no reduction of TG by selectively annexin A5-treated RBC we consider as proof-of-evidence of the high-affinity retainment of annexin A5 to RBC, unable to switch over to the phosphatidylserine-exposing platelets that are formed during the TG process. Kinetic analysis indicated that in whole blood the supporting role phosphatidylserine-exposing platelets was secondary to that of RBC. Similarly, we found that common platelet antagonists were less effective in blood than in PRP, although prior GPVI activation enhanced the platelet contribution.

The presently developed manner of complete TG curves provides novel insight into the role of phosphatidylserine-exposing RBC in the regulation of coagulation. An earlier subsampling method did not detect an initiating role of blood-borne tissue factor in whole blood coagulation, unless monocytes were pre-stimulated with lipopolysaccharide [16]. in a follow-up study, it was concluded that TG negatively correlated with phosphatidylserine expression on RBC [4]. In earlier studies from our group [19,23], no enhancing effect of RBC on TG could be identified, because the red cells and clots caused disturbances in the signal detection. In another method of TG measurement in mouse blood, also the role of RBC was not investigated, as that work focused on coagulation amplification via factors XI and IX [39].

For long, the examined link of RBC abnormalities with venous or arterial thrombotic complications have been suggestive for a procoagulant function of RBC [9, 10, 40]. Our present data indicate that at low trigger doses the coagulation process develops faster in whole blood than in PRP. Furthermore, we found in reconstitution experiments that negative of positive manipulation of phosphatidylserine on RBC (with annexin A5 or ionomycin, respectively) markedly affected the TG process. Together, this strongly indicates that such RBC play an active role in the blood coagulation. Furthermore, we showed that phosphatidylserine-blocked RBC no longer supported a fast-onset TG, a role that could be taken over by GPVI-activated platelets. By inference, the procoagulant role of RBC may be most relevant under conditions of local blood stasis or in semi-static red venous blood clots.

Earlier papers did not find a role of WBC-derived (blood borne) tissue factor in the whole blood coagulation process [16,26]. We confirmed this by checking the effect of factor VII inhibition on Rvv-X-activated blood samples. The expression of active tissue factor by platelets is still a matter of debate, with positive [41] and negative [42] evidences. A recent paper states that especially in smaller platelets its activity is antagonized by platelet-derived tissue factor pathway inhibitor (TFPI) [43]. Given the relatively high mRNA and protein expression of secretory TFPI in human platelets, when compared to tissue factor [44], our results may be explained by an overshoot of TFPI, *e.g.*, released by CRP-XL, thus preventing tissue factor activity in whole blood or PRP.

In contrast, it appeared that pretreatment of blood with corn trypsin inhibitor delayed the TG process in (reconstituted) blood samples containing RBC. Recently, it was reported that RBC-derived extracellular vesicles can trigger the contact activation by a classic factor XIIa-XI-IX pathway as well as by direct kallikrein activation of factor IX [45]. Given the low levels of such vesicles seen in freshly isolated blood samples, we speculate that also intact RBC can have such an effect, likely in a phosphatidylserine-dependent way. However, this requires further research.

Red blood cells are by far the most abundant cells in the blood circulation. Earlier papers indicated that a small fraction of about 0.5% of freshly isolated RBC exposes phosphatidylserine [2,46]. In patients with polycythemia very, phosphatidylserine exposure on isolated RBC can increase from 1.4 to 3.6% [47,48]. The underlying process is known as eryptosis developing by ageing, in vitro storage, and a variety of other conditions, inducing removal of the erythrocytes from the circulation [28,46]. Mechanistically, RBC phosphatidylserine externalization is regulated by phospholipid transporters such as ATP11C [7] and anoctamin-6 [49]. For instance, a mutation in the *ATP11C* gene associates with RBC dysfunction and hemolytic anemia [50]. Also in congenital sickle cell disease, RBC dysfunction can lead to an anemic condition. In our view, comparative measurements of TG in blood and plasma samples can now help to better resolve how blood cell-associated abnormalities alter the coagulation process.

In the experiments, we noticed for several coagulation triggers, in particular factor Xa, an only shallow dose-response on TG parameters. Our tentative explanation is that low factor Xa distributes among the relatively large surface of phosphatidylserine-expressing RBC, thus preventing extra enforcement of the prothrombinase loop. An interesting finding was that PAR1 and PAR4 antagonists caused no more than small effects on the blood and PRP TG parameters. Recent work points to the formation of procoagulant platelets via S100A-protein interactions with GPIbα [51] or via Fas ligand-receptor interactions [52]. Such pathways may complement the roles of the platelet thrombin receptors, but this needs further examination.

Our findings in patients with (congenital) polycythemia vera or erythrocytosis with essentially normal blood cell counts showed similar TG responses as those from healthy controls, likely linked to the normalized the RBC counts during treatment. On the other hand, we found a strong versatility in TG parameters in the heterogeneous group of patients with anemia (low RBC counts). In three patients, *i.e.,* with hemolytic anemia or congenital sickle cell disease, the high TG was dose-dependently suppressed with annexin A5, supporting a procoagulant role for phosphatidylserine on RBC.

Several other clinical conditions can induce the hemostatic response, often linked to increased risk of thrombosis, such as antiphospholipid syndrome, heparin-induced thrombocytopenia and SARS-CoV-2-induced infection [53]. This suggests that qualitative and quantitative platelet traits also contribute to the overall coagulation profile. In those patients, whole blood TG can give better insight in the interplay between RBC, platelets and the coagulation system.

Limitations of our study are the small number of patients with expected RBC abnormalities investigated. Especially the anemia patients formed a heterogenous group with a wide variety of causes of the low RBC counts (**Table 1**). On the other hand, the included patients with primary polycythemia showed normal RBC properties due to periodic phlebotomy. Whilst our data

suggest that the overall level of phosphatidylserine exposure in both quality and quantity determines the TG in patient blood samples, more work is needed to draw clinically relevant conclusions.

Authors' contributions

S.S. performed experiments, analyzed results and drafted the manuscript; S.T. and J.Z. performed experiments and edited the manuscript; J.K., J.W. and D.H. provided technical support and edited the manuscript; D.I.F. analyzed experiments and edited the manuscript, C.P.M.R. provided reagents; P.G.d.G. and B.d.L. provided supervision and edited the manuscript; P.S. and E.C. recruited patients, collected blood samples and edited the manuscript. J.W.M.H. and M.R. supervised research and wrote the manuscript. All authors approved the final version of the manuscript.

Acknowledgements

The authors thank Dr. F. Swieringa for providing assistance for the image study and Dr. L. Spiezia for collecting patient samples. The authors thank the volunteers who donated blood for this study. This work was supported by the China Scholarship Council (S. S.: CSC 201906220218, and J.Z. CSC 201909370052).

Disclosures

B.d.L., J.K., D.H., J.W. and M.R. are employees of the Synapse Research Institute Maastricht (member of the Stago Diagnostic group), P.G.d.G. and J.W.M.H. are advisors of the same institute. The other authors do not report a conflict of interest.

References

1 Borissoff JI, Spronk HM, ten Cate H. The hemostatic system as a modulator of atherosclerosis. *N. Engl. J. Med*. **2011**, *364*, 1746-1760.

2 Byrnes JR, Wolberg AS. Red blood cells in thrombosis. *Blood*. **2017**, *130*, 1795-1799.

3 Aleman MM, Byrnes JR, Wang JG, Tran R, Lam WA, Di Paola J, Mackman N, Degen JL, Flick MJ, Wolberg AS. Factor XIII activity mediates red blood cell retention in venous thrombi. *J. Clin. Invest*. **2014**, *124*, 3590-3600.

4 Whelihan MF, Lim MY, Mooberry MJ, Piegore MG, Ilich A, Wogu A, Cai J, Monroe DM, Ataga KI, Mann KG, Key NS. Thrombin generation and cell-dependent hypercoagulability in sickle cell disease. *J. Thromb. Haemost*. **2016**, *14*, 1941-1952.

5 Faes C, Ilich A, Sotiaux A, Sparkenbaugh EM, Henderson MW, Buczek L, Beckman JD, Ellsworth P, Noubouossie DF, Bhoopat L, Piegore M, Renoux C, Bergmeier W, Park Y, Ataga KI, Cooley B, Wolberg AS, Key NS, Pawlinski R. Red blood cells modulate structure and dynamics of venous clot formation in sickle cell disease. *Blood*. **2019**, *133*, 2529-2541.

6 Whelihan MF, Lim MY, Key NS. Red blood cells and thrombin generation in sickle cell disease. *Thromb. Res*. **2014**, *133* Suppl. 1, S52-53.

7 Arashiki N, Takakuwa Y, Mohandas N, Hale J, Yoshida K, Ogura H, Utsugisawa T, Ohga S, Miyano S, Ogawa S, Kojima S, Kanno H. ATP11C is a major flippase in human erythrocytes and its defect causes congenital hemolytic anemia. *Haematologica*. **2016**, *101*, 559-565.

8 Vijay R, Guthmiller JJ, Sturtz AJ, Crooks S, Johnson JT, Li L, Lan LY, Pope RL, Chen Y, Rogers KJ, Dutta N, Toombs JE, Wilson ME, Wilson PC, Maury W, Brekken RA, Butler NS. Hemolysis-associated phosphatidylserine exposure promotes polyclonal plasmablast differentiation. *J. Exp. Med*. **2021**, *218*, e20202359.

9 Griesshammer M, Kiladjian JJ, Besses C. Thromboembolic events in polycythemia vera. *Ann. Hematol*. **2019**, *98*, 1071-1082.

10 Guglielmelli P, Vannucchi AM. Current management strategies for polycythemia vera and essential thrombocythemia. *Blood Rev*. **2020**, *42*, 100714.

11 Nguyen DB, Wagner-Britz L, Maia S, Steffen P, Wagner C, Kaestner L, Bernhardt I. Regulation of phosphatidylserine exposure in red blood cells. *Cell Physiol. Biochem*. **2011**, *28*, 847-856.

12 Wesseling MC, Wagner-Britz L, Huppert H, Hanf B, Hertz L, Nguyen DB, Bernhardt I. Phosphatidylserine exposure in human red blood cells depending on cell age. *Cell Physiol. Biochem*. **2016**, *38*, 1376-1390.

13 Wadud R, Hannemann A, Rees DC, Brewin JN, Gibson JS. Yoda1 and phosphatidylserine exposure in red cells from patients with sickle cell anaemia. *Sci. Rep*. **2020**, *10*, 20110.

14 Kremers RM, Peters TC, Wagenvoord RJ, Hemker HC. The balance of pro- and anticoagulant processes underlying thrombin generation. *J. Thromb. Haemost*. **2015**, *13*, 437-447.

15 Binder NB, Depasse F, Mueller J, Wissel T, Schwers S, Germer M, Hermes B, Turecek PL. Clinical use of thrombin generation assays. *J. Thromb. Haemost*. **2021**, *19*, 2918-2929.

16 Butenas S, Bouchard BA, Brummel-Ziedins KE, Parhami-Seren B, Mann KG. Tissue factor activity in whole blood. *Blood*. **2005**, *105*, 2764-2770.

17 Ninivaggi M, Apitz-Castro R, Dargaud Y, de Laat B, Hemker HC, Lindhout T. Whole bloodthrombin generation monitored with a calibrated automated thrombogram-based assay. *Clin. Chem*. **2012**, *58*, 1252-1259.

18 Li L, Roest M, Sang Y, Remijn JA, Fijnheer R, Smit K, Huskens D, Wan J, de Laat B, Konings J. Patients with multiple myeloma have a disbalanced whole blood thrombin generation profile. *Front. Cardiovasc. Med*. **2022**, *9*, 919495.

19 Wan J, Konings J, Yan Q, Kelchtermans H, Kremers R, de Laat B, Roest M. A novel assay for studying the involvement of blood cells in whole blood thrombin generation. *J. Thromb. Haemost*. **2020**, *18*, 1291-1301.

20 Versteeg HH, Heemskerk JW, Levi M, Reitsma PH. New fundamentals in hemostasis. *Physiol. Rev*. **2013**, *93*, 327-358.

21 Vanschoonbeek K, Feijge MA, van Kampen RJ, Kenis H, Hemker HC, Giesen PL, Heemskerk JW. Initiating and potentiating role of platelets in tissue factor-induced thrombin generation in the presence of plasma, subject-dependent variation in thrombogram characteristics. *J. Thromb. Haemost*. **2004**, *2*, 476-484.

22 Van Geffen JP, Brouns S, Batista J, McKinney H, Kempster C, Sivapalaratnam S, Baaten CB, Bourry N, Frontini M, Nagy M, Swieringa F, Turro E, Verdoold R, Cavill R, Kuijpers MJ, Ouwehand WH, Downes K, Heemskerk JW. High-throughput elucidation of thrombus formation reveals sources of platelet function variability. *Haematologica*. **2019**, *104*, 1256-1267.

23 Wan J, Roberts LN, Hendrix W, Konings J, Ow TW, Rabinowich L, Barbouti O, de Laat B, Arya R, Patel VC, Roest M, Lisman T, Bernal W. Whole blood thrombin generation profiles of patients with cirrhosis explored with a near patient assay. *J. Thromb. Haemost*. **2020**, *18,* 834-843.

24 Herrmann RG, Lacefield WB, Crowe VG. Effect of ionic calcium and magnesium on human platelet aggregation. *Proc. Soc. Exp. Biol. Med*. **1970**, *135*, 100-3.

25 Van der Meijden PE, Feijge MA, Swieringa F, Gilio K, Nergiz-Unal R, Hamulyák K, Heemskerk JW. Key role of integrin αIIbβ3 signaling to Syk kinase in tissue factor-induced thrombin generation. *Cell. Mol. Life Sci*. **2012**, *69*, 3481-3492.

26 Brouns S, van Geffen JP, Campello E, Swieringa F, Spiezia L, van Oerle R, Provenzale I, Verdoold R, Farndale RW, Clemetson KJ, Spronk H, van der Meijden PE, Cavill R, Kuijpers MJ, Castoldi E, Simioni P, Heemskerk JW. Platelet-primed interactions of coagulation and anticoagulation pathways in flow-dependent thrombus formation. *Sci. Rep*. **2020**, *10*, 11910.

27 Sang Y, Roest M, de Laat B, de Groot PG, Huskens D. Interplay between platelets and coagulation. *Blood Rev*. **2021**, *46*, 100733.

28 Dreischer P, Duszenko M, Stein J, Wieder T. Eryptosis, programmed death of nucleus-free, iron-filled blood cells. *Cells*. **2022**, *11*, 503.

29 Ghashghaeinia M, Wesseling MC, Ramos E, Petkova-Kirova P, Waibel S, Lang E, Bissinger R, Alzoubi K, Edelmann B, Hosseinzadeh Z, Dreischer P, Shahvaroughi-Farahani A, Mrowietz U, Köberle M, Kaestner L, Bernhardt I, Martínez-Ruiz A, Wieder T, Lang F. Trifluoperazine-induced suicidal erythrocyte death and S-nitrosylation inhibition, reversed by the nitric oxide donor sodium nitroprusside. *Cell Physiol. Biochem*. **2017**, *42*, 1985-1998.

30 Guo L, Tong D, Yu M, Zhang Y, Li T, Wang C, Zhou P, Jin J, Li B, Liu Y, Liu R, Novakovic VA, Dong Z, Tian Y, Kou J, Bi Y, Zhou J, Shi J. Phosphatidylserine-exposing cells contribute to the hypercoagulable state in patients with multiple myeloma. *Int. J. Oncol*. **2018**, *52*, 1981-1990.

31 Chung HY, Bian Y, Lim KM, Kim BS, Choi SH. Martx toxin of Vibrio vulnificus induces RBC phosphatidylserine exposure that can contribute to thrombosis. *Nat. Commun*. **2022**, *13*, 4846.

32 Kenis H, Reutelingsperger C. Targeting phosphatidylserine in anti-cancer therapy. *Curr. Pharm. Des*. **2009**, 15, 2719-2723.

33 Wallace EL, Smyth SS. Targeting platelet thrombin receptor signaling to prevent thrombosis. *Pharmaceuticals (Basel)*. **2013**, *6*, 915-928.

34 Derszniak K, Przyborowski K, Matyjaszczyk K, Moorlag M, de Laat B, Nowakowska M, Chlopicki S. Comparison of effects of anti-thrombin aptamers HD1 and HD22 on aggregation of human platelets, thrombin generation, fibrin formation, and thrombus formation under flow conditions. *Front Pharmacol*. 2019, 10, 68.

35 Nimjee SM, Oney S, Volovyk Z, Bompiani KM, Long SB, Hoffman M, Sullenger BA. Synergistic effect of aptamers that inhibit exosites 1 and 2 on thrombin. *RNA*. 2009, 15, 2105-11.

36 Carvalho FA, Connell S, Miltenberger-Miltenyi G, Pereira SV, Tavares A, Ariëns RA, Santos NC. Atomic force microscopy-based molecular recognition of a fibrinogen receptor on human erythrocytes. *ACS Nano*. **2010**, *4*, 4609-4620.

37 Whelihan MF, Zachary V, Orfeo T, Mann KG. Prothrombin activation in blood coagulation, the erythrocyte contribution to thrombin generation. *Blood*. **2012**, *120*, 3837-3845.

38 Al Mamun Bhuyan A, Lang F. Inhibition of erythrocyte cell membrane scrambling following energy depletion and hyperosmotic shock by alectinib. *Cell Physiol Biochem*. **2018**, *51*, 1996-2009.

39 Wan J, Tanratana P, Roest M, Gruber A, Pawlinski R, Wolberg AS, Mackman N, Grover SP. A novel mouse whole blood thrombin generation assay sensitive to FXI- and FIX-mediated amplification of coagulation. *Blood Adv*. **2023**, *7*, 1915-1925.

40 Bettiol A, Galora S, Argento FR, Fini E, Emmi G, Mattioli I, Bagni G, Fiorillo C, Becatti M. Erythrocyte oxidative stress and thrombosis. *Expert Rev Mol Med*. **2022**, *24*, e31.

41 Panes O, Matus V, Sáez CG, Quiroga T, Pereira J, Mezzano D. Human platelets synthesize and express functional tissue factor. *Blood*. **2007**, *109*, 5242-5250.

42 Østerud B, Olsen JO. Human platelets do not express tissue factor. *Thromb. Res*. **2013**, *132*, 112-115.

43 Brambilla M, Rossetti L, Zara C, Canzano P, Giesen PL, Tremoli E, Camera M. Do methodological differences account for the current controversy on tissue factor expression in platelets? *Platelets*. **2018**, *29*, 406-414.

44 Huang J, Swieringa F, Solari FA, Provenzale I, Grassi L, De Simone I, Baaten CC, Cavill R, Sickmann A, Frontini M, Heemskerk JW. Assessment of a complete and classified platelet proteome from genome-wide transcripts of human platelets and megakaryocytes covering platelet functions. *Sci. Rep*. **2021**, *11*, 12358.

45 Noubouossie DF, Henderson MW, Mooberry M, Ilich A, Ellsworth P, Piegore M, Skinner SC, Pawlinski R, Welsby I, Renné T, Hoffman M, Monroe DM, Key NS. Red blood cell microvesicles activate the contact system, leading to factor IX activation via 2 independent pathways. *Blood*. **2020**, *135*, 755-765.

46 Lang E, Pozdeev VI, Xu HC, Shinde PV, Behnke K, Hamdam JM, Lehnert E, Scharf RE, Lang F, Häussinger D, Lang KS, Lang PA. Storage of erythrocytes induces suicidal erythrocyte death. *Cell Physiol. Biochem*. **2016**, *39*, 668-676.

47 Fujita H, Sakuma R, Tomiyama J, Hamaki T, Ohwada A, Kurosawa S, Nishimura S. Increased phosphatidylserine exposure on the erythrocyte membrane in patients with polycythaemia vera. *Br. J. Haematol*. **2011**, *152*, 238-240.

48 Tan X, Shi J, Fu Y, Gao C, Yang X, Li J, Wang W, Hou J, Li H, Zhou J. Role of erythrocytes and platelets in the hypercoagulable status in polycythemia vera through phosphatidylserine exposure and microparticle generation. *Thromb. Haemost*. **2013**, *109*, 1025-1032.

49 Yan M, Xu M, Li Z, An Y, Wang Z, Li S, Chen Y, Xia Y, Wang L, Wang L, Ji S, Dong W, Shi J, Gao C. TMEM16F mediated phosphatidylserine exposure and microparticle release on erythrocyte contribute to hypercoagulable state in hyperuricemia. *Blood Cells Mol. Dis*. **2022**, *96*, 102666.

50 Arashiki N, Niitsuma K, Seki M, Takakuwa Y, Nakamura F. ATP11C T418N, a gene mutation causing congenital hemolytic anemia, reduces flippase activity due to improper membrane trafficking. *Biochem. Biophys. Res Commun*. **2019**, *516*, 705-712.

51 Colicchia M, Schrottmaier WC, Perrella G, Reyat JS, Begum J, Slater A, Price J, Clark JC, Zhi Z, Simpson MJ, Bourne JH, Poulter NS, Khan AO, Nicolson PL, Pugh M, Harrison P, Iqbal AJ, Rainger GE, Watson SP, Thomas MR, Mutch NJ, Assinger A, Rayes J. S100A8/A9 drives the formation of procoagulant platelets through GPIbα. *Blood*. **2022**, *140*, 2626-2643.

52 Klatt C, Krüger I, Zey S, Krott KJ, Spelleken M, Gowert NS, Oberhuber A, Pfaff L, Lückstädt W, Jurk K, Schaller M, Al-Hasani H, Schrader J, Massberg S, Stark K, Schelzig H, Kelm M, Elvers M. Platelet-RBC interaction mediated by FasL/FasR induces procoagulant activity important for thrombosis. *J. Clin. Invest*. **2018**, *128*, 3906-3925.

53 Sun S, Urbanus RT, ten Cate H, de Groot PG, de Laat B, Heemskerk JW, Roest M. Platelet activation mechanisms and consequences of immune thrombocytopenia. *Cells*. **2021**, *10*, 10123386.

Supplementary Materials to Chapter 7

Materials

Recombinant tissue factor (TF; Innovin) was purchased from Siemens Healthineers (Marburg, Germany). Fluorogenic thrombin substrate Z-Gly-Gly-Arg-aminomethylcoumarin (ZGGR-AMC) was purchased from Bachem (Basel, Switzerland). Glycoprotein VI (GPVI) agonist, collagen-related peptide (CRP-XL) was from CambCol (Cambridge, United Kingdom). TG calibrator (α_2-macroglobulin-thrombin complex) was prepared in house, as described [1]. Annexin A5 and mutant annexin A5 were obtained from Tau Technologies (Kattendijke, The Netherlands) [2]. Atopaxar was purchased from Axon Medchem (Groningen, The Netherlands), vorapaxar from MedChem Express (Princeton, NJ, USA), and BMS-986120 from ChemeGen (Riverside, CA, USA). Integrin αIIbβ3 inhibitor tirofiban came from Bayer (Essen, Germany), Syk inhibitor PRT-060318 from ApexBio (Houston, TX, USA). Aptamer 1 blocking thrombin exosite I (HD1), aptamer 2 blocking thrombin exosite II (HD22), aptamer 1+2 blocking thrombin exosite I and II (combined HD1 and HD22) [3] and FITC-conjugated annexin A5 were obtained from ThermoFisher Scientific (Eindhoven, The Netherlands). Russell's viper venom factor X activator (Rvv-X, 0.189 OD) was purified, as described before [4]. Active-site inactivated FVIIa (FVIIai) came from Novo Nordisk (Bagsvaerd, Denmark). Ionomycin was from Calbiochem (San Diego, CA, USA). Human thrombin, factor Xa and factor XIa were produced by Synapse Research Institute (Maastricht, The Netherlands).

Blood preparation and separation

Blood samples were collected into 3.2 % trisodium citrate Vacuette tubes (Greiner Bio-One, Alphen a/d Rijn, The Netherlands). Corn trypsin inhibitor (CTI) was added, if indicated. Platelet-rich plasma (PRP) at autologous platelet count was obtained by centrifugation of blood at 220 *g* for 15 minutes at room temperature [2]. The blood and collected PRP were used within 4 hours after preparation. Platelet-poor plasma (PPP) was obtained through two runs of centrifugation at 2840 *g* for 10 minutes at room temperature. Washed RBC were prepared by double centrifugation at 890 *g* for 15 minutes in Hepes buffer pH 7.35 (136 mM NaCl, 2.7 mM KCl, 10 mM Hepes, 2 mM $MgCl_2$, 0.1% w/v bovine serum albumin and 0.1% w/v glucose) [5]. Where indicated, autologous PPP or PRP were combined with RBC to generate reconstituted samples with 20-40% hematocrit.

The collection of blood samples from healthy controls and patients on citrate suppresses eryptosis induced by high Ca^{2+} levels [6,7]. Before use, all blood samples were checked on the absence of clots. Yet, we cannot fully exclude phosphatidylserine expression due to sample handling, although such effects would be similar for control subjects and patients.

Blood cell parameters

Blood cell parameters were measured with a coulter counter analyzer (Beckman Coulter, Woerden, The Netherlands), or were determined with a Cell-Dyn Emerald 22 (Abbott Medical, Sesto San Giovanni, Italy).

Pre-incubation of blood and plasma samples

When required, samples in wells were pre-incubated for 10 minutes at 37 °C with vehicle control medium, PAR1 inhibitor atopaxar (0.04-10 μM), PAR1 inhibitor vorapaxar (0.04-10 μM), PAR4 inhibitor BMS-986120 (0.04-10 μM), thrombin exosite inhibitors aptamer 1 (0.5-15 μM), aptamer 2 (0.5-15 μM) or aptamer 1+2 (0.5-15 μM) [3]. Other wells were preincubated with integrin αIIbβ3 inhibitor tirofiban (0.3-5.0 μg/mL) or Syk kinase inhibitor PRT-060318 (0.04-10 μM). Vehicle controls were run at the same concentration of DMSO solvent or Hepes buffer pH 7.35.

Blood mixing and calibration in for thrombin generation experiments

Citrated whole-blood, PRP or PPP was mixed with substrate solution (Z-GGR-AMC dissolved into BSA-60 buffer, containing 20 mM Hepes, 6% w/v bovine serum albumin, pH 7.35) and trigger solution (coagulation trigger, 11 mM $CaCl_2$ and 5.5 mM $MgCl_2$ dissolved into BSA-5 buffer, containing 20 mM Hepes, 140 mM NaCl, 0.5% w/v bovine serum albumin, pH 7.35). The final volume ratio of WB or plasma, trigger solution and substrate solution was 3:2:1. The optimized final concentration of Z-GGR-AMC was 417 μM.

The procedure using 96-well plates were as follows. Trigger solution 120 μL (row A) and the mixture of 120 μL whole-blood or plasma plus 40 μL substrate solution (row B) were prewarmed at 37 °C for 10 minutes. Then, 80 μL trigger solution was transferred from row A to row B, followed by 8 times mixing using a multi-channel pipette. Subsamples were transferred to the recording wells (rows D-F), and measurements were started. In calibration wells, the trigger solution was replaced by α_2-macroglobulin-thrombin complex (corresponding to 320 nM thrombin activity).

Red blood cell annexin A5 treatment and wash

Washed RBC (35% hematocrit) were preincubated with annexin A5 (18.5-75 μg/mL) in the presence of 1 mM $CaCl_2$ for 15 minutes at room temperature. After the addition of 25× Hepes buffer plus 1 mM $CaCl_2$, the cells were centrifuged at 800 *g* for 15 minutes. The wash step in the presence of $CaCl_2$ was repeated three times. This procedure retained the annexin A5-binding to the phosphatidylserine-exposing RBC.

The washed RBC were then resuspended in the presence of 1 mM $CaCl_2$ at required hematocrit for TG measurements. Since the binding of annexin A5 is Ca^{2+}-dependent [2], care was taken to keep $CaCl_2$ present in all steps of RBC treatment. Procedures with 96 well plates were modified as follows. Trigger solution 120 µL plus RBC sample 90 µL (row A), as well as autologous PRP or PPP 60 µL plus substrate solution 40 µL (row B) were prewarmed for 10 minutes. Subsequently, 140 µL from row A was transferred to row B with 8 times mixing using a multi-channel pipette. Subsamples were transferred to the recording wells (rows D-F), and fluorescence measurements were started.

Red blood cell treatment and reconstitution

To block exposed phosphatidylserine, washed RBC (35% hematocrit) in isotonic Hepes buffer (10 mM Hepes, 136 mM NaCl, 2.7 mM KCl, 2 mM $MgCl_2$, 5.5 mM glucose, 0.1% BSA, pH 7.35) supplemented with 1 mM $CaCl_2$ were preincubated with annexin A5 (18.5-75 µg/mL) or vehicle in the presence of 1 mM $CaCl_2$ for 15 minutes at room temperature. After incubation, the cells were triple washed with Hepes buffer plus 1 mM $CaCl_2$.

Flow cytometric analysis

Freshly washed RBC (10% hematocrit) were preincubated with ionomycin (10 µM) with or without unlabeled annexin A5 (7.50 µg/mL) in the presence of 2 mM $CaCl_2$ for 10 minutes at 37 °C. Cells were then labeled with FITC-conjugated annexin A5 in the presence of 2 mM $CaCl_2$ for 15 minutes in the dark. After 20× dilution in Hepes buffer pH 7.35 containing BSA, glucose and 2 mM $CaCl_2$, fluorescence was measured with an Accuri C6 flow cytometer (BD Biosciences, Flanklin Lakes, NJ, USA) [8].

Light transmission microscopy

Freshly washed RBC (10% hematocrit) were preincubated with ionomycin (10 µM) or vehicle in the presence of 2 mM $CaCl_2$ for 10 minutes at 37 °C. The samples were diluted 3 times with Hepes buffer pH 7.35 containing 2 mM $CaCl_2$, and examined by an inverted light transmission microscope with 63× objective (Leica DFC 3000 G, Wetzlar, Germany).

Measurement of factor Xa activity

To measure RBC-dependent factor X activation [9], 30 µL of washed RBC (10% hematocrit) were mixed with 20 µL substrate solution (containing 417 µM ZGGR-AMC and 2 mM $CaCl_2$), and 70 µL purified factor Xa (20 µM, fc.). Fluorescence development was measured for 70 minutes at fluorescence wavelengths of λ_{ex} 355 nm and λ_{em} 460 nm using Fluoroskan Ascent Software (version 2.6). The cells were preincubated with annexin A5 and/or ionomycin in the presence of 2 mM $CaCl_2$ (10 minutes at 37 °C), as indicated.

References

1 Bloemen S, Zwaveling S, Douxfils J, Roest M, Kremers R, Mullier F. The anticoagulant effect of dabigatran is reflected in the lag time and time-to-peak, but not in the endogenous thrombin potential or peak, of thrombin generation. *Thromb. Res*. **2018**, *171*, 160-166.

2 Vanschoonbeek K, Feijge MA, van Kampen RJ, Kenis H, Hemker HC, Giesen PL, Heemskerk JW. Initiating and potentiating role of platelets in tissue factor-induced thrombin generation in the presence of plasma: subject-dependent variation in thrombogram characteristics. *J. Thromb. Haemost.* **2004**, *2*, 476-484.

3 Derszniak K, Przyborowski K, Matyjaszczyk K, Moorlag M, de Laat B, Nowakowska M, Chlopicki S. Comparison of effects of anti-thrombin aptamers HD1 and HD22 on aggregation of human platelets, thrombin generation, fibrin formation, and thrombus formation under flow conditions. *Front. Pharmacol*. **2019**, *10*, 68.

4 Lindhout MJ, Kop-Klaassen BH, Hemker HC. Activation of decarboxyfactor X by a protein from Russell's viper venom. Purification and partial characterization of activated decarboxyfactor X. *Biochim. Biophys. Acta*. **1978**, *533*, 327-341.

5 Ninivaggi M, Apitz-Castro R, Dargaud Y, de Laat B, Hemker HC, Lindhout T. Whole bloodthrombin generation monitored with a calibrated automated thrombogram-based assay. *Clin. Chem*. **2012**, *58*, 1252-1259.

6 Lang F, Birka C, Myssina S, Lang KS, Lang PA, Tanneur V, Duranton C, Wieder T, Huber SM. Erythrocyte ion channels in regulation of apoptosis. *Adv. Exp. Med. Biol*. **2004**, *559*, 211-217.

7 Cilla A, López-García G, Collado-Díaz V, Amparo Blanch-Ruiz M, Garcia-Llatas G, Barberá R, Martinez-Cuesta MA, Real JT, Álvarez Á, Martínez-Hervás S. Hypercholesterolemic patients have higher eryptosis and erythrocyte adhesion to human endothelium independently of statin therapy. *Int. J. Clin. Pract*. **2021**, *75*, e14771.

8 De Simone I, Baaten CC, Jandrot-Perrus M, Gibbins JM, ten Cate H, Heemkerk JW, Jones CI, van der Meijden PE. Coagulation factor XIIIa and activated protein C activate platelets via GPVI and PAR1. *Int. J. Mol. Sci*. **2022**, *23*, 10203.

9 Al Dieri R, Bloemen S, Kelchtermans H, Wagenvoord R, Hemker HC. A new regulatory function of activated factor V: inhibition of the activation by tissue factor/factor VII(a) of factor X. *J. Thromb. Haemost*. **2013**, *11*, 503-511.

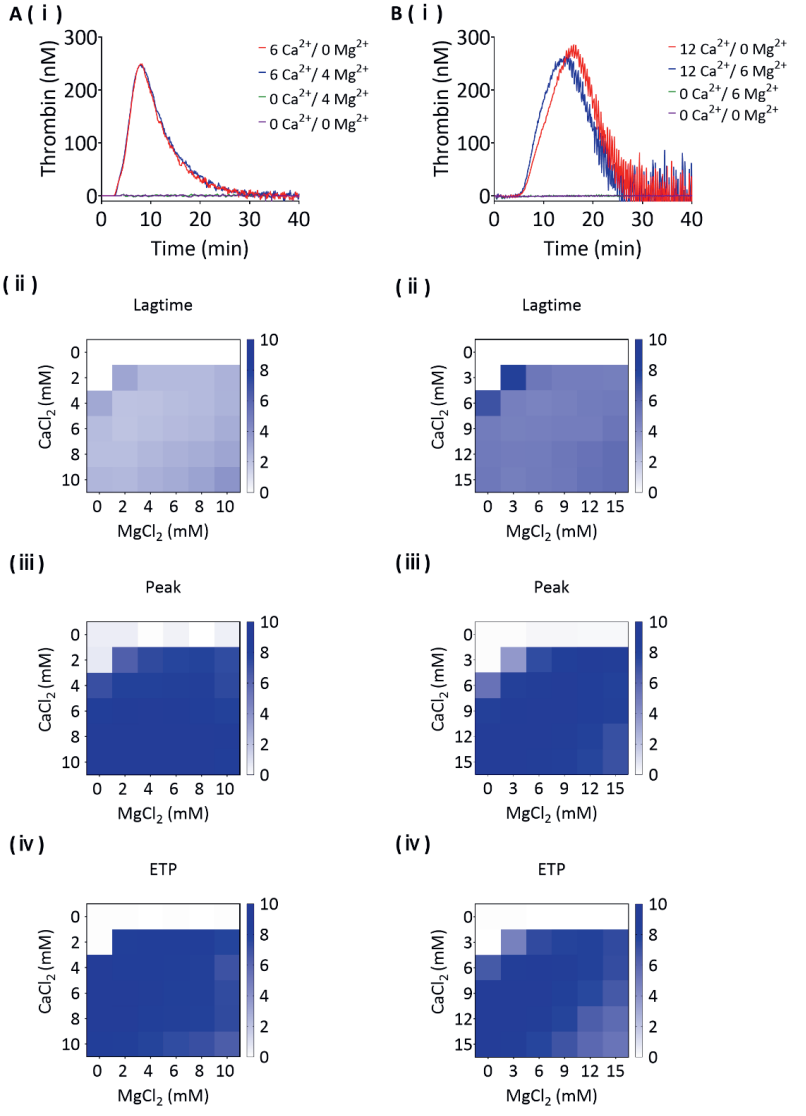

Suppl. Figure 1. Optimal recalcification with $CaCl_2$ and $MgCl_2$ for thrombin generation in citrated whole blood and PRP. Parallel samples of citrated whole blood (**A**) and PRP (**B**) were supplemented with indicated concentration of $CaCl_2$ (0-15 mM) and/or $MgCl_2$ (0-15 mM), after which TG was triggered with tissue factor (TF, 1 pM). Shown are representative TG curves (**i**) at indicated conditions, as well as heatmap values of the curve parameters, lagtime (**ii**), thrombin peak level (**iii**) and ETP (**iv**). For the comparisons, we assumed a 33% hematocrit, meaning that 10 mM in whole blood equaled 15 mM in PRP. For heatmapping, parameter values were scaled 0-10 across conditions. Data are means from three experiments. Note that higher concentrations of $MgCl_2$ initially stimulated and then decreased the peak and ETP parameters (panels **A ii-iv**).

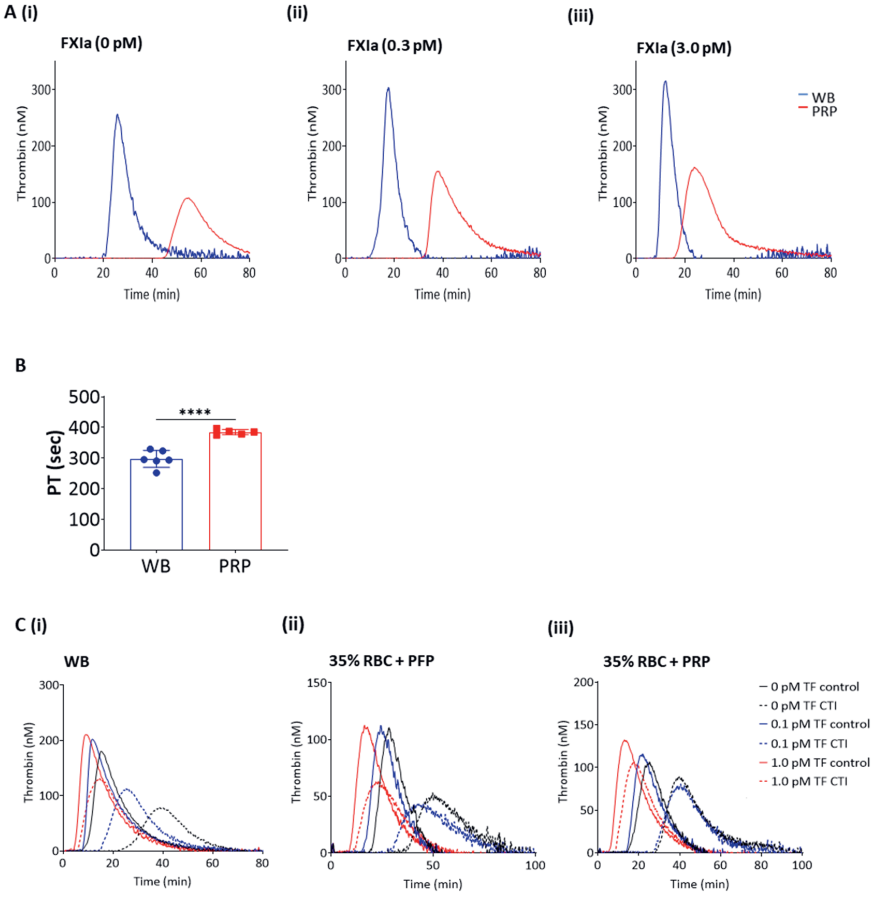

Suppl. Figure 2. Trigger-induced thrombin generation and clotting in (reconstituted) whole blood and in corresponding plasma samples. (**A**) Thrombin generation in whole blood (WB, blue lines) or autologous PRP (red lines) was triggered in the presence of $CaCl_2/MgCl_2$ with vehicle medium or factor XIa (FXIa, 0.3-3.0 pM). Representative curves are shown (n = 3). (**B**) Recalcified WB or autologous PRP was triggered with 0.1 pM tissue factor, and mechanical prothrombin times (PT) were measured. Data are presented as means ± SD (n = 6), ****P<0.0001 (t-test). (**C**) Whole blood on citrate was pretreated with corn trypsin inhibitor (CTI, 50 µg/mL) or left untreated (control). Samples were used for the collection of RBC, PRP and PFP, followed by reconstitution of the plasmas with RBC at 35% hematocrit. Thrombin generation was measured in parallel in whole blood and the reconstituted blood. Coagulation was triggered upon recalcification with $CaCl_2/MgCl_2$ by 0.1 pM or 1.0 pM TF, as indicated. Representative calibrated TG curves are shown (n = 3).

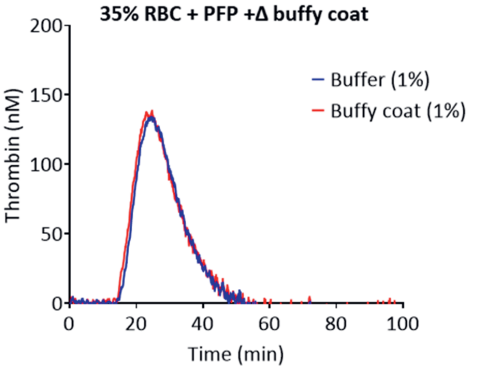

Suppl. Figure 3. Contribution white blood cells to phosphatidylserine-dependent thrombin generation. Autologous PFP was reconstituted with washed RBC (35% hematocrit) plus 1 vol% of buffer or buffy coat (corresponding to the buffy coat volume in whole blood). Thrombin generation was triggered with $CaCl_2$/$MgCl_2$ and a low dose of 0.1 pM TF. Shown are TG traces, representative for 3 experiments. Final counts for buffer (buffy coat): RBC 3.53 (3.82) × 10^{12}/L, WBC 2.70 (5.70) × 10^9/L, platelets 4.1 (191.3) × 10^9/L.

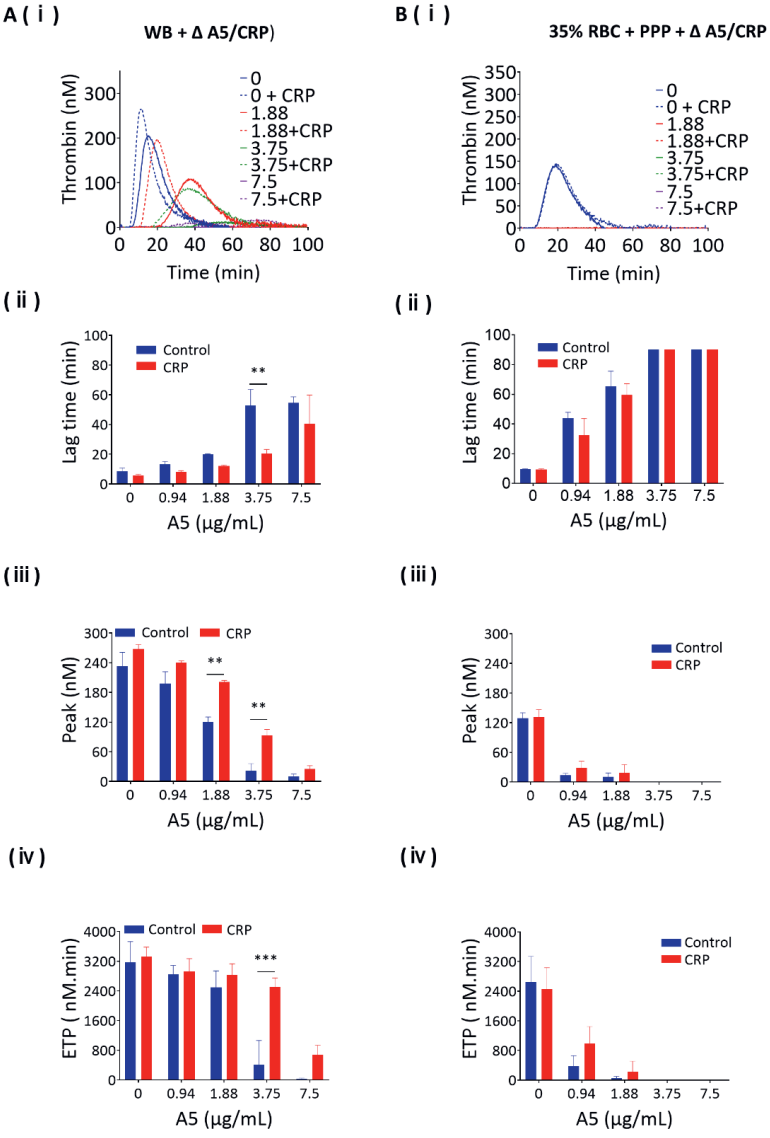

Suppl. Figure 4. Effect of annexin A5 (A5) addition on thrombin generation in whole blood and platelet-rich plasma. Whole blood of 35% hematocrit (**A**) or RBC reconstituted with plasma (**B**) was pre-incubated with CRP-XL (25 µg/mL) and/or annexin A5 (0-7.5 µg/mL) as indicated, and subsequently triggered with 0.1 pM tissue factor for measurement of TG. Shown are representative TG curves, indicating the effects of annexin A5 and CRP-XL (**i**). Furthermore, quantified lag times (**ii**), thrombin peak levels (**iii**) and ETP values (**iv**), as a function of the added annexin A5 concentration. Data are means ± SD (n = 3), one-way ANOVA, ***P*<0.01 and ****P*<0.001.

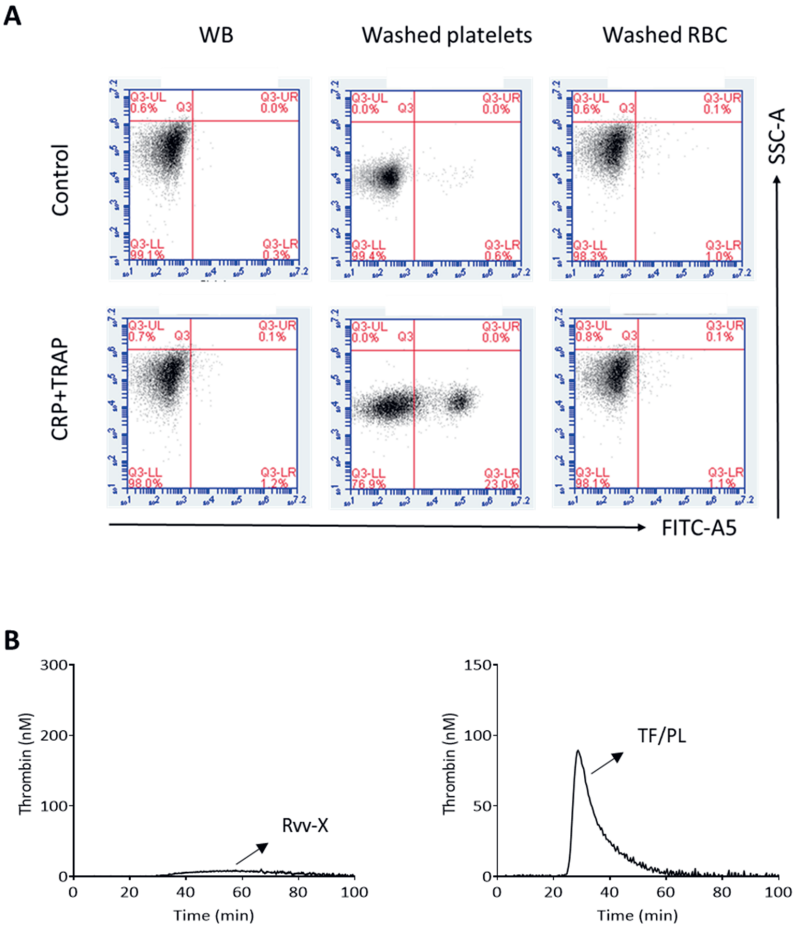

Suppl. Figure 5. Phosphatidylserine expression on blood cells and extracellular vesicles. (**A**) Flow cytometric analysis of phosphatidylserine exposure of freshly isolated whole blood, autologous washed platelets and washed RBC. Blood cell preparations were pre-labeled with FITC-annexin A5. Where indicated, the preparations were pretreated for 10 minutes with 25 µg/mL CRP and 10 µM TRAP6. SSC = side scatter. Representative data from >3 experiments. (**B**) Platelet-free plasma (PFP) was isolated from citrate-anticoagulated blood samples (healthy subjects). Thrombin generation was after recalcification with $CaCl_2$/$MgCl_2$. Triggering was either by Rvv-X (dilution $1e^{-6}$) or by tissue factor/phospholipids (TF, 1 pM TF, phospholipids 4 µM). Curves are representative for three experiments. Note the essential absence of TG with Rvv-X.

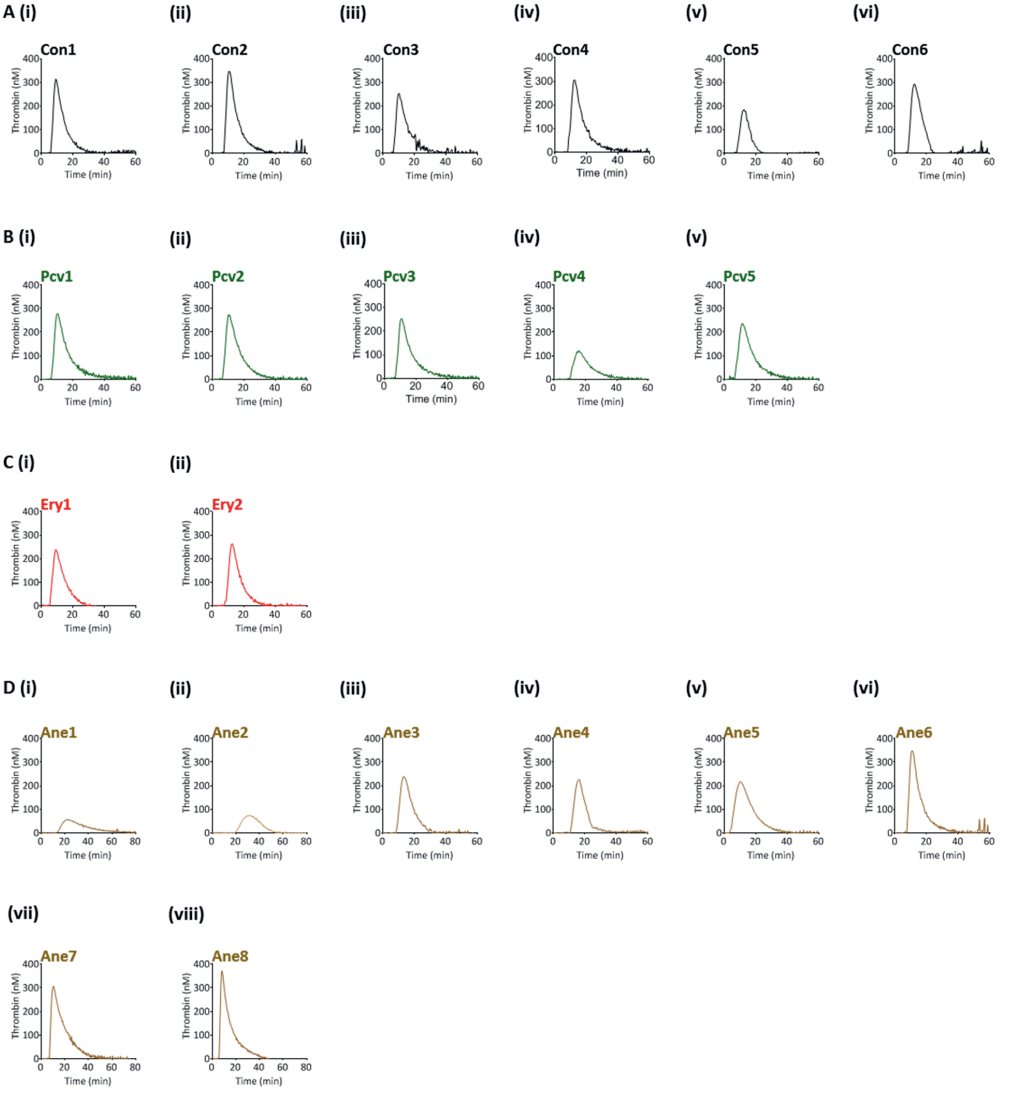

Suppl. Figure 6. Thrombin generation curves with blood from investigated patients with RBC abnormalities. Blood samples from individual day-control subjects (Con, **A**), or from patients with polycythemia vera (Pcv, **B**), erythrocytosis (Ery, **C**) or anemia (Ane, **D**) were investigated for TG in response to 0.1 pM tissue factor. Representative curves are shown.

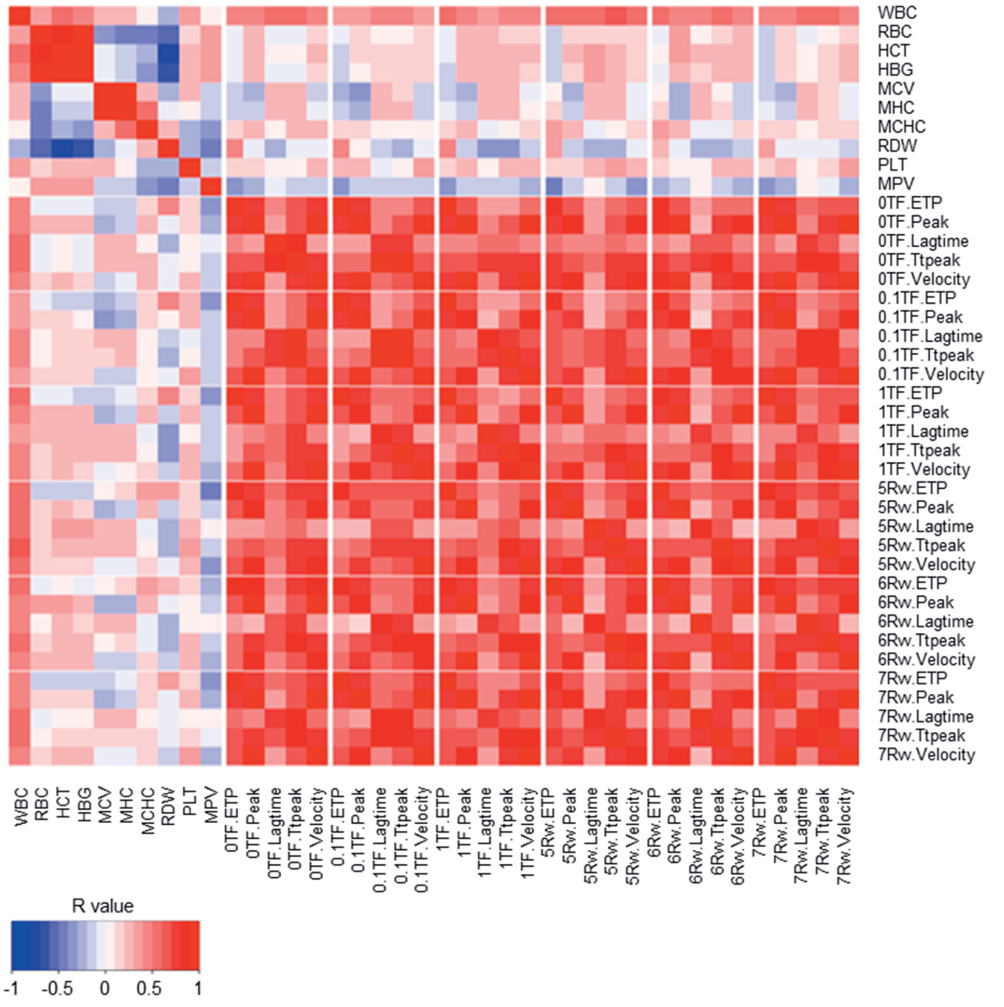

Suppl. Figure 7. Multivariate Spearman correlation. Analysis was performed of hematological parameters and six conditions of thrombin generation (TG) parameters for cohort of 21 control subjects and patients with altered red blood cell traits. For incorporated subjects and variables, see Figure 7A. Note the overall high consistency of all TG parameters independent of trigger. Color code: blue, negative relation; red, positive relation.

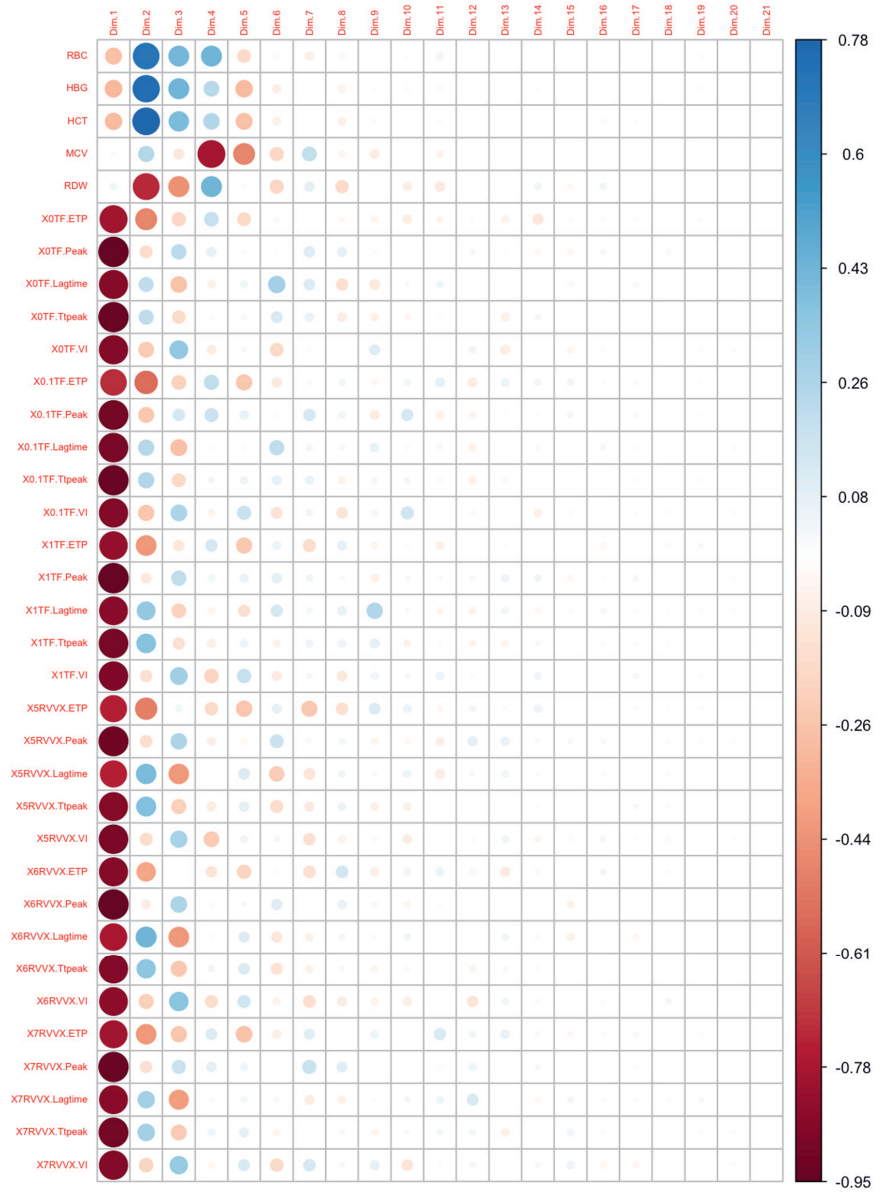

Suppl. Figure 8. Principal component matrix of TG and blood cell traits in investigated patients. Shown is the relative contribution to dimensions 1-21 of the principal component analysis of combined TG and hematological parameters for cohort of 21 control subjects and patients. For incorporated subjects and variables, see Figure 7A. Visualized is per dimension the relative contribution of each variable. Positive correlations are shown in blue, negative correlations in red.

Chapter 8

General discussion

Blood platelets are essential for normal hemostasis, *i.e.,* the cessation of blood loss upon vascular injury, and also play a key role in the development and formation of arterial thrombosis (Chapter 1). In these (patho)physiological processes, platelets trigger the formation of occlusive clots, such in interplay with the coagulation process. It is considered that the (un)disturbed vessel wall controls the delicate balance between platelet aggregation and platelet-dependent coagulation in hemostasis to halt bleeding on one side, and intravascular thrombus formation on the other side. Additional control of this regulation remains an issue in the treatment of arterial cardiovascular disease, which still is a leading cause of death globally [1]. In 2020, an estimated 523 million people suffered from some form of cardiovascular disease, requiring drug treatment to suppress platelet activation and/or the coagulation process [2]. Importantly, current antiplatelet and anticoagulant drugs to prevent (secondary) thrombotic events are accompanied by unwanted bleeding side effects. In this thesis, I investigated key mechanisms evoking transient or persistent platelet activation and blood clotting, aiming to better define the versatility of these processes in hemostasis and thrombosis. As discussed below, the obtained results provide clues for improving the safety and efficacy of antiplatelet medication.

Time dependency of platelet activation

The overall process of platelet aggregation and thrombus formation in hemostasis and thrombosis relies on a variety of platelet agonists, receptors and signaling mechanisms [3,4]. Key platelet responses are integrin-dependent adhesion, αIIbβ3 activation, granule release, and procoagulant activity. Usually, two types of receptors are distinguished, G protein-coupled receptors (GPCR) and tyrosine kinase-activating receptors, of which glycoprotein VI (GPVI) is best known. These receptor types activate the isoforms phospholipase Cβ2/3 (PLCβ2/3) and PLCγ2, respectively, which enzymes produce the second messengers cytosolic Ca^{2+} and diacylglycerol (DAG) [5]. The formed DAG is critical for activation of the broad substrate protein kinase C (PKC), mediating granule release and integrin αIIbβ3 activation. In several chapters, we focused on the temporal character of these platelet responses by assessing the time frame in which they can be modulated by (ant)agonists.

Temporal integrin αIIbβ3 activation and platelet-platelet interactions in aggregation

As reviewed in Chapter 2, several platelet agonists and signaling pathways induce the enhanced affinity of integrin αIIbβ3 that is required for fibrinogen binding and, thereby, plays a key role in hemostasis and thrombosis [6]. This integrin is a clinically recognized antithrombotic target, but with a risk of bleeding [7]. Searching through the current literature learned that especially ADP (autocrine produced) distinguishes between transient and persistent ligand binding to integrin αIIbβ3 [8,9]. With this as a starting point, in Chapter 3 we found that also upon platelet

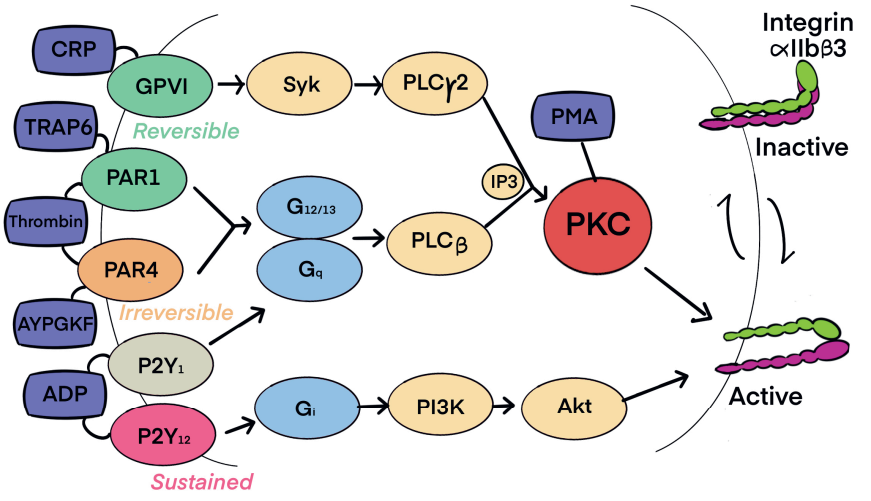

Figure 1. Pathways leading to partly reversible integrin αIIbβ3 activation in platelets. Activation of the receptors GPVI and PAR1 induces a mostly transient integrin αIIbβ3 activation. The current and other studies indicated that especially ADP-induced $P2Y_{12}$ activation is essential for keeping the integrin αIIbβ3 in active state. The PKC pathway appears to be a most crucial regulator for integrin activation.

activation by the GPCR PAR1 (protease activated receptor-1) or by the tyrosine kinase-stimulating GPVI the activation of integrin αIIbβ3 partly reverses over a time period of 20 minutes. The reversibility of PAR1- and GPVI-induced integrin activation may be related to a transient phosphoinositide 3-kinase (PI3K) activity and to transient ADP receptor ($P2Y_1$/$P2Y_{12}$) functions [10,11]. On the other hand, platelet PAR4 stimulation caused a rather irreversible αIIbβ3 activation. This is schematically shown in **Figure 1**.

In Chapter 3, we tested a panel of signal molecule inhibitors on the time-dependent activation processes induced by GPVI, PAR1 or PAR4 agonists, using flow cytometry. We found that under conditions of pan-PKC inhibition (*i.e.,* of conventional and novel isoforms, cPKC and nPKC, respectively) or of $P2Y_{12}$ inhibition, the activation of integrin αIIbβ3 strongly reverted (see **Table 1**). This indicated that both PKC and autocrine ADP signaling contribute to a persistent integrin αIIbβ3 activation state and hence, to stabilized platelet aggregates. Additional, less prominent pathways contained the signaling molecules GSK3α/β (contributing to both PI3Kβ/Akt-dependent and PI3K-independent pathways) and β-arrestins (regulating GPCR activities). These signaling routes are known to be activated in response to GPVI or PAR1 stimulation [12,13]. On the other hand, the specific blockage of PI3Kβ (a main PI3K isoform in platelets) or of Ras-related pathways did not affect the longer-term GPVI- or PAR1-triggered integrin αIIbβ3 activation. Further assessment of the platelet spreading response showed that inhibition of either PKC or $P2Y_{12}$ led to a partial reversion of platelet shape changes. In relation

to our results, it was earlier reported that the platelet $P2Y_{12}$ receptors act in a way more dependent on PI3K than on PKC [10]. The Bergmeier group, focusing on the small G-protein regulator CalDAG-GEFI and downstream effector Rapb1, has shown additional roles regarding integrin activation of the PKC and PI3K pathways [14,15]. Our present results, in confirmation with this literature, suggest that $P2Y_{12}$-based (or PI3K-based) antiplatelet therapy cannot only inhibit platelet activation, but can also revert previously activated platelets into the circulation.

In Chapter 4, we assessed functional consequences of this time-dependent integrin αIIbβ3 activation using light transmission aggregometry. We were particularly interested to find if the aggregation of platelets in response to PAR1 or GPVI agonists could be reverted by pre- or post-treatment with agents causing cAMP elevation, Syk tyrosine kinase inhibition, or blocking αIIbβ3 itself. An important finding was that the aggregation response was completely eliminated when cAMP was elevated either prior to or simultaneous with the GPVI or PAR1 agonist. However, when compared to PAR1 activation using TRAP6 (peptide SFLLRN), the GPVI activation using CRP (collagen-related peptide) had a shorter time frame for responding to cAMP elevation by the prostacyclin analog iloprost. Conversely, others have measured a rapid decline of cAMP in collagen-stimulated platelets [16].

Pre-inhibition of the tyrosine kinase Syk was only effective in case of GPVI stimulation. This is in agreement with other papers from our laboratories, pointing to a more continued – and thereby perhaps less reversible – activation signal with GPVI stimulation, when compared to GPCR stimulation [17,18]. On the other hand, it was verified that GPVI-mediated platelet signaling through Syk kinase was limited to the initial moments of thrombus formation. The reversal by αIIbβ3 antagonists of particularly the PAR1-induced aggregation response can be explained by a high sensitivity of the PAR1 response to autocrine ADP inhibition (Chapter 3).

Temporal aspects of platelet cytosolic Ca^{2+} rises

All functional responses of platelets, including shape change, integrin activation, granule secretion and procoagulant activity are mediated by intracellular second messengers, of which especially cytosolic Ca^{2+} is an essential factor [19]. As explained in Chapter 1, the platelet Ca^{2+} response consists of mobilization of Ca^{2+} from stores in the endoplasmic reticulum, along with extracellular Ca^{2+} entry, especially via the mechanisms of store-operated or receptor-operated Ca^{2+} entry pathways. The fluorescent ratio dye Fura-2 has for long been used in cuvette-based assays to measure, in a calibrated way, nanomolar changes in cytosolic $[Ca^{2+}]_i$ in platelets [18]. Early findings have shown that platelet stimulation via PAR1 induces a fast and transient $[Ca^{2+}]_i$ rise, whereas stimulation via GPVI results in a slower and persistent $[Ca^{2+}]_i$ rise [20]. In Chapter 4, we employed a 96-well plate high-throughput assay using Fura-2-loaded platelets to demonstrate the ability of platelets to consecutively respond to PAR1, $P2Y_{1/12}$ and GPVI stimulation. We found that, after pre-stimulation with CRP (GPVI agonist), the subsequent administration of TRAP6 (PAR1 agonist) led to an additional, transient increase in $[Ca^{2+}]_i$ level on top of the prior CRP-induced signal. See overview **Table 1**. On the other hand, after initial stimulation by TRAP6 or CRP, the subsequent administration of CRP produced a prolonged Ca^{2+} signal. This indicated that, in terms of Ca^{2+} signaling, prior GPVI but not PAR stimulation

provokes a prolonged, high activation state of the platelets, while the platelets can still respond to a second agonist. The continuous Ca^{2+} signaling evoked by CRP stimulation implies that platelets are enduring a protracted or hyperactivated phase in this case. This protracted state has been considered as a property of the GPVI-induced signaling via tyrosine kinases [21, 22], with our new data in Chapter 6 are suggesting that at least part of the mechanism is provided by releasing PKC-dependent suppression of Ca^{2+} entry process. Accordingly, general PKC stimulation with phorbol ester PMA downregulated the platelet Ca^{2+} responses (**Table 1**).

The mechanism of platelet Ca^{2+} signaling, controlled by Ca^{2+} channels such as Orai1, we have explored in Chapter 5 via parallel $[Ca^{2+}]_i$ measurements of agonist stimulation in the presence of extracellular $CaCl_2$ or of calcium chelating EGTA, using the same 96-wells high-throughput assay. We found that at either condition the $[Ca^{2+}]_i$ rises induced by the weaker agonists collagen and

Agonist	Receptor	Pathway	Reversible (integrin $\alpha_{IIb}\beta_3$)	Calcium curve	Extent of activation (Ca^{2+} µM)	Chapter
CRP	GPVI	Syk PLC$\gamma_{1/2}$ PKC $\alpha_{IIb}\beta_3$	Y		100-300	3-6
Convulxin					200-250	6
TRAP6	PAR1	Gq,G12/13 PLCβ $\alpha_{IIb}\beta_3$	Y		100-200	3-6
Thrombin	PAR1, PAR4		N	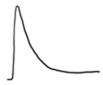	100-300	3-6
AYPGKF	PAR4		N		170	3
ADP	P2Y1	Gq PLCβ $\alpha_{IIb}\beta_3$	Y		50	3
	P2Y12	Gi PI3K - Akt $\alpha_{IIb}\beta_3$				
PMA		PKC $\alpha_{IIb}\beta_3$	N		25	3, 6

Table 1. Key agonists and pathways in (reversible) agonist-induced integrin αIIbβ3 activation and Ca^{2+} rises.

TRAP6 were more dependent on release of the secondary mediators ADP and thromboxane A_2 than those of the strong agonists CRP and thrombin. Inhibition of the back-pumping of cytosolic Ca^{2+} via sarco- and endoplasmic reticulum Ca^{2+}-ATPases, with thapsigargin [23], resulted in a prolonged and amplified Ca^{2+} signal. Markedly, combining thapsigargin with the GPVI or PAR1/4 stimulation strongly increased the Ca^{2+} entry ratio from 4 to 400 (GPVI) or to 40 (PARs), indicating a significant receptor-pathway dependent enhancement of store-operated Ca^{2+} entry. By pharmacological blockage, we found that the Orai1 channel inhibitor 2-APB and the Na^+/Ca^{2+} exchange (NCX) inhibitor ORM-10103 were most effective with all agonists used. Accordingly, Orai1 and NCX appear to be major Ca^{2+} carriers that regulate GPVI- and PAR-induced Ca^{2+} entry in human platelets. This finding is supported by the signaling and functional defects of platelets from patients with dysfunctional Orai1 and from mice lacking Orai1 [24,25]. Our results are also consistent with another report that inhibition of NCX suppresses the prolonged Ca^{2+} response required for procoagulant platelet formation [26].

Differential roles of PKC isoforms in platelet activation

It is known that the various PKC isoforms in platelets play distinct roles, some of which are antagonistic to one another [27]. As explained in Chapter 1, platelets express the conventional PKC (cPKC) isoforms α and β, which are activated by Ca^{2+} and DAG; and additionally the novel PKC (nPKC) isoforms δ, η and θ, which only have a DAG-binding domain [28]. In Chapter 3, we observed that the inhibition of all PKC isoforms caused integrin αIIbβ3 closure. In addition, the combined inhibition of PKCα/β (compound Gö6976) and PKCθ (compound PKCθ-IN) could suppress the αIIbβ3 activation. This pointed to additive roles of cPKC and nPKC isoforms in the regulation of integrin activation.

For a long time, it is known from platelets and other cells that PKC activity modulates the entry of extracellular Ca^{2+} [30-32], although the mechanism was not well understood. In Chapter 6, we investigated how PKC isoforms regulated this process in platelets stimulated via GPVI or PAR1/4. It appeared that the activation of PKC isoforms via GPVI in platelets resulted in a potent suppressive effect on extracellular Ca^{2+} entry through the Orai1 channel in connection with the sensor protein STIM1. This in turn downregulated platelet procoagulant activity and coagulation. Our results with thapsigargin pre-treated platelets from patients with a mutation in the Orai1 channel confirmed that the Ca^{2+} entry mechanism is entirely dependent on this pathway. We concluded that in human platelets, phosphorylation events by cPKC and nPKC acts as a potent negative regulator of store-regulated Ca^{2+} entry, extending to blood clotting.

The adaptor protein BIN2 has been identified as a crucial connector of the IP_3 receptor to the Ca^{2+} storage sensor STIM1 in the endoplasmic reticulum membrane. Mouse knockout studies indicated that BIN2 thereby controls store-operated Ca^{2+} entry via Orai1 channels [29]. We used an advanced label-free, bottom-up phosphorylation proteomics method to pinpoint four heavily phosphorylated polar domains in the human BIN2 protein, three of which were altered in response to GPVI stimulation and were predicted substrates for PKC isoforms. The STIM1 protein also contains one of such phosphorylation sites. From this, we inferred that the PKC-

induced phosphorylation alters the conformations of BIN2 and STIM1 in a way to decreases the Orai1 Ca^{2+} channel activity. Based on the present findings, these data can now be interpreted as an inhibitory effect of platelets on the STIM1-BIN2-Orai1 axis induced by multiple PKC isoenzymes.

Additive contribution of red blood cells and platelets in thrombin generation

Under certain conditions, red blood cells can support the formation of blood clots and enhance the thrombus stability [33,34]. Considering transiency in the platelet activation state, this may indicate that in blood clotting red blood cells can take over the role of platelets under certain conditions. The process of thrombin generation provides a manner to investigate the relative contributions of these and other blood cells in clotting. Based on a previous 'incomplete' thrombin generation assay, in Chapter 7 we describe an improved method for whole-blood thrombin generation measurements using 96-well plates. This method provides the first quantitative comparison of coagulation kinetics in whole blood and platelet-rich plasma from the same subject. Our findings suggest that red blood cells play an initial role in supporting thrombin generation, whereas white blood cells have a minor contribution. Activated platelets on the other hand play a supportive role in the thrombin generation process via GPVI and PAR1/4, which role though becomes enhanced when the red blood cells are silenced. We found that low concentrations of coagulant triggers − including tissue factor, factor X-dependent stimuli and thrombin −, resulted in a faster and initially higher thrombin generation and a shorter coagulation onset time in whole blood than in platelet-rich plasma. The thrombin generation accelerated with increased hematocrit values, and was delayed if the red blood cells were treated with phosphatidylserine-blocking annexin A5. Interestingly, profiles for patients with hemolytic anemia but not with polycythemia vera were altered, likely due to a different procoagulant activity of the blood cells. These results hence indicate that next to procoagulant platelets, also red blood cells need to be taken into account in assessment of the the balance of pro- and anticoagulant processes underlying thrombin generation [35,36].

Concluding remarks and future work

Overall, this thesis provides better understanding of the transient mechanisms of human platelet activation via the receptors GPVI, PAR1/4, and $P2Y_{1/12}$. The findings include: *(i)* persistency of the integrin αIIbβ3 activation state and consequently stabilized platelet aggregation is facilitated by signaling via PKC and autocrine ADP; *(ii)* when compared to PAR or P2Y receptor stimulation, GPVI stimulation has a longer-lasting, more potent priming and memory effect on platelets; *(iii)* the dominant Ca^{2+} carriers controlling Ca^{2+} entry via GPVI and PAR in platelets are Orai1 and NCX; *(iv)* conventional and novel PKC isoforms acts as strong negative regulators of the Ca^{2+} entry, thereby suppressing procoagulant activity; *(v)* the thrombin generation process is aided next to platelets by procoagulant red blood cells.

The results presented in this thesis highlight that at one side the transiency of platelet activation and at the other side Ca^{2+}-dependent platelet procoagulant activity are aspects to take into account when considering the roles of platelets in thrombosis and hemostasis. The investigated pathways underlying these processes may prove to be suitable targets for antiplatelet drugs. Furthermore, this thesis introduces as novel target the channels and ion exchange proteins that are involved in GPVI- and PAR-induced Ca^{2+} entry.

References

1. van der Meijden PE, Heemskerk JW. Platelet biology and functions: new concepts and clinical perspectives. *Nat. Rev. Cardiol.* **2019**, *16*, 166-179.
2. Coronado F, Melvin SC, Bell RA, Zhao G. Global responses to prevent, manage, and control cardiovascular diseases. *Prev. Chronic Dis.* **2022**, *19*.
3. Becker RC, Sexton T, Smyth SS. Translational implications of platelets as vascular first responders. *Circ. Res.* **2018**, *122*, 506-522.
4. Stefanini L, Bergmeier W. CalDAG-GEFI and platelet activation. *Platelets*. **2010**, *21*, 239-243.
5. Receveur N, Mouriaux C, Nieswandt B, Gardiner EE, Gachet C, Jandrot-Perrus M, Mangin PH. Differential role of glycoprotein VI in mouse and human thrombus progression and stability. *Thromb. Haemost.* **2020**, *121*, 543-546.
6. Durrant TN, van den Bosch MT, Hers I. Integrin αIIbβ3 outside-in signaling. *Blood.* **2017**, *130*, 1607-1619.
7. Janus-Bell E, Mangin PH. The relative importance of platelet integrins in hemostasis, thrombosis and beyond. *Haematologica.* **2023**, *108*, 1734.
8. Moser M, Bertram U, Peter K, Bode C, Ruef J. Abciximab, eptifibatide, and tirofiban exhibit dose-dependent potencies to dissolve platelet aggregates. *J. Cardiovasc. Pharmacol.* **2003**, *41*, 586-592.
9. Cosemans JM, Munnix IC, Wetzker R, Heller R, Jackson SP, Heemskerk JW. Continuous signaling via PI3K isoforms β and γ is required for platelet ADP receptor function in dynamic thrombus stabilization. *Blood.* **2006**, *108*, 3045-3052.
10. Kauffenstein G, Bergmeier W, Eckly A, Ohlmann P, Leon C, Cazenave J, Nieswandt B, Gachet C. The P2Y12 receptor induces platelet aggregation through weak activation of the αIIbβ3 integrin: a phosphoinositide 3-kinase-dependent mechanism. *FEBS Lett.* **2001**, *505*, 281-290.
11. Gilio K, Munnix IC, Mangin P, Cosemans JM, Feijge MA, van der Meijden PE, Olieslagers S, Chrzanowska-Wodnicka MB, Lillian R, Schoenwaelder S, Koyasu S, Sage SO, Jackson SP, Heemskerk JW. Non-redundant roles of phosphoinositide 3-kinase isoforms α and β in glycoprotein VI-induced platelet signaling and thrombus formation. *J. Biol. Chem.* **2009**, *284*, 33750-33762.
12. Moore SF, van den Bosch MT, Hunter RW, Sakamoto K, Poole AW, Hers I. Dual regulation of glycogen synthase kinase 3 (GSK3) α/β by protein kinase C (PKC) α and Akt promotes thrombin-mediated integrin αIIbβ3 activation and granule secretion in platelets. *J. Biol. Chem.* **2013**, *288*, 3918-3928.
13. Van Gastel J, Hendrickx JO, Leysen H, Santos-Otte P, Luttrell LM, Martin B, Maudsley S. β-Arrestin based receptor signaling paradigms: Potential therapeutic targets for complex age-related disorders. *Front. Pharmacol.* **2018**, *9*, 1369.

14. Cifuni SM, Wagner DD, Bergmeier W. CalDAG-GEFI and protein kinase C represent alternative pathways leading to activation of integrin αIIbβ3 in platelets. *Blood.* **2008**, *112*, 1696-1703.
15. Cosemans JM, Iserbyt BF, Deckmyn H, Heemskerk JW. Multiple ways to switch platelet integrins on and off. *J. Thromb. Haemost.* **2008**, *6*, 1253-1261.
16. Margarucci L, Roest M, Preisinger C, Bleijerveld OB, van Holten TC, Heck AJ, Scholten A. Collagen stimulation of platelets induces a rapid spatial response of cAMP and cGMP signaling scaffolds. *Mol. Biosyst.* **2011**, *7*, 2311-2319.
17. De Simone I, Baaten CC, Gibbins JM, ten Cate H, Heemskerk JW, Jones CI, van der Meijden PE. Repeated platelet activation and the potential of previously activated platelets to contribute to thrombus formation. *J. Thromb. Haemost.* **2023**, *21*, 1289-1306.
18. Fernández DI, Provenzale I, Cheung HYF, van Groningen J, Tullemans BM, Veninga A, Dunster JL, Honarnejad S, van den Hurk H, Kuijpers MJ, Heemskerk JW. Ultra-high-throughput Ca^{2+} assay in platelets to distinguish ITAM-linked and G-protein-coupled receptor activation. *Iscience.* **2022**, *25*.
19. Navarro S, Stegner D, Nieswandt B, Heemskerk JW, Kuijpers M J. Temporal roles of platelet and coagulation pathways in collagen-and tissue factor-induced thrombus formation. *Int. J. Mol. Sci.* **2021**, *23*, 358.
20. Versteeg HH, Heemskerk JW, Levi M, Reitsma PH. New fundamentals in hemostasis. *Physiol. Rev.* **2013**, *93*, 327-358.
21. Heemskerk JW, Feijge MA, Henneman L, Rosing J, Hemker HC. The Ca^{2+}-mobilizing potency of α-thrombin and thrombin-receptor-activating peptide on human platelets: concentration and time effects of thrombin-induced Ca^{2+} signaling. *Eur. J. Biochem.* **1997**, *249*, 547-555.
22. Zhang P, Solari FA, Heemskerk JW, Kuijpers MJ, Sickmann A, Walter U, Jurk K. Differential regulation of GPVI-induced Btk and Syk activation by PKC, PKA and PP2A in human platelets. *Int. J. Mol. Sci.* **2023**, *24*, 7776.
23. Mammadova-Bach E, Nagy M, Heemskerk JW, Nieswandt B, Braun A. Store-operated calcium entry in thrombosis and thrombo-inflammation. *Cell Calcium.* **2019**, *77*, 39-48.
24. Heemskerk JW, Vis P, Feijge M, Hoyland J, Mason W, Sage S. Roles of phospholipase C and Ca^{2+}-ATPase in calcium responses of single, fibrinogen-bound platelets. *J. Biol. Chem.* **1993**, *268*, 356-363.
25. Nagy Á, Lánczky A, Menyhárt O, Győrffy B. Validation of miRNA prognostic power in hepatocellular carcinoma using expression data of independent datasets. *Sci. Rep.* **2018**, *8*, 9227.
26. Braun A, Varga-Szabo D, Kleinschnitz C, Pleines I, Bender M, Austinat M, Bösl M, Stoll G, Nieswandt B. Orai1 (CRACM1) is the platelet SOC channel and essential for pathological thrombus formation. *Blood.* **2009**, *113*, 2056-2063.
27. Aliotta A, Bertaggia Calderara D, Zermatten MG, Alberio L. Sodium–calcium exchanger reverse mode sustains dichotomous ion fluxes required for procoagulant COAT platelet formation. *Thromb. Haemost.* **2020**, *121*, 309-321.
28. Gilio K, Harper MT, Cosemans JM, Konopatskaya O, Munnix IC, Prinzen L, Leitges M, Liu Q, Molkentin JD, Heemskerk JWM, Poole AW. Functional divergence of platelet protein kinase C (PKC) isoforms in thrombus formation on collagen. *J. Biol. Chem.* **2010**, *285*, 23410-23419.
29. Harper M, Poole A. Diverse functions of protein kinase C isoforms in platelet activation and thrombus formation. *J. Thromb. Haemost.* **2010**, *8*, 454-462.
30. Volz J, Kusch C, Beck S, Popp M, Vögtle T, Meub M, Scheller I, Heil HS, Preu J, Schuhmann MK, Hemmen K, Premsler T, Sickmann A, Heinze KG, Stegner D, Stoll G, Braun A, Sauer M, Nieswandt B. BIN2 orchestrates platelet calcium signaling in thrombosis and thrombo-inflammation. *J. Clin. Invest.* **2020**, *130*, 6064-6079.

31. Shibata K, Kitayama S, Morita K, Shirakawa M, Okamoto H, Dohi T. Regulation by protein kinase C of platelet-activating factor-and thapsigargin-induced calcium entry in rabbit neutrophils. *Jpn. J. Pharmacol.* **1994**, *66*, 273-276.
32. Xu Y, Ware JA. Selective inhibition of thrombin receptor-mediated Ca^{2+} entry by protein kinase C β. *J. Biol. Chem.* **1995**, *270*, 23887-23890.
33. Kawasaki T, Ueyama T, Lange I, Feske S, Saito N. Protein kinase C-induced phosphorylation of Orai1 regulates the intracellular Ca^{2+} level via the store-operated Ca^{2+} channel. *J. Biol. Chem.* **2010**, *285*, 25720-25730.
34. Aleman MM, Byrnes JR, Wang J-G, Tran R, Lam WA, Di Paola J, Mackman N, Degen JL, Flick MJ, Wolberg AS. Factor XIII activity mediates red blood cell retention in venous thrombi. *J. Clin. Invest.* **2014**, *124*, 3590-3600.
35. Faes C, Ilich A, Sotiaux A, Sparkenbaugh EM, Henderson MW, Buczek L, Beckman JD, Ellsworth P, Noubouossie DF, Bhoopat L, Piegore M, Renoux C, Bergmeier W, Park Y, Ataga KI, Cooley B, Wolberg AS, Key NS, Pawlinski R. Red blood cells modulate structure and dynamics of venous clot formation in sickle cell disease. *Blood.* **2019**, *133*, 2529-2541.
36. Kremers RM, Peters TC, Wagenvoord RJ, Hemker HC. The balance of pro- and anticoagulant processes underlying thrombin generation. *J. Thromb. Haemost.* **2015**, *13*, 437-447.
37. Binder NB, Depasse F, Mueller J, Wissel T, Schwers S, Germer M, Hermes B, Turecek PL. Clinical use of thrombin generation assays. *J. Thromb. Haemost.* **2021**, *19*, 2918-2929.

Chapter 9

Summary

Samenvatting

总结

Impact

Curriculum vitae

Publications

Acknowledgements

Summary

Blood platelets establish the formation and development of arterial thrombi and orchestrate normal hemostasis. Current antiplatelet agents prescribed for the prevention of (secondary) thrombotic events are associated with bleeding side effects. It is considered that improved drugs will arise from a better understanding of the complex mechanisms of platelet activation. Human platelets can be stimulated via multiple receptors, with clear (patho)physiological importance of the signaling collagen receptor, glycoprotein VI (GPVI), the protease-activated receptors for thrombin, PAR1 and PAR4, the receptors for ADP, $P2Y_1$ and $P2Y_{12}$, and the thromboxane A_2 receptor TP. Crucial outcomes of the platelet activation process are a change in the fibrin(ogen) receptor integrin αIIbβ3 from the inactive to the active, ligand-binding state; the secretion of storage granules (assessed as P-selectin expression); and the development of procoagulant activity. In this thesis, I examined the intrinsic reversibility of integrin αIIbβ3 activation, such in contrast to the irreversible secretion process. Furthermore, I studied the transiency in Ca^{2+} signaling of activated platelets, and I compared the development of procoagulant activity of platelets with that of red blood cells. The thesis thereby focuses on key signaling pathways contributing to transient state of platelet activation.

Chapter 1 provides a brief, general background on the roles of key platelet receptors in thrombosis and hemostasis. Particular attention is paid to GPVI and PAR1/4, with as downstream signaling modes the activation of protein tyrosine kinases and protein kinase C (PKC). The chapter furthermore introduces how, next to PKC isoforms, elevated cytosolic Ca^{2+} can be placed in the center of the platelet activation process, also mentioning the main Ca^{2+} transporters in store-regulated Ca^{2+} entry, including the Orai1 channel. Furthermore, I describe the blood coagulation as a process that can be monitored by determining the generation and inactivation of thrombin. **Chapter 2** provides an in-depth review, describing the current knowledge on platelet agonists and conditions that lead to a reversible platelet aggregation as a result of transient ligand binding to integrin αIIbβ3. Highlighted herein are the roles of the platelet ADP receptors, and the signaling pathways downstream of these via phosphoinositide 3-kinase (PI3K) isoforms. Argued is how a transient $P2Y_{1/12}$ receptor function and PI3K activity relate to the observed GPVI- and PAR-dependent reversibility of integrin activation.

To better understand how other signaling pathways contribute to a transient platelet integrin αIIbβ3 activation, in **Chapter 3**, we used a panel of pharmacological inhibitors to pre-treat or post-treat platelets activated via the GPVI, PAR, or P2Y receptors. These inhibitors targeted PKC or PI3K isoforms, glycogen synthase kinase-3 (GSK3), Ras-related proteins or β-arrestins. The most responsive platelet receptors in terms of transiency appeared to be PAR1 (triggered by the peptide TRAP6), $P2Y_{12}$ (triggered by ADP) and GPVI (triggered by collagen-related peptide). We established that platelet pre-treatment with the inhibitors decreased GPVI- and PAR-induced αIIbβ3 activation and P-selectin expression in the order of PKC > GSK3 > β-arrestin > PI3K. In addition, the post-treatment with inhibitors revealed secondary αIIbβ3 inactivation (not P-selectin expression), in the same order, in which case the reversibility was confined to GPVI and PAR1 agonists. It appeared that a combined inhibition of the so-called conventional and novel PKC isoforms was more effective for integrin closure than the use of isoform-specific inhibitors

alone. Platelet spreading assays revealed that either PKC or $P2Y_{12}$ inhibition provoked a partial conversion from lamellipods to a more discoid platelet shape. We concluded that PKC isoforms and autocrine ADP contribute to the persistent integrin αIIbβ3 activation state and hence a stabilized platelet response.

In **Chapter 4**, we examined the time-dependency of effects of consecutive addition of agonists of the GPVI and PAR1/4 receptors. Outcome measurements were platelet aggregation and cytosolic Ca^{2+} rises. We confirmed that an iloprost-induced elevation of cAMP level, either before or simultaneously with GPVI or PAR1 stimulation, completely eliminated the aggregation responses. However, PAR signaling demonstrated a longer time sensitivity for post inhibition than GPVI signaling. Furthermore, also tirofiban (integrin αIIbβ3 blocker) and Syk kinase inhibition sub-acutely modulated platelet aggregation, in other words halted this process even when applied after an agonist. We also examined whether platelets are capable to react to sequential stimulation. After initial activation via PAR, the cells still responded to GPVI, but they failed to respond to repeated PAR stimulation. Cytosolic Ca^{2+} measurements indicated that, in comparison to prior PAR stimulation, prior GPVI stimulation induced a more persistent, priming activation state, which influenced the response to a next agent. Overall, our work revealed a high degree of versatility of platelets to rapidly react to a second receptor agonist, with a longer-term signal memory effect after GPVI than after PAR stimulation.

Similarly to other cells, cytosolic Ca^{2+} is in platelets an important second messenger that regulates the majority of functional responses. **Chapter 5** describes time-dependent effects of GPVI and PAR1/4 stimulation on intracellular Ca^{2+} mobilization and the accompanied extracellular Ca^{2+} entry, with a 96-well plate-based method also allowing calculation of the Ca^{2+} entry ratios. We established that, when compared to CRP and thrombin, collagen and TRAP6 act as weaker Ca^{2+}-rising agonists that are also more dependent on the secondary mediators ADP and thromboxane A_2. We also investigated the effect of the compound thapsigargin, which blocks the back-pumping of cytosolic Ca^{2+} by Ca^{2+}-ATPases. When CRP or thrombin were combined with thapsigargin, the Ca^{2+} entry ratios greatly increased to 400 (GPVI stimulation) or 40 (PAR stimulation). This pointed to a major role of the so-called store-operated Ca^{2+} entry. By using a panel of pharmacological inhibitors, we could establish that the main Ca^{2+} carriers that control both the GPVI- and PAR-induced Ca^{2+} entry into platelets are the channel Orai1 and Na^+/Ca^{2+} exchange proteins. Much less important were the ATP receptor $P2X_1$ (only initial curve value), and the channels TRPC6 and Piezo-2.

In the connected **Chapter 6**, we investigated the impact of novel and conventional PKC isoforms on store-operated Ca^{2+} entry. We found a redundant contribution by both types of isoforms in the suppression of this process. Key involvement of the Orai1 channel was confirmed using platelets from patients with a mutation in the *ORAI1* gene. GPVI activation through both PKC isoforms had a significant suppressive effect on the Ca^{2+} entry process. When checking for an important mediator of the Orai1-STIM1 interactions, namely the adapter protein BIN2, we identified by label-free analysis of the platelet phosphoproteome 45 regulated phospho-sites in BIN2 and 18 in STIM1, of which four had the characteristics of PKC multi-isoform substrates. Functional platelet testing indicated that the negative PKC-dependent regulation of Ca^{2+} entry

was accompanied by a downregulation of GPVI-dependent phosphatidylserine exposure and a suppressed thrombin generation in the presence of plasma.

In addition to platelets, red blood cells also play a role in the modulation of thrombus stability, and hence contribute to thrombosis and clot formation. In **Chapter 7**, we describe a novel whole-blood fluorogenic assay to elucidate the complementary roles of platelets and red blood cells in the process of thrombin generation. We find an enhancement of thrombin generation by phosphatidylserine-exposing red blood cells, independent of the coagulant trigger. Blockage of the exposed phosphatidylserine with annexin A5 appeared to enhance the GPVI-induced procoagulant activity of platelets. In patients with (hemolytic) anemia or erythrocytosis, cluster analysis revealed both high and low whole-blood thrombin generation profiles. We concluded that better determination of the whole blood hypo-or hyper-coagulant activity may help to characterize a bleeding or thrombosis risk. **Chapter 8** discusses the main findings and conclusions of this thesis in the light of relevant literature. Foreseen is that the current analysis of transient aspects of platelet activation will lead to the development of improved antiplatelet medications, limiting the current bleeding risk.

Samenvatting

Bloedplaatjes zorgen voor de vorming en ontwikkeling van arteriële trombi en bewerkstelleen de normale hemostase. De huidige plaatjesaggregatieremmers, die worden voorgeschreven ter preventie van (secundaire) trombose-incidenten gaan regelmatig gepaard met bloeding als bijwerking. Aangenomen kan worden dat de werkzaamheid van nieuwe geneesmiddelen verhoogt, wanneer we een beter begrip krijgen van de complexe mechanismen van plaatjesactivering. Humane plaatjes worden gestimuleerd via meerdere receptoren, waarin duidelijk van (patho)fysiologisch belang zijn de signalerende collageenreceptor, glycoproteïne VI (GPVI), de protease-geactiveerde receptoren voor trombine, PAR1 en PAR4, de receptoren voor ADP, $P2Y_1$ en $P2Y_{12}$, en de tromboxaan A_2-receptor TP. Belangrijke responsen van het activeringsproces zijn: een structurele verandering in de fibrinogeenreceptor integrine αIIbβ3 van een inactieve naar een actieve, ligandbindende toestand; de secretie van opslag-granula (gemeten als P-selectine-expressie); en het ontstaan van procoagulante activiteit. In dit proefschrift heb ik de intrinsieke omkeerbaarheid van de integrine αIIbβ3-activatie bestudeerd, in tegenstelling tot het niet omkeerbare secretieproces. Verder heb ik de reversibiliteit in de Ca^{2+}-signalering van geactiveerde plaatjes onderzocht, en heb ik de procoagulante activiteit van plaatjes vergeleken met die van rode bloedcellen. Het proefschrift richt zich daarmee op belangrijke signaalroutes, die bijdragen tot een transiënte toestand van de plaatjesactivering.

Hoofdstuk 1 geeft een kort, algemeen overzicht van de functie van belangrijke plaatjesreceptoren bij trombose en hemostase. Bijzondere aandacht is besteed aan GPVI en PAR1/4, met als signalerings-mechanismes de activering van proteïne tyrosinekinasen en van proteïnekinase C (PKC). Het hoofdstuk beschrijft verder hoe, naast PKC-isovormen, verhoogd cytosolisch Ca^{2+} centraal staat in de plaatjesactivering. Ook worden de belangrijkste Ca^{2+}-transporters genoemd in de zogeheten *store-regulated* Ca^{2+} instroom middels Orai1 Ca^{2+}-kanalen. Verder beschrijf ik de bloedstolling als een proces dat kan worden benaderd door het bepalen van de vorming en inactivatie van trombine. **Hoofdstuk 2** biedt een diepgaand overzicht, waarin de huidige kennis wordt beschreven over plaatjesagonisten en omstandigheden, die leiden tot een reversibele plaatjesaggregatie als gevolg van transiënte ligandbinding aan integrine αIIbβ3. In het hoofdstuk wordt ook de rol benadrukt van de ADP-receptoren, en de signaalroutes opgewekt door deze receptoren middels fosfoinositide 3-kinase (PI3K). Beargumenteerd is hoe een transiënte $P2Y_{1/12}$-receptorfunctie alsmede PI3K-activiteit relateert aan een reversibele GPVI- en PAR-opgewekte integrine-activering.

Om beter te begrijpen hoe ook andere signaleringsroutes bijdragen aan een tijdelijke activering van integrine αIIbβ3, hebben we in **Hoofdstuk 3** een panel van farmacologische remmers gebruikt. Daarmee werden plaatjes vóór- of nabehandeld, bij activering van de GPVI-, PAR- of P2Y-receptoren. De remmers waren gericht tegen PKC- of PI3K-isovormen, glycogeensynthase-kinase-3 (GSK3), Ras-gerelateerde eiwitten of β-arrestines. De meest responsieve plaatjesreceptoren in termen van transiëntie bleken PAR1 (geactiveerd door het peptide TRAP6), $P2Y_{12}$ (geactiveerd door ADP) en GPVI (geactiveerd door een collageen-peptide). We konden vaststellen dat de voorbehandeling van plaatjes leidde tot vermindering van de GPVI- en PAR-geïnduceerde αIIbβ3-activering en P-selectine-expressie in de volgorde van PKC > GSK3 > β-arrestine > PI3K. Nabehandeling met deze remmers resulteerde in secundaire αIIbβ3-inactivering (niet P-selectine-expressie) in dezelfde volgorde, alhoewel hier de omkeerbaarheid beperkt bleef tot GPVI- en PAR1-agonisten. Combinatieremming van de zogeheten conventionele en nieuwe PKC-isovormen bleek effectiever voor de integrinesluiting dan een isovorm-specifieke remming alleen. Plaatjes-spreidingstesten gaven aan dat de remming van PKC of $P2Y_{12}$ leidde tot een gedeeltelijke teruggang van lamellipoden naar de oospronkelijke schijfvormige plaatjesstructuur. We concludeerden dat naast PKC-isovormen ook autocriene ADP bijdraagt aan een persistente integrine αIIbβ3-activeringstoestand en daarmee aan een permanente plaatjesrespons.

In **Hoofdstuk 4** onderzochten we de tijdsafhankelijkheid van effecten van een opeenvolgende toevoeging van GPVI en PAR1/4 agonisten. Uitkomstmetingen waren plaatjesaggregatie en stijging van de cytosol Ca^{2+}-concentratie. We vonden dat de door iloprost geïnduceerde verhoging van cAMP, vóór of gelijktijdig met GPVI- of PAR1-stimulering, de aggregatiereactie volledig remde. De PAR-signalering vertoonde echter een langere gevoeligheid voor post-remming dan de GPVI-signalering. Daarnaast zorgden ook tirofiban (integrine αIIbβ3-blokker) en Syk-kinase-remming voor subacute onderdrukking van de plaatjesaggregatie. Met andere woorden, deze stoffen werkten remmend, zelfs als ze werden toegediend na een agonist. We hebben ook bekeken of plaatjes in staat zijn te reageren op een tweede stimulatie. Na een initiële activering via PAR bleken ze nog steeds te reageren op GPVI, maar niet meer op een herhaalde PAR-stimulatie. Verder gaven Ca^{2+}-metingen aan dat, in vergelijking met voorafgaande PAR-stimulering, GPVI-stimulering een meer persistente activeringstoestand induceerde, die ook de respons op een volgende agonist beïnvloedde. Over het geheel genomen toont dit werk een hoge mate van veelzijdigheid van plaatjes om snel te reageren op een tweede receptoragonist, met een langer geheugeneffect na GPVI- dan na PAR-stimulering.

Net als in andere cellen vormt cytosolisch Ca^{2+} in plaatjes een belangrijke *second messenger*, die de meeste plaatjesfuncties controleert. **Hoofdstuk 5** beschrijft tijdsafhankelijke effecten van de

GPVI- en PAR1/4-stimulering op de intracellulaire Ca^{2+}-mobilisatie en de daarmee gepaard gaande extracellulaire Ca^{2+}-instroom. Hierbij gebruikten we een op 96-well platen gebaseerde methode, die ook berekening van de Ca^{2+}-instroom ratio mogelijk maakte. Het bleek dat collageen en TRAP6, vergeleken met CRP en trombine, werken als zwakkere Ca^{2+}-mobilizerende agonisten die meer afhankelijk zijn van de secundaire mediatoren ADP en tromboxaan A_2. We onderzochten ook het effect van de verbinding *thapsigargin*, die het terugpompen van Ca^{2+} door Ca^{2+}-ATPasen blokkeert. Wanneer CRP of trombine werd gecombineerd met *thapsigargin*, nam de Ca^{2+}-instroom ratio sterk toe tot wel 400 (GPVI stimulering) of 40 (PAR stimulering). Dit duidde op een belangrijke rol van de zogeheten *store-operated* Ca^{2+}-instroom. Middels een panel van farmacologische remmers konden we vaststellen dat de belangrijkste Ca^{2+}-*carriers*, die zowel de GPVI- als PAR-geïnduceerde Ca^{2+}-instroom in plaatjes controleren, bestaan uit het kanaaleiwit Orai1 en Na^+/Ca^{2+} transporteiwitten. Veel minder belangrijk waren de ATP-receptor $P2X_1$ (alleen initiële curvewaarde) en de kanaaleiwitten TRPC6 en Piezo-2.

In het gekoppelde **hoofdstuk 6** onderzochten we de impact van nieuwe en conventionele PKC-isovormen op de *store-operated* Ca^{2+}-instroom. We maten een combi bijdrage van beide typen isovormen in de suppressie van dit proces. Betrokkenheid van het Orai1-kanaal kon worden bevestigd aan de hand van plaatjes van patiënten met een mutatie in het *ORAI1*-gen. GPVI-activering via beide PKC-isovormen had een significant onderdrukkend effect op de Ca^{2+}-instroom. Voor bepaling van een belangrijke mediator van Orai1-STIM1-interacties, namelijk het adaptereiwit BIN2, voerden we een labelvrije analyse van het plaatjes-fosfoproteoom uit. Deze gaf 45 gereguleerde fosforylerings-plaatsen in BIN2 en 18 in STIM1, waarvan er vier de kenmerken van PKC-substraat hadden. Functionele plaatjes testen gaven aan dat de negatieve PKC regulering van Ca^{2+}-instroom gepaard ging met een downregulatie van de GPVI-geïnduceerde fosfatidylserine-expositie en een onderdrukte trombinevorming in de aanwezigheid van plasma.

Ook rode bloedcellen kunnen een rol spelen bij de modulatie van de trombusstabiliteit, daarmee bijdragen aan trombose en stolselvorming. In **Hoofdstuk 7** beschrijven we een nieuwe fluorogene test in volbloed om de complementaire functies van plaatjes en rode bloedcellen bij het proces van trombinevorming op te helderen. We vonden een verbetering van de vorming van trombine door rode bloedcellen met geëxposeerd fosfatidylserine, onafhankelijk van de stollingstrigger. Na blokkade van het fosfatidylserine met annexine A5 bleek de GPVI-geïnduceerde procoagulante activiteit van plaatjes toegenomen. Clusteranalyse van de resultaten met bloed van patiënten met (hemolytische) anemie of erytrocytose toonde zowel hoge als lage trombinevormings-profielen. Onze conclusie is dat bepaling van de hypo- of hyperstollingsactiviteit in volbloed kan helpen bij het karakteriseren van een bloedings- of

tromboserisico. **Hoofdstuk 8** bespreekt de belangrijkste bevindingen en gevolgtrekkingen van dit proefschrift in het licht van relevante literatuur. Verwacht kan worden dat de huidige analyse van temporele aspecten van de plaatjesactivering zal leiden tot de ontwikkeling van verbeterde plaatjesremmers, waarmee het huidige bloedingsrisico kan worden beperkt.

总结

血小板能促进动脉血栓的形成和发展，并协调正常的止血过程。目前用于预防（继发性）血栓事件的抗血小板药物与出血副作用有关。人们认为，只有更好地了解血小板活化的复杂机制，才能改进药物。人体血小板可通过多种受体受到刺激，其中信号胶原受体糖蛋白 VI (GPVI)、凝血酶蛋白酶活化受体 PAR1 和 PAR4、ADP 受体 $P2Y_1$ 和 $P2Y_{12}$ 以及血栓素 A_2 受体 TP 在（病理）生理方面具有明显的重要性。血小板活化过程的关键结果是纤维蛋白（原）受体整合素 αIIbβ3 从非活性状态转变为活性的配体结合状态；分泌储存颗粒（评估为 P-选择素的表达）；以及产生促凝活性。在这篇论文中，我研究了整合素 αIIbβ3 激活的内在可逆性，这与不可逆的分泌过程形成了鲜明对比。此外，我还研究了活化血小板 Ca^{2+} 信号的瞬时性，并比较了血小板与红细胞促凝活性的发展。因此，论文重点研究了导致血小板活化瞬时状态的关键信号通路。

第一章简要介绍了血小板主要受体在血栓形成和止血中的作用。本章特别介绍了 GPVI 和 PAR1/4，其下游信号模式是激活蛋白酪氨酸激酶和蛋白激酶 C(PKC)。本章进一步介绍了除 PKC 同工酶外，细胞膜 Ca^{2+} 的升高如何成为血小板活化过程的中心，还提到了储存调节 Ca^{2+} 进入的主要 Ca^{2+} 转运体，包括 Orai1 通道。此外，我还将血液凝固描述为一个可通过确定凝血酶的生成和失活来监测的过程。**第二章**提供了一篇深入的综述，描述了目前有关血小板激动剂的知识，以及由于瞬时配体与整合素 αIIbβ3 结合而导致血小板可逆聚集的条件。本文强调了血小板 ADP 受体的作用，以及这些受体下游通过磷酸肌酸 3- 激酶（PI3K）同工酶发出信号的途径。本文论证了瞬时 $P2Y_{1/12}$ 受体功能和 PI3K 活性与所观察到的 GPVI 和 PAR 依赖性整合素激活的可逆性之间的关系。

为了更好地了解其他信号通路是如何促成瞬时血小板整合素 αIIbβ3 激活的，在**第三章**中，我们使用了一组药理抑制剂，对通过 GPVI、PAR 或 P2Y 受体激活的血小板进行预处理或后处理。这些抑制剂靶向 PKC 或 PI3K 同工酶、糖原合酶激酶-3 (GSK3)、Ras 相关蛋白或 β-阻遏素。就瞬时性而言，反应最灵敏的血小板受体似乎是 PAR1（由多肽 TRAP6 触发）、$P2Y_{12}$（由 ADP 触发）和 GPVI（由胶原相关肽触发）。我们发现，用抑制剂预处理血小板可降低 GPVI 和 PAR 诱导的 αIIbβ3 活化和 P 选择素表达，其顺序为 PKC > GSK3 > β-restin > PI3K。此外，用抑制剂进行后处理后发现继发性 αIIbβ3 失活（不是 P-选择素表达），顺序相同，在这种情况下，可逆性仅限于 GPVI 和 PAR1 激动剂。联合抑制所谓的传统 PKC 和新型 PKC 同工酶似乎比单独使用同工酶特异性抑制剂对整合素封闭更有效。血小板铺展试验显示，无论是 PKC 还是 $P2Y_{12}$ 抑制剂都会导致血小板从片状部分转变为更圆盘状。我们的结论是，PKC 同工酶和自分泌 ADP 有助于整合素 αIIbβ3 的持续激活状态，从而使血小板反应趋于稳定。

在**第四章**中，我们研究了连续添加 GPVI 和 PAR1/4 受体激动剂的效果随时间的变化。测量结果是血小板聚集和细胞膜 Ca^{2+} 上升。我们证实，在 GPVI 或 PAR1 刺激之前或同时，伊洛前列素诱导的 cAMP 水平升高可完全消除聚集反应。然而，与 GPVI 信号传导相比，PAR 信

号传导对抑制后的时间敏感性更长。此外，替罗非班（整合素αIIbβ3 阻断剂）和 Syk 激酶抑制剂也能亚急性调节血小板聚集，换句话说，即使在激动剂之后使用，也能阻止这一过程。我们还研究了血小板是否能对连续刺激做出反应。通过 PAR 首次激活后，细胞仍对 GPVI 有反应，但对重复的 PAR 刺激却没有反应。细胞膜 Ca^{2+} 测量结果表明，与之前的 PAR 刺激相比，之前的 GPVI 刺激会诱导更持久的引物激活状态，从而影响对下一种药剂的反应。总之，我们的研究揭示了血小板对第二种受体激动剂做出快速反应的高度多功能性，与 PAR 刺激相比，GPVI 刺激后的信号记忆效应更持久。

与其他细胞类似，细胞膜 Ca^{2+} 在血小板中也是调节大多数功能反应的重要第二信使。第 5 章描述了 GPVI 和 PAR1/4 刺激对细胞内 Ca^{2+} 动员和伴随的细胞外 Ca^{2+} 进入的时间依赖性效应，基于 96 孔板的方法还可以计算 Ca^{2+} 进入比率。我们发现，与 CRP 和凝血酶相比，胶原蛋白和 TRAP6 是较弱的 Ca^{2+} 上升激动剂，而且更依赖于次级介质 ADP 和血栓素 A_2。我们还研究了 thapsigargin 这种化合物的作用，它能阻断 Ca^{2+}-ATP 酶对细胞膜 Ca^{2+} 的反泵作用。当 CRP 或凝血酶与葡糖甘结合使用时，Ca^{2+} 进入比率大大增加到 400（GPVI 刺激）或 40（PAR 刺激）。这表明所谓的储存操作 Ca^{2+} 进入起了重要作用。通过使用一系列药理抑制剂，我们可以确定，控制 GPVI 和 PAR 诱导的 Ca^{2+} 进入血小板的主要 Ca^{2+} 载体是通道 Orai1 和 Na^{+}/Ca^{2+} 交换蛋白。ATP 受体 $P2X_1$（只有初始曲线值）以及通道 TRPC6 和 Piezo-2 的重要性要小得多。

在接下来的**第六章**中，我们研究了新型和传统 PKC 同工酶对储存操作的 Ca^{2+} 进入的影响。我们发现这两种同工酶在抑制这一过程中的作用都是多余的。使用 *ORAI1* 基因突变患者的血小板证实了 Orai1 通道的主要参与作用。通过两种 PKC 同工酶激活 GPVI 对 Ca^{2+} 进入过程有显著的抑制作用。在检查 Orai1-STIM1 相互作用的一个重要介质（即适配蛋白 BIN2）时，我们通过对血小板磷酸蛋白组进行无标记分析，在 BIN2 和 STIM1 中分别发现了 45 个和 18 个受调控的磷酸化位点，其中 4 个具有 PKC 多异构体底物的特征。血小板功能测试表明，PKC 对 Ca^{2+} 进入的负调控伴随着 GPVI 依赖性磷脂酰丝氨酸暴露的下调以及血浆存在时凝血酶生成的抑制。

除血小板外，红细胞也在调节血栓稳定性方面发挥作用，从而促进血栓形成和血块形成。在**第七章**中，我们介绍了一种新型全血荧光测定法，以阐明血小板和红细胞在凝血酶生成过程中的互补作用。我们发现，暴露于磷脂酰丝氨酸的红细胞能增强凝血酶的生成，而与凝血剂的触发无关。用 annexine A5 阻断暴露的磷脂酰丝氨酸似乎能增强 GPVI 诱导的血小板促凝活性。在（溶血性）贫血或红细胞增多症患者中，聚类分析显示全血凝血酶生成情况有高有低。我们的结论是，更好地确定全血低凝血活性或高凝血活性可能有助于确定出血或血栓形成风险的特征。**第八章**根据相关文献讨论了本论文的主要发现和结论。可以预见的是，目前对血小板活化瞬时性的分析将有助于开发出更好的抗血小板药物，从而限制目前的出血风险。

Impact

Cardiovascular diseases still are a leading cause of death worldwide, and costed the European Union economy €282 billion in 2021 [1]. Platelets, the smallest blood cells, play a major role in arterial thrombosis as well as in physiological hemostasis. The use of antiplatelet therapy has become an essential component of cardiovascular disease treatment. While the inhibition of platelet responsiveness has decreased the occurrence of ischemic events, it also led to side effects of bleeding, thus perpetuating the therapeutic challenge of preventing thrombosis whilst preserving hemostasis. The future of antiplatelet therapy depends on finding new drugs that target specific platelet functions, based on better methods for assessing the risks of bleeding and thrombosis-induced ischemia [2]. The platelet integrin αIIbβ3, the collagen receptor GPVI, the thrombin receptors PAR1/4, and the ADP receptors $P2Y_{1/12}$ are all suitable targets. In this thesis, I focus on a better understanding of transient platelet activation pathways by investigating how platelets can respond to different agonists and inhibitors in a time-dependent way.

Integrin αIIbβ3, expressed at high level, stays in an inactive conformation on resting platelets. After platelet stimulation, it converts due to an inside-out signal from the low-affinity state into a high-affinity state, able to bind fibrinogen and other ligands. The ligand binding also promotes clustering of integrin molecules and, in turn, triggers the process of outside-in signaling [3]. This signaling cascade sets into motion a variety of cellular processes, crucial for platelet functions like spreading, aggregation, clot retraction, and the consolidation of thrombus formation. Thus, the integrin αIIbβ3-related signaling pathways are regarded as potential points for antithrombotic treatment. In Chapters 2-3, our objective was to enhance current understanding of the reversibility of integrin αIIbβ3 activation.

In Chapter 3, we showed that platelet stimulation via GPVI or PAR1 caused transient integrin αIIbβ3 activation, while stimulation via PAR4 led to permanent αIIbβ3 activation. We also confirmed that the protein kinase C pathway is crucial for integrin αIIbβ3 activation, and that autocrine responses via $P2Y_{12}$ are essential for a sustained integrin αIIbβ3 opening. Flow cytometry was employed in this chapter, which method can also be used for clinic testing, as it can rapidly analyze thousands of cells in complex mixtures per second. By detecting the degree of integrin activation, it assesses whether platelets are activated or not. Flow cytometry can also assist in determining the clinical dosage of drugs, and thereby improve the risk prediction of thrombosis and bleeding.

In various clinical situations, it can be needed to quickly assess the hemostasis process, for instance in patients with acute bleeding symptoms. In Chapter 4, we tested several agonists that rapidly trigger platelet aggregation. Our findings suggest that it is still effective to administer antiplatelet drugs, while aggregation is already occurring. However, when compared to PAR activation, GPVI activation shows a more restricted time frame for interference in the

aggregation process. This may be helpful in clinical treatment of thrombosis with suspected roles of different receptors.

In Chapters 5-6, we used a high throughput method to assess the GPVI and PAR-induced Ca^{2+} mobilization in platelets. In Chapter 5, we find that this response with weaker agonists relied more on secondary mediators, when compared to stronger agonists like collagen-related peptide and thrombin. Our findings also provide novel quantitative insight into the importance of Ca^{2+} entry for platelet activation. We confirmed that Na^{+}/Ca^{2+} exchangers and Orai1 channels are crucial in this process, thereby building upon earlier reports [4]. In the next Chapter 6, we investigated the roles of different protein kinase C (PKC) isoforms in the regulation of Ca^{2+} entry. We showed that overall PKC activation via GPVI led to a robust inhibitory effect on the entry through Orai1 channels. In addition, this inhibition also suppressed platelet procoagulant activity and the coagulation process. Notably, we discovered that PKC-dependent phosphorylation of the signaling proteins BIN2 and STIM1 associates with a decreased Orai1 Ca^{2+}-channel activity. Indeed, PKC isoforms served as potent negative regulators of the process of store-operated Ca^{2+} entry. These findings offer fresh perspectives on the exploration and creation of novel drugs aimed at modulating these molecular pathways.

In the last experimental Chapter 7, we describe a method for obtaining calibrated thrombin generation curves in 96-well plates, thereby providing the first comprehensive quantitative comparison of this coagulation process in whole blood and platelet-rich plasma from the same subject. Our results indicated that red blood cells play an initial role in the thrombin generation, whilst activated platelets later support this process. Thrombin generation accelerated as the hematocrit level increased, and delayed when the erythrocytes were treated with annexin A5, which blocks phosphatidylserine. These findings on red blood cell properties are valuable for assessing the risk of bleeding or thrombosis in a clinical setting.

Overall, this thesis elaborates how transient activation via GPVI and PARs is a major response function of platelets, and thereby likely is relevant for thrombosis and hemostasis. In addition, the thesis provides new insights into the regulation of platelet Ca^{2+} responses and thrombin generation. My expectation is that these discoveries will help to drive the development of antiplatelet medications and to enhance the clinical assessments of thrombosis and bleeding risks.

References

1. Luengo-Fernandez R, Walli-Attaei M, Gray A, Leal J. Economic burden of cardiovascular diseases in the European Union: a cardiovascular diseases in the European Union: a population-based cost study. *Eur. Heart J.* **2023**.
2. Gelbenegger G, Jilma B. Clinical pharmacology of antiplatelet drugs. *Expert Rev. Clin. Pharmacol.* **2022**, 15, 1177-1197.
3. Huang J, Li X, Shi X, Zhu M, Wang J, Huang S, Huang X, Wang H, Li L, Deng H. Platelet integrin αIIbβ3: signal transduction, regulation, and its therapeutic targeting. *J. Hematol. Oncol*. **2019**, 12, 1-22.
4. Nagy M, Mastenbroek TG, Mattheij NJ, de Witt S, Clemetson KJ, Kirschner J, Schulz AS, Vraetz T, Speckmann C, Braun A. Variable impairment of platelet functions in patients with severe, genetically linked immune deficiencies. *Haematologica* **2018**, 103, 540.

Curriculum Vitae

Jinmi Zou was born on the 23rd of February 1992 in Shandong, China. In 2010 he started his study of Pharmacy at the Shandong University, China, where he received his bachelor's degree in 2014. He then started a master study of Medicinal Chemistry at Shandong University under the supervisor of Prof. Xinyong Liu. After completing his master's degree in 2018 with honors, he obtained an international bursary of the China Scholarship Council. In 2019, he started the PhD project at the Department of Biochemistry at the University of Maastricht (the Netherlands) and at Synapse Research Institute Maastricht (the Netherlands), under the joint supervision of Prof. Johan Heemskerk, Prof. Hugo ten Cate and Dr. Frauke Swieringa. During the years 2019-2023, he performed research on platelet functions in relation to thrombosis and hemostasis, as described in this thesis.

Publications

1. **Zou J**, Gao P, Hao X, Xu H, Zhan P, Liu X. Recent progress in the structural modification and pharmacological activities of ligustrazine derivatives. *Eur. J. Med. Chem.* **2018**, *147*, 150-162.

2. Kang D, Feng D, Ginex T, **Zou J**, Wei F, Zhao T, Liu X. Exploring the hydrophobic channel of NNIBP leads to the discovery of novel piperidine-substituted thiophene [3,2-d] pyrimidine derivatives as potent HIV-1 NNRTIs. *Acta Pharm. Sin. B.* **2020**, *10*, 878-894.

3. **Zou J**, Wu J, Roest M, Heemskerk JWM. Long-term platelet priming after glycoprotein VI stimulation in comparison to protease-activating receptor (PAR) stimulation. *PloS One.* **2021**, *16*, e0247425.

4. **Zou J**, Swieringa F, de Laat B, de Groot PG, Roest M, Heemskerk JWM. Reversible platelet integrin αIIbβ3 activation and thrombus instability. *Int. J. Mol. Sci.* **2022**, *23*, 12512.

5. Cheung HYF*, **Zou J***, Tantiwong C, Fernandez DI, Huang J, Ahrends R, Roest M, Cavill R, Gibbins JM, Heemskerk JWM. High-throughput assessment identifying major platelet Ca^{2+} entry pathways via tyrosine kinase-linked and G protein-coupled receptors. *Cell Calcium*, **2023**, *112*, 102738.

6. Li P, Ju H, Zhang Y, Achi JG, Kang D, **Zou J**, Zhan P. Discovery of ligustrazine and chalcone derivatives as novel viral nucleoprotein nuclear export inhibitors against influenza viruses. *J. Med. Virol.* **2023**, *95*, e28968.

7. Sun S, Campello E*, **Zou J***, Konings J, Huskens D, Wan J, Fernandez DI, Reutelingsperger, CP, ten Cate H, Toffanin S, Bulato C, de Groot PG, de Laat B, Simioni P*, Heemskerk JWM*, Roest M. Crucial roles of red blood cells and platelets in whole-blood coagulation. *Blood Adv.* **2023**, in press.

8. Huang J, Fernandez DI, **Zou J**, Wang X, Heemskerk JWM, García A. Restrained glycoprotein VI-induced platelet signaling by tyrosine protein phosphatases independent of phospholipase Cγ2. *Blood Thromb. Vasc. Biol.* **2023**, in press.

Submitted papers

9. **Zou J**, Sun S, De Simone I, ten Cate H, de Groot PG, de Laat B, Roest M, Heemskerk JWM, Swieringa F. Platelet activation pathways controlling reversible integrin αIIbβ3 activation. **2023** (submitted).

10. **Zou J***, Zhang P*, Solari FA, Mattheij NJA, Schönichen C, Kuijpers MJE, Sickmann A, Swieringa F, Zieger B, Jurk K, Heemskerk JWM. Negative regulation of store-operated calcium entry in platelets by protein kinase C isoforms. **2023** (submitted).

11. Fernández DI, Sobota V, Tullemans BME, van Groningen J, Troitiño S, **Zou J**, van den Hurk H, García A, Hornanejad S, Kuijpers MJE, Heemskerk JWM. Ultra-high throughput screening to identify antiplatelet drugs with discriminative receptor-dependent action mechanism. **2023** (submitted).

Abstracts and posters

1. **Zou J**, Sun S, De Simone I, ten Cate H, de Groot PG, Heemskerk JW, de Laat B, Roest M. Establishing the signalling pathways regulating reversible platelet integrin activation. International Society of Thrombosis and Haemostasis (ISTH), London, UK, July 2022.
2. Fernández DI, **Zou J**, Sobota V, Tullemans BME, van Groningen J, van den Hurk H, García A, Hornanejad S, Kuijpers MJE, Heemskerk JWM. Ultra-high throughput screening identifies novel calcium-dependent antiplatelet drugs with discriminative mode of receptor-dependent action. EUPLAN meeting, Milan, Italy, September 2022.
3. Sun S, **Zou J**, Konings J, Huskens D, Wan J, Reutelingsperger CP, ten Cate H, de Groot PG, de Laat B, Heemskerk JW, Roest M. Complementary roles of red blood cells and platelets in high-throughput whole-blood thrombin generation. International Society of Thrombosis and Haemostasis (ISTH), London, UK, July 2022.
4. Sun S, Konings J, Urbanus RT, Huskens D, Swieringa F, de Laat-Kremers R, **Zou J**, de Groot PG, Roest M, Heemskerk JWM, de Laat B. Diversity of plasmatic thrombin pools regulate thrombin generation and blood clotting: interference by a novel nanobody. American Society of Hematology Annual Meeting (ASH), San Diego, California, USA, December 2023.

Acknowledgement

I extend my deepest gratitude to the numerous individuals and institutions whose unwavering support has been instrumental in the completion of this doctoral thesis.

First and foremost, I would like to express my heartfelt appreciation to my supervisor Prof. Johan Heemskerk, Prof. Hugo ten Cate and my co-promotor Dr. Frauke Swieringa. Dear **Johan**, thank you for your guidance, expertise and encouragement which have been invaluable throughout this journey. Your guidance not only shapes my research direction but also inspires me to pursue excellence. I am grateful for the countless discussions that have been very beneficial in my journey as a researcher. Dear **Hugo**, I am very grateful for your support and help with my extension. I also appreciate your constructive feedback during my PhD. Dear **Frauke**, I'm happy to have you as my co-promoter. Thank you for teaching me many experimental techniques and for reviewing my manuscript. By the way, the cake you made is delicious.

I would like to thank the assessment committee of my thesis. Dear Prof. **Rory Koenen**, Prof. **Chris P.M. Reutelingsperger**, Prof. **Alastair Poole**, Prof. **David Stegner**, and Dr. **Ingrid Dijkgraaf**, thank you very much for spending time reading my thesis. Your expertise greatly enhanced the quality of this work.

I'm happy to be part of the Platelet Group and appreciate the collaboration and learning opportunities it provides. Dear **Claudia**, thank you for your useful advice and blood drawing. Dear **Giorgia**, thank you for all the help in the lab and fun moments. Dear **Simone**, thank you for bringing happiness and laugh at work and thank you for helping me find reagents countless times. Dear **Titus**, thanks for all your help and happy time. Dear **Bibian, Sanne, Alicia, Gina, Natalie, Isabella,** and **Daniëlle**, I have learnt a lot from you, and I am very grateful for all your help. Dear **Marijke**, thanks so much for all your advice and lab work. Dear **Paola, Contance,** and **Magdi**, thank you for your kind help. Dear **Judith**, I would like to thank you for your helpful advice and support during my PhD studies, as well as for the meaningful chats you have had with me outside of work. Thanks to all Chinese friends who have joined the platelet group. **黄竞男**，感谢你对我实验上的帮助以及各种吐槽。**张鹏宇**，**张任丰**，感谢你们对文章的贡献以及快乐的聊天。**罗琪**，很开心和你打麻将。

I am grateful to the Biochemistry Department for providing the necessary resources and research facilities, fostering an environment conducive to academic growth, thank all Biochemistry Department members. Dear **Trees** and **Lidewij**, thank you for all your help and nice chats. Dear **Stella, Elisabetta,** and **Cengiz**, thanks for the nice chat with you.

I sincerely thank my colleagues and researchers at the Synapse Research Institute for sharing their knowledge and providing valuable feedback. I would like to extend my thanks to **Bas** and **Mark**, thank you for giving me the opportunity to interview and for all the suggestions you made during the weekly meetings. Dear Prof. **Philip**, thank you for your advice on my experiments and manuscripts. Dear **Joke**, thank you for helping me in the lab. Dear **Marisa, Dana, Romy, Debora, Eric,** and **Rob**, thank you for your support and for great chats at Synapse. Dear **Ilaria**, thank you for your useful advice and help in university and Synapse. Dear **Harmen, Rachel, Ruth, Veronica, Anouk,** and **Lily,** thank you for all the help and fun moments. Thanks to all synapse's Chinese colleagues and friends. 感谢**翠**帮我找到各种东西以及工作和生活上的建议，感谢你，**Armando** 和 **Aron** 的款待。感谢**思雨**在工作和生活中的热心帮助，感谢你邀请我们聚餐、麻将以及对多多的照顾，祝你早日毕业。感谢**俊**对我实验上的指导和工作规划，感谢你和**珊珊**的聚餐邀请。感谢实验室的师兄师姐**殷冬梅、桑亚秋、黄盛世、闫秋婷**及**李莉**的帮助。感谢新加入的**云鹏、俊雄**和**翔**，感谢你们以及**小松**和**娟芝**的聚餐邀请，祝你们实验顺利，早日毕业。

I would like to express my gratitude to my family for their unwavering support and understanding. Their encouragement has been a constant source of motivation during the challenging phases of this research endeavor. 感谢**爸爸妈妈**的无条件支持和默默付出。

I also want to thank many friends I met in Maastricht! 感谢**李老师**生活上给与的帮助。感谢**吴瞻哲**和**李美铮**的约饭、喝酒、聊天。感谢**何磊**和**翁洪娟**，**宋柯**，**许蛟婧**，**赵沅蒂**，**罗鸿幸**和**列永蝉**，**檀秀香**，**吴文博**，**罗维**，**王珊**，很开心在荷兰认识你们。

Finally, I extend my deepest appreciation to my wife. **张幸真**，感谢这五年在荷兰对我的鼓励和帮助，没有你我没法完成这趟旅程。感谢你在背后的默默支持和付出以及对我的宽容。

This thesis would not have been possible without the collective contributions of these individuals and institutions. I am truly thankful for their support, and I dedicate this work to them.